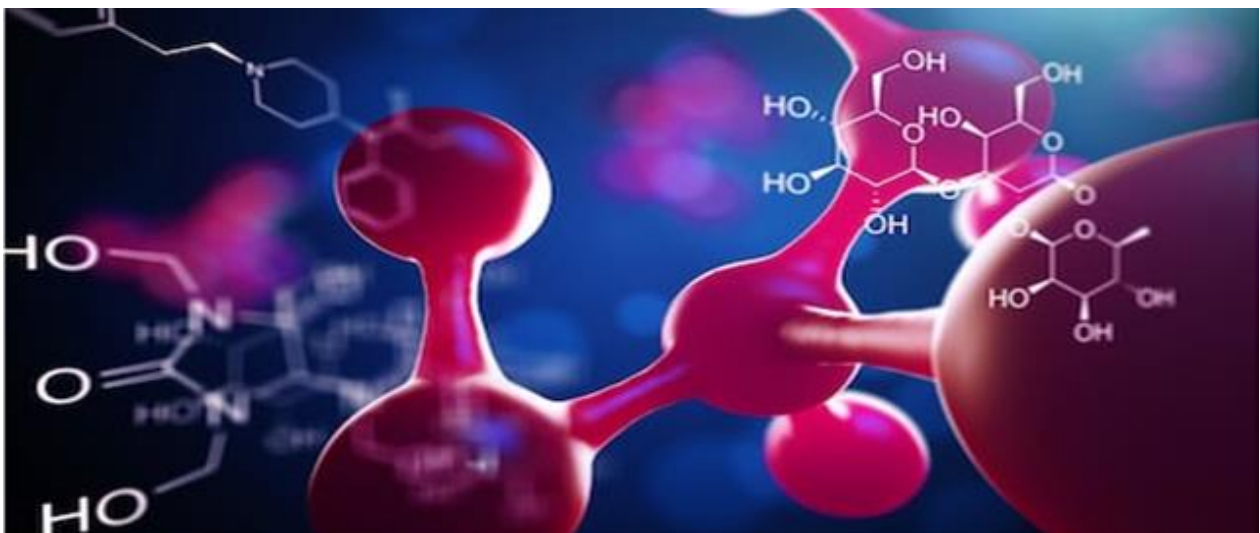# A route to fully wine-derived plastics: Wine wastes as source, additives and fillers for different polymers and biopolymers

Alessandro Nanni

University of Modena and Reggio Emilia
Department of Engineering "Enzo Ferrari"

PhD school in Industrial and Environmental Engineering

A route to fully wine-derived plastics: Wine wastes as source, additives and fillers for different polymers and biopolymers

PhD Thesis in Polymer Engineering

Candidate:
Alessandro Nanni

Advisor:
Prof. Massimo Messori

Doctorate Cycle: XXXII | [2016-2019]

Doctorate Directors: Prof. P. Tartarini / Prof. A. Muscio

External Revisers: Prof. F. Bignotti / Prof. A. Pegoretti

Abstract

In the last decades, the increasing global environmental concern has lead industry and scientific academia to focus in new eco-friendly and renewable processes, materials and systems. Considering the plastics sector, biodegradable and bio-based polymers have gained a great attention as promising solutions to solve or reduce the crude oil dependence and/or the plastic pollution issues. By the way, these natural polymers still cover restricted portion of the market because of both their high prices and the lack of knowledge, if compared with classical petrochemical polymers. Therefore, from an overall point of view, the present dissertation should be seen as a detailed part of a broader context in which it is attempted to bridge the maturity gap between the concepts of petrochemical and bio-refineries and to promote their progressive switch in large-scale by the contribution of new ideas, results and know-hows. Going into details, the present work has investigated the possibility to valorize the agro-industrial wastes derived from the wine companies within different polymers and biopolymers following several different approaches. Two apparently distinct processes as plastic and winemaking have been put in contact, offering new suitable products able to solve at the same time the green materials necessity and the agro-wastes disposal problems in accordance with the principles of sustainability, circular economy, renewability and low environmental footprint. Different solid wine wastes have been collected, characterized and exploited in different ways depending on their evaluated properties and potentiality. Generally, wastes rich in polyphenols and/or their extracts have been tested as natural stabilizers within Polypropylene (PP), Poly(hydroxybutyrate) (PHB) and Poly(butylene Succinate) (PBS) investigating the response of the bio-stabilizers to short and long-terms degradation (thermal and/or UV) as well as to biodegradation in different environments. At the same time, wastes characterized by high inorganic or lignocellulosic fractions have been studied as reinforcement cost-effective natural fillers within Poly(hydroxybutyrate) (PHB), Poly(3-hydroxybutyrate-*co*-hydroxyhexanoate) (PHBH), Poly(3-hydroxybutyrate-*co*-hydroxyvalerate) (PHBV), Poly(butylene Succinate) (PBS), Polyamide 11 (PA11) and Poly(lactic acid) (PLA). Bio-composites have been mainly investigated from a thermal, mechanical and rheological point of view, exploiting also micro-mechanics models to deeper understand the effect of the wine-derived fillers on the biopolymers properties. Finally, steps to directly synthesise *scl*-Poly(hydroxyalkanoate)s (PHAs) starting from wine wastes as substrate have been also partially discussed. Each treated topic has been handled from a theoretical and experimental point of view in order to model and control the behaviour of these new wine-based materials and simultaneously, economical essays have been carried out in order to point out the concrete feasibility to transfer these wine-based materials to large-scale apparatuses.

Abstract

Negli ultimi decenni, a causa della sempre maggiore e più diffusa preoccupazione ambientale, l'industria e la ricerca scientifica si sono concentrati sullo sviluppo di nuovi processi, materiali e sistemi più ecosostenibili e meno impattanti. Così, nel mondo della plastica, i polimeri da fonte rinnovabile (bio-based) e/o quelli biodegradabili hanno guadagnato una grande attenzione in quanto promettenti soluzioni per la risoluzione (o riduzione) della dipendenza dal petrolio e/o del problema dell'inquinamento della plastica. Tuttavia, questi nuovi polimeri naturali coprono ad oggi solo ristrette porzioni di mercato in quanto sono più costosi e meno conosciuti in termini di know-how rispetto ai polimeri convenzionali di origine petrolchimica. Quindi, da un punto di vista globale più ampio, la presente dissertazione deve essere vista come un capitolo facente parte di un insieme collettivo di più ricerche animate dal fine condiviso di favorire la bio-raffineria in larga scala a scapito della raffineria petrolchimica, ricucendo il loro gap di competenze tramite l'apporto di nuove idee e risultati. Entrando nel vivo degli argomenti, il presente lavoro ha investigato la possibilità di valorizzare gli scarti agro-industriali provenienti dalle cantine vitivinicole nel mondo dei polimeri e biopolimeri utilizzando diversi approcci. In tal modo, mettendo in contatto due mondi apparentemente separati come quelli della plastica e del vino, si è sia reso possibile lo sviluppo di nuovi materiali eco-friendly che fornite nuove soluzioni per lo smaltimento dei rifiuti della lavorazione del vino, in linea con quanto voluto dalle nuove politiche di sostenibilità, rinnovabilità ed economia circolare. Diversi sottoprodotti vitivinicoli sono stati campionati, trattati, caratterizzati e sfruttati a seconda delle loro proprietà e potenzialità. In genere, gli scarti ricchi di polifenoli e/o i loro estratti sono stati testati come stabilizzanti naturali all'interno del Polipropilene (PP), del Poli(idrossibutirrato) (PHB) e del Poli(butilene succinato) (PBS), investigando la risposta di tali bio-stabilizzanti sia alla degradazione a breve e lungo termine (termica e/o da UV) che alla biodegradazione in diversi ambienti. Parallelamente, gli scarti lignocellulosici o contenenti frazioni importanti di materiale inorganico sono stati studiati come filler naturali rinforzanti a basso costo all'interno del Poli(idrossibutirrato) (PHB), Poli(idrossibutirrato-*co*-idrossiesanoato) (PHBH), Poli(idrossibutirrato-*co*-idrossivalerato) (PHBV), Poli(butilene succinato) (PBS), Poliammide 11 (PA11) e del Poli(acido lattico) (PLA). I bio-compositi sono stati investigati da un punto di vista termico, meccanico e reologico, sfruttando anche differenti modelli micromeccanici per la comprensione dell'effetto del filler vitivinicolo sulle proprietà dei biopolimeri. Infine, gli step necessari per sintetizzare direttamente i Poli(idrossialcanoati) (PHAs) a catena corta (-scl) utilizzando gli scarti vitivinicoli come substrato di fermentazione sono stati parzialmente discussi. Ogni argomento è stato trattato da un punto di vista sia teorico che sperimentale in modo tale da modellare, comprendere e controllare il comportamento dei nuovi materiali che, nello stesso tempo, sono stati anche oggetti di valutazioni economiche per la fattibilità del loro trasferimento in larga scala.

"I think having land and not ruining,
it is the most beautiful art
that anybody could ever want"
A. Warhol

Alla mia famiglia,
alla mia compagna
e ai miei amici.

TABLE OF CONTENTS

1. INTRODUCTION

1.1 CONVENTIONAL PLASTICS

The prophetic words "I just want to say one word to you, Ben. Just one word – plastics" pronounced to D. Hoffman in the movie *The Graduate* can perfectly resume the influence of the plastic material on the human everyday common life. It was the 1967 and the global plastic production amounted to 23 millions of tons (Mt) with an incredible registered +360% in only 10 years. In that year, plastic production also surpassed the one of all combined metals, pointing out an incoming revolution in the fields of materials. Nowadays, it is reasonable to state that prophecy has come true: considering and stating plastics as one of the most affecting and revolutionary materials of the 20th century is in fact not overrated, as testified by their selves production numbers. From 1967, in only 50 years, plastic industry has exponentially increased its production of more than 10 times, arriving to the 2017 worldwide production of 348 Mt (Fig.1) (not considering polymer fibers and polymer additives; in that case would arrive to nearly 420 Mt)).
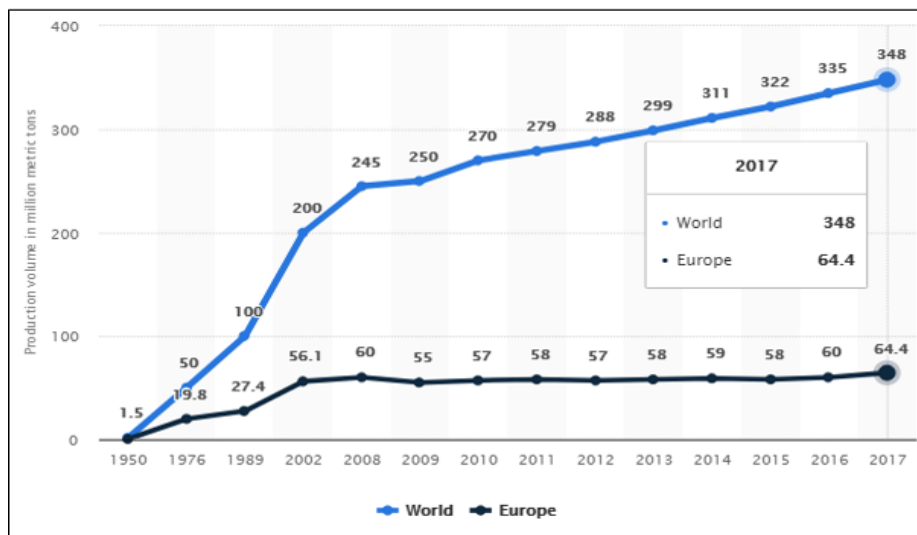
Fig.1 Worldwide and European plastic production trend in last 70 years (not considering polymer additives and fibers). Taken from [1].

Moreover, despite the European production trend depicted in Fig.1 would appear as tempting to an asymptote from 2000s, the 2016-2017 plastic production has increased of 7.3% (more than each other continent) from 60 to 64.4 Mt, highlighting a not still complete market saturation. Thus, today, plastic represents the second most produced matrial in the earth, being slightly behind only to paper and in advantage to other common materials as metals, glasses, ceramics and woods (Fig.2a).
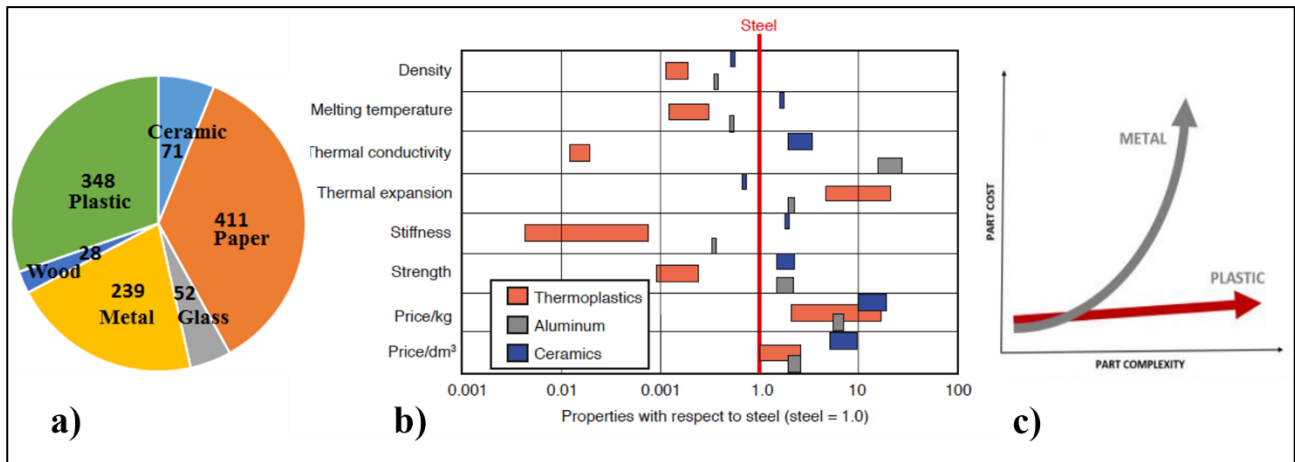
Fig.2 Comparison between plastics and other materials in terms of a) production (2018, Mt) b) properties (taken from [2]) and c) price for part complexity.

From a geographical point of view, Asia is the major producing continent carrying the 50% of the total production, with China absolute leader (29.4%), followed by Europe (18.4%) and North America (17.4%). Considering the typology, thermoplastics represent the most produced polymers (73%), followed by polymer fibers (12%), thermosets (10%) and polymer additives (5%). Among thermoplastics, polyolefin family represent nearly the 60% of the total production, with polyethylene (both light and high density, LDPE and HDPE) and Polypropylene (PP) able to cover the 45% of the world plastic market (Table 1 and Figure 3b). All this numbers make European Plastic the seventh most valued industry, at the same level as the pharmaceutic and very close to the chemical industry. In 2017, it has been able to contribute to 32.5 billion euros to public finances and welfare, to have a market turnover business of 355 billion euros and to involve more than 60.000 companies giving direct employment to over 1.5 million people [1].

Table 1 Polymer production data. European data do not consider additives and fibers. Adapted from

Polymer type	2015, World Production [Mt][a]	%	2017, Europe Production [Mt][b]	%
LLDPE, LDPE	64	15.7	11.3	17.5
MDPE, HDPE	52	12.8	7.9	12.3
PP	68	16.7	12.4	19.3
PS, EPS	25	6.1	4.3	6.6
PVC	38	9.3	6.6	10.2
PET	33	8.1	4.8	7.4
PUR	27	6.6	5.0	7.7
PP&A fibers	59	14.5	-	-
Additives	25	6.1	-	-
Others	16	3.9	19.0	12.2
Total	407	100	64.4	100

[a] Considering Fibers and additives; [b] Without considering fibers and additives

Plastic market has born as answer to improve the everyday life of most people, making products that were previously considered luxuries available to everyone. The success of plastic to replace many other materials has been due mainly because of its ability to be easily and fast formed in every imaginable shapes and not because of its intrinsic cheapness as often erroneously reported. In fact, the polymer pellet price is not so low, since it can range from 1 to 10 €/kg depending on polymer typology. Economically, the real plastics benefit lies on the fact that even complex parts do not require exponential costs as would happen for metals part (Fig.2c). In addition, plastics exhibit low densities (lightness), great optical properties (transparency and brightness), wide and customizable mechanical and thermal properties and low electric and thermal conductivities, if compared with other materials (Fig.2b).
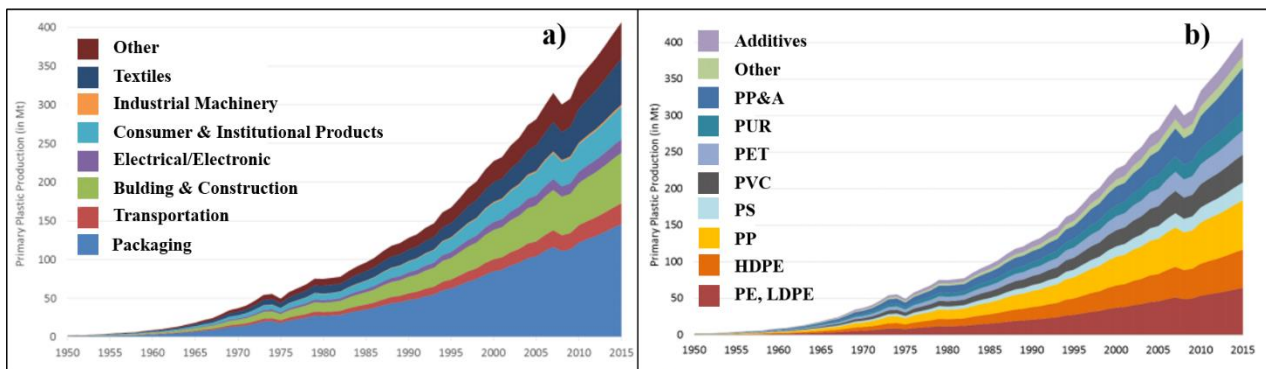
Fig.3 Global polymer production trends (1950-2015) in terms of a) application and b) polymer typology.

The easily plastic processing as well as their wide range of possible properties has lead plastic to find space in many different fields and applications as reported in Fig.3a and in Table 2.

Table 2 Distribution of European plastics demand by application and segments in 2016.

Market sector	2015,World [Mt][a]	%	2017, Europe [Mt][b]	%
Packaging	146	35.9	25.7	39.9
Transportation	27	6.6	-	-
Building and Construction	65	16.0	12.7	19.7
Electrical/Electronic	18	4.4	4.0	6.2
Consumers goods	42	10.3	-	-
Industrial Machinery	3	0.7	4.8	7.4
Textiles	59	14.5	5.0	7.7
Automotive	-	-	6.4	10.0
Household, Leisure & sport	-	-	2.7	4.2
Agriculture	-	-	2.1	3.3
Other	47	11.5	10.0	16.7
Total	407	100	64.4	100

[a] Consider Fibers and additives; [b] Do not consider fibers and additives

By the way, in the last decades, the global increasing environmental concerns have started to demand new more sustainable products to all industrial sectors, including the plastic one. In fact, as it shall be subsequently shown, the conventional plastics have been one of the main responsible for the land and ocean pollution as well as for the CO_2 emissions and the related global weather changes. Therefore, the well-established plastic sector has been today called to give answers to community in terms of new eco-friendly technologies and products in order to preserve its financial solidity, prosperity and reliability. Within this 21th century plastic revolution, bio-based and/or biodegradable polymers have started to gain a great attention and a central role within both Industry and scientific academia because their potential to solve or decrease both crude oil dependence and plastic pollution.

1.1.1 Fossil fuels issues

The rate of fossil fuels (crude oil, coal and natural gas) consumption has increased rapidly from industrialization age until today providing cheap and continuous power in favour to the development of the Western economies, mostly. The data published on "BP Statistical Review of World Energy" [3] assert that global energy consumption of 2018 has been of 13865 million tons of oil equivalent (mtoe) (+2.8% respect to 2017) and that almost the 85% of the used energy has been based on fossil fuels (Fig.3). Crude oil has been exploited for the 33.6%, natural gas for the 23.9%, coal for the 27.2%, hydroelectric for the 6.8, nuclear energy for the 4.4% and the renewable energy (solar, wind, geothermal energy and biomasses) for the 4.0%.
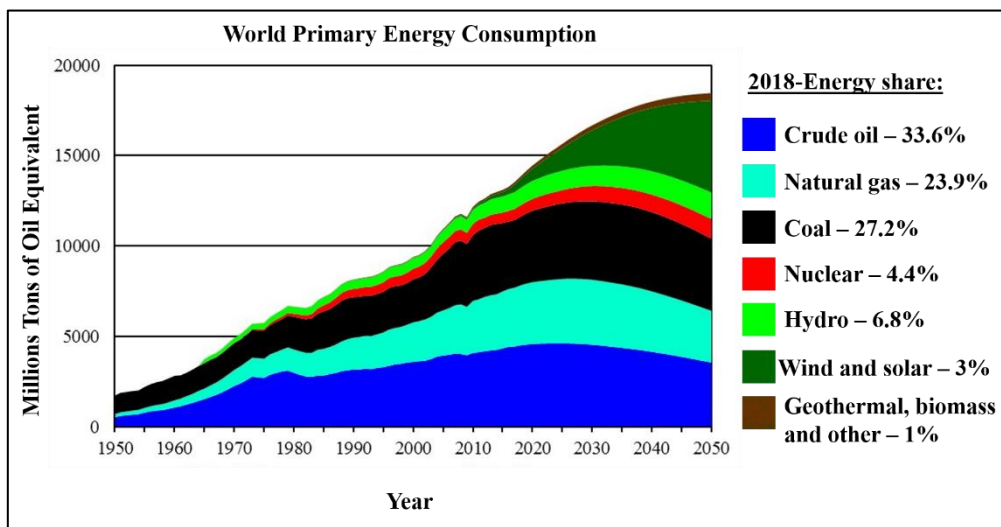
Fig.4 World Primary Energy Consumption expressed as Million Tons of Oil Equivalent. Taken and adapted from [4].

Despite this evident domain, several concerns have progressively started to raise up against the fossil dependence in the last years. The two main concerns have regarded the effect of the fossil fuels on the environment and the fossil resource scarcity. Speaking about the first issue, fossil fuels have been criticized because their effect on the soil carbon sequestration [5] and mainly for their contribution to the CO_2 and other greenhouse effect gases (GHG) emissions [6] and to the related climate changes [7]. In 2018, global CO_2 emissions have been amounted to almost 34 billion of tons recording a worrying +2.0% with respect to 2017. Oil and Gas industries, consuming about the 57% of the global worldwide produced fuels, have been responsible of more than 50% of whole GHG emissions. For

this reason, main industries have endorsed and adopted new ways for sustainability and carbon footprint reduction. Briefly, the main adopted implementation and strategies carried out by the Oil and Gas plants to decrease CO_2 emissions have been:

a) The integration of renewable energies to supply the Oil & Gas plants energy requests (e.g. solar and wind energy combined with classic diesel generators and gas turbines [8, 9]).

b) The conversion of produced CO_2 in high-value chemicals as synthetic natural gas (SNG) or methanol [10, 11].

c) The exploitation of the produced CO_2 to improve the performance of depleted oil and gas reserves through the "carbon capture and storage" [12] techniques integrated with new technologies of "enhanced oil (or gas) recovery) [13].

d) The progressive substitution of coal in favour to natural gas (Coal to Gas). Coal plants generates CO_2/MWh emissions that are almost double than those produced by Natural Gas plants and moving from Coal to Gas would reduce the world emissions of 15% [14].

Nevertheless, the adaptation of Oil and Gas industries to these new processes is still in a transition phase where technologies are under investigation to be optimized in terms of costs and efficiencies. Thus, fossil fuels prices are in an overall increasing trend that will not be stopped in next decades as testified by the projection charts reported in Fig.4 [15] .
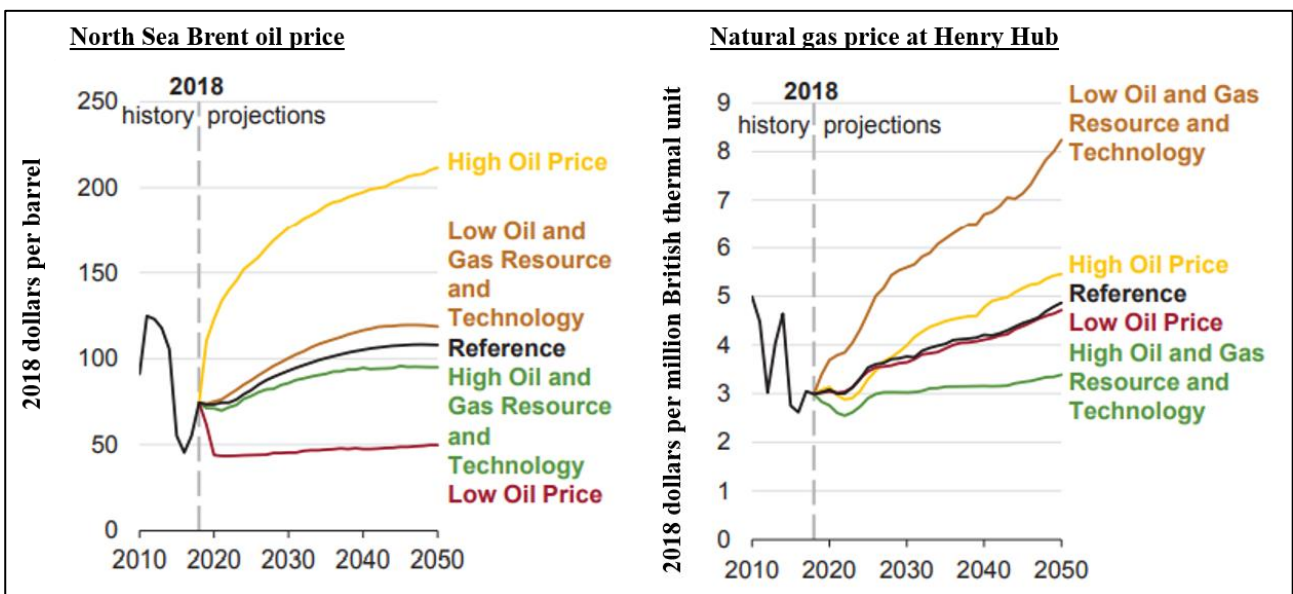
Fig.5 Projection chart of oil and natural gas prices. Taken and adapted from [15].

In addition, also fossil scarcity is contributing to make fossil fuels more unstable and less attractive to investors. The R/P factor is a parameter that estimate the time needed before the extinguishment of a not renewable resource relating its amount expressed in terms of proved reserves to its yearly consumption rate. In 2018, R/P times of fossil fuels have not been exciting (132 years for the coal extinction, 50.9 years for the natural gas and 50.0 years for the crude oil), especially considering that coal will be progressively substituted by natural gas, as previously mentioned. Moreover, the heterogeneity and disparity between the geolocation of fossil fuels reserves, consumers and producers

(Fig.5) could lead to possible incoming energy-supply security problems and geopolitical tensions that would increase the risk and instability of the Oil and Gas sector within the free market [16].
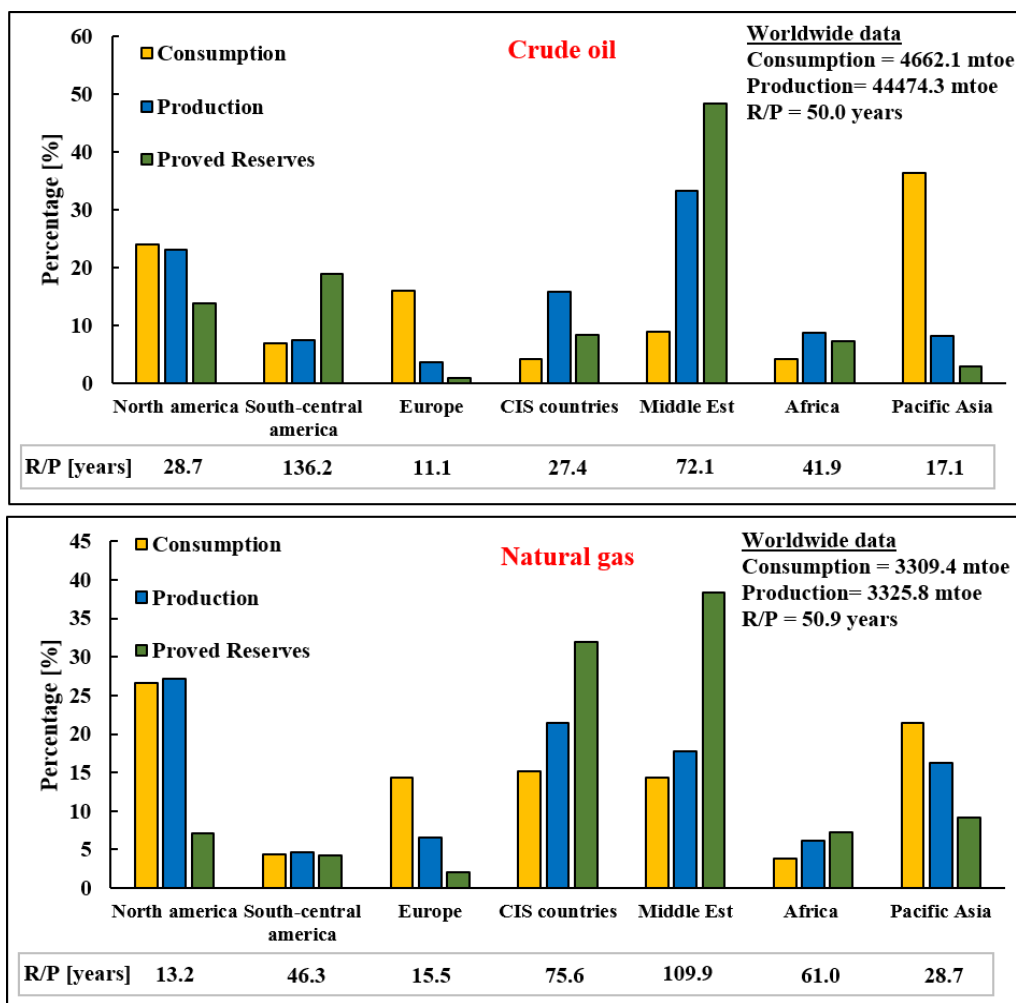
Fig. 6 Worldwide and distributive data of the consumption, production and proved reserves of crude oil and natural gas. Generated using data from [3].

It is from and within this complex economical, ecological and geopolitical context, in which short-terms problem (CO_2 emissions) and long-terms problems (fossil scarcity) are connected and branched, that bio-based polymers have started to be attractive in large scale and are now growing up and are being more and more required. In fact, even if only the 5-7% of oil and gas production is destined to polymers synthesis (45% transports, 42% heating and electricity, 4-5% chemicals, 5% other utilities), the same dynamics regarding the oil & gas sector are also reflected on the plastic sector as testified by Fig. 16 in which petroleum and polymer prices report the same price trend.

1.1.2 Plastic pollution

Plastic pollution is one of the main environmental problem of our era. The huge plastic waste generation is a direct consequence of the fact that most plastics products are designed to have a short lifetime. In this way, every year, the amount of wasted plastic is very similar to the amount of produced plastic pointing out significant intrinsic problems on the plastic disposal and management.

In 2015, the plastic waste generation has been of 302 Mt, representing almost the 75% of the total produced plastic in the same year, and being roughly equivalent in mass to the two-thirds of the world population. As easily imaginable, packaging is the sector that more contribute to waste generation and plastic pollution, and about a 96% of the yearly produced packaging items is wasted in the same year (Fig.7).
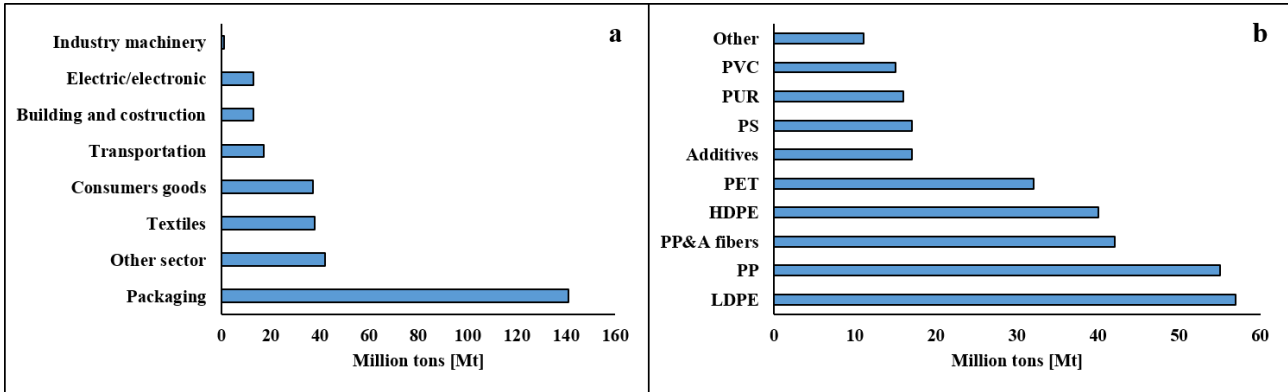
Fig. 7 World plastic waste generation in 2015 in terms of a) sector and b) polymer typology.

The situation becomes more dramatic if it is considered the cumulative plastic wastes generation over the year. It is estimated that since 1950, the world has produced nearly 8 billion tons (Bt) of plastic of which almost 5 Bt have been discarded to landfill just after one use. Landfilling has in fact represented the unique destination for each wasted plastics for almost 40 years, and it has been only from 1990's that different managing approaches have started to be considered and applied in large scale to limit the not eco-friendly landfilling. This environmental revolution has been conducted on two levels: i) by the means of awareness campaigns aimed to educate consumers and societies to the reuse and to the reduced use of the plastics and ii) by the optimization and the scaling up of plants for the plastic waste treatment and valorization. Therefore, plastic wastes are nowadays generally treated in four different ways: i) mechanical recycling, ii) chemical recycling, iii) incineration and energy recovery and iv) disposal in landfill (Fig.8a). Among them, from an environmental point of view, recycling is the most preferred meanwhile landfilling is the least favourite, as pointed out by the waste treatment hierarchy (Fig.8b) stilled by the US Environmental Protection Agency (EPA). Positive and negative aspects of each mentioned treatment have been briefly reported in Table 3.
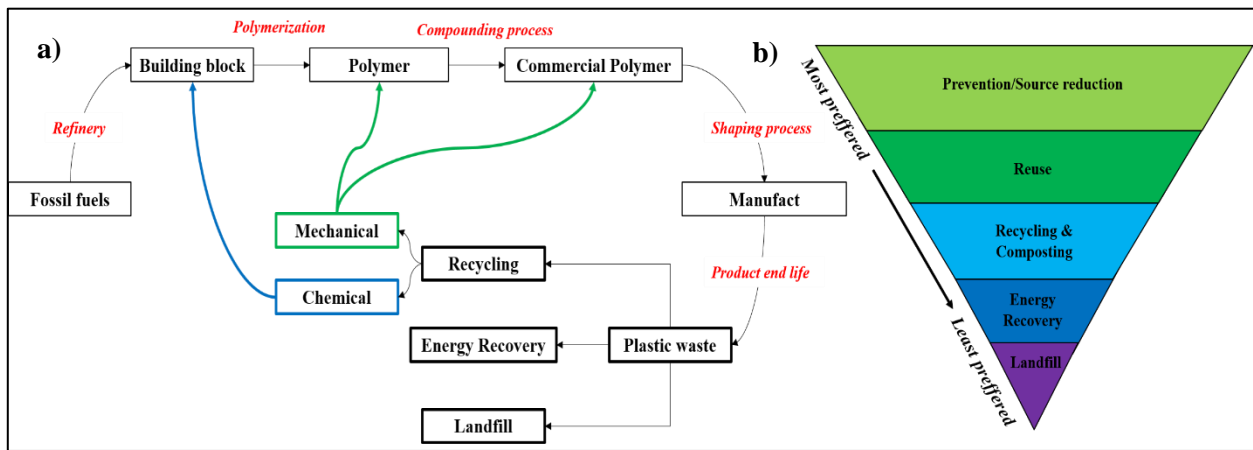
Fig. 8 a) Conventional plastic life cycle and b) waste treatment hierarchy stilled by EPA.

Thus, today, in western society, landfilling has started to be finally abandoned in favour to mechanical recycling and energy recovery as testified by the European trends depicted in Fig.9. Recycling has registered a +79% growing rate, and the amount of the recycled plastics has finally surpassed the amount of the landfilled ones in 2014. Even if these trends are really positive, it has to mentioned that mechanical recycling still suffers several drawback. It can be scarcely applied on plastic objects formed by different components and the polymer typology sorting is often a critic step, it induces degradation on the polymer matrix causing a limitation on the number of the possible recycling cycles (Table 3). Now, mechanical recycling alone cannot close the loop of the plastic life cycle even if progresses have been made as the optimization of the chain extenders additives for the PET molecular weight preservation [17] or the optimization of the sorting step [18, 19]. Thus, mechanical recycling should be exploited as more as possible and at the same time collaborates with energy recovery when polymer cannot be recycled or cannot be anymore recycled. Another important and positive parameter that arise from Fig.9 is the +11% registered trend in terms of total collected plastic wastes. Some important countries have still some difficulties in this step, as for example Italy, that in the 2006-2016 period has recorded only a +2% in collecting plastic wastes (Germany, +46%). It is clear that collection step represents the *sine qua non* of a green disposal management policy. A lack in this phase can invalidate all the efforts made to enhance and promote recycling and energy recovery. Considering packaging materials and comparing their post-life data, a worrying leakage (32%) between generated wastes and treated wastes (landfill, recycling and energy recovery) has been observed, and only the 2% of the recycled packaging has been able to close the loop.

		Collection, 2016	2006-2016 grow rate
♻	Recycling	8.4 Mt (31.1%)	+79%
⏻	Energt Recovery	11.3 Mt (41.6%)	+61%
🚛	Landfill	7.4 Mt (27.3%)	-43%
♳	Total collected	27.1 Mt	+11%
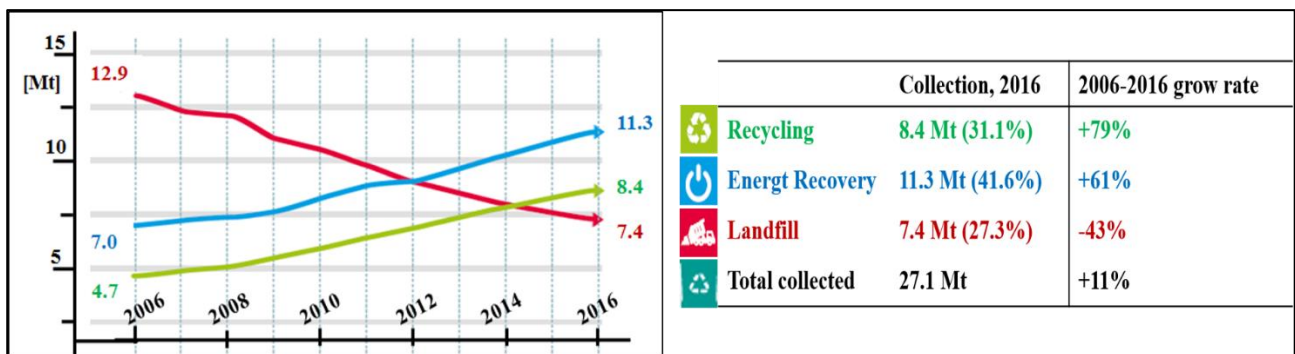
Fig. 9 European management data of the plastic wastes, 2006-2016. Adapted from [20].

Unfortunately, the positive European reported data are not uniformly diffused in the world, where landfilling still continue to be the global most used treatment. More precisely, in 2015, landfilled plastic wastes have been the 55% of the total plastic wastes, meanwhile the incinerated the 25.5% and the recycled only the 19.5%, as shown in Fig.9.
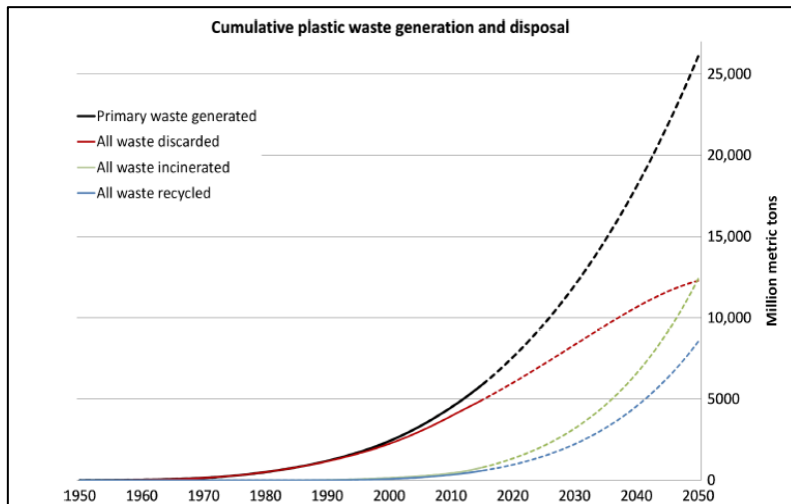
Fig.9 Historical and projection trends of the cumulative plastic waste generation and disposal. Taken from [21].

Thus, this historical and present massive use of landfills as well as the difficulty on collecting and reusing plastic wastes, has led to environmental problems due by the creation of mismanaged wastes. For mismanaged wastes are intended the sum of all plastic material that being either littered or inadequately disposed, as for example, disposal in open and uncontrolled landfills, have an high risk of entering the ocean via inland waterways, wastewater outflows or being transported by wind or tides [22]. Plastic waste mismanagement is mostly present in countries located in East Pacific Asia (60%) and South Asia (11%) (Fig. 10) in which are also located, as consequence, the most important plastic polluting sources for the ocean. As example, considering the contribute of the rivers to the ocean pollution, it is possible to estimate that Asian rivers transport the 86% of the total plastic inputted into oceans by rivers [23].
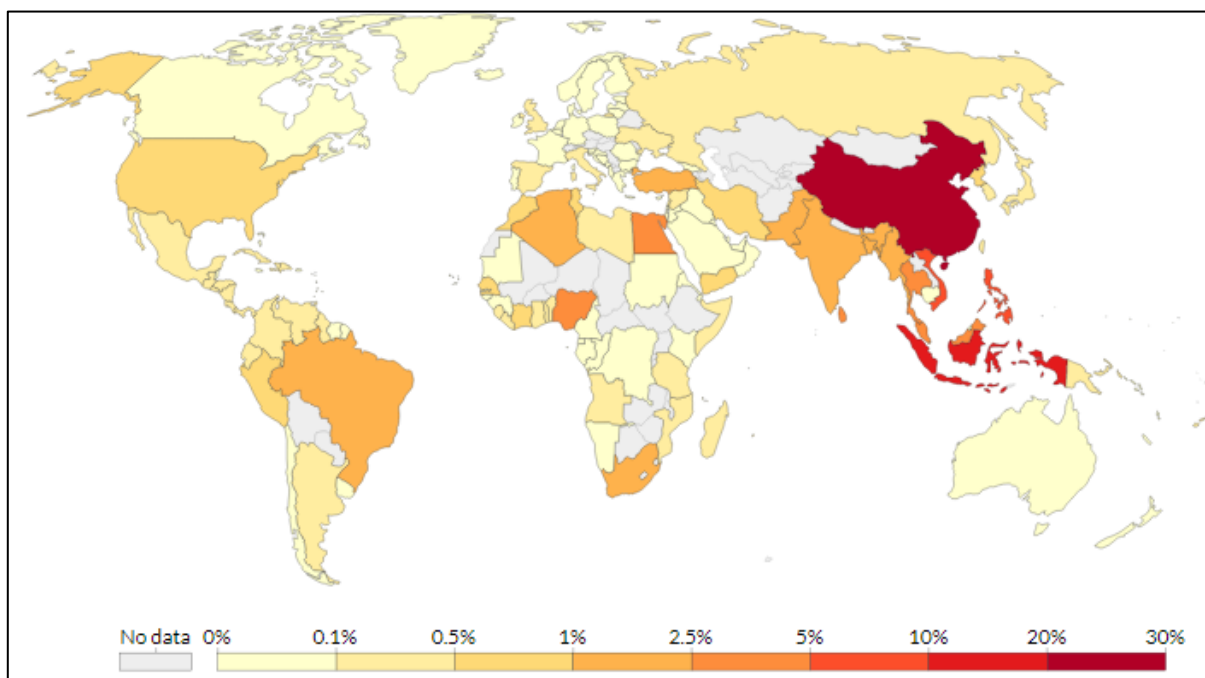
Fig.10 Global mismanaged plastic by region, 2010. Taken from [22, 24].

21

Moreover, plastic wastes are introduced into the ocean also through other pathways as coastlines and tides (together with rivers form the "land sources", responsible of the 80% ocean plastic input) or by marine sources as fishing nets, ropes or other objects connected with the fishing activities. For this reason, the plastic floating on the oceans and sea surfaces has been accounted to be almost 270.000 tons [25] and the estimation could be also underrated. There is in fact a discrepancy between the accounted plastic inputting into oceans and the revealed one, especially if it is considered the cumulative wastes ended into oceans over the years. This gap is well known in literature as a long-standing question "where is the missing plastic going?" The most accredited theories have indicated that ocean plastic underestimation could be due by a) incorporation and ingestion of small plastic pieces by organism [26] b) sink and sedimentation of plastics pieces in deep-sea sediments [27] and c) burial of plastic in shorelines [28]. Following these theories, the real cumulative plastic inputted on ocean between 1950 and 2015 has been terrifying. Nearly 82 Mt of macro-plastic (greater than 0.5 cm) and 40 Mt of micro-plastic (smaller than 0.5 cm) have been reversed on the dry lands of the shoreline, 150 Kt (macro) and 80 Kt (micro) on the shallow waters of the coastal and 1 Mt (macro) and 0.5 Mt (micro) have sunk in offshore deeper waters.
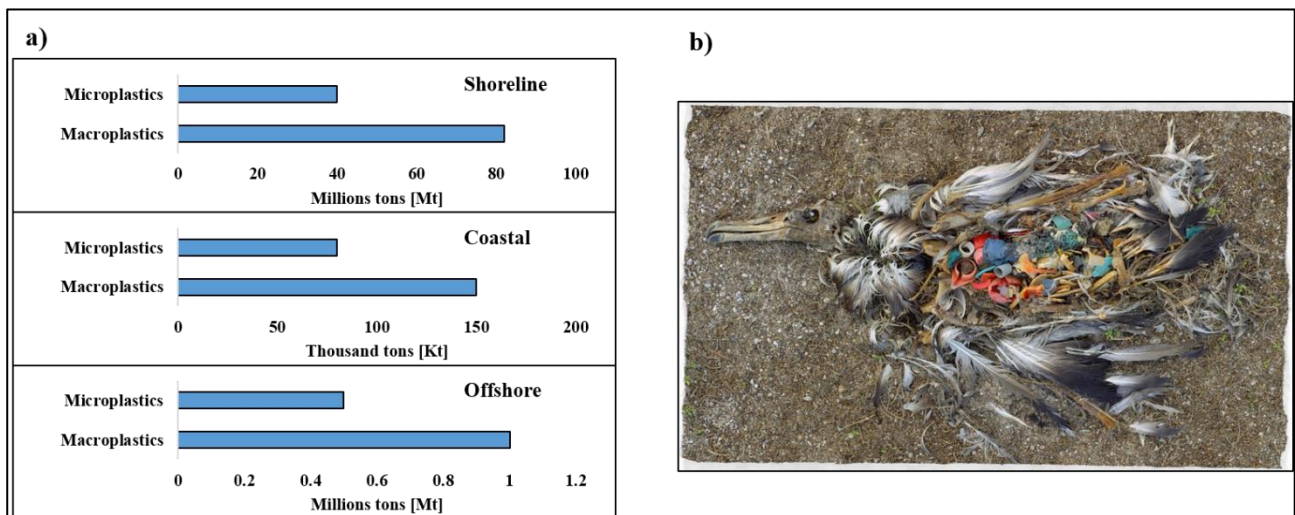
Fig.11 a) Cumulative micro and macro plastic pollution in the oceans (1950-2015). b) Example of plastic within a sea-bird body. Plastic pollution affects the marine wildlife environment and the food chain.

Clearly, this pronounced pollution has started to affect the wildlife environment significantly. Many cases of entanglements, ingestion and interaction between marine organism and plastic debris have been documented and studied. Plastic has caused in marine organisms many negative consequences as death, tissue abrasions, biochemical/cellular modification, altered genetic assemblages and reductions or increases in population size [22, 29, 30]. This not eco-friendly chain is now propagating to human population. It is possible for micro and nano-plastics to be passed up to higher levels in food chain (Fig. 11b). This is possible when a species consumes organisms of lower levels in the food chain that have micro or nano plastics within them, in the gut or tissue [31]. Therefore, these micro and nano plastics are the greatest concerns for human health [22]. Example of plastic ingestion trough water and marine products consumptions as well as of plastic inhalation trough air containing

particles have been documented [32, 33], confirming the presence of micro and nano plastics at higher levels of the food chain [34].

Therefore, it has been from and within this complex environmental challenge that biodegradable polymers have started to gain a great importance in the last decade. Their capacity to degrade in comparatively low times into mainly CO_2 and water after their life cycle in different natural or industrial environments (soil and water, digesters and fermenters) has attracted companies and society to their use in large scale in order to furnish a new more possibility to solve the plastic pollution issues. Indeed, biodegradable polymers have not to be seen as invitation in littering ("so much are degradable"), but as useful materials able to prevent or at least limit the lacks in wastes collecting or in wastes management. Therefore, biodegradable polymers should not considered as in competition with classical recycling and recovery tools, but as a parallel useful tool. Public awareness and technological research on plastic recycling, recovery and management need to be pursed at the same time and at the same level as biodegradable polymers need to be extended in large scale.

Table 3 Plastic waste treatments: positive and negative aspects.

Plastic waste treatment	Main Positive aspects	Main negative aspects	Ref
Mechanical recycling	a) Reduction of new petrochemical sources. b) Circular economy principles.	a) Difficulty on polymer sorting. b) Degradation as treatment limit. c) Performable only on single polymer plastics. d) Customers responsibility.	[35-37]
Chemical recycling	a) Recovery of the initial building block for new polymers or other purposes (e.g. chemicals, gases). b) Reduction of new petrochemical sources. c) Suitable also for thermosets.	a) High consumptions of energy and/or solvents. b) Hazardous products often involved (e.g. acid/basis). c) Difficulty on scaling up.	[38-40]
Energy recovery	a) Electric energy production. b) Thermal energy for plant facility. c) Useful in case of contaminated or not easily sortable plastics. d) Useful when recycling is no longer possible. e) Huge and fast plastic wastes reduction; suitable especially for countries with not good disposal management.	a) Possible release of toxic substances (e.g. dioxins). b) CO_2 emissions: "zero emissions" target not possible. c) Generation of ashes and scoriae (special wastes treatment) and of toxic powders from filters (toxic wastes treatment.	[37, 41]

Landfill	a) Still better than littering. b) Close and controlled landfills can be exploited for methane recovery.	a) Absence/lack of valorization and circular economy principles. a) High risks of micro, meso and macro plastics migration into oceans. b) Hazardous products can leach in soil and aquifers (e.g. bisphenol A). d) Open or uncontrolled landfill input methane in atmosphere.	[42-44]

1.2 BIOPLASTICS

As described in 1.1.1 and 1.1.2, oil & gas crisis and plastic pollution issues have respectively incentivized the bio-based and biodegradable polymers demand in large scale. Firstly, it is needed to define these two classes of polymers and their connection with the more general term biopolymer in order to avoid confusion. As shown in Fig.12, polymers can be classified in terms of origin and biodegradability. In accordance to European bioplastics, a plastic material is defined as bioplastic (or biopolymer) if it is either bio-based (both fully and partially), biodegradable or features both properties [45]. From an ecological and environmental point of view, it is easily to state that bioplastics both bio-based and biodegradable are the most preferred.

	Biodegradable	Non-biodegradable
Bio-based	CA, CAB, CAP, CN, PHB, PHBV, PLA, starch, chitosan	PE (LDPE), PA 11, PA 12, PET, PTT
Partially bio-based	PBS, PBAT, PLA blends, starch blends	PBT, PET, PTT, PVC, SBR, ABS, PU, epoxy resin
Fossil fuel-based	PBS, PBSA, PBSL, PBST, PCL, PGA, PTMAT, PVOH	PE (LDPE, HDPE), PP, PS, PVC, ABS, PBT, PET, PS, PA 6, PA 6.6, PU, epoxy resin, synthetic rubber

Fig.12 Polymer classification in terms of origin and biodegradability. Red rectangles group biopolymers as defined by European Bioplastics.

1.2.1 Bio-based polymers

The term "bio-based" is defined in European standard EN 16575 as "derived from biomass" and for biomass, it is intended a material of biological origin not embedded in geological formations and/or fossilized. Examples regard paper and wood or bioplastics such as PLA and PHAs that derive from sugars. The term renewable depends on the exploited feedstock and it can be used when the feedstock is naturally replenished on a human timescale, in contrast to fossil oils which need millions of years to be formed [46]. As consequence, bio-based do not intrinsically involve renewable (e.g. peat is not considered renewable and tropical hardwood is only if well managed). Thus, bio-based polymers refers to polymers of which starting blocks are derived, fully or partially, from renewable biomasses. The bio-based content can be expressed in terms of mass content or, more usually, in terms of carbon content (EN 16640 or ASTM 6866). These bioplastics are technically equivalent to their fossil counterparts in terms of properties and processability, are recyclable too, but simultaneously, they reduce the product's overall carbon footprint. Their ideal life cycle would consist on a reuse phase trough mechanical recycling (as many times as possible), followed by the energy recovery step. Thus, the final by-products generated in the incinerator (CO_2, water and compost) would represent the input for the plant growth and for the new renewable feedstocks in order to close the *virtuoso* loop shown in Fig. 13.
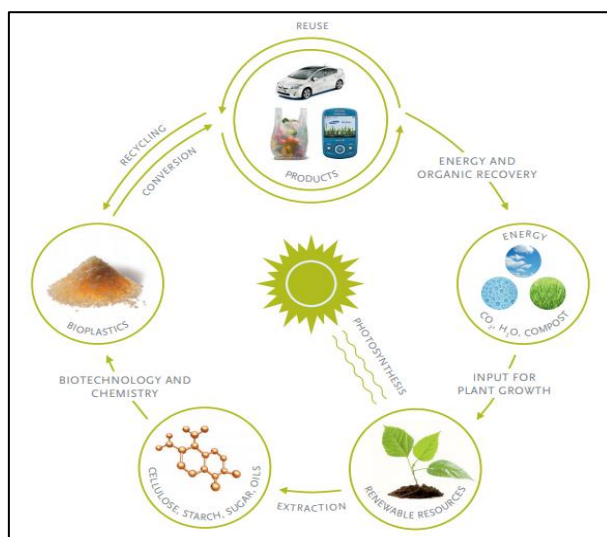
Fig.13 Ideal life-cycle of the bio-based plastics. Taken from [47].

In 2018, the production of bio-based polymers (not biodegradable) has been of only 1.2 Mt (0,35% of the total polymer production) and it is predicted to raise up 1.328 Mt (+10.6%) in 2023 (Fig.14). Among them, the most produced polymers in 2018 have been bio-PET (46%) followed by polyamides (PA) (20.1%), bio-PE (16.4%), bio-PTT (15.9%) and others (1.6%), meanwhile bio-polypropylene (bio-PP) and bio-poly(ethylene florurate) (bio-PEF) are currently in development and their market availability has been predicted for 2023.

2018 Production data	10^3 tons	Share
● PE	201	16%
● PET	562	46%
● PA	245	20%
● PP*	-	-
● PEF*	-	-
● PTT	194	16%
○ Others	19	2%
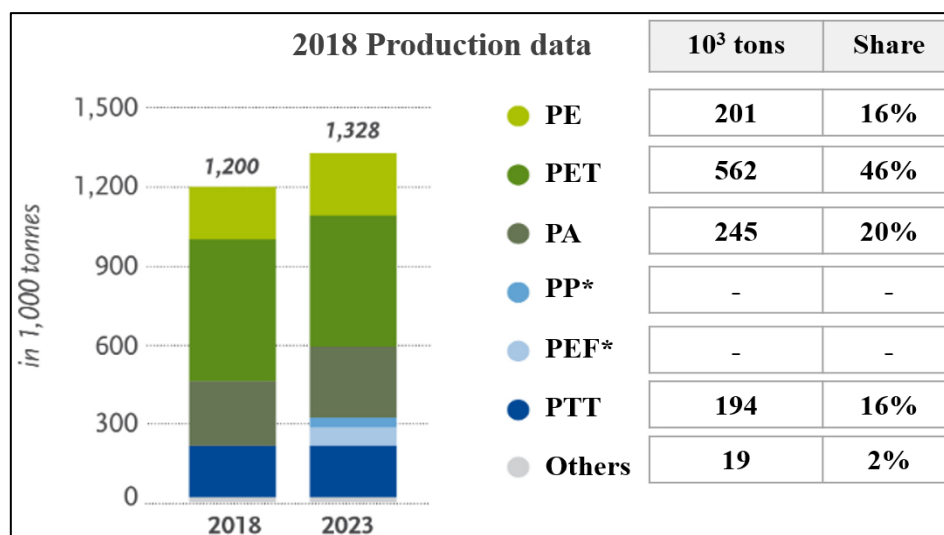
Fig. 14 Production data in 2018 and projection at 2023 of bio-based polymers (not degradable). Adapted from [45].

The challenges to increase the bio-based polymers production are mainly connected with the initial used feedstock and with the final product costs. Raw materials can be classified as of first, second and third generation. First generation feedstocks are food crops generally rich in carbohydrates, sugars and/or fats (oily or animal). Examples can regard corn, wheat, rapeseed, cassava (starchy) or sugar cane and sugar beet juices (sugary) as well as oils from palm, soybean and sunflower (oily). Second generation feedstocks are non-food lignocellulosic crops such as residues from agricultural and forest industries or woody and fibrous by-products. Examples may regard wheat straw, corn stover and sugar cane bagasse or molasses. Finally, third generation feedstocks are represented by algae. Bio-based polymers are nowadays mainly obtained through the fermentation of first generation feedstock, that being food competitive have lead scientific academy and industry to contrasting opinions. From one side it is believed that as consequence of the fossil fuels increasing prices, larger portions of lands will be dedicated to biomaterials instead of using them to produce food and thus, food price will raise up pointing out ethical implications. In addition, some studies have pointed out that the CO_2 emissions and fossil energy consumptions to produce biomaterials and biofuels are not always low as believed because of the high energy in put required for crop cultivation and conversion [48-50]. For these authors, second generation feedstocks should be preferred even if their conversion in large scale is expected only in 10-15 years. Conversely, the other way of thinking believes that first generation feedstock should be not seen in a negative light since the land destined to biopolymers is still very low (0.016% of the global agricultural area in 2018) and would remain acceptable even for higher biopolymers productions (predicted to be the 0.02% in 2023) as shown in Fig. 15 [47]. Moreover, higher productions of biomaterials and/or biofuels could relieve the price-pressure on the oil & gas sector and, indeed, on the food price, and not the reverse. Finally, it is also suggested that further new lands dedicated for biomaterials production should be assigned again to first generation crops because of their higher conversion yields and their cascade effect on the by-production of other residues and/or second-generation feedstocks suitable for further conversions [51].
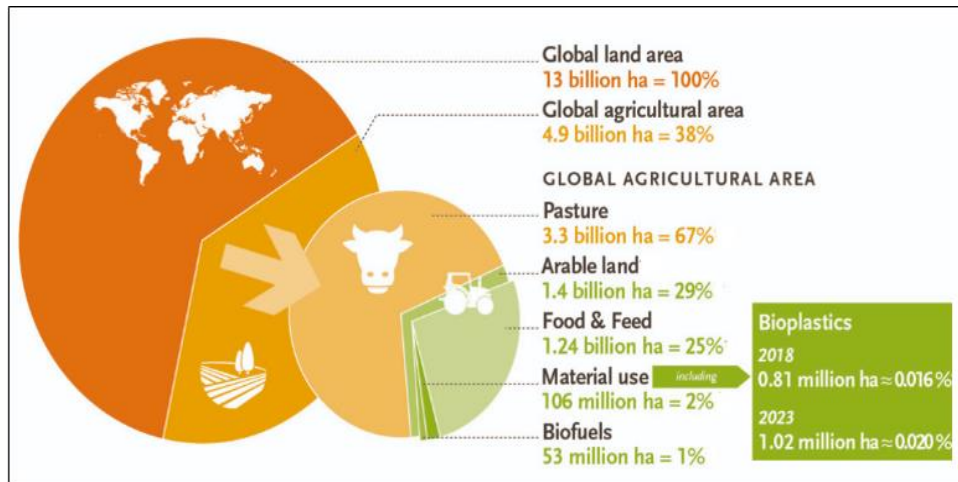
Fig.15 Partition of the global land area. In 2018, land used for bioplastics have been of 0.81 ha and they are expected to raise to 1.02 ha in 2023. Taken from [47].

Regarding the prices, it is possible to notice from Table 4 that bio-based polymers cost generally more than conventional plastics since the technological knowledges to obtain bio-based building block are not still enough or optimized. This is a consequence of the fact that bio-based materials have gained attention in large-scale only in the last decades. Conversely, fossil plastics prices are low because their processing steps have been deeply investigated and optimized from 1950's but they are also depend on and fluctuate with oil prices that are increasing for environmental and availability reasons (paragraph 1.1. and Fig.16). Thus, bio-based materials are favoured to be more and more invested and researched, and it is therefore expectable that the maturity gap between bio and fossil plastics could be repaired in the near future, leading to comparable market prices. Moreover, the optimization of the bio-refiners processes could also reduce the ethical problems connected with the lands uses. By the way, even today, there are several exception in which bio-based or biodegradable polymers are economically preferred than conventional plastics. For example, because the higher stiffness of PLA compared to PS, PLA final products can be down-gauged in thickness allowing material saving (e.g. a traditional HIPS Danone dairy cup of 0.89 mm wall thickness could be down-gauged to 0.66 mm thickness using PLA [46, 52]). Similarly, in agriculture, economical benefits could be obtained replacing PE mulch films with soil biodegradable mulch films: labour costs and film thickness would be in fact reduced since the not necessity of removing films after their use (PE mulch films are 2 times thicker than required to allow their recognition and removing) [46].

Finally, politics and governments should promote bioplastics demand but proceeding hand in hand with the gradual increases production levels in order to avoid inequalities between demand and supply that could raise up biopolymers prices apart from their technological progresses.

Table 4 Price costs (2016/2019) and densities of conventional plastics and bioplastics. Adapted from [46, 53, 54].

Plastics	Price [€/ton]	Density [kg m^{-3}]	Bioplastics	Price [€/ton]	Density [kg m^{-3}]
LDPE	1250-1450	910-940	PBAT	2200-3500	1250
HDPE	1200-1500	930-970	Bio-PE	+20-40%	910-970
PS	1250-1430	1040	PLA	2000-3000	1250

PET	850-1050	1370-1390	Bio-PET	No information	1370-1390
PP	1000-1200	900-920	Bio-PP	+40-50%	900-920
PA6	1970-2300	1140	Bio-PA	+10-20%	1030-1140
PVC	800-930	1100-1450	Bio-PBS	4000-5000	1260
PC	2600-3000	1220	PHAs	5000-6000	1200-1250
HIPS	1350-1525	1080	CA	5000	1200-1300
EPS	1500-1900	11-32	PTT	4000-5000	1320
ABS	1600-1950	1060-1080	Starch blends	2000-4000	1250-1350
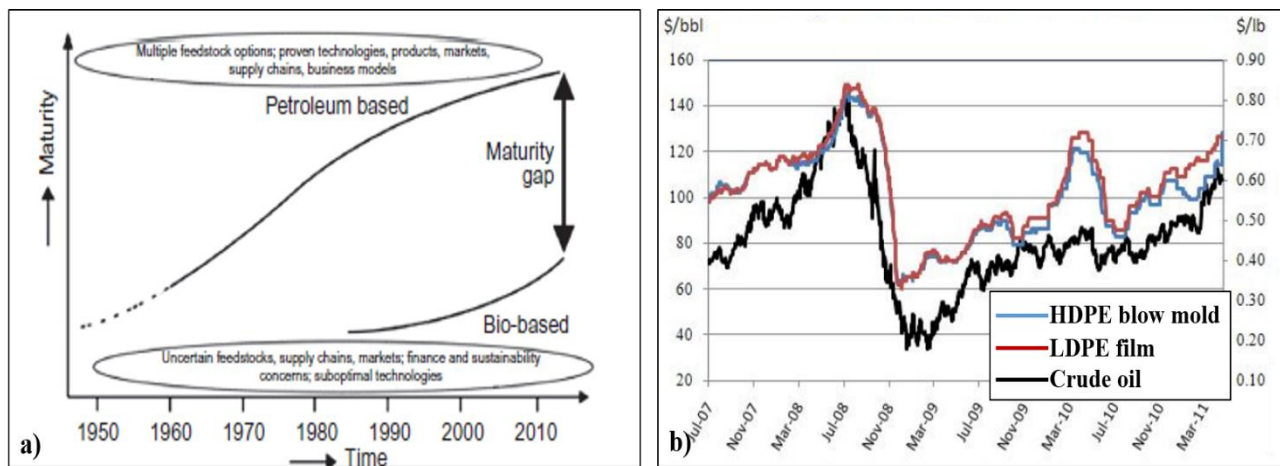
Fig.16 a) Technological knowledge maturity over time for petroleum and bio-based plastics. b) Fluctuation of the conventional plastics and crude oil prices where it is notable the same pathway. Adapted from [46, 55].

1.2.2 Biodegradable polymers

As previously mentioned, biodegradable polymers are fossil and/or bio-based polymers that can be degraded by microorganism after their lifecycle. By the way, the term "biodegradable" often generates confusion or is overlapped with other similar but different terms. Therefore, in order to be more accurate and avoid misunderstanding, the following definitions are now introduced.

- Biodegradable materials. They are materials that can be broken down by microorganism as bacteria or fungi into water, natural gases as carbon dioxide (CO_2) and/or methane (CH_4) and biomass. Biodegradability depends on environmental conditions as temperature, microorganism concentration and oxygen and water contents. Therefore, the biodegradation rate of biodegradable polymers can be different in the soil, on the soil, in surface waters, in marine waters or in human systems like home composter, industrial composer or anaerobic digesters. Clearly, biodegradation rate depends also on product itself thickness.
- Industrially compostable materials. They are materials that break down at industrial composting conditions, which are optimal in terms of temperature (55-60 °C), humidity and oxygen levels. Compared to the other common biodegradation conditions as in or on soil, in surface water and in marine water, the industrial composter ensures the best biodegradation rates. Generally, biodegradable plastics are certificated industrially compostable trough the EN13432 standard. Clearly, the product thickness affect the biodegradation rate and therefore,

it is taken into account for the certification (e.g. the existence of an industrial compostable fork do not guarantee that a thicker fork, made off the same biopolymer, could be certified too).

- Home compostable materials. They are materials that break down under domestic conditions of a home composter, where temperatures and aeration are lower than in industrial composter and not constant during the process. The biodegradation rate is slower than within industrial composter and thus, a home compostable material can be also composted industrially but and not *vice-versa*. The Belgian company Vincotte has its own test standard for home composting certification, meanwhile an EN standard is currently under developing [56] (in Italy many authors deal with UNI 11183:2006).

- Durable materials. This term is often seen as opposite to biodegradable. By the way, durability refers to the material ability to offer its performance for a long period without significant deteriorations induced by its use and aging. Thus, depending on the product and on its conditions, compostable polymers could be also labelled as durable (e.g., a PLA product at indoor conditions has a life span of 10-20 years).

Therefore, it can be said that biodegradability refers to an overall and intrinsic ability of a polymer to be degraded by microorganism under at least one environmental condition, meanwhile the terms industrially and home compostable (same principle for marine water or in/on soil compostable) are subgroups that specify the conditions under which biodegradation has been tested and certified. It has also to be specified that with the EU directive 94/62/EC of 20 December 1994, composting and anaerobic digestion have been considered as recycling forms (organic recycling). Thus, the post life fate of a biodegradable and mechanically recyclable polymer both depends on the product application itself and on the consumer decision. Generally, compostable flexible packaging (e.g. films or bags) should be discarded in organic trash or in home composter in order to prevent pollution, meanwhile mechanically recyclable and compostable thicker items (e.g. toothbrush) could be deposed both in plastic and in organic trash (Fig.17).
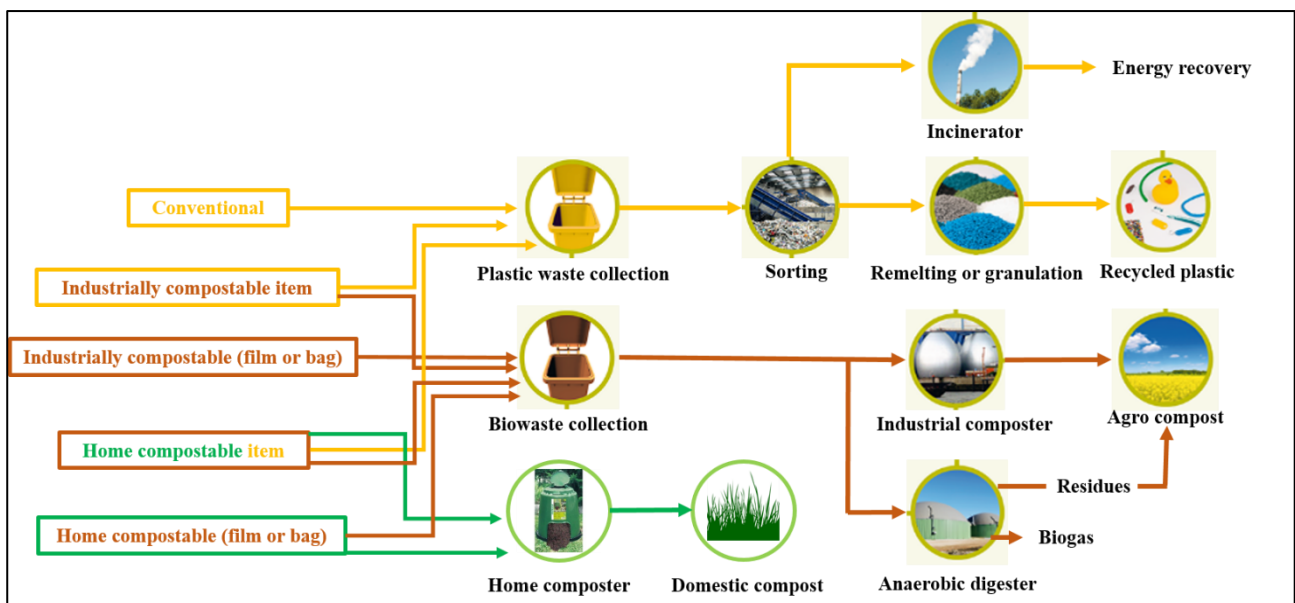
Fig.17 Discarding possibilities of conventional and industrially/home compostable plastics.

In 2018, the biodegradable polymers production has been of 0.912 Mt (less than 0.5% of the toal production) and it is predicted to reach nearly 1.3 Mt (+42.5%) in 2023 (Fig.18). Among them, PLA and PHAs are also fully bio-based, meanwhile the PBS and PBAT average biomass contents are expected to raise up to 80 and 50% in 2020 respectively, and starch is usually compounded with other polymers at 40%.
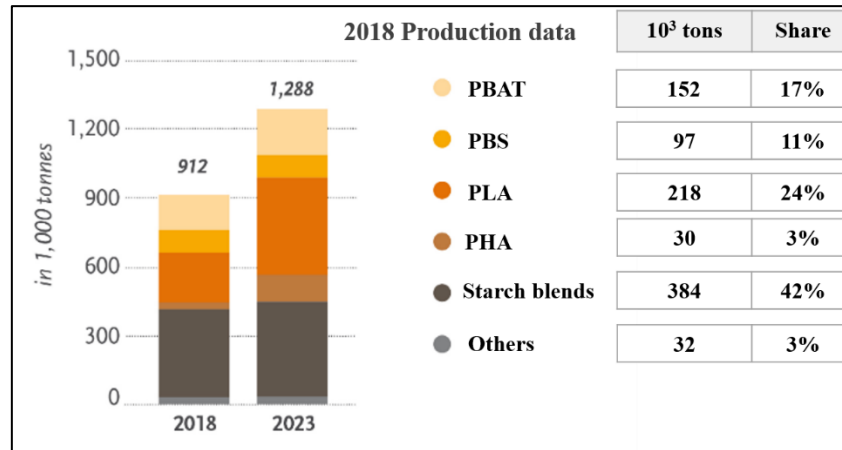
Fig. 18 Production data in 2018 and projection for 2023 of biodegradable polymers. Adapted from [45].

Therefore, being mostly bio-based or, at least, in the process of becoming bio-based, the challenges to extent biodegradable production to higher market levels are again connected with the necessity to optimize bio-refiners plants, as previously described in paragraph 1.2.1. In addition, not all applications could be suitable for biodegradable polymers. Thus, nowadays, biodegradable polymers are mainly exploited within those market segments in which biodegradability is a plus (e.g. agriculture) or in which environmental pollution want to be prevented (e.g. packaging). In Fig.19, it emerges what has been just said: rigid and flexible packaging are the market segments in which bio-based and biodegradable polymers are most used. More precisely, it could be noticed that biopolymers are more involved in packaging than conventional plastics as testified by the fact that almost the 58% of produced biopolymers has been destined to packaging meanwhile "only" a 36-40% share-ratio is recognizable when considered conventional plastics (Table 2). Similarly, biopolymers seems to be preferred also in textile and agriculture market segments in which their shares are of 11.3% and 5.7%, respectively, and are again higher than ones of conventional plastics (7.7% and 3.3%).
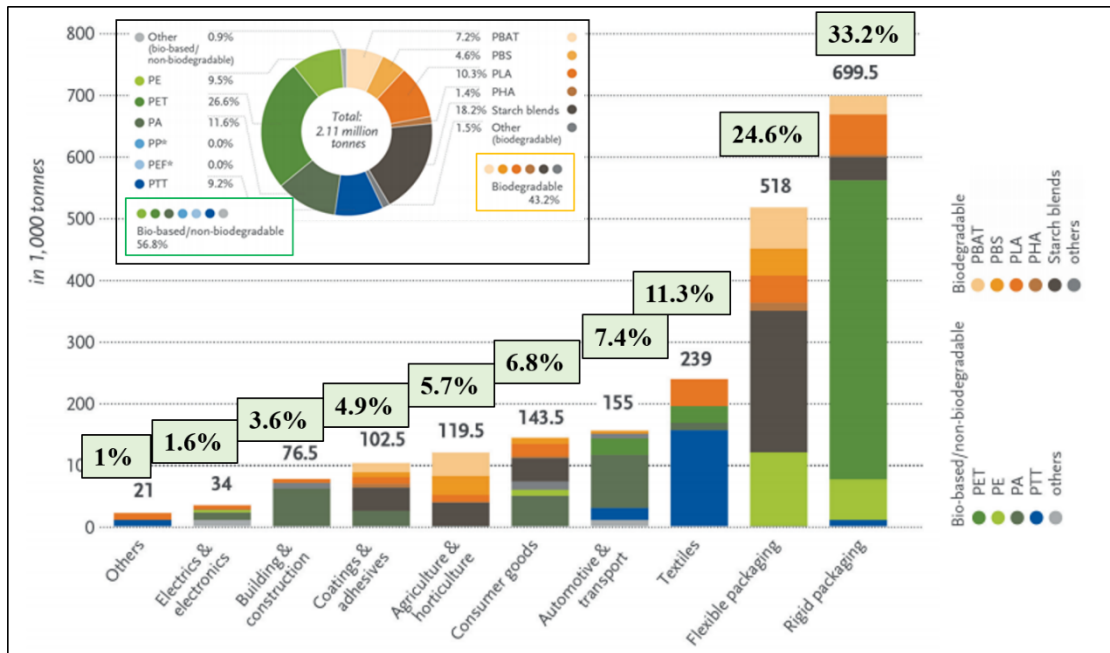
Fig.19 Biopolymers consumption data in terms of market sector, 2018. Adapted from [45].

2. STATE OF THE ART: BIO-BASED POLYMERS

Previously, bio-based polymers have been defined as polymers of which building blocks are partially or fully derived from natural and renewable sources. Going more into details, three ways to produce bio-based polymers are actually possible. As reported in Fig.20, bio-based polymers can be obtained: a) by direct extraction from biomass (e.g. polysaccharides, proteins or lipids), b) by polymerization of building blocks partially or fully derived from natural feedstocks (e.g. PLA obtained using lactic acid derived from carbohydrates fermentation) and c) by direct production of microorganism such as PHAs or Pullulan and Xanthan gum.
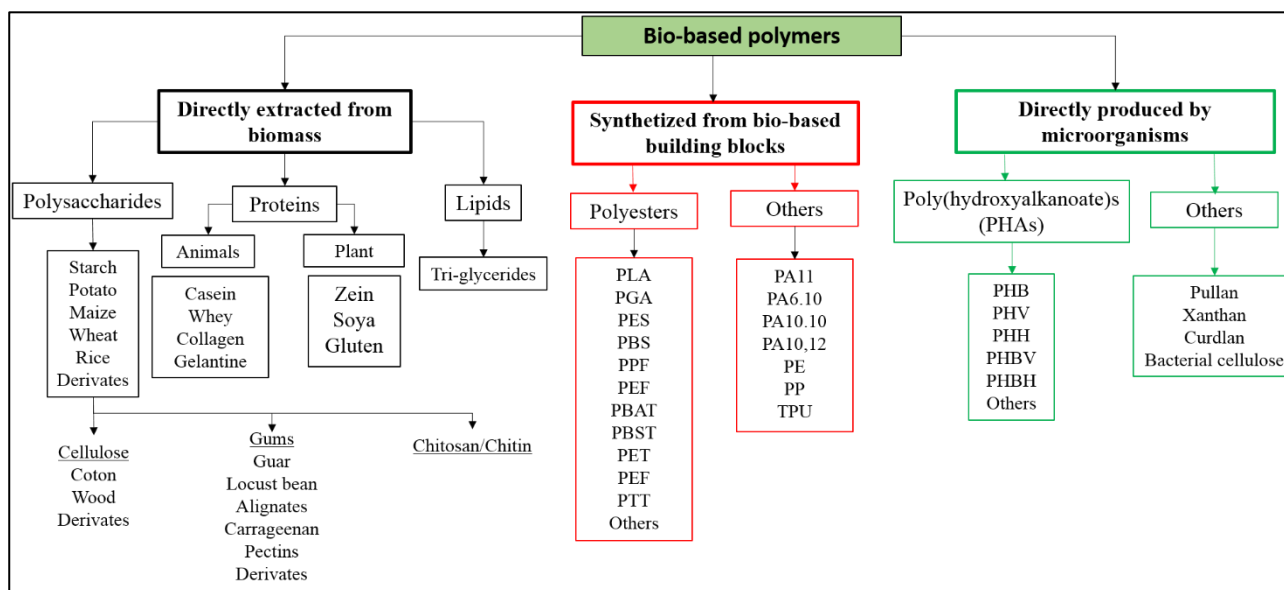
Fig. 20 Classification of bio-based polymers in terms of production approach.

From a technological and industrial point of view, bio-based polymers directly extractable from biomasses (a) are scarcely used as they are since their mechanical properties and their processability are not good enough or are not adaptable to the conventional plastics technologies. These polymers are mainly investigated as starting source for the biosynthesis of suitable bio-based building blocks or as polymer additives. On the other hand, polymers obtained using partially or fully bio-based building blocks (b), are gaining more and more importance since they are identical in terms of properties to the petrochemical polymer with the advantage to derive from renewable sources. These polymers are the most investigated both academically and industrially since bio-based compounds could be exploited also for other goals (not only polymers) in perfect agreement with the bio-refinery concepts. Similarly, despite their scaling up difficulty, polymers directly synthetized from microorganism (c) (especially PHAs), are still very attractive since they would not need further chemical transformation and they would be able to easy and eco-friendly biodegrade. Thus, in this chapter, most important bio-based polymers (b and c) will be presented, discussing their synthesis pathway and the state of art of the incoming developments.

2.1 GENERAL REMARKS

Generally, the processes to obtain polymeric building blocks from natural feedstocks involve the use of a natural renewable biomass. As previously mentioned, the raw materials generally used are starchy, sugary and oily materials (1st generation) or lignocellulosic materials (2nd generation). In the first step, each starchy, sugary or lignocellulosic material need to be treated in order to release a sugar medium suitable for the obtainment of the polymer building block. Sugary first generation crops as sugar cane and beet juices or their by-products as molasses do not need pre-treatmenst since they already release simple sugars that can be metabolized by microorganisms. In starchy materials, two different polysaccharides fractions are present: the amylose, a long linear glucose polymer with few branched chains, and the amylopectin, a short highly branched polymer of the α-glucose. To obtain glucose solutions, starchy materials are firstly liquefied by thermostable α-amylase and subsequently saccharified by α-amylase and amyl-glucosidase to avoid starch gelatinization [57]. Finally, the lignocellulosic materials are formed by long chains of glucose (cellulosic fraction) and by long chains of hexoses and pentose sugars (hemi-cellulosic fraction). In this case, pre-treatments to breakdown the lignocellulosic structure and hydrolysis reactions (acid, basic or enzymatic) to release simple sugars, are needed [58, 59]. Lignocellulosic hydrolysis can also lead to important amounts of unwanted products such as furfural, 5-hydroxymetyl furfural (5-HMF), organic acids (acetic acid), polyphenols and lignin that must be removed in order to not affect further processes as fermentation. In fact, these products are microorganism inhibitor and thus, detoxification treatments as activate charcoal, over liming, dephenolyzation and delignification are carried out on the sugar hydrolysate [60-62]. In other cases, however, sugar's by products as 5-HMF could be converted in useful products as levulinic acid [63] that could be further transformed in succinic acid [64]. Thus, biomass treatments depends on the initial raw material typology as well as on the desired final product. In Fig. 21, the synthesis routes involved for the production of important building-blocks or polymer precursor have been reported. Sugar media can be generally transformed chemically or biologically. Chemical processes regard sugar oxidation, dehydration, hydrolysis, hydrogenation and catalytic conversion, meanwhile fermentation is the main biological process. On the other hand, oily feedstocks are generally treated and converted in useful building blocks chemically.
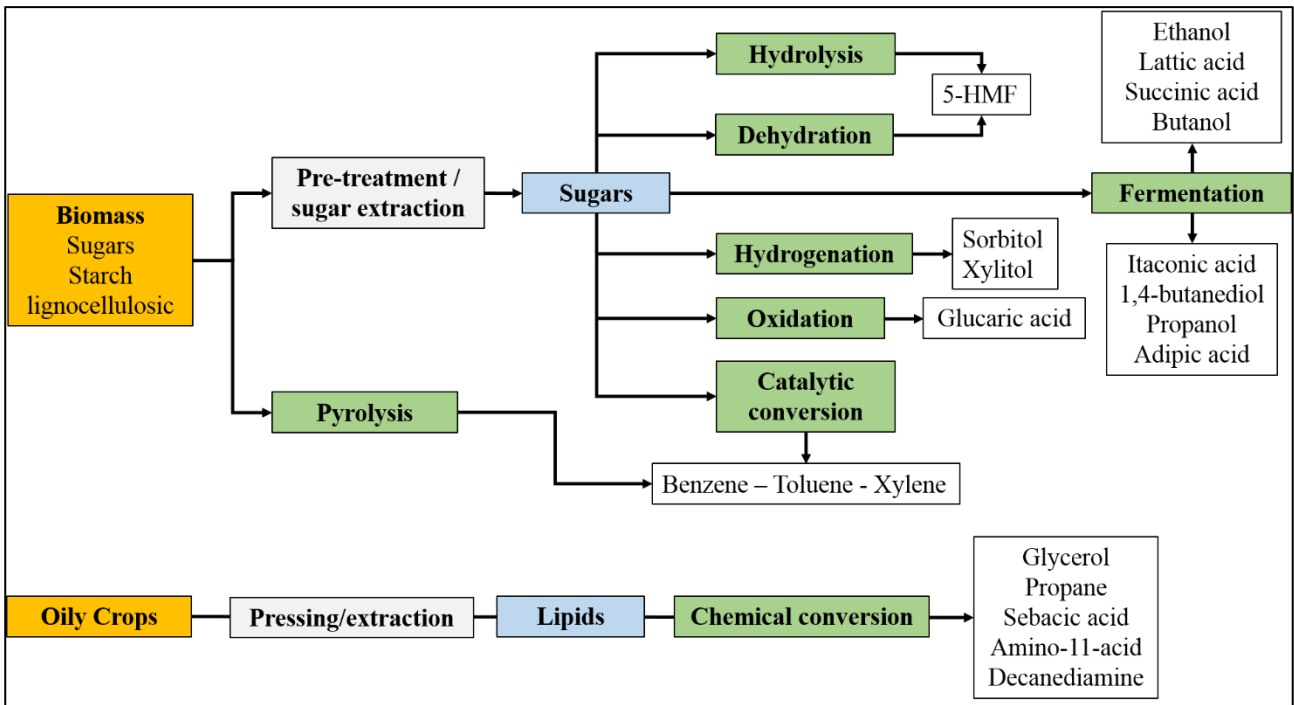
Fig.21 Biological and chemical routes to transform sugary, starchy, lignocellulosic and oily crops in useful bio-based building blocks or polymer precursor.

Finally, because most important building blocks or polymer precursor as lactic acid, ethanol, succinic acid and butanol as well as PHAs are mostly obtained through fermentation, an example of this biological process has been shown in Fig.22., where it is possible to notice that PHAs and bio-building blocks have different downstream steps (extraction, purification and concentration).
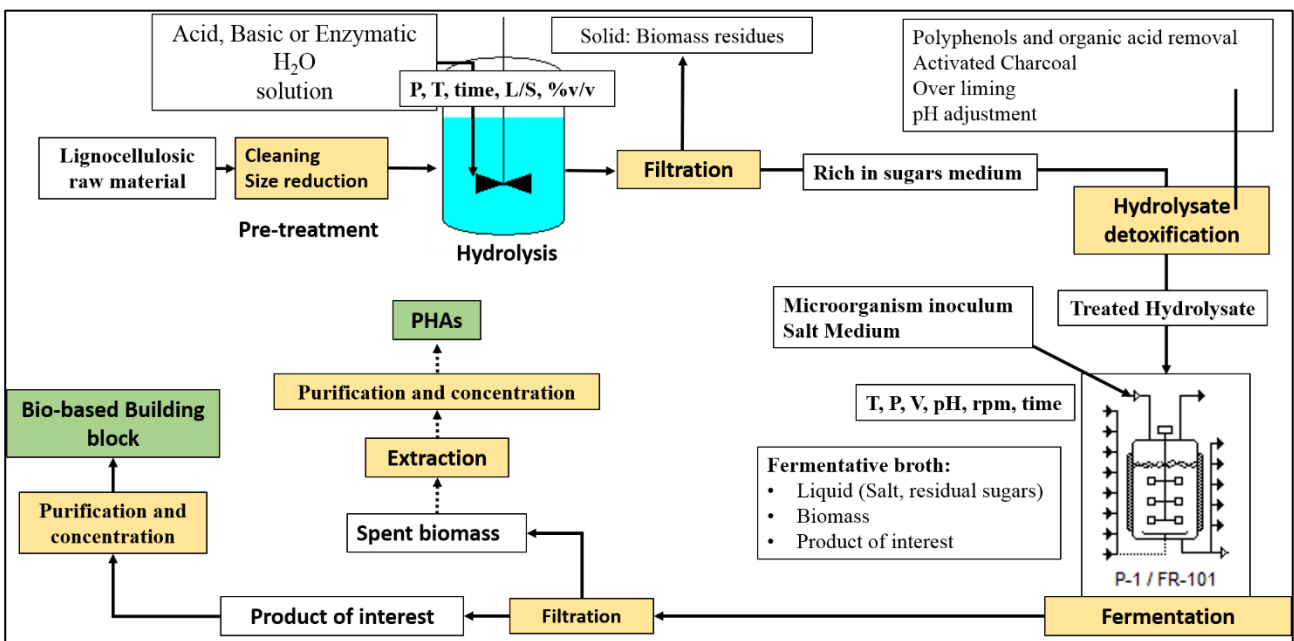
Fig.22 General processing scheme for the obtainment of bio-based building blocks using lignocellulosic raw materials.

2.2 VINYL POLYMERS

As seen in the introduction chapter, vinyl polymers (or polyolefin) represent the globally largest produced plastics. They are produced by chain-growth polymerization of alkene monomers and in the last decade, research and Industry have been more and more interested in find solution to obtain bio-based vinyl monomers. Now, the most important bio-based vinyl polymer is the bio-PE that in 2018 has reached the production of 200 kton. Bio-PE is generally obtained through the catalytic dehydration of bio-ethanol that in large-scale is derived mostly from sugar cane. Bio-ethanol is used also within the fuel market, but, because of its saturation, it is believed that the bio-ethanol fraction destined to polymer applications will increase in the next years in order to produce also other new bio-based polymers and/or chemicals. In fact, bio-based ethylene could be transformed in other several building blocks via currently applied chemical conversions. As example, bio-ethylene could be easily converted with chlorine into 1,2-dichloroethane that yield in its turn vinyl chloride (PVC monomer) by dehydrochlorination (well-known chemical process). Similarly, bio-ethanol could be converted in acetic acid [65] that, if combined with ethylene, would yield bio-poly(vinyl alcohol) (bio-PVA). In parallel, many investigations are now trying to optimize the use of lignocellulosic materials as substrate for the bio-ethanol production in order to scale-up more eco-friendly processes. Considering bio-polypropylene (bio-PP), it is possible to state it has been announced to be commercially available in 2023 [66]. Theoretically, bio-propylene could be obtained in several ways [67]:

 a) Dimerization of ethylene into 1-butene and its isomerization into 2-butene and further metathesis of ethylene and 2-butene to yield propylene. In this case, polypropylene would be entirely derived from bio-ethanol.

b) Similarly to method a), but with the obtainment of 1-butene trough *n*-butanol dehydration.

c) Fermentation of sugars to acetone and its reduction to isopropanol and further reduction to propylene [68].

d) Fermentation of sugars into isopropanol and its dehydration into propylene [68].

 e) Dehydrogenation of propane, obtained from glycerol, a bio-diesel by-products [69].

Among them, it seems that processes based on metathesis of ethylene and 2-butene (a-b) will be the most likely possibilities for large-scale productions [67]. Finally, considering the other main vinyl polymers as poly (methyl methacrylate) (PMMA), polystyrene (PS) and poly (acrylic acid)s (PAA), it can be said that despite their bio-based versions are still not the market, they are under investigation at lab and R&D scale since their theoretical feasibility (Fig.23).
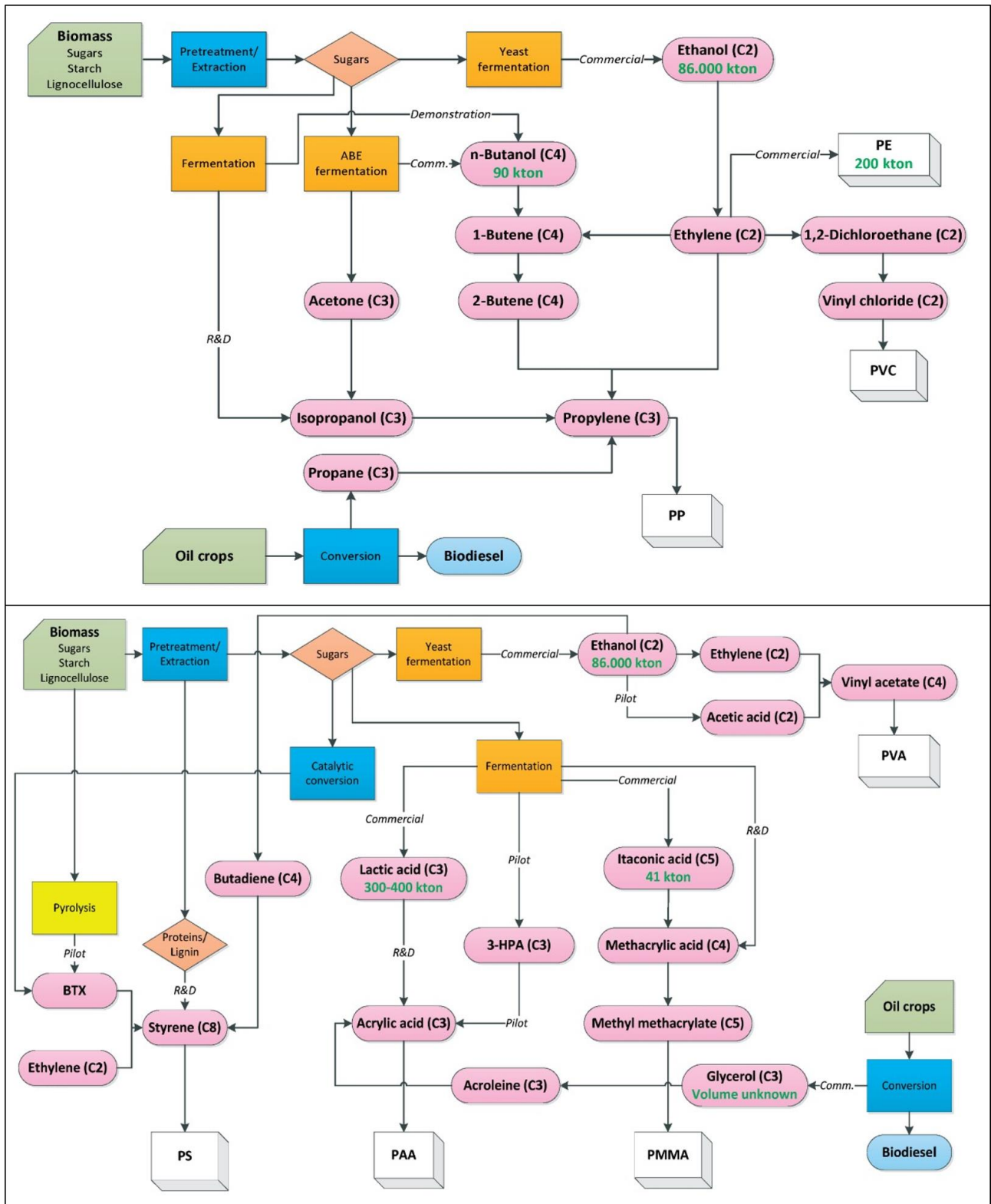
Fig.23 Commercial and possible routes for the obtainment of bio-based vinyl polymers. Taken from [67].

2.3 BIO-POLYESTERS

Polyesters represent the polymer family at which most of bio-based and/or biodegradable polymers belong. In 2018, nearly the 60-70% of produced biopolymers have been polyesters. In terms of

chemical structure, polyesters can be divided in two main sub-families: a) the poly(hydroxyl acid)s, which are aliphatic polyesters synthesized from hydroxyl-carboxylic acids and b) the poly(alkylene di-carboxylate)s, which are polyesters derived by the poly-condensation of diols and dicarboxylic acids [70]. Poly (hydroxyl acid)s can be further subdivided into three classes depending on the typology of the carboxylic acid involved, and similarly, Poly(alkylene di-carboxylate)s can be subdivided into three classes depending on the starting dicarboxylic acid (aliphatic, aromatic or their mixture) as shown in Fig. 24.
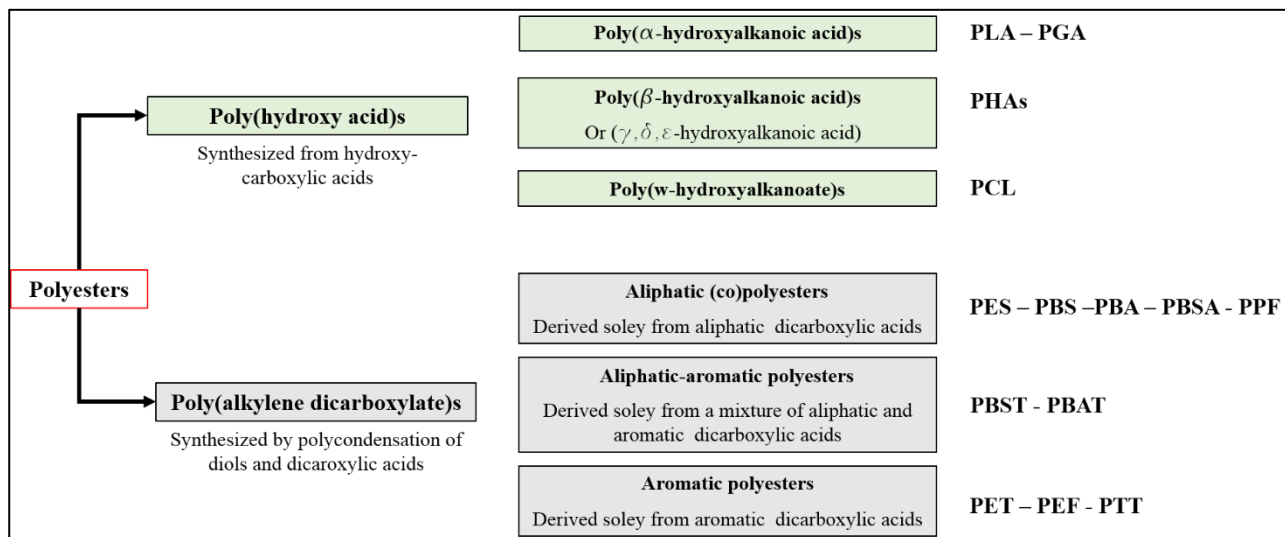
Fig. 24 Classification of bio-polyesters in terms of chemical structure.

2.3.1 Poly(lactic acid) (PLA)

Poly (lactic acid) (PLA) is one of the most investigated and produced biopolymer (218 Kt in 2018). PLA is a biodegradable linear aliphatic polyester derived from lactic acid, the simplest α-carboxylic acid. Nowadays, approximately the 90-95% of the total lactic acid is produced by bacterial fermentation of sugars and for this reason, PLA resins are today almost fully bio-based [71].
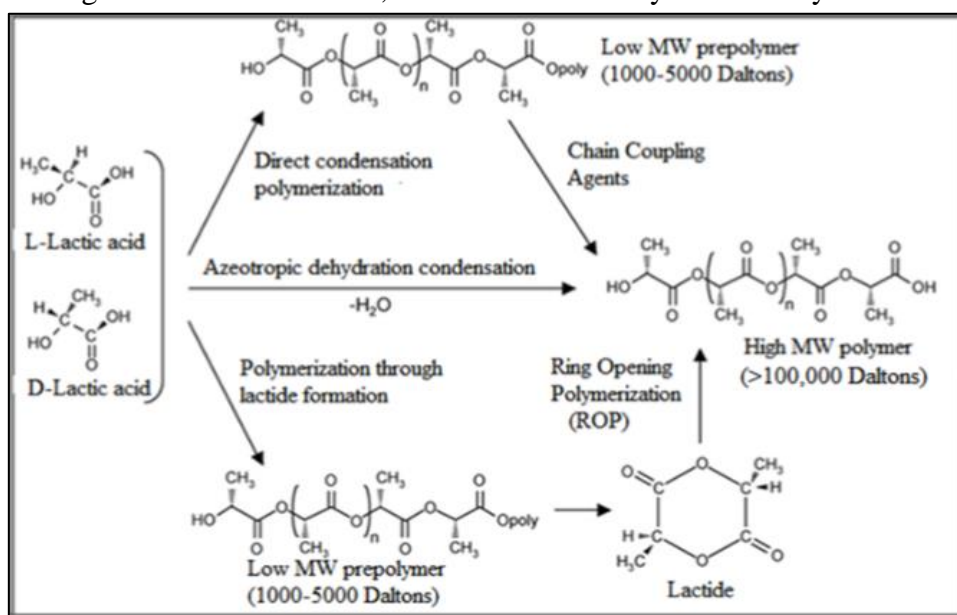
Fig.25 Synthesis methods for PLA. Adapted from [72].

38

PLA can be obtained through three different polymerization routes (Fig. 25). The direct condensation polymerization of lactic acid is scarcely present in large scale since it leads to low molecular weight PLA (M_w of 1000-5000 Da) that necessity chain coupling agents (e.g. anhydrides, epoxides and isocyanates) or esterification-promoting agents to enhance its MW, affecting significantly the processes costs and complexity. The azeotropic dehydration condensation is a method developed by Mitsui Chemicals (Japan) in which lactic acid and a catalyst are azeotropically dehydrated in a refluxing high boiling solvent under reduced pressures to obtain high chain lengths PLA. The main drawback of this method is the significant catalyst residues and impurities that remain on the final product. In large-scale PLA polymerization is generally conducted through the ring opening polymerization (ROP) of the lactide, the lactone cyclic di-ester derived from lactic acid. Lactide is obtained by the depolymeryzation of low-M_w PLA (or PLA oligomers) under reduced pressure. Successively, the ROP takes place at 140-180 °C and under the action of catalytic tin compounds leading to the production of high M_W (>100,000 Da) and pure PLA. For this reason, PLA is also known as poly(lactide)). Lactic acid exist in two different optically actives forms: *L*-lactic acid and *D*-lactic (Fig.26a), and therefore, three forms of lactide can be obtained, depending on typology of lactic acids involved in the reactions. It can exist: a) the *L*-lactide, formed by two *L*-lactic acid molecules, b) the *D*-lactide, formed by two *D*-lactic acid molecules and c) the meso-lactide (or *L,D*-lactide) formed by one *L*-lactid acid molecule and one *D*-lactid acid molecule). Finally, an equimolar mixture of *L*- and *D*-lactides can also exist, leading to the *rac*-lactide (raceme lactide). Since this chirality of the lactide monomer, the modulation of the polymer stereochemistry during the polymerization can lead to several PLA forms as: a) poly(*L*-lactic acid) (PLLA), b) poly(D-lactic acid) (PDLA) and c) poly(D,L-lactic acid) (PDLLA) (either syndiotactic and attactic), that are tremendously different in terms of mechanical properties (Fig.26b).
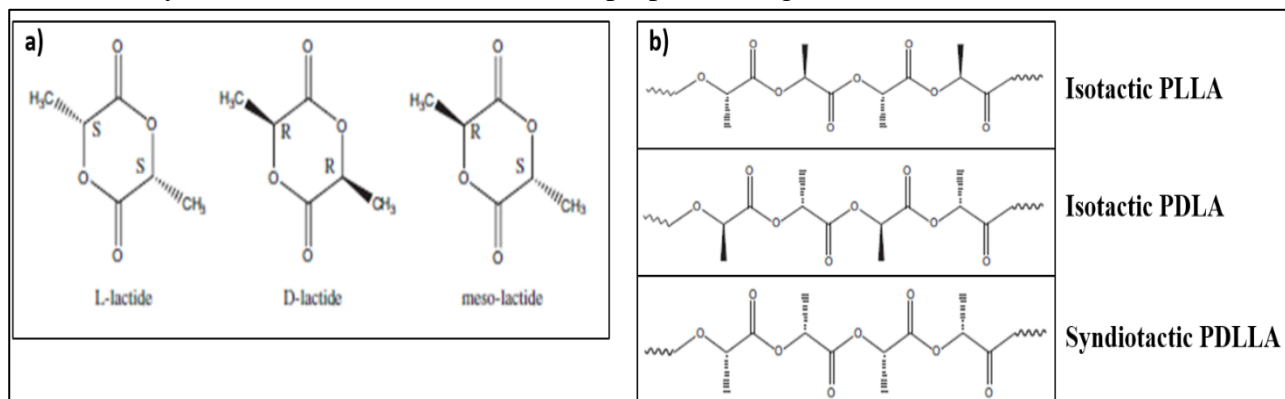
Fig.26 a) Lactide enantiomers and b) examples of different PLA structures.

As example, PLLA, the most commercialized resin, is a semi-crystalline, hard and brittle polymer with a melting temperature (T_m) of 165-185 °C and a glass transition temperature (T_g) in the 55-65 °C range, meanwhile attactic PDLLA is a completely amorphous material (T_g at 58 °C) with much lower tensile strength. Generally, the degree of crystallinity of PLA significantly depends on L-lactic acid content: PLA resins with more than 93% of L-acids are mainly semi-crystalline, meanwhile yet with 85% L- content, PLA is amorphous [73]. The difficulty on obtaining pure *L*-lactic acid trough common chemical synthesis has also favoured the bio-fermentation approach in which *L*-lactic acid can be produced more easily. In nature, L-lactic acid form is the most abundant one (e.g. mammalian organism only produce this kind of isomer since it is more easily assimilated during metabolism) and

39

many microorganism can synthetize it. Lactic acid can be produced by either hetero-fermentative microorganism or homo-fermentative microorganism; the first category lead to low yields (nearly 1.8 mol of lactic acid per mole of sugar) and many by-products as acetic acid, ethanol, glycerol and carbon dioxide are produced, meanwhile with homo-fermentative method, greater yields and lower by-products are obtained. Industrially, homo-fermentative microorganism are preferred and they mainly used belong to the *Lactobacillus* family. Most of the organisms produce the *L*-isomer such as *Lactobacilli amylophilus*, *L. bavaricus*, *L. casei*, and *L. maltaromicus* but *D*-lactic acid or an *L*- and *D*- mixture can be also obtained using *L. delbrueckii, L. jensenii, and L. acidophilus* [72, 74]. Lactic acid is currently produced in large-scale from sugar-rich and starch-rich biomass such as sugarcane and maize, but several companies are working to develop processes involving lignocellulosic raw materials. Example of lactic acid biosynthesis using different substrates have been reported in Table 5.

Table 5 Production of lactic acid using different raw materials, bacteria and fermentation strategies.

Raw material	Bacteria	Fermentation type	Lactic acid [g/L]	Yield[*] [g/g]	Proudctivity [g/Lh]	Ref.
Oak wood	*Lactobacillus RKY2*	Cell-recycle	34	0.94	6.5	[75]
Vine shoot	*Lactobacillus pentosus*	Batch	15.5	0.70	3.1	[76]
Corn cobs	*Lactobacillus casei*	Cell-recycle	34.1	0.68	3.4	[77]
Brewer'spent grain	*Lactobacillus delbrueckii UFV H2B20*	Batch	35.5	0.99	0.59	[78]
Paper sludge	*Lactobacillus rhamnosus ATCC 7469*	Batch SSF	73.0	0.97	2.9	[79]
Apple pomace	*Lactobacillus rhamnosus ATCC 9595*	Batch	32.5	0.88	5.41	[80]
Rice and wheat bran	*Lactobacillus RKY2*	Batch	129	0.95	2.9	[81]
Cassava bagasse	*Lactobacillus casei*	Batch SSF	83.8	0.96	1.40	[82]
Sugar cane juice	*Lactobacillus sp. strain FCP2*	Batch	28-104	0.93	2.8-0.9	[83]
Cane sugar molasses	*Lactobacillus delbrueckii mutant Uc-3*	Batch	129	0.96	4.30	[84]

* Yield: g of lactic acid / g of available sugar.

2.3.2 Poly(butylene succinate) (PBS)

Poly(butylene succinate) represents one of the most promising biodegradable polymer because its excellent ductility and melt processing capability that make it suitable for many fields as flexible packaging, agriculture and consumers goods. It is a semi-crystalline thermoplastic with a low melting temperature (110-120 °C), a low Young Modulus (300-800 MPa), noteworthy tensile strength values (30-40 MPa) and excellent elongation at break values (200-400%). From a structural point of view, PBS is an aliphatic polyester derived by an aliphatic dicarboxylic acids, the succinic acid, and a polyol, the 1,4-butandiol. Poly-condensation is usually carried out in two steps: firstly succinic acid and 1,4-butanediol are directly esterified forming PBS oligomers and removing water, and subsequently, PBS oligomers are trans-esterified under vacuum using suitable catalysts as titanium, zirconium, germanium and tin to obtain high molecular weight PBS polymer. Until recently, both PBS building blocks were generally obtained through several reactions starting from petrochemicals products (Fig.27a). Example may regard the oxygenation of butane to maleic anhydride that hydrated forms maleic acid that can be yielded in succinic acid through hydrogenation or the BASF's Reppe method able to convert acethylene and formaldehyde (1:2 mol/mol) into 1,4-Butynediol that, if further hydrogenated, yield 1,4-butanediol. Thus, PBS has been considered until last years as a biodegradable but not bio-based polymer. Nevertheless, nowadays, these monomers have started to be obtained also trough fermentation of agro-industrial sources and the biomass-derived content of PBS has been estimated to represent nearly the 80% in 2018 [85] (Fig. 27b).
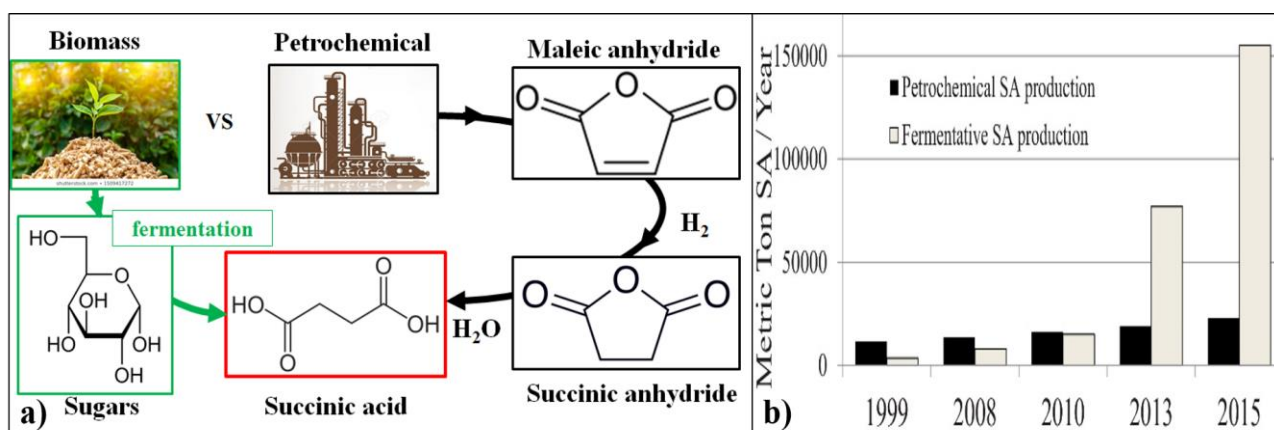
Fig.27 Biomass and petrochemical succinic acid production: a) general routes and b) production data over the last 10 years. Taken from [86].

Bio-based succinic acid is mostly produced trough the fermentation of fermentative sugars medium obtained by several feedstocks and using different microorganism such as *Escherichia coli* (genetically engineered and not), *Actinobacillus succiniproducens, Anaerobiospirillum succiniproducens* and *A. succinogenes* [86-89] (Table 6). In large-scale, bio-based succinic acid's producers are: BioAmber (CA), Myriant (US), Succinity (DE), and Reverdia (NL) [86-89]. Despite fermentative succinic acid production has a lower efficiency, if compared with petrochemical production, from an economical point of view, bio-based succinic acid is nowadays competitive with important petrochemical feedstocks such as maleic anhydride and further cost reductions could be obtained involving at the same time biomasses derived from first to third-generation [86-88]. Pinazo et al. [86], reported that succinic acid price could pass from 1.2 (only 1st generation) to 0.6 €/kg exploiting 3rd generation wastes derived from sorghum and 0.4 €/kg in the case of the sugar-beet. In

each prospective, however, final succinic acid cost seems to be much lower than using maleic anhydride (2.5 €/kg). Finally, the increasing interest in bio-based succinic acid is also explainable by the fact that this dicarboxylic acid can be involved as key-intermediate also for the production of other several chemical compounds such as solvents, adhesives, printing inks and plasticizers [90] (Fig.28).
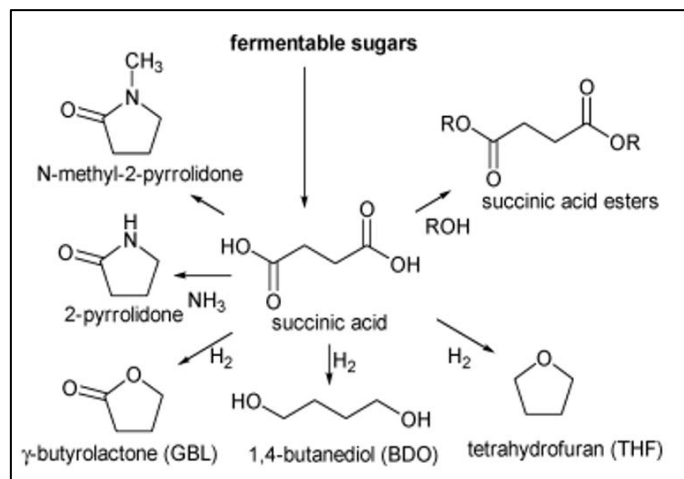
Fig.28 Bio-based succinic acid as platform of several bio-based chemicals.

In addition, succinic acid can be also converted in bio-based 1,4-butanediol, the other PBS building block (Fig.28) trough hydrogenation even if only BASF and Bioamber companies have started this kind of production. In general, nowadays, 1,4-butanediol is still almost entirely produced trough fossil carbon resources. Direct fermentation of this polyol is difficult since is a non-natural compound and metabolic pathway for its production are totally absent within living microorganisms [91]. Nevertheless, in recent years *E.coli* has been genetically engineered and it has become able to directly synthetize 1,4-butanediol using glucose as carbon source and achieving a not negligible productivity of 18 g L^{-1} [91]. This promising approach has been exploited in large-scale by Genomatica and DuPont that have started to produce approximately 2000 tons of bio-based 1,4-butanediol using conventional sugars as fermentative medium. Finally, it is noteworthy underline that bio-based production of 1,4-butanediol has also gained interest because it could be transformed in adipic acid by carboxylation [87]. Bio-based adipic acid is not still avaible in large-scale and it could be useful for the production of polyamide 6,6 (PA6,6), polyurethanes and poly(butylene adipate-*co*-terephthalate) (PBAT) [85, 87].

Table 6 Production of succinic acid using different raw materials, bacteria and fermentation strategies.

Raw material	Bacteria	Fermentation type	Succinic acid [g/L]	Yield* [g/g]	Proudctivity [g/Lh]	Ref
Glucose	*M.succiniciproducens*	Fed-batch	52.4	0.76	1.8	[92]
Glycerol	*B.succiniciproducens*	Batch	8.4	1.2	0.9	[93]
Glucose	*E.Coli*	Batch SSF	99.2	1.1	1.3	[94]
Cassava starch	*E.Coli*	Batch SSF	127	0.86	3.23	[95]

Whey and corn liquor	*M.succiniciproducens*	Batch	13.4	0.71	1.18	[96]
Bread waste	*A. succinogenes*	Batch	47.3	0.55	1.12	[97]
Bakery waste	*A. succinogenes*	Batch	31.7	0.35	0.87	[98]
Coffee husk	*A. succinogenes*	Batch	19.3	0.95	0.54	[99]
Sorghum bagasse	*A. succinogenes*	Batch	17.8	0.61	-	[100]
Potato waste	*E.Coli (engineered)*	Batch	18.65	0.94	-	[101]
Corn stover	*B.succiniciproducens*	Batch SSF	30	0.69	0.43	[102]

* Yield: g of succinic acid/ g of available sugars.

2.3.3 Poly (butylene adipate-*co*-terephthalate) (PBAT)

Poly(butylene adipate-*co*-terephthalate) (PBAT), is a biodegradable semi-aromatic random copolymer obtained by the random copolymerization of three different building blocks: 1,4-butanediol (BDO) , adipic acid (AA) and terephthalic acid (TPA). In particular, aliphatic unit is obtained using BDO and AA acid, meanwhile the aromatic unit is synthesized using BDO and TPA, and aliphatic and aromatic units are subsequently copolymerized by transesterification in presence of a titanium catalyst. In terms of structure (Fig.29), PBAT is a random copolymer and thus it is generally scarcely crystalline and/or with a wide melting point [103]. Because of its high ductility, toughness, biodegradability and its poor mechanical properties (low elastic modulus and stiffness), it is general used as film in flexible packaging and in agriculture. Nowadays, PBAT is mostly fossil-based, but theoretically, it could arrive up to 50% bio-based contents in next years since bio-based AA is not available yet in large scale being still at the research stage [85], meanwhile it is believed that BDO (as seen previously for the PBS) and TPA (as further shown) will be soon available. For this reason, PBAT is generally compounded with starch [104] in order to increase the overall bio-based content without altering the PBAT main properties.
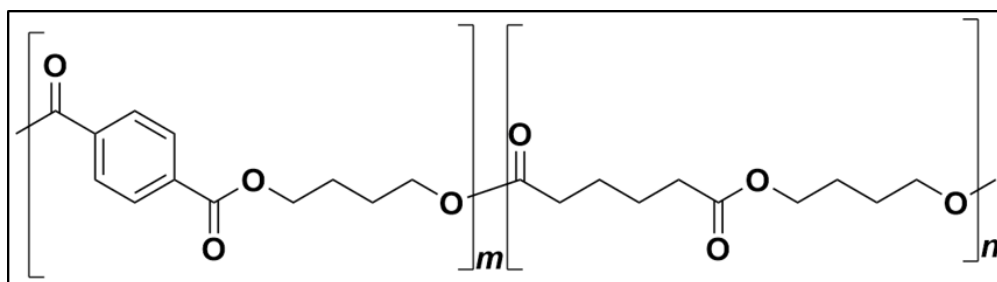
Fig.29 PBAT structure.

2.3.4 Bio-Poly(ethylene terephthalate) (bio-PET)

Bio-Poly(ethylene terephthalate) (bio-PET) has been the most produced bio-based (and biopolymer) in 2018. It is a non-biodegradable aromatic polyester obtained from ethylene glycol (EG) and terephthalic acid (TPA). Coca Cola® disclosed such bio-based PET in 2009 (WO2009120457 A2)

claiming the formulations comprising 25-75%wt. of TPA, 20-50%wt. of EG, wherein at least 1%wt. (preferably 10%wt.) of the EG and/or TPA component was derived from a bio-based material such as corn and potato [105]. Recently, Coca-Cola has developed a renewable bottle, the PlantBottle ™, converting the sugarcane into EG which represented the 30wt% of the PET composition [106]. Traditionally, EG is obtained by petroleum sources, through the ethylene oxidation by water addition (Fig.30a). Since bio-ethanol is easily obtainable by natural feedstocks and it can be converted in ethylene trough catalytic dehydration, many companies have tried to oxide this bio-ethylene to obtain bio-EG. Even if this method would be technically feasible, today it is not still much sustainable in terms of yields. Therefore, other more efficient strategies to obtain bio-EG are under investigation. In last decade, because of the huge increase of biodiesel production, glycerol has become very attractive as feedstock for the EG production. In fact, glycerol can be transformed in EG, 1,2- and 1,3-propylene trough catalytic hydrogenolysis [107] (Fig.30b). Similarly, other promising methods are based on the catalytic hydrogenolysis of bio-based hydrogenated sugars such as xylitol [108, 109] and sorbitol[110]. Nevertheless, these processes are not yet available in large scale and thus, the oxidation of the petrochemical ethylene still represents the most widely used process.
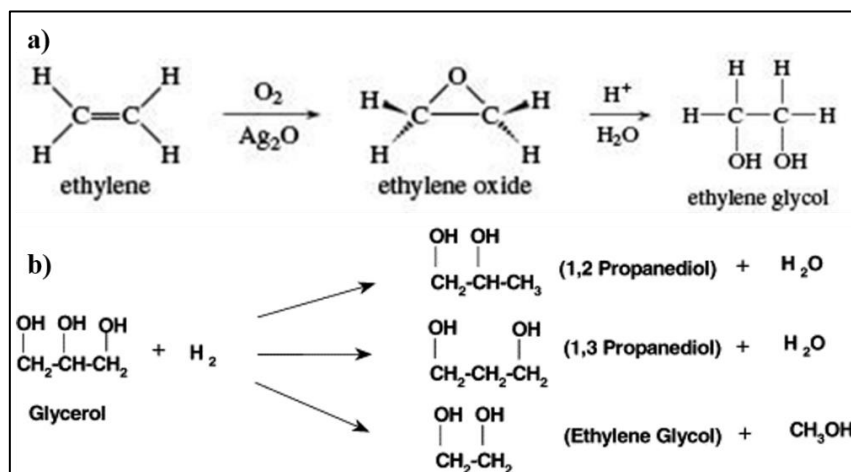
Fig.30 a) Ethylene oxidation and b) glycerol catalytic hydrogenolysis

From another hand, the derivation of TPA from nature has been much more difficult. Industrially, TPA is mainly obtained through catalytic oxidation of petrochemical *p*-xylene and thus, several routes to obtain bio-based *p*-xylene have been investigated. Briefly, bio-based *p*-xylene can be obtained by the pyrolysis of biomass, the yeast fermentation of sugars into isobutanol and by the chemical conversion of carbohydrates [87, 111]. In large-scale, in 2011, the Japanese company Toray announced the production of the first fully renewable bio-based PET made from *p*-xylene obtained by Gevo (USA) through the conversion of cornstarch sugars into butanol that, after subsequent chemical reactions, was transformed in streams of aromatics compounds containing more than 90% of *p*-xylene [106]. Finally, interesting and promising lab-scale researches are now trying to obtain TPA using as intermediate the furfural which is industrially obtained from inedible cellulosic biomass by the cycloaddition of acrylic acid and isoprene (both bio-based) and by the isolation of xylenes from lignin [112] . Main routes of TPA production have been shown in Fig.31.
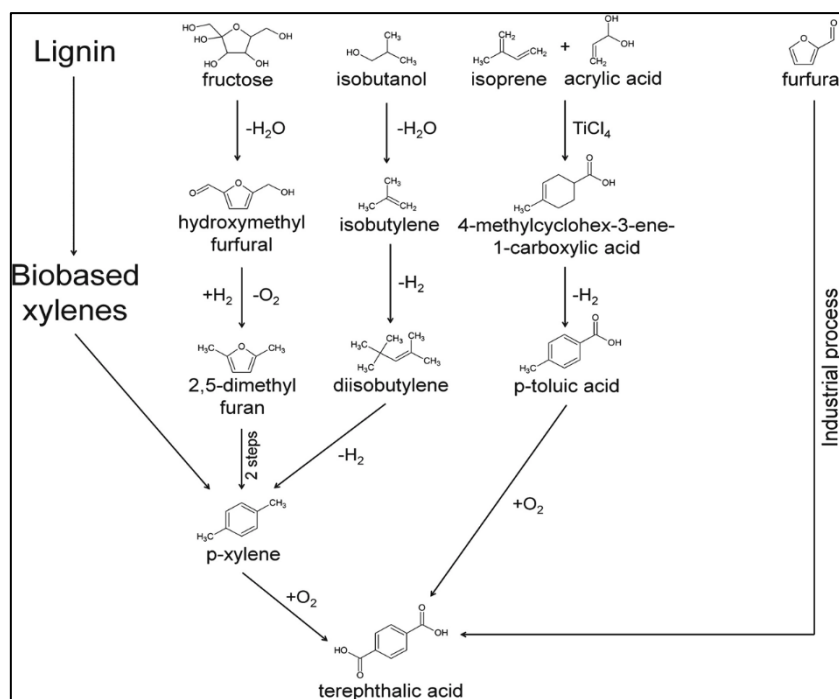
Fig.31 Different routes for the TPA obtainment. Taken from [87].

2.3.5 Poly(hydroxyl alkanoates)s (PHA)s

Poly (3-hdroxyalkanoate)s, (PHA)s, belong to a family of fully biodegradable polyesters that generally consist of 3-, 4-, 5- and 6- hydroxyl-carboxylic acids. PHAs are usually accumulated by bacterial fermentation [113] or, less often, by transgenic microorganism [114] and plants [115] in intracellular granulates as carbon and energy reserves when nutrient supplies are imbalanced. PHAs are very interesting biopolymer because of their renewability, biodegradability, biocompatibility and extreme versatility. The versatility of PHAs depends on the PHAs constituent monomer and on the carbon numbers. Depending on synthesis pathway, processing conditions, used substrate and bacterial culture more than 150 kinds of hydroxyl-carboxylic acids may be obtained as PHAs monomers [116] and carbon number may vary from 3 to 16 (Fig. 32). This aspect gives PHAs an extended spectrum of associated properties, which may make PHAs similar both to thermoplastics poly-olefins (short-chain length, *scl*-PHAs, 3-5 carbon units) and to elastomers and adhesives (medium-chain length, *mcl*-PHAs, 6-14 carbon units) [117]. For these reasons, it is believed that PHAs could be able to replace the 33% of common commercial petroleum polymers [118, 119].

R	n=1	n=2	n=3
H	Poly(3-hydroxypropionate) (PHP)	Poly(4-hydroxybutirrate) (P4HB)	Poly(5-hydroxyvalerate) (P5HV)
CH_3	Poly(3-hydroxybutirrate) (PHB)	Poly(4-hydroxyvalerate) (P4HV)	Poly(4-hydroxyhexanoate) (P5HH)
C_2H_5	Poly(3-hydroxyvalerate) (PHV)		
C_3H_7	Poly(3-hydroxyhexanoate) (PHH)		
C_5H_{11}	Poly(3-hydroxyoctanoate) (PHO)		
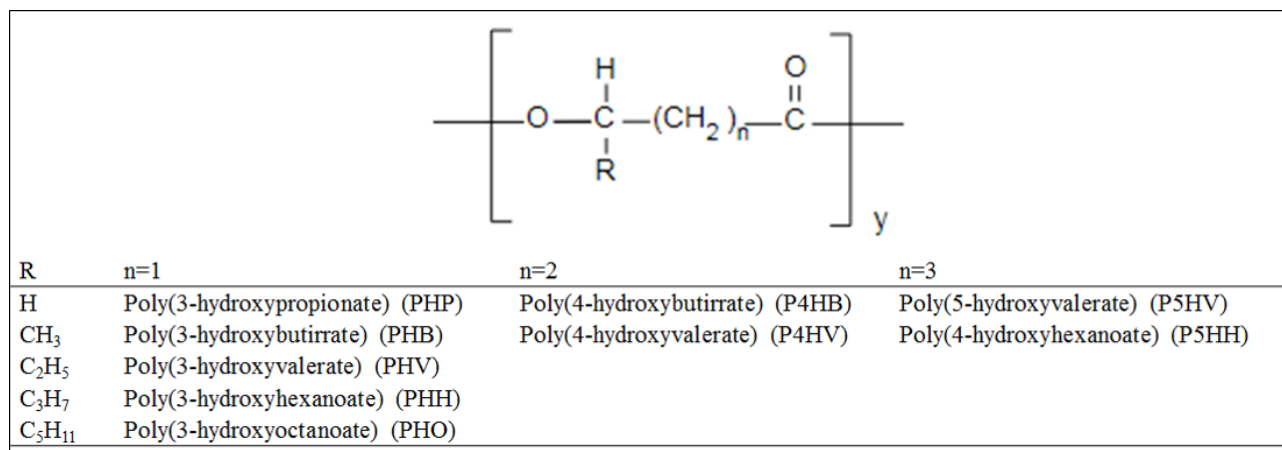
Fig.32 PHAs general structure and most important PHAs polymers.

Among all PHAs family, poly(3-hydroxybutirrate) (PHB) is certainly the most investigated polymer. PHB was discovered in 1920's inside bacteria's nucleus [120] and despite its promising properties (fair mechanical properties, excellent biodegradation and good biocompatibility), it nowadays covers only limited marked portions. This can be explained by the three main PHB drawbacks that are: i) its brittleness, ii) its bad processability and iii) its high cost that is generally 3-5 times higher than on of classical petroleum polymers [121]. PHB is a brittle material since it is characterized by high amounts of crystalline domains that involve poor elongation at breaks values and scarce impact resistances. The PHB narrow processing window is caused by the fact that PHB melting and degradation temperatures are very close and thus, degradative mechanisms often affect final PHB properties. The first two problems (brittleness and scarce processability) are often solved copolymerizing PHB with 5-20% of poly(3-hydroxyvalerate) (PHV) or poly(3-xydroxyexanoate) (PHH) yielding PHBV and PHBH copolymers, respectively. In fact, both PHV and PHH polymers are characterized by lower melting temperatures (145-150 °C vs 175 ° of PHB) and by less crystalline domains (40-50% vs 70-80% of PHB) that partially solve the above mentioned PHB problems. On the other hand, to decrease the PHB cost, three crucial aspects need to be investigated. Firstly, it is needed to intervene on the PHB downstream processes represented by PHB recovery and purification steps [122] . Until recently, PHB extraction has been generally conducted using chloroform but this method is now in process to be abandoned since the solvent is toxic, not-ecofriendly and expensive from an energetic point of view (it need to boil) [123]. The most promising and adopted alternatives of PHB recovery are the mechanical cell disruption, the chemical or enzymatic non-PHB cell mass digestion and, when possible, osmotic extractions [124]. In parallel, new techniques based on the utilization of green solvents such as lactic acid esters [125] or of solvents derived by the same biopolymer fermentative plant, are under investigation. According to the last mentioned technique, it is useful report that the Brazilian company PHBISA obtains PHB from sugar cane using the iso-pentanol (also obtained by sugar cane) as PHB extractive solvents, integrating bio-fuels and biopolymers in order to respect circular economic principles and to decrease downstream costs [123, 126]. Secondly, to decrease the PHB costs, also fermentative processes should be optimized and deeper studied. Until recently, most PHB synthesis have been conducted under discontinues conditions (batch bioreactors). Nevertheless, it is recognized that different apparatuses such as cell-recycle or continuous fermenters could lead to better PHB yields and to decrease the overall processing costs [127]. One of the most promising

configuration is represented by the utilization of multi-stage bioreactor cascades [128]. Following this approach, several (from 2 to 5) bioreactors are disposed in series in order to simulate tubular continuous reactors conditions, and to optimize each PHB production phase. Thus, the microorganism growth is conducted within the first reactor under ideal cultivation conditions, meanwhile within the following others reactors, PHB accumulation is carried out and optimized (Fig.33) in accordance with PHB production kinetics (linear increase of PHB concentration). This approach (5-SCR), as observable in Table 7, can lead to significant improvements of the PHB yields and productivities, if compared with other fermentation systems.
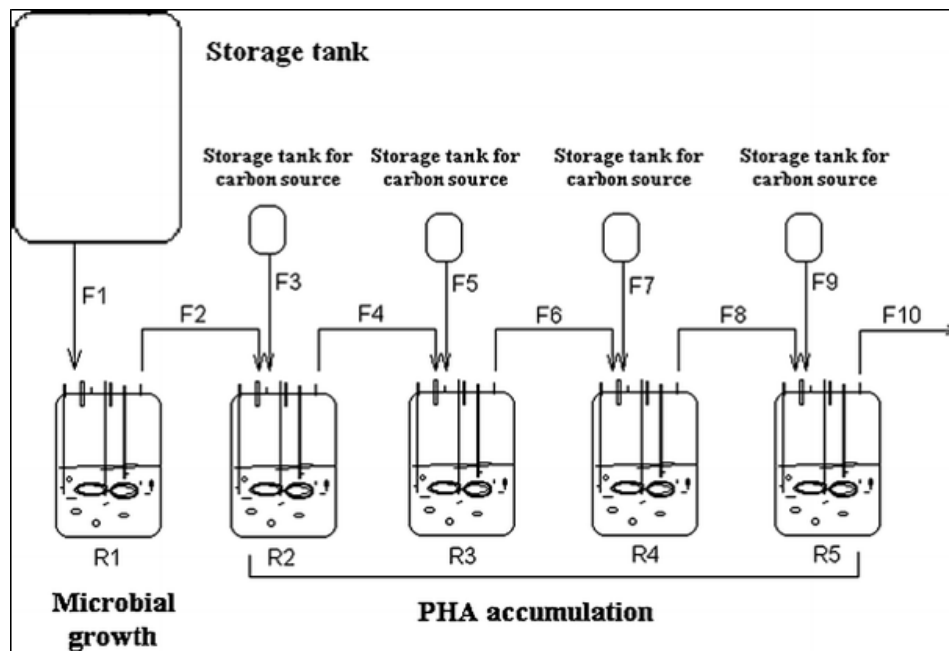
Fig.33 Five stage continuous reactor (5-SCR) system for PHAs production. Taken from [128].

Finally, another way to decrease the PHB price is represented by the utilization of inexpensive and non-food competitive raw materials for the obtainment of the sugar medium [129]. In fact, the exploited substrate plays a cost-effective key role since it affects up to the 38-50% the final PHB costs [130-132]. Thus, lignocellulosic agro-industrial materials are being massively investigated as potential PHB substrate because they are abundant, cheap and not in competition with the human food chain. By the way, their use in large-scale is still a challenge for several factors such as the necessity of pre-treatments as hydrolysis and the variability of the raw material components from year to year [130, 133]. In Table 7, some PHB results obtained using different substrates as well as different fermentative systems have been reported.

Table 7 PHB synthesis using different substrates and fermentation systems.

Raw material	Bacteria	Fermentation type	PHB [g/L]	Yield* [g/g]	Proudctivity [g/Lh]	Ref
Glucose	*C.necator*	Fed-batch	70	0.68	1.44	[134]
Glucose	*C.necator*	2-SCR	31	0.72	1.23	[135]
Glucose	*C.necator*	5-SCR	63	0.77	1.85	[127]

Wheat straw	*B. sacchari*	Fed-batch	105	0.72	1.6	[136]
Sugar cane bagasse	*B. sacchari*	Batch	36	0.60	0.47	[137]
Coffee ground	*B. cepeacia*	Batch	2.7	0.55	-	[138]
Oil palm fruit brunch	*B.magaterium*	Batch	12.5	0.52	0.26	[138]
Potato waste	*H.boliviensis*	Batch	4.0	0.50	0.1	[139]

* Yield= g of PHB/ g of biomass cell dried weight (CDW)

2.4 POLYAMIDES

Polyamides (PA) are polymers of which main chain is formed by amide groups (R-CO-NH-R') and they can be fully, partially and not bio-based. Bio-based PA are generally formed by poly-condensation of a) diamines and dicarboxylic acids (e.g. PA10,10 - PA4,10 – PA6,10), b) ω-amino carboxylic acids bi-functional monomers (e.g. PA11) and c) α-amino carboxylic acids bi-functional monomers as poly(glutamic acid) (γ-PGA) and poly(L-lysine) (ε-PL). In addition, it useful mention that non bio-based PA, as PA6 and PA12 are generally produced by ring-opening polymerization (ROP) of caprolactam and laurolactam, respectively. In Fig.34, most important polyamides have been shown evidencing the origin of their building block.
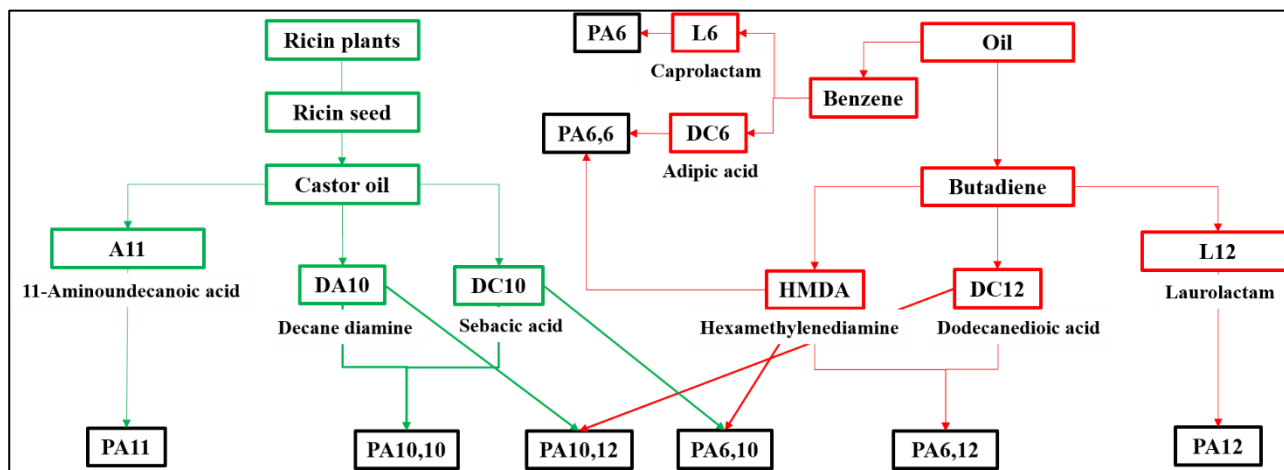
Fig.34 Main PA polymers and their building block origin. Green and red indicate bio-based and petrochemicals routes, respectively.

From an industrial point of view, nowadays, fully bio-based PA11 (10-20 kton/year) and PA10,10 as well as partially bio-based PA6,10 - PA4,10 and PA10,12 are commercially available in the market meanwhile fully bio-based PA6,6 are in pilot-plant production and bio-based processes for caprolactam (monomer of PA6) are at R&D stage [67]. Decanediamine (DA10), sebacic acid (DC10) and 11-aminoundecanoic acid (A11) are all derived from castor oil [140] that, its turn is extracted from the *Ricinus Communis* [141], a plant that mainly grows in India, Brazil and China. The plant

seeds contain nearly 50%wt of castor oil, a unique triacglycerol that is composed of 85-90% by ricinoleic acid, an unsaturated fatty acid with one hydroxyl group, that after several chemical processes is transformed in suitable PA building blocks [142]. In Fig.35 reaction scheme for the obtainment of PA11 have been shown.
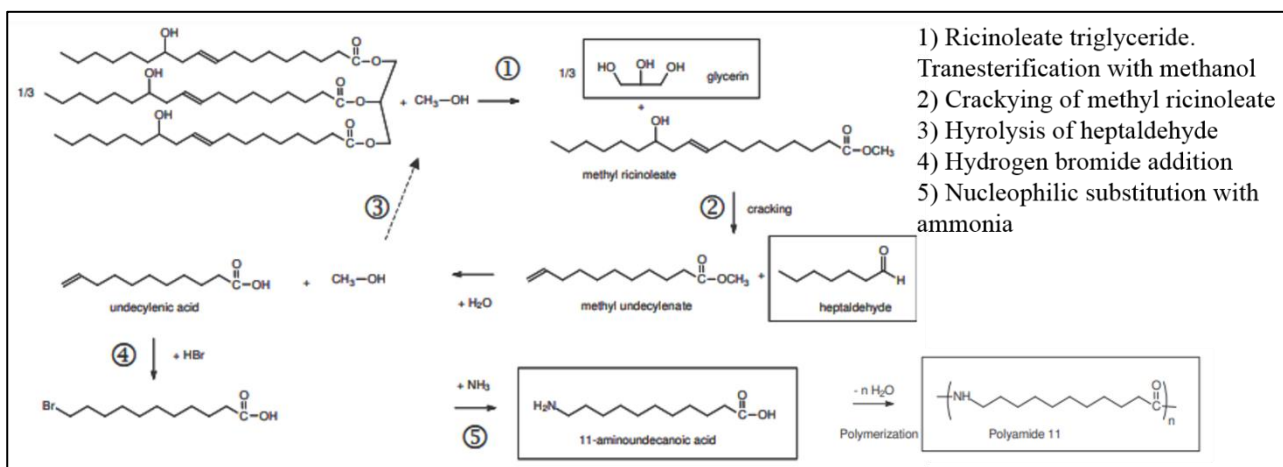
Fig.35 Reaction scheme of PA11. Taken and adapted from [142].

3. STATE OF ART: BIOCOMPOSITES

Biocomposites are material of great importance because able to provide unique properties that do not exist naturally. Their properties can be tailored depending on selective design composition, processing and final application. Thus, biocomposites can find place in different sectors such as aerospace, automotive, building and construction, human goods and so on. Polymer composite science is an age-old study that dates back to 1910' when glass fibers where firstly exploited within synthetic plastics [143]. Similarly, bio-fibers where firstly introduced in 1941, when Henry Ford introduced biocomposites using hemp, sisal and cellulose as natural reinforcing fillers [144]. Since then, lot of research has been dedicated to biocomoposites both industrially and academically. The number of publications concerning biofiller and/or biocomposites has passed from 50, in 2005, to 250 in 2013, meanwhile in the United States, the amount of involved fillers has increased from 525 kton (1967) to 2 million ton (Mt) in 1998 and to 3.9 Mt in 2010 [145]. Biocomposites materials consist of two or more distinct components that once joined produce a new material with very different properties from those of the individual components. Generally, with the term polymer biocomposite are intended all composites formed by a) natural fillers/fibers (NF) within a polymer/or biopolymer matrix and/or b) synthetic fillers within a biopolymer matrix. From an ecological point of view, NF included within biopolymers represent the greenest solution, but anyway, the use of NF within synthetic polymers is also important from an industrial point of view because the high production volumes of the conventional polymers. Finally, the use of synthetic fillers within bio-based or biodegradable polymers seems the less attractive solution because it would damage the intrinsic eco-friendly properties of the bioplastics. NF-reinforced materials present several and significant environmental advantages such as reduced dependency on non-renewable sources, reduced consumption of fossil energy, lower pollutant emissions and lower processing costs. Moreover, if compared with synthetic fillers, NF present also higher toughness, lower densities, reduced tool wear (less abrasive to processing equipment [146]), CO_2 neutrality (when burned) and biodegradability [147, 148]. Therefore, NF represent an eco-friendly and cost-advantage alternative to the conventional reinforcing fibers such as glass and carbon that require important energetic contributes and their cost is not negligible (1.2-1.8 €/kg and 30 GJ/ton for glass fibers and 12.5-15 €/kg and 130 GJ/ton for carbon fibers [149]). Thus, the aim of this chapter is to show the main aspects, properties and effects regarding the utilization of NF within thermoplastic polymers.

3.1 NATURAL FILLERS/FIBERS CLASSIFICATION

3.1.1 Shape classification

Natural fillers/fibers (NF) can be generally classified in basis to their source and origin and in basis to their shape and dimensions. Firstly, in order to avoid misunderstanding between the terms fillers and fibers is necessary to show their difference starting with the NF classification based on the shape dimensions. These terms are often used as synonyms in literature and their difference is rarely reported within the biocomposites reviews. Generally, fibers are intended as parallelepiped/cylinder shape elements characterized by important L/D aspect ratio (100-1000) that can be classified as short (2-6 mm) and long (12-25 mm) fibers. Generally, short-fibers (or whiskers) can be either all oriented along one direction or randomly oriented within the polymer matrix (Fig.37). In the first case, composite material would tend to be markedly anisotropic (orthotropic) meanwhile in the second

case, it could be regarded as a quasi-isotropic composite [150]. Long fibers are able to reinforce the polymer matrix in the most efficient way in terms of stiffness and strength since they can be disposed continuously and in parallel among several direction, or oriented at right angles to each other (crossply or woven fabrication) [150]. On the other hand, with the filler term is intended a group of particles characterized by various size and shape where no significant L/D aspect ratio are detectable (Fig.36). Filler's shape can be a sphere, a cube, a block or a flake but in each case, the mean size diameter is reported as the equivalent spherical diameter (EDS). In general, fillers are randomly dispersed within the polymer matrix and thus, filled-composites can be regarded as quasi-homogeneous and quasi-isotropic materials [150]. From an overall point of view, it can be stated that short-fiber and fillers are mainly applied within thermoplastics polymers by the means of processing apparatuses such as twin-screw extruders and injection moulding machines, meanwhile long-fibers are preferred to be processed within thermosets by compression moulding.

Finally, it is useful remind that also the mean particle size affects the final properties of the polymer composites and when one or more particle dimension is under 100 nm (nano-filler or nano-fiber), mechanical properties of the composite are significantly enhanced [151].
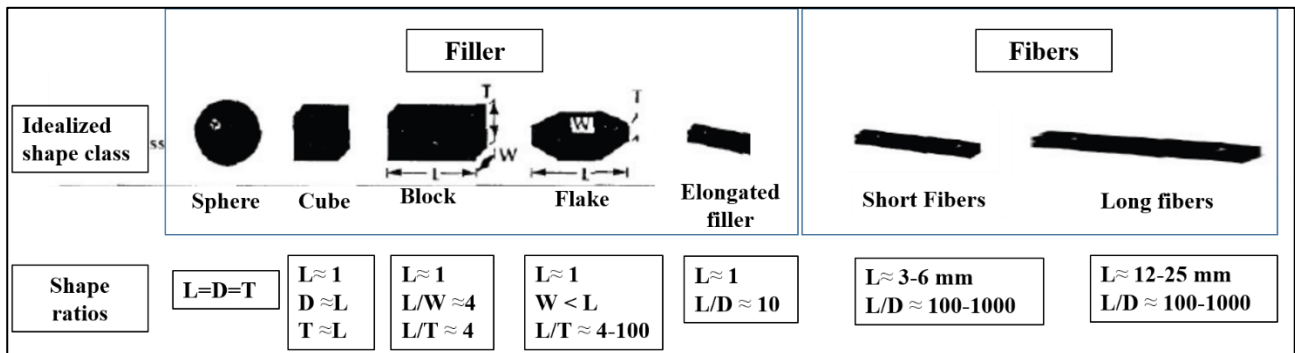
Fig.36 Shape ratios and shape classes of fillers and fibers.
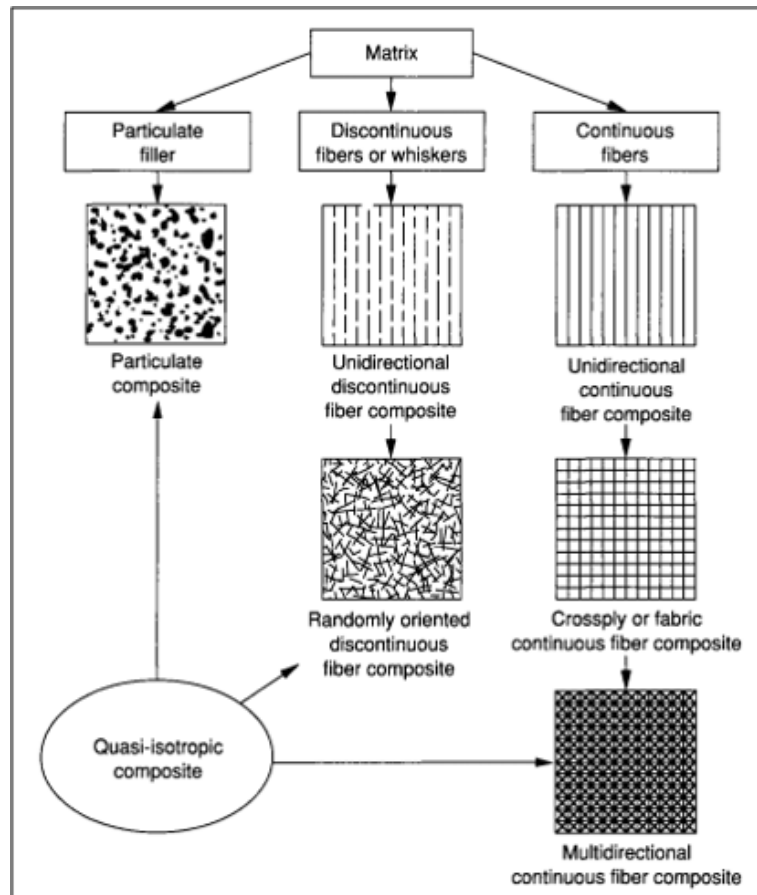
Fig.37 Example of polymer composites structures using fillers and short and long fibers. Taken from [150].

3.1.2 Origin classification

Apart from their shape and dimensions, natural fillers/fibers (NF) can be classified on the basis of their origins. In Fig.38, a diagram with a detailed NF classification has been reported. Briefly, it can be noticed that fillers/fibers can be divided as natural, synthetic and lignocellulosic. Indeed, these latter fillers are natural too, but because of their huge presence and massive investigation, they are generally shown separately from the other natural fillers.
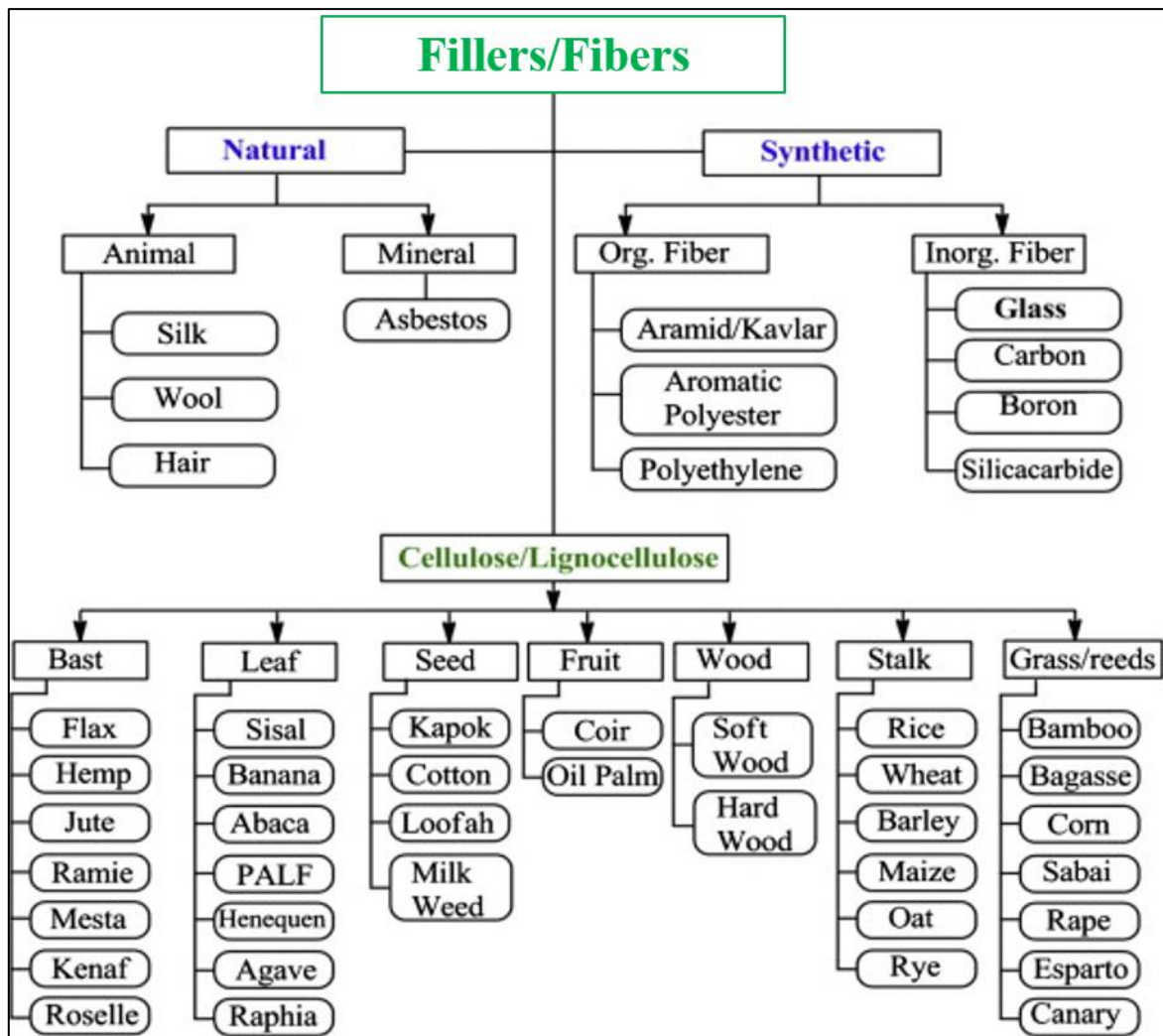
Fig.38 Classification of natural, synthetic and lignocellulosic fibers/fillers. Taken from [152].

Main difference between plant and animal fillers/fibers is that the first one are composed by lignocellulosic materials meanwhile animal fibers are mostly formed by protein compounds (hair, silk and wool). Plant fillers/fibers include bast, leaf, seed, fruit wood, cereal straw and other grass fibres. Finally, it is useful remind that in the last years, fillers and fibers derived from food waste have also started to be tested. In fact, because of their non-food competitiveness (as the lignocellulosic materials), they have been more and more investigated since their possibility to be scaled up without ethical concerns. Example may regard the use of eggshell, shell wastes, shellfish, shrimps shell, tea mill wastes, and spent coffee grounds as reinforcing fillers within thermoplastics, thermosets and/or elastomers [145].

3.2 BIO-FILLERS/FIBERS COMPOSITION AND PROPERTIES

The information on the chemical composition of the natural filler/fiber (NF) is essential since it determines their final properties and thus their applications. Lignocellulosic materials are generally formed by three primary chemical constituents, namely cellulose, hemicellulose and lignin and by minor components such as pectin, waxes or lipids and water soluble substances [153]. These chemical components are distributed troughout the primary and secondary wall cell layers and vary from plant to plant as within different parts of the same plant. The chemical properties of the most common NF

have been summarized in Table 8. Generally, the different amounts of cellulose and hemi-cellulose affect the NF mechanical properties since cellulose's Young's modulus (nearly 140 GPa) is higher than one of hemicellulose (8 GPa) [154]. This consideration is observable also comparing Tables 8 and 9, in which emerge that NF with high cellulose contents such as Flax, Hemp and Kenaf have excellent intrinsic mechanical properties. Finally, it is also well known that lignin fraction increases the NF tensile strength, which range between 1.6 and 3 MPa, by acting as compatibilizer between cellulose and hemicellulose [147, 152, 155].

Table 8 Chemical composition of some common natural fillers [147] .

Fiber	Cellulose (wt%)	Hemicellulose (wt%)	Lignin (wt%)	Waxes (wt%)
Bagasse	55	17	25	–
Bamboo	26–43	30	21–31	–
Flax	71	19-21	2.2	1.5
Kenaf	72	20-21	9	–
Jute	61–71	14–20	12–13	0.5
Hemp	68	15	10	0.8
Ramie	68-76	13–16	0.6–0.7	0.3
Abaca	56–63	20–25	7–9	3
Sisal	65	12	9.9	2
Coir	32–43	0.15–0.25	40–45	–
Oil palm	65	–	29	–
Pineapple	81	–	12.7	–
Curaua	73.6	9.9	7.5	–
Wheat straw	38–45	15–31	12–20	–
Rice husk	35–45	19–25	20	14–17
Rice straw	41–57	33	8–19	8–38

Table 9 Mechanical properties and density of some of the most common NF [147].

Fiber	Tensile strength (MPa)	Young's modulus (GPa)	Elongation at break (%)	Density [g/cm³]
Abaca	400	12	3–10	1.5
Bagasse	290	17	–	1.25
Bamboo	140–230	11–17	–	0.6–1.1

Fiber	Tensile strength (MPa)	Young's modulus (GPa)	Elongation at break (%)	Density [g/cm³]
Flax	345–1035	27.6	2.7–3.2	1.5
Hemp	690	70	1.6	1.48
Jute	393–773	26.5	1.5–1.8	1.3
Kenaf	930	53	1.6	–
Sisal	511–635	9.4–22	2.0–2.5	1.5
Ramie	560	24.5	2.5	1.5
Oil palm	248	3.2	25	0.7–1.55
Pineapple	400–627	1.44	14.5	0.8–1.6
Coir	175	4–6	30	1.2
Curaua	500–1150	11.8	3.7–4.3	1.4

3.3 BIOFILLERS MODIFICATION

One of the most important mechanical properties of polymeric materials is the tensile strength. In composites, this property is strongly affected by the particle-matrix adhesion. Poorly bonded particles are in fact not able to transfer the stress through the interface, generating discontinuities and de-wetting phenomena that involve crazy mechanisms for low applied stresses, if compared with well bonded particles [156, 157]. Natural fillers (NF), being generally polar, are not so affine to the polymer matrices (in general not polar) and thus, obtained biocomposite could have not enough tensile strength values. To overcome this problem, NF can be treated with the aim to make them more hydrophilic. The NF modification can be made by physical and/or chemical treatments as shown in Fig.39.
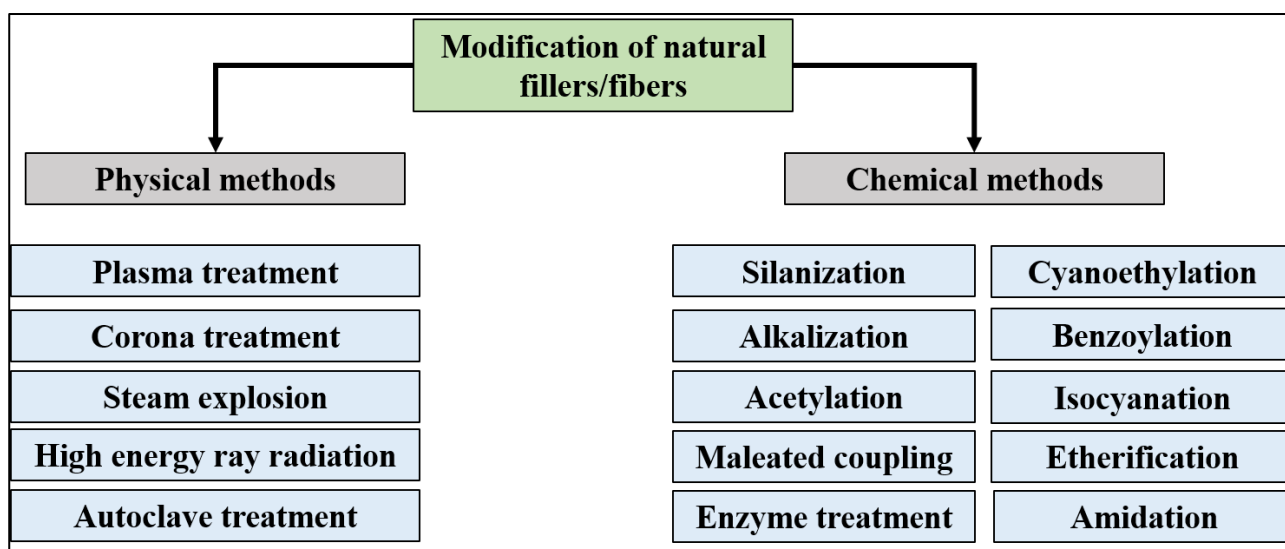
Fig.39 Physical and chemical treatments for the natural filler modification.

3.3.1 Physical modification of natural fillers

Physical treatments are able to change the structural and surface properties of the natural fillers influencing their mechanical bonding with the polymers. In other words, physical methods do not massively affect the chemical composition of the fillers and the interface is mostly enhanced by the increment of the mechanical bonding between filler and polymer matrix [147]. The treated filler-matrix adhesion is improved by reducing the difference between hydrophilic/hydrophobic characters of fillers and polymer matrix. Physical treatments appear as the most eco-friendly treatments because the absence of any kind of chemical.

Plasma treatment is one of the most exploited physical treatment and it is able to modify the chemical and physical structure of both filler and polymeric surfaces without compromising the bulk characteristics of the material. Depending on the type and on the nature of the used gases, with plasma it is possible produce and add reactive free radicals on the filler surface, increase or decrease the filler surface energy and introduce cross-linking reactions. This treatment is generally used for the food packaging applications in order to increase the film surface hydrophilicity and adhesion ability through the formation of polar groups on film surface [152]. Example of plasma treatment and their relative enhancement can be find within the following works on biocomposites: i) PHB and flax fibers [158], ii) PHBV and wood flour [159], iii) PLA and jute fibers [160] and iv) PLA and silk fibers [161]. Similarly, the corona treatment, (sometimes referred also as air plasma) has been found able to activate oxidation on the filler surface. This process has been tested using jute fibers and epoxy resins [162], hemp and PP [163] and flax and a tannin-hexamine lignin matrix [164] and in each case, the tensile strength of biocomposites with treated fillers has been found enhanced.

On the other hand, steam explosion is a high-pressure process that lead the filler to high temperatures and pressures and subsequently to a mechanical disruption trough violent steam discharges [152]. Steam explosion has been found able to improve the properties of lignocellulosic materials, reducing their stiffness, smoothing their surfaces and improving their bending properties [165]. Finally, other physical treatments able to improve the filler-matrix adhesion are the high energy ray radiation processing [166] and the autoclave treatment [167].

3.3.2 Chemical modification of natural fillers

In literature, many chemical modification techniques have been found able to improve the filler-matrix adhesion. Examples may regard silanization, alkalization, acetylation, cyanoethylation, benzoylation, treatment with isocyanates, dewaxing, esterification, etherification, graft copolymerization, crosslinking treatments with formaldehyde, nitration, dinitrophenylation and transesterification [152]. In each case, the involved chemical needs to react with the filler's surface forming a chemical bond bridge between the filler and the matrix. In this section, the most adopted and successful chemical modification strategies have been described meanwhile their reaction scheme are observable in Fig. 40.

Alkaline treatment (or mercerization), is one of the oldest, cost-advantage and most used chemical treatments for natural fillers that need to be used within thermoplastic matrices. This treatment is based on the capacity of the alkaline to ionize the filler hydroxyl group that become an alkoxide (filler—O⁻Na⁺) [168] and can be applied to lignocellulosic materials in order to remove the lignin, hemicellulose, wax and oils that cover the filler surface.

Silane is a multifunctional molecule that has been found to be the most effective chemical treatment for many natural filler/fibers. The silane efficiency depends on many factors such as hydrolysis time, the typology of the organofunctional group, the reaction temperature and the pH. After silanization, one end group of silanol will be able to react with the hydroxyl groups of the filler (Si-O-filler) and, at the same time, the other silanol end group will be able to bond with the polymer matrix (Si-polymer) [169].

Acetylation is a chemical treatments that consist in an esterification reaction between the acetyl group (-CH₃COO) of the involved coupling agent (generally, acetic anhydride) with the hydrophilic hydroxyl group of the filler/fiber in order to takes out the existed moisture. As consequence, treated filler is more hydrophobic and the dimensional stability as well as the dispersion of the filler within the polymer matrix is enhanced. Moreover, after acetylation the filler hygroscopic charter is significantly reduced because the irreversible substitution of hydroxyl groups with acetyl groups [170].

Finally, it is useful mention that another possibility to improve the filler-matrix adhesion is represented by the direct use of silanes or other coupling agents (e.g. maleic anhydride grafted polymer or compatibilizers or Joncryl®) within the processing step. In this case untreated fillers and polymers are compounded with the addition of few percentages of coupling agent leading to a reactive process (e.g. reactive twin-screw extrusion) aimed to improve the polymer-matrix interface. This approach is usually less efficient than the direct chemical treatment of the filler but it is very attractive in large scale because of its intrinsic cheapness.
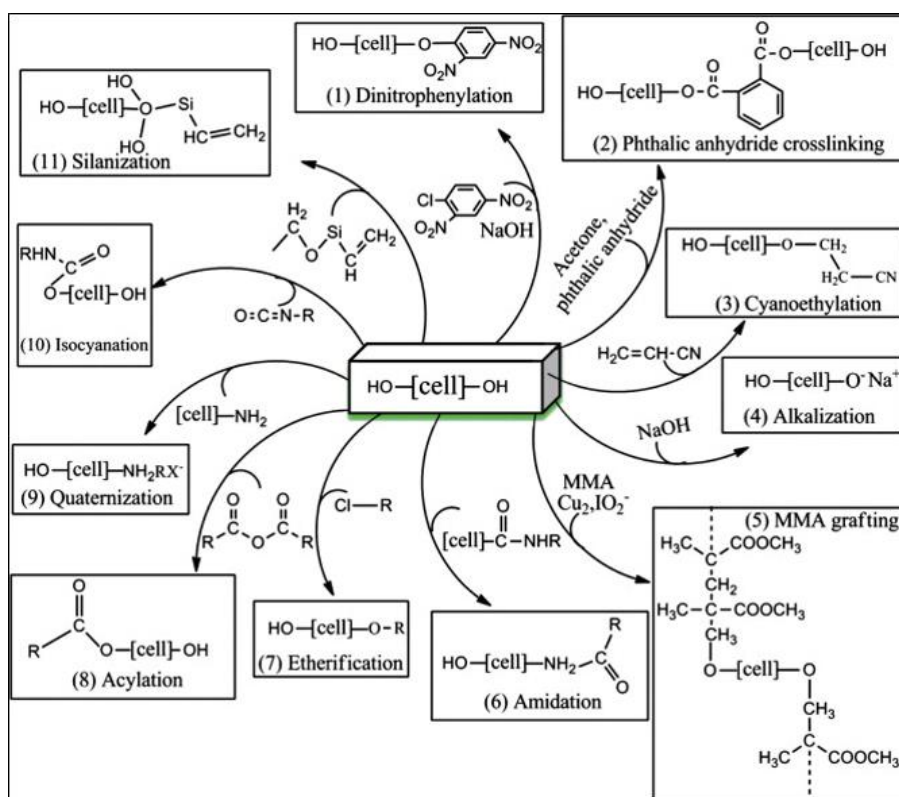
Fig.40 Several chemical modification routes involved for the enhancement of the filler-polymer adhesion.

3.4 BIOCOMPOSITE PERFORMANCE

In this section, the main properties of biocomposites will be discussed focusing on the role of the filler particle. It is noteworthy underline within this discussion, the difference between filler and fiber is relevant because the shape ratio affects the final biocomposite properties. This discussion will be more focused on biocomposites filled by particle shape filler but, anyway, natural fibers will be also considered in some cases.

3.4.1 Mechanical properties

Natural fillers are suitable for reinforcing plastics because they possess high strength and stiffness values and low densities that can than can be exploited within biocomposites. The main tensile properties (Young'modulus (E), tensile strenght (σ_M) and elongation at break (ε_b)) of polymer composites filled with natural particles generally depend on three parameters: filler size, filler-particle adhesion and filler loading [156]. Among all these factors, Young's modulus is mainly affected by the particle loading. The gain in elastic modulus is explained by the fact that natural fillers have generally higher stiffness than polymer matrices. In many works, Young's modulus has been found to be enhanced by the filler content in a proportional way [171-173]. Nevertheless, in other cases the linearity between elastic modulus and filler's content has been observed less marked, and over a certain filler content value, the elastic modulus has been observed tending to an asymptotic value [174-176]. This unconventional mechanical behaviour has been explained as consequence of two possible concomitant effects [177]. Firstly, as the filler content increase, polymer chains become more and more hindered to orient their selves along the resistant section during the injection moulding. This pattern is especially possible when short fibers are involved. Secondly, in semi-crystalline thermoplastic composites, high filler contents could form aggregates able to decrease the crystallinity percentage that is also related to the elastic modulus. Thus, these two opposite effects would balance the final Young's modulus of the composite to an asymptotic value. Finally, it is possible to state that filler size is able to affect the Young's modulus only when filler mean diameter value is below a critic value (often placed at 30 nm [178-180]) and that particle-matrix adhesion phenomena do not significantly affect this property since it is evaluated at low deformations not able to cause interface separations [156]. The maximum tensile strength (σ_M) of biocomposites, as previously mentioned, mainly depends on the adhesion between filler and polymer matrix because poorly bonded particles are not able to transfer the applied stress through the matrix-filler interphase. The originated discontinuity make impossible to handle any stress load and craze formation happens earlier than when dealing with well-bonded particles [156]. Generally, if filler surface is not physically or chemically modified, the tensile strength values decrease increasing the filler content. Nevertheless, when a bio-thermoplastic is involved as matrix, the tensile strength loss could be no so dramatic. In fact, biopolymers such as PHB, PHBV, PBS, PLA and PA11, because of the presence of ammine (N-H) and ester groups (C=O) within their backbone are less hydrophobic than convention petrochemical polymers. Finally, tensile strength is also affected by particle size and particle loading. Generally, decreasing the particle size, the composite tensile strength is enhanced because the higher particle specific areas (inversely proportional to the mean size) guarantee better stress transfers between particle and polymer matrix. On the other hand, at higher particle loading, tensile strength is decreased because agglomerated particles deteriorates the stress transfer efficiency [172]. Considering the elongation at break values of composites it is possible to state that it usually decreases abruptly, even

at low filler loadings. This fact is explainable as consequence of the intrinsic brittleness of the used particles that are not able to deform. To overcome this mechanical loss, it is necessary decrease significantly the main diameter size of the used particles in order to avoid significant discontinuities and/or to modify the filler surface to improve the particle-matrix adhesion. Nevertheless, is noteworthy underline that in certain cases, it is possible to obtain smoother elongation at break losses using natural fillers characterized by not negligible amounts of lipid or waxes fractions that could partially act as plasticizer improving the chain mobility and the elongation at break resistance [157]. In table 10, the variation of tensile properties (with respect to neat biopolymer) obtained using different natural fillers has been reported.

Finally, similar reasoning can be done considering other two important mechanical properties as flexural and impact resistances. Flexural properties mainly depends on the elastic modulus and on the moment of inertia of the biocomposite material. Thus, it is possible to affirm that biofillers generally improve the polymer flexural resistance since their induced stiffening effect. Analogously, the ability to resist fracture under stress applied at high speed (impact resistance) is generally decreased using filler for the same reasons previously reported discussing the elongation at break.

Table 10 Variation of tensile properties (with respect to the net biopolymer) of different biocomposites.

Polymer	Filler	ΔE (%)	$\Delta \sigma_M$ (%)	$\Delta \varepsilon_b$ (%)	Ref
PA11	25%wt. lignin	+67	+5	-95	[181]
PA11	20phr wine lees	+19	-23	-45	[157]
PA10.10	20%wt. rice husk	+44	-22	-95	[182]
PA6.10	10%wt. rice husk	+15	-14	-86	[182]
PBS	30%wt. lignin	+80	-26	-96	[183]
PBS	10%wt. oil palm fibers	+20	-31	-96	[184]
PBS	20phr wine lees	+27	-28	-52	[157]
PLA	20%wt. banana fiber*	+95	+37	-49	[185]
PLA	30%wt. flax fiber	+144	+6	-50	[174]
PLA	5%wt chicken fiber	+20	+16	+14	[186]
PHBV	30%wt corn straw	+220	-1	-80	[187]
PHBV	30%wt. soy stalk	+120	-13	-61	[187]
PHBV	10phr wine lees	+6	+15	equal	[177]
PHBH	40phr wine lees	+25	-28	-33	[177]
PBAT	10%wt. coffee grounds	+150	-42	-35	[188]

* Surface modification trough alkalization and silanization

3.4.2 Thermo-mechanical properties

In addition to the classical mechanical properties generally evaluated at room temperature, natural fillers should be able to enhance the polymer resistance also at higher temperatures. In fact, the ability of a composite material to manifest important mechanical properties also at high temperatures is a required skill for many applications. This aspect is particularly remarkable for disposable biopolymers such as PHB, PHBH, PHBV, PLA and PBS designed for the food packaging in which materials need to be resistant even at 80-100 °C. In general, the most important tests involved for the

determination of the applicative temperature ranges are the Dynamic Mechanical Analysis (DMA), the Heat Deflection Temperature test (HDT) and the Vicat method.

Trough DMA, the bio-composite storage (E') and loss (E'') moduli are monitored over a wide temperature's range (generally from -50/0 °C to 100-150°C). Generally, natural fillers are able to improve the storage modulus of the polymer matrix over the whole range of temperatures, testifying that the natural filler stiffening effect is also maintained at higher or lower temperatures. In [157], the storage modulus of several biopolymers such as PA11, PLA, PHB, PHBH and PBS filled with the same filler (wine lees) has been plotted as filler function pointing out a common correlative formula for the E' prediction of the biocomposite (Fig.41). In addition, another possibility to further enhance the biocomposite storage modulus values is represented by the natural filler surface modification. In fact, similarly to what expressed for the tensile properties, an improved filler-matrix adhesion can induce benefit also at the viscoelastic properties of the composite. Nevertheless, in the case of highly-amorphous biopolymers such as PLA, natural filler are not able to induce any benefit to the storage modulus values above the glass transition temperature (Tg), pointing out the predominant role of the morphology [189] over the involved filler. Finally, it useful remind that, at high filler loadings, the polymer glass transition temperature (T_g) could be increased as consequence of the polymer chains immobilization made by the particle along the particle-matrix interface [190-192].
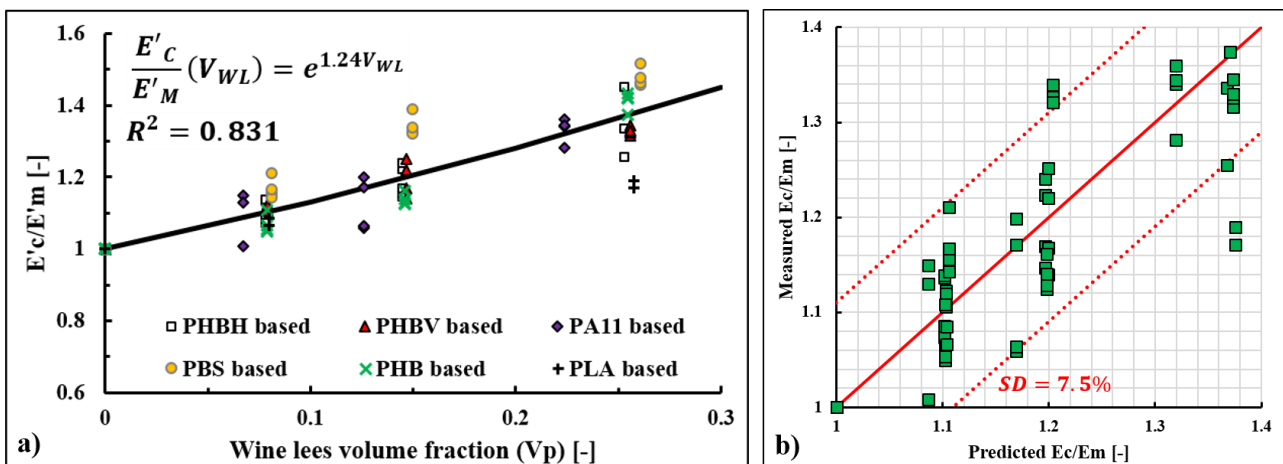
Fig.41 Storage modulus of different wine lees-filled biocomposite as natural filler content. Taken from [157].

HDT and Vicat tests are useful methods to estimate the maximum application temperature of a material. HDT is the temperature at which a rectangular sample immersed in a ramp-heated bath (2 °C/min) deforms of 0.25 mm under a constant flexural load. Similarly, the Vicat softening temperature is represented by the temperature at which a flat-ended needle is penetrated to a depth of 1 mm within the tested sample (again immersed in a ramp-heated bath). Generally, natural fillers enhance this parameter of nearly 1-15 °C depending on both polymer matrix and natural fillers involved. The surface modification of natural fillers can further significantly increase the heat resistance as evidenced by [185], in which banana fibers modified both trough alkalization and silanization have been found able to enhance the PLA HDT of almost 80 °C, and by [187], where alkali treated wheat straw has been found able to improve the PHBV HDT of 23 °C. Nevertheless, it is opportune to mention that, through surface modification, so increased values could have been due

also by partial cross-linking reactions that, in the case of biodegradable polymers, would be unappreciated because inhibitors of biodegradation.

Table 11 Heat Deflection Temperatures variation (ΔHDT) of several bio-composites.

Polymer matrix	Filler	ΔHDT [°C]	Ref
PA11	20%wt. wood fiber	+1-2	[193]
PA11	40 phr wine lees	+6	[157]
PA10.10	20%wt. rice husk ash	+1	[182]
PA6.10	10%wt. rice husk ash	+7	[182]
PBS	30%wt. lignin	+5	[183]
PBS	40 phr wine lees	+11	[157]
PLA	40 phr banana fiber *	+77	[185]
PLA	20%wt. rice husk ash	+1	[182]
PLA	30%wt. pineapple flour	+9	[194]
PHBV	30%wt. corn straw	+12	[187]
PHBV	30%wt. soy straw	+9	[187]
PHBV	30% wheat straw**	+23	[187]

* Surface modification trough alkalization and silanization

** Surface modification trough alkalization

3.5 SUMMARY

There are thousands of different possible fillers/fibers in the world and, nowadays, only few of them have been deeply investigated and even less have been industrialized. Despite the increasing interest in this polymeric field, there is still a lack of knowledge concerning the filler chemical composition, its variability related to location and time of harvest, its processing conditions and or its sensitivity to temperature, moisture and/or UV radiations. In addition, many promising lab-scale fillers are often not scalable at industrial levels because they are scarcely available during the year, or because they are food competitive and/or because their high production cost. In fact, even if the raw materials is often cheap, economic consideration on steps such as transport, drying, grounding and surface modification are scarcely conduced at lab-scale. Thus, more works connected with these industrial realities should be done to promote in large-scale new different bio-composites.

From a technological point of view, it is possible to state that natural fillers are able to enhance many properties of the neat biopolymers such as tensile, flexural and dynamic-mechanical. In addition, natural fillers can also enhance the maximum application temperatures of many biodegradable polymers pointing out new interesting possibilities for application in which biodegradability and heat resistance are simultaneously needed (e.g. disposable plastic cutlery). From another hand, impact strength and ductility are the only undesirable weak points of these materials in terms of mechanical performance but better results could be achieved using additives as coupling agents, compatibilizers or chain extenders. Besides these properties, also long-term performance (creep test) and compressive properties of biocomposites are generally investigated for structural, aerospace and automotive purposes, and even in these cases, the filler response is often positive.

In conclusion, it is possible to say that biocomposites appear very promising in terms of properties, application, cost-effectiveness and sustainability but in order to expand their commercial markets, they should become governable in terms of desired and predicted performances. To obtain this goal, many parameters such as filler pretreatments, filler characterization, processing conditions, the biocomposite non-linear behavior, the matrix-filler adhesion and the filler dispersion should be deeper investigated and optimized.

4. STATE OF ART: PLAYING WITH THE DEGRADATION

Polymer properties depends on the chemistry of their repeating unity, on their macromolecular structure and on the interactions between their chains. Each chemical or physical mechanism that lead to an irreversible modification of the molecular weight and/or to the modification of the chemical structure of a generic polymer is recognized as degradative process. Since even few degradative reactions occurred at microscopic scale, can affect significantly the macroscopic physical-mechanical properties of a polymeric matrix, the knowledge of the degradation mechanisms as well as of stabilization's strategies is very important during the polymer design phase. Nevertheless, at the same time, when dealing with biodegradable polymers, it is also needed to know the possible mechanisms and solution to modulate the degradation on demand, in accordance with the purposes of the product. Therefore, in this chapter, the main degradative mechanisms and the most important ways to postpone and accelerate degradation will be discussed.

4.1 GENERAL REMARKS

The most common way to classify the various types of degradation is by the nature of the degradative agents. The main agents that initiate degradation can be divided in physical, chemical and biological agents. Physical agents are heat, light (UV), mechanical stress and high-energy radiations such as X- and γ-rays, most common chemical agents are oxygen, ozone, water and chemical compounds such as solvents, acids and basis and finally, biological agents are represented by microorganisms such as bacteria and fungi. Clearly, polymer degradation can be conducted simultaneously by different degradative agents. The most important degradative pathway have been reported in Table 12, indicating also the polymer life-phase in which those degradative pathway generally occur. In fact, polymer degradation occurs during the polymer processing (e.g. extrusion, injection molding) where heat, mechanical stress and sometimes oxygen (it depends on the polymer the oxygen diffusivity) are the main degradative agents as well as during the product life time where other degradative agents (e.g. UV, heat, oxygen, chemicals) continue to degrade the polymer matrix. In addition, in the case of biodegradable polymers, microbial degradation also occurs during the post-life phase.

Table 12 Degradative processes and polymer life-phase in which they generally occur.

Degradative agent	Degradation name	Polymer life-phase
Heat	Thermal degradation	Processing
Heat + Oxygen	Thermo-oxidation	Processing/life time
UV light	Photo-degradation	Life time
UV light + oxygen	Photo-oxidation	Life time
Mechanical stress	Mechanical degradation	Processing/life time
Microorganism	Anaerobic biodegradation (digester)	Post life
Microorganism + oxygen	Aerobic biodegradation (composter)	Post life
Microorganims + marine water	Biodegradation in marine water	Post life

The degradative agents influence the polymer degradation pathway in terms of by-products and modification, but anyway, they are not the unique affecting factors. In fact, degradation depends also on the degradative agents load and on the exposure time and from this point of view, degradation is usually distinguished in short-term or long-term degradation. Short-term degradation occurs when

degradative agents are applied at very-high loads and for short times (processing conditions), meanwhile long-term degradation appears with modest loads applied for long times (product lifetime). There are many differences between these two degradations pathways such as radical typology and quantity, oxygen levels and physical state (Table 13) and thus, either contributes need to be considered during the polymer design phase. Finally, considering the alteration caused by degradation is possible to say that initial polymer chains can be de-polymerized into initial monomers, fragmented in several oligomers, cross-linked in network structures and chemically modified in terms of repeating unit (Fig.42).
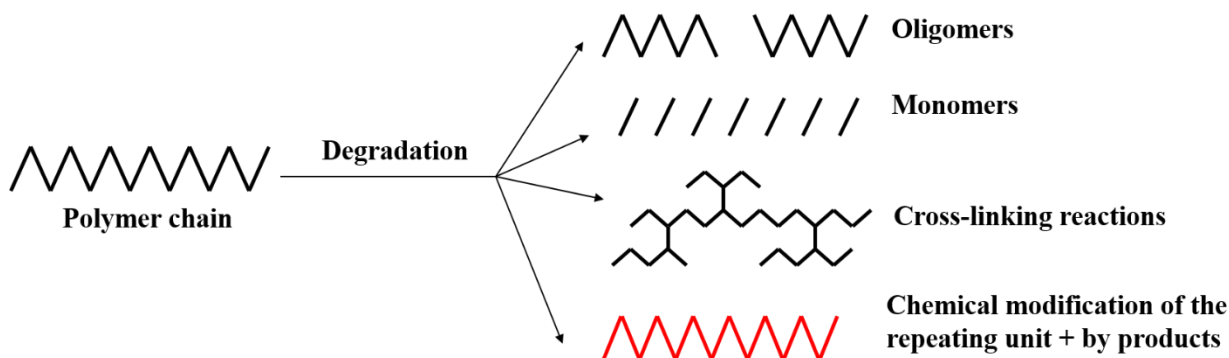
Fig.42 Polymer chain irreversible alterations caused by degradation.

In conclusion, polymer degradation can occur through different degradative agents, during different product life phases and with different loads and exposure times; all these contributes have to be considered during the polymer design phase in order to guarantee the product desired properties.

Table 13 Differences in short and long-term degradation pathways [195].

Parameter	Processing [Short-terms]	Use [long-terms]
Load typology	Temperature; Mechanical stress	Temperature; UV rays
Load intensity	High	Low
Load times	Short	Long
Physical state	Liquid (melt)	Solid
Oxygen	Oxygen-poor	Oxygen-saturation
P• concentration	[P•] >> [POO•]	[P•] << [POO•]
POOH concentration	Low	High

4.2 THERMAL DEGRADATION

Thermal degradation of thermoplastic polymers occurs during processing at high temperatures (over the melting temperature) when polymer is transformed from solid to melt. Under these conditions, the oxygen contribute is usually negligible if compared with the heat load and with the mechanical stress. Degradation reaction can attack both the polymer chain backbone and the side-chain substituents. In the first case, monomers and oligomers are the main degradation's products, meanwhile in the second case, elimination or cyclization reactions change the initial chemical composition. The degradation mechanism depends on the polymer typology but three phases (initiation, depropagation and termination) are always recognizable.

4.2.1 Vyinl polymers

According to Frache and Camino [196], vinyl polymers degradation starts through a random homolytic scission of a C-C bond along the polymer backbone that generate macro-radicals (P•). Formed macro-radicals are able to propagate the degradation in two different ways: through the unzipping process and trough the inter- and intra-molecular chain transfer (also called unbuttoning reactions). Unzipping process produces the starting vinyl monomers, meanwhile the inter- and intra-molecular hydrogen transfer usually leads to oligomeric fragments (Fig.43). Hydrogen transfer reactions are favored by the reactivity of the macro-radicals and by the mobility of the hydrogen atoms. These thesis are empirically supported by the fact that, as example, propylene formation during PP degradation is almost totally absent meanwhile poly(methyl methacrylate) (PMMA) is totally depolymerized (Table 14). In fact, PP radicals are very reactive and they very mobile tertiary hydrogen atoms, meanwhile PMMA, having a phenol ring, stabilizes the radical that is thus not able to transfer the degradation. At the end of degradation, termination reactions take places in forms of disproportionation and recombination. In the case of recombination, crosslinked or branched structures can be formed if the unpaired electron is not in terminal position. Finally, it has to be mentioned that polyvinylchloride (PVC) degrades with the elimination reactions of the side-chain substituents modifying its chemical composition. In fact, PVC loses its chloride acid side-chain molecules (HCl) forming double bonds along the polymer backbone.

Table 14 Thermal degradation products of vinyl polymers.
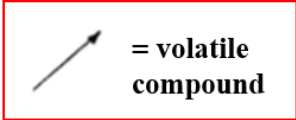
Polymer	Monomer [%]	Depropagation pathway
Poly(methyl methacrylate) (PMMA)	100	Unzipping
Poly(α-methyl styrene) (PMS)	100	Unzipping
Poly(tetrafluorothylene) (PTFE)	100	Unzipping
Polystyrene (PS)	40	Unzipping/molecular transfer
Polyisobutene (PIB)	30	Unzipping/molecular transfer
Polypropylene (PP)	2	Molecular transfer
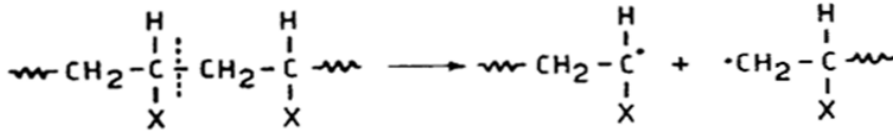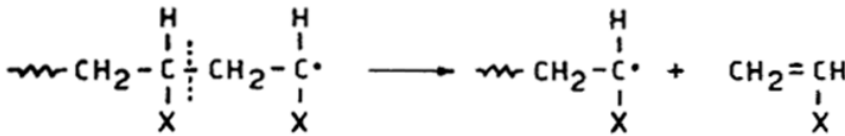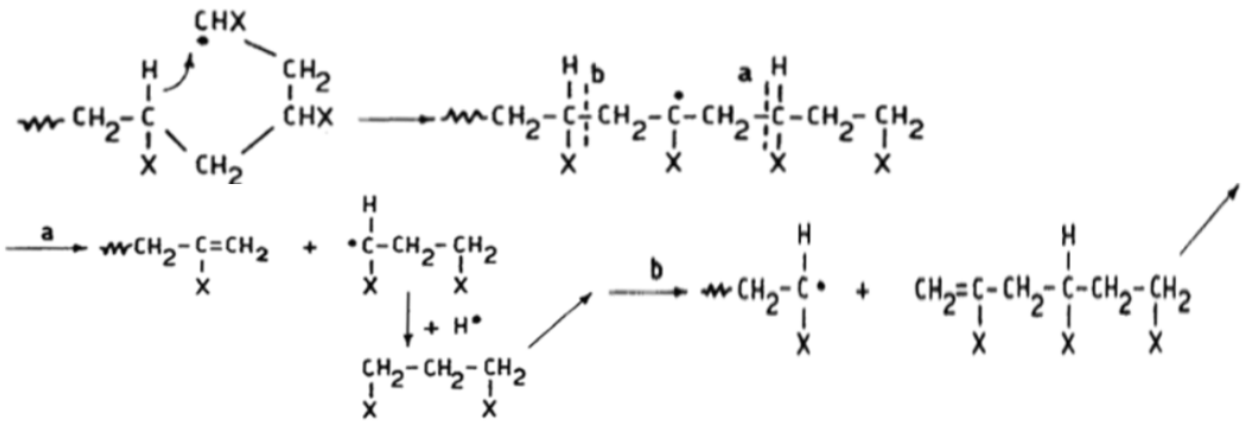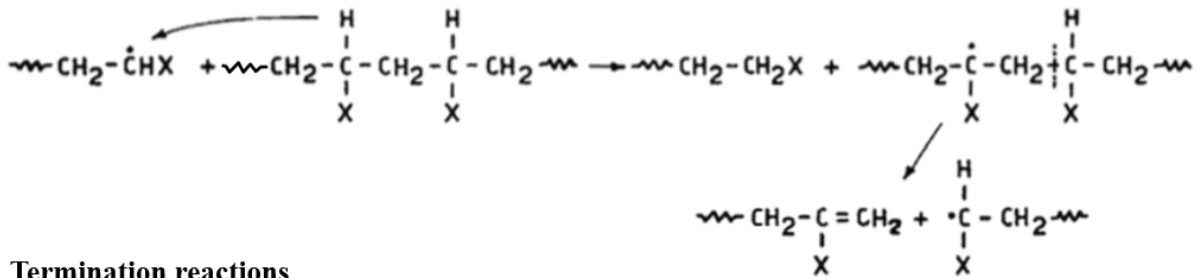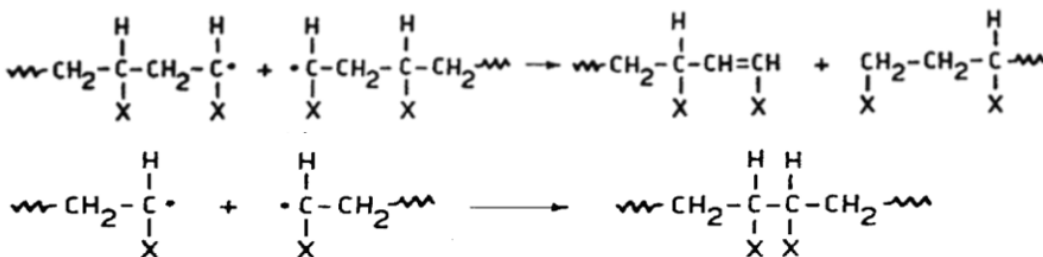
Fig.43 Thermal degradation of vinyl polymers. Adapted from [196].

4.2.2 Polyesters

Thermal degradation of polyesters description is more complicated to be generalized since depends on many factors and it is particularly affected by the involved temperatures. It can be only said that backbone esters groups are the first groups to react because their activation temperatures are lower than ones of C-C bonds are, and that radical reactions are often negligible and surely much less predominant than in the case of vinyl polymers.

4.2.2.1 Poly(3-hydroxybutyrate) (PHB)

Thermal degradation of PHB has been deeply investigated and described in literature [197-202]. Briefly, PHB becomes thermally unstable even before of its melting temperature, in the 160-200 °C range. In this phase, the main degradative pathway is represented by random chain scission (cis-elimination) that lead to low molecular weight PHB oligomers with a carboxylic acid and an unsutarated propenyl as ends groups. It is very widely accepted that chain scission usually occurs by ester decomposition mechanism involving a six-memered ring transition state. Before the M_W reduction, it is believed that esterification reactions between hydroxyl and acid groups origanally present as the end group of the PHB polymer could take place leading to M_W increases, and that M_W starts to decline only when hydroxyl groups are consumed. Random chain scission reactions will continue untill formed oligomers will be volatile enough to leave the matrix. Crotonic acids and their dimers and trimers represent the first and most formed volatile compounds [203, 204] that at high temperatures (ca. 500 °C) can be further degraded by decarboxylation reactions leading to carbon dioxide and propene (especially) as well as to ketene and acetaldhyde. The PHB degradation pathway is schemized in Fig.43, meanwhile the above mentioned reactions are reported in Fig.44. At PHB processing temperatures (170-190 °C), volatile products are pratically never produced since they are mostly genereted at 200-300 °C or, at lower temperaturers, for degradation times significantly higher than processing residence times. This is explained by the fact that since thermal degradation occurs almost exclusively via random chain scission reactions, the probability of volatile species are lower than chain scission probabilities [205], and even at 220 °C, mass losses could be scarcely detactable [205]. By the way, processed PHB exhibits significantly decreased M_W and important oligomeric fractions as random chain scission consequence [206].
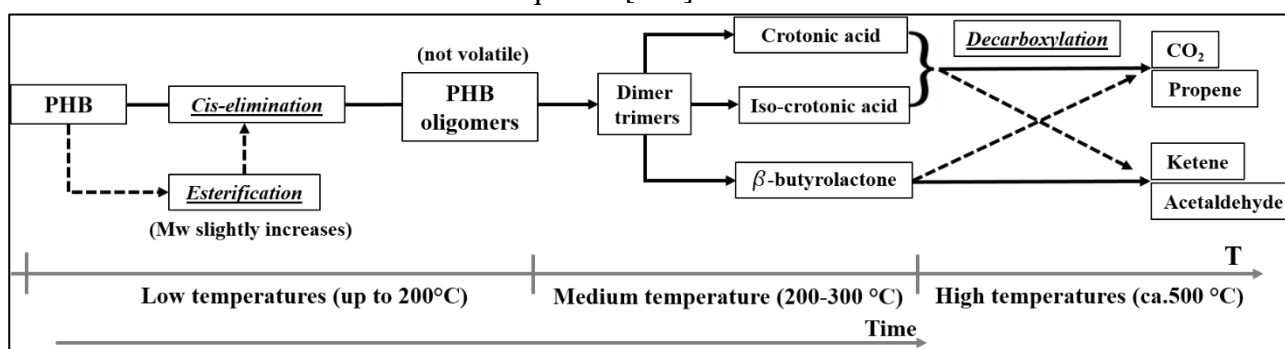
Fig.44 PHB thermal degradation pathway
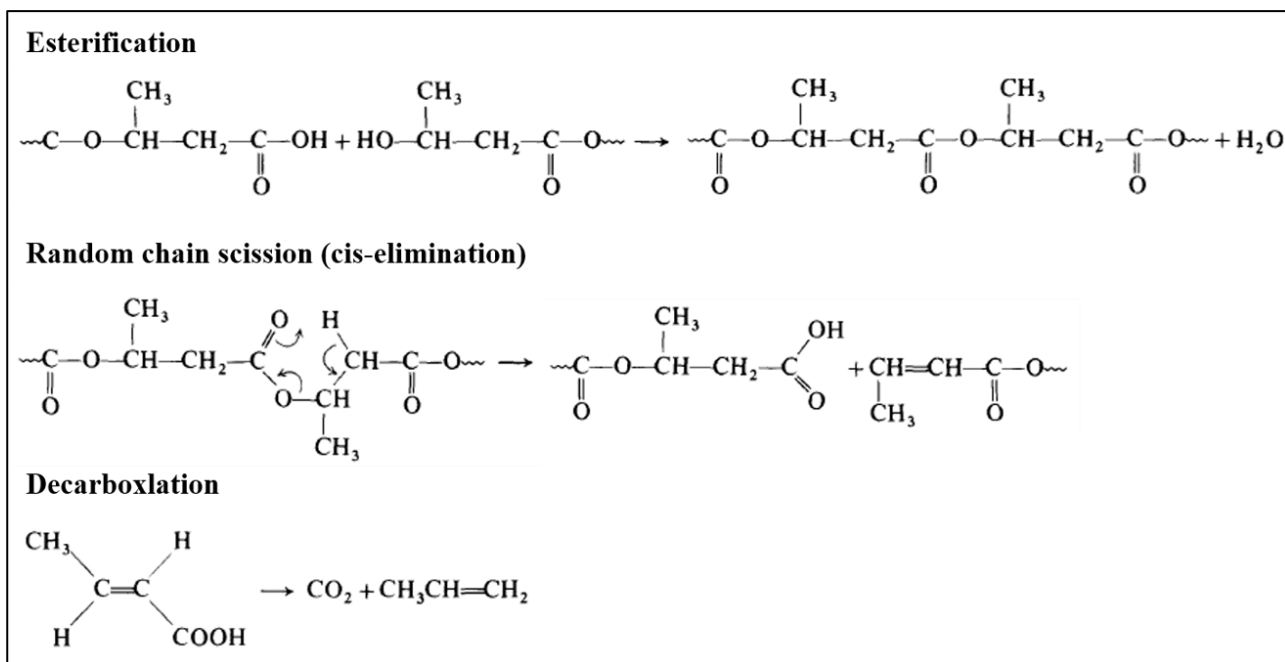
Fig.44 Main reactions occurring during PHB thermal degradation.

4.2.2.2 Poly(lactic acid) (PLA)

For PLA, thermal degradation seems to proceed by a very complicated mechanism which does not allow simple representative schemes. Many factors such as moisture, hydrolysed monomers, residual metals, molecular weight and PLA stereochemistry can affect the PLA thermal degradation [205] that can therefore occur through several different reactions depending on the above mentioned parameters [106, 207]. According to McNeill and Leiper [208, 209], the main thermal degradation PLA reaction is a non-radical unbuttoning ester interchange reaction involving the hydroxyl end-groups (Fig.45). This hypothesis has been supported experimentally by the fact that acetylated PLA showed increased thermal stability. Following this theory, the degradation products can be a lactide molecule, an oligomeric ring or acetaldehyde plus carbon monoxide depending on the backbone point at which degradation reaction has occurred. Radical reactions are assumed to start with either an alkyl-oxygen or an acyl-oxygen and carbon-centred macro-radicals can be formed, but in both cases, PLA produces mainly cyclic oligomers. According to Kopinke [210], PLA thermal degradation above 200 °C involves five reaction pathways that can be summarized as follow:

i)   Intra- and intermolecular ester exchange that yield lactides and cyclic oligomers.
ii)   Cis-elimination reactions that lead to acrylic acid and acyclic oligomers.
iii)   Radical and connected non-radical reactions that form acetaldehyde and carbon monoxide.
iv)   Radical reactions that yield methyl-keten, acetaldehyde and carbon dioxide.
v)   Unzipping selective reactions that form exclusively lactides.
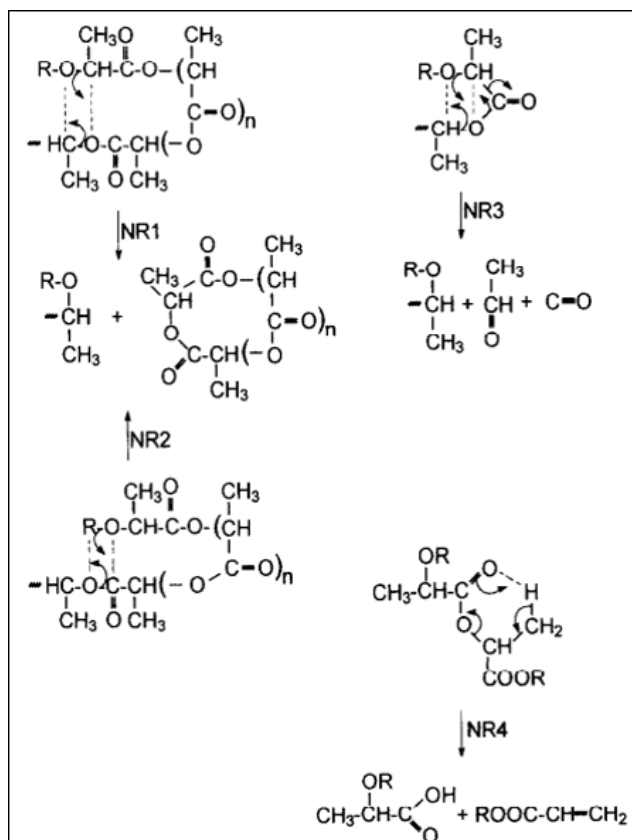
Fig.45 Non-radical (NR) reaction of PLA during thermal degradation. Taken from [210]

4.2.2.3 Poly(butylene succinate) (PBS)

Rizzarelli et al. [211], studied the thermal degradation and thermo-oxidation of different PBS grades applying MALDI-TOF mass spectrometry. They proposed that PBS degrades thermally through the β-hydrogen transfer mechanism forming oligomers terminated with olefin groups and species bearing 1,4-butandiol at one end an olefin group at the other end. Even if the β-hydrogen transfer rearrangement is rather usual for polyesters in thermal degradation, the PBS thermal degradation is quite different. In fact, during the β-hydrogen transfer mechanism, the rearranged hydrogen is usually attached to the carbonyl oxygen of the di-acid and its transfer leads to the formation of two ions of which one has a carboxylic acid end groups, meanwhile in PBS thermal degradation no oligomers containing succinic acid end groups have been detected. Thus, following author's hypothesis, it is reasonable to believe that succinic acid end molecules are decomposed and cyclized in succinic anhydride as also supported by similar results obtained through the investigation of the poly(propylene succinate) degradation [212] in which succinic anhydride was also found. In Fig.46, the PBS β-hydrogen transfer reactions and the succinic anhydride formation have been reported.
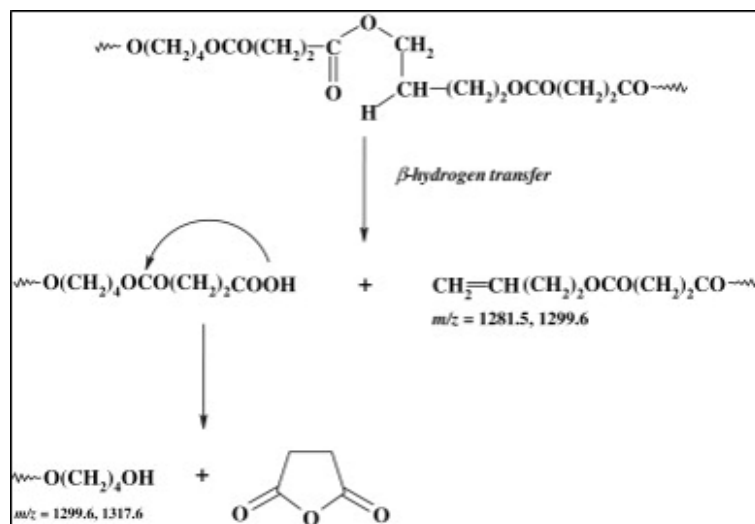
Fig.46 Thermal degradation mechanism of PBS. Taken from [211].

4.3 PHOTO-DEGRADATION

Photo-degradation is a degradative pathway derived by the fact that some polymer groups, namely chromophore groups, can absorb the visible and UV (200-400 nm) incident photonic radiations. The absorbed energy surplus make the chromophore groups highly unstable and thus, they can react photo-chemically leading to a homolytic chain scission. Thus, the initiation mechanisms of photo-degradation, represented by the in series steps of absorbance and scission, is quite different from the thermal degradation initiation that do not require any absorbance phase. Nevertheless, from a qualitative point of view, the further degradation steps (unzipping, molecular transfer and termination reactions) are qualitatively identical to the ones previously described for the thermal degradation. The other difference regards the composition of the degradation products because photo-degradation involves cross-linking reactions more frequently [105]. This can be explained by the fact that photo-degradation usually occurs at temperatures much lower than the ones involved during the thermal degradation. For example, as previously seen, polystyrene degradative products during thermal degradation are styrene monomers (40%) and oligomers meanwhile during photo-degradation it releases hydrogen, it forms network structures and become yellow. Similarly, PMMA, that under thermal loads fully de-propagates trough unzipping (100% of monomer), during photo-degradation forms cross-linking reactions and yield to gaseous products such as CO, CO_2 and CH_4 and to methanol and methyl formate [196].

4.4 THERMO/PHOTO-OXIDATION

Thermo- and photo-oxidation are degradative mechanisms that are mainly induced during the lifetime of the polymer product. It is caused by the combination of heat or light and oxygen that nevertheless, do not react directly with the polymer. In fact, as shown in Fig.47, the initiation step is represented by the formation of the polymer macro-radical (P•) trough pure thermal or photo-degradation. Successively, in the propagation phase, molecular oxygen reacts with P• to form the peroxyl POO•. This reaction is generally very fast and it is accompanied by another slower reaction of propagation in which POO• reacts with a polymer molecule forming an hydro-peroxide (POOH) and another new

macro-radical P•. Finally, POO• is involved in termination reactions in which crosslinking phenomena may occur meanwhile POOH can be further degraded in oxyl polymer (PO•) and in hydroxyl radicals able to form degradation products such as alcohols, ketones, acids and esters [196].
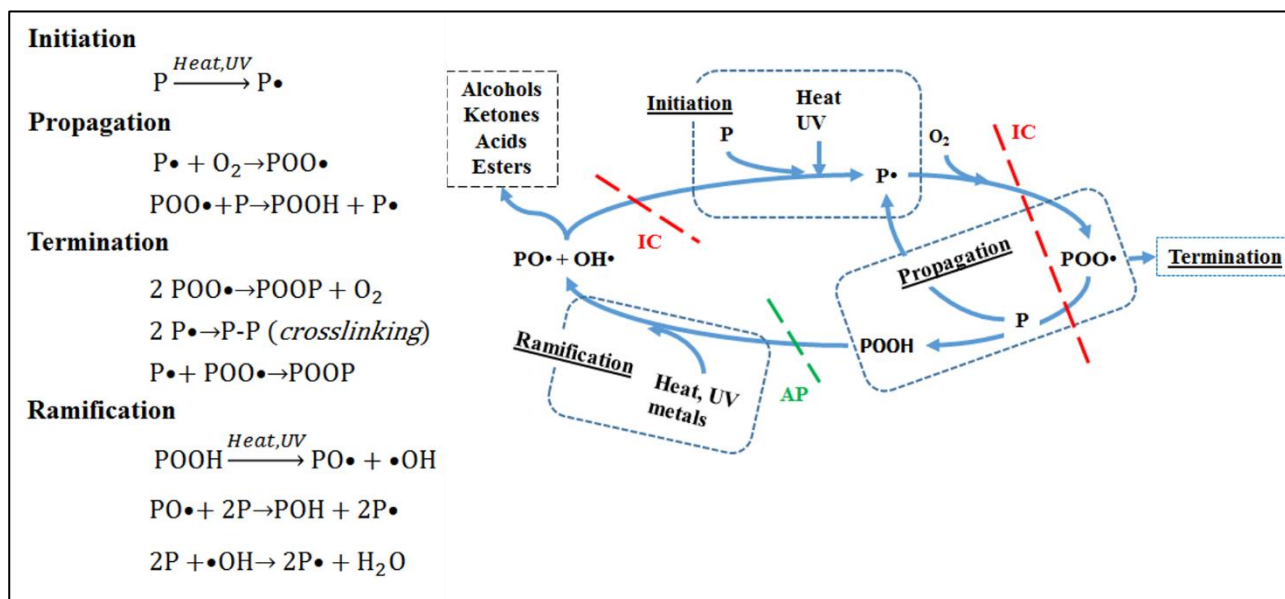
Fig.47 Thermo/Photo-oxidation scheme and reactions.

In conclusion, it is noteworthy underline that thermo/photo-oxidative degradation mainly occurs during the polymer product lifetime. During the polymer processing, these degradative mechanisms are often negligible, especially when dealing with polymers characterized by scarce oxygen permeability (e.g. polypropylene) or when processing is conducted under vacuum (e.g. extrusion). In addition, since oxygen reacts with polymer macro-radicals, it is easily to understand that oxidative degradation is more present when dealing with radical degradation pathways. Nevertheless, it is also important mention that thermo-oxidation minor contributes have been found out also within polyesters (not-radical degradation) after processing as for example, within PHB [213-215].

4.5 BIODEGRADATION

Biodegradation can occur in aerobic or anaerobic conditions. In the first case, biomass (humus and compost) and carbon dioxide are the main biodegradation's products; meanwhile in the second case biomass and methane are generally formed. The biopolymer yield conversion in biomass is usually of 10-40% depending on the biopolymer itself. Biodegradation rate depends on many factors such as product thickness, environmental conditions and temperature, pH, oxygen and water contents. In terms of pathway, biodegradation mainly consists of three phases: i) bio-deterioration, ii) bio-fragmentation and iii) assimilation [216].

Bio-deterioration is the superficial degradation that modifies mechanical, physical and chemical properties of a given material. In addition, abiotic degradations, as previously described, provoke deterioration. Bio-deterioration can be seen as the result of the activity of microorganisms growing on the surface and/or inside a given material [216, 217]. Microorganisms involved in bio-deterioration can form a consortia with a common structured organization (biofilm) that can provoke serious damages on different biopolymers [218]. This biofilm can attack the biopolymer in three different and concomitant ways: mechanically, chemically and enzymatically. The physical way involves the

secretion of a kind of glue (complex matrix of natural polymers) that infiltrates within the porous structures of biopolymers [219]. The aim of this infiltration is to protect the microorganisms from unfavorable conditions such as desiccation and UV rays and to allow them to develop their mycelia frameworks within the biopolymer. In addition, the glue increases the size of pores and provokes cracks that decrease the overall polymer resistance and durability [220]. Chemical bio-deterioration is conduced simultaneously by two degradative agents: microorganisms and water. From one side, developing successively into the biopolymers bulk, microorganisms can release active chemicals such as nitrous acid, nitric acid, sulphuric acid [221] or organic acids such as oxalic, citric, gluconic and fumaric [222], that clearly damage the polymer chains. From another side, water can enters in the polymer matrix and lead to abiotic or biotic hydrolysis reactions that forms and releases compounds such as succinic acid, adipic acid and lactic acid within the biopolymer. These acids can react with components of the material and increase the surface erosion [223], others can form stable complex sequestrating cations present into the matrix and still others can be used as carbon sources from microorganisms that extend their mycelia [224]. Finally, bio-deterioration can be induced by enzymes secreted by microorganisms such as lipases, esterases, ureases and proteases [225].

Bio-fragmentation is the middle step that bridge the bio-deterioration and the assimilation phase. Here, it is indispensable to cleave several bonds to obtain a mixture of low-molecular weight oligomers/monomers that can further be digested by microorganisms. Microorganisms generally use three ways to cleave polymers: i) enzymatic hydrolysis, ii) enzymatic oxidation and iii) radical oxidation [216] depending on both polymer typology and on environmental conditions. Anyway, in each case, the polymer de-polymerization is carried out and the obtained oligomer/monomer mixture can be assimilated by microorganisms. The assimilation phase is the unique event in which there is a real integration between atoms from fragments of polymeric materials and microbial cells. Through this integration, microorganisms can uptake the necessary sources of energy, electrons and elements indispensable for the formation of the cell structure. During assimilation microorganism can grow and reproduce while consuming the polymeric substrate from the environment. Monomers need to go through the cellular microorganism membranes in order to be assimilated. Inside the cell, monomers are therefore oxidized (catabolic pathway) leading to the adenosine triphosphate (ATP) production and to the all other constitutive cell structure elements. Thus, in accordance with the environmental conditions (aerobic or anaerobic), microorganism's respiration will lead to carbon dioxide or methane, respectively, meanwhile the undigested polymer fragments will constitute the spent biomass (humus and compost). A stylized scheme of biodegradation pathway is shown in Fig.48.
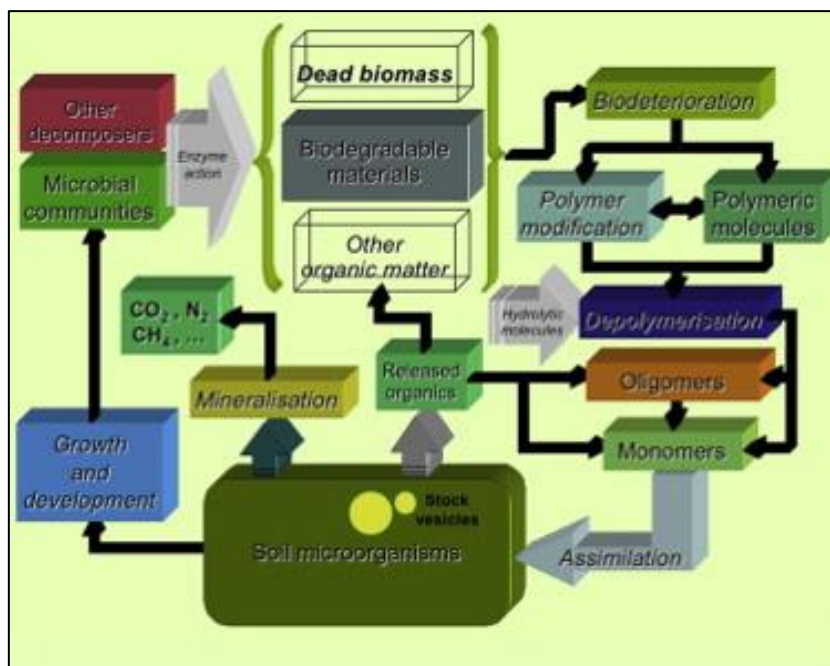
Fig.48 Polymer biodegradation scheme. Taken from [216].

4.6 POLYMER STABILIZATION

Degradation and biodegradation can be undesired phenomena since they affect the ultimate mechanical properties of the polymer product. To withstand or postpone degradation phenomena two types of action are generally possible (also concomitantly): i) the intervention on the polymer structure and ii) the use of stabilizers (or antioxidants). Stabilizers can be further classified as thermal or UV stabilizers in accordance to the type of degradation that want be prevented (Fig.49).
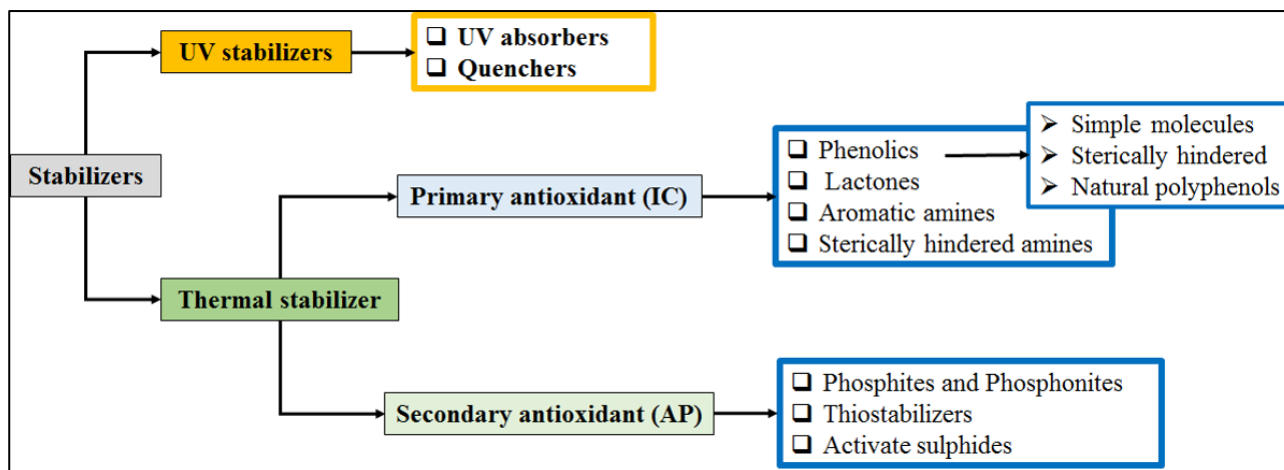
Fig.49 Classification of the stabilizers

4.6.1 Thermal stabilizers

As seen in Fig.47, thermal stabilizers can work in two different ways: a) as interrupters of the radical chain mechanism (IC) and b) as hydro-peroxides decomposer (AP= action preventive). These types of antioxidants are also know with the name of primary antioxidant (IC) and secondary antioxidant

(AP), respectively. Nevertheless, a combination of both stabilizers is generally required their synergetic effect.

4.6.1.1   Primary antioxidants

Primary antioxidant are radical scavengers that are able to stop the radical degradative propagation by the donation of an hydrogen atom. The most used primary antioxidants are: a) phenolic compounds, b) lactones, c) sterically hindered amines and d) aromatic amines. Primary antioxidants (A) mainly act with the (POO•) peroxyl radicals but theoretically they can take part to the following stabilization reactions:

a) $POO \bullet + AH \rightarrow POOH + A \bullet$

b) $PO \bullet + AH \rightarrow POH + A \bullet$

c) $OH \bullet + AH \rightarrow H_2O + A \bullet$

d) $POO \bullet + A \bullet \rightarrow POOA$

Antioxidant A need to be stable to the air, do not be toxic, its radical A• radical have to not react with the polymer (P) or with the oxygen and it need to be stable. As example, phenolic antioxidant are the most common used hydrogen-donator antioxidants because they are able to stabilize the unpaired electron through the ring resonance (Fig.50).
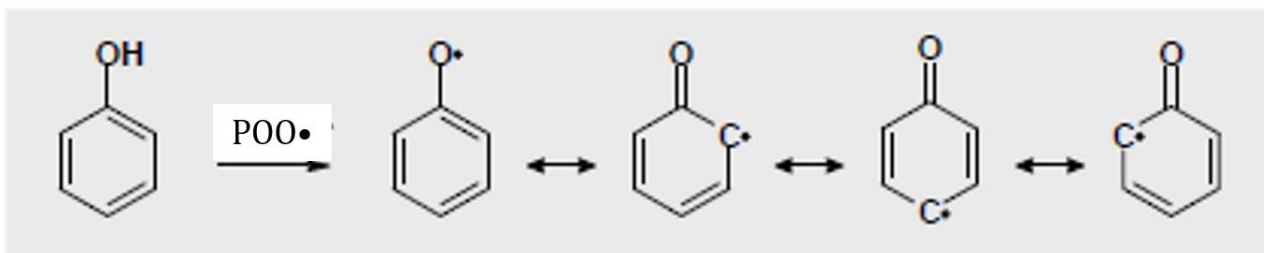
Fig.50 Mechanism of the phenol resonance stabilization.

The primary antioxidant efficiency depends also in other two parameters. Firstly, perossyil radical can extract the antioxidant hydrogen only if the Bond Dissociation Energy (BDE) of A-H is lower than the BDE of the hydro-peroxide (POOH). The antioxidant's BDE depends mainly on its stability and on the stability of its radical A•. As example, comparing two simple phenols as the Guaiacol and Catechol (Fig.51) it is possible to state that Catechol, having a lower BDE, is more efficient because its radical is more stable. In fact, Catechol radical is characterized by the fact that it still has the hydrogen bonding that instead is not present within the Guaiacol radical.

a) *o*-Methoxyphenol (Guaiacol)   **b)** 1,2-Benzenediol (Catechol)
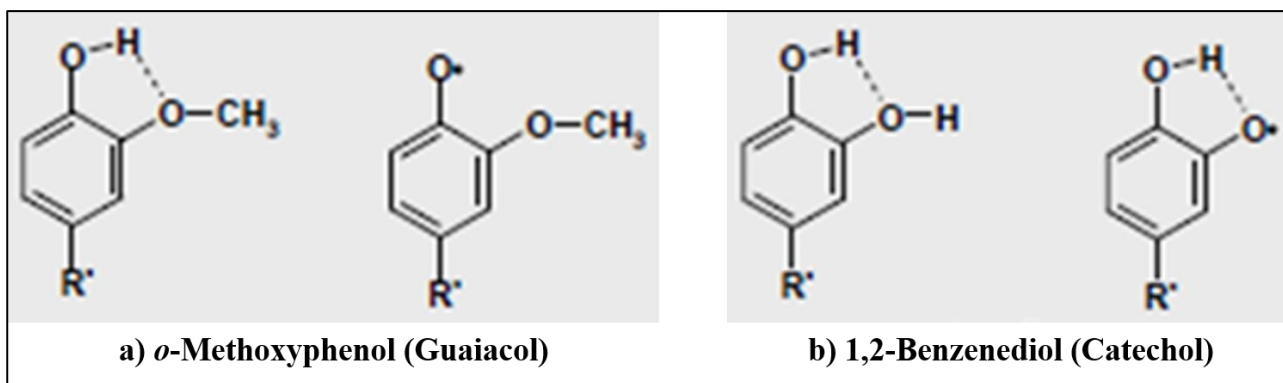
Fig.51 Guaiacol, Catechol and their radicals. Catechol antioxidant efficiency is higher (lower BDE).

In addition, the steric hindrance also affects the stabilization's mechanism since the dimensions of the substituents are inversely proportional to the antioxidant's efficiency. In fact, increasing the substituents dimensions, less efficient impacts between antioxidants and peroxyl radicals will take place (Fig.52) [226]. By the way, large substituents could be useful to prevent the reaction of the phenol radicals with the polymer chain and the dimerization of two phenol radicals [227]. Thus, the choice between simple phenols or sterically hindered phenols generally depends on the polymer typology as well as on the expected degradative conditions. Finally, it is noteworthy underline that also natural polyphenolic extracts can work as radical chain interrupters antioxidant and their use is more and more investigated since they are eco-friendly and able to maintain bio-based polymers fully natural. Natural polyphenols have been further and deeper discussed within sections 6.2, 7.2, 7.3 and 7.6.
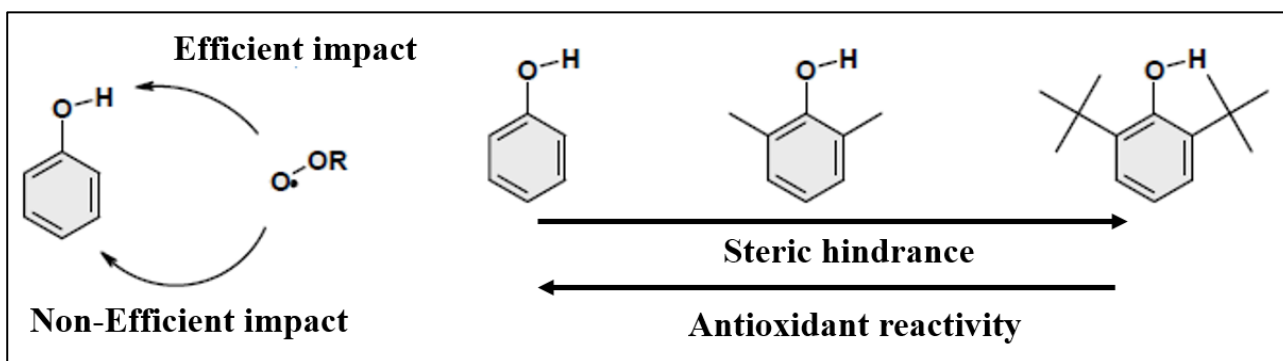
Fig.52 Antioxidant reactivity as steric hindrance function.

4.6.1.2 Secondary antioxidant

Secondary antioxidants (AP) are used with the aim to decompose hydroperoxides (POOH) intto non-radical compounds, preventing the formation of new radical decomposition products (PO• and •OH). They are often used in combination with primary antioxidants in order to delay the consumption of the latter and for these reasons they are called as synergists or co-stabilizers. The most important secondary antioxidant are a) phosphites and phosphonites, b) thiostabilizers and c) activated sulfides. Among them, phosphites and phosphonites as well as activated sulfites are the most effective hydroperoxide decomposers since they react stoichiometrically with the POOH oxidizing their selves. Sulfur compounds are already active at room temperature, meanwhile phosphites are active only at

higher temperatures. In addition, the phosphites contribution to long-term stabilization is small because they scarcely react with oxygen and thus, they are almost exclusively used in combination with phenolic antioxidant. Reaction of phosphites and sulfur compounds with hydroperoxides are:

$$P(OR)_3 + POOH \rightarrow O = P(OR)_3 + POH$$

$$RS + POOH \rightarrow O = SR + POH$$
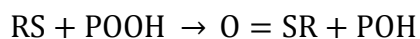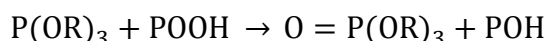
4.6.2 Light stabilizers

To stabilize polymers to outdoors purposes, light-stabilization is needed. The previous mentioned thermal stabilizers (radical scavenger and hydroperoxide decomposers) are also efficient against photo-oxidation since its degradative mechanism, when triggered, is the same of thermo-oxidation, as also previously seen. Therefore, for light stabilizers are intended those compounds able to inhibit the chromophore photon absorption that causes the homolytic scission. The most used strategies for the light protection involve the use of a) UV absorbers and/or b) Quenchers. The principle of the UV absorbers is inherent in the idea of using suntan lotion to reduce harmful radiations. These compounds absorb the UV light in the harmful wavelength range and transform the absorbed radiation energy in harmless energy such as heat [227]. They have to not absorb in the visible light range because they would lead to undesired colour modification. Examples of UV absorbers are the hydroxyl benzophenones and the hydroxyphenyl benzotriazoles since they are able to absorb in the UV wavelength region (280-400 nm) [228]. The UV stabilizers efficiency depends on the absorption characteristics, on the stabilizer concentration and on the thickness of the object. UV radiations decreases in fact exponentially with the distance from the surface, and using 0.1-0.6% of UV stabilizer this value drops to zero nearly at 0.1 mm from the surface [227, 229]. Thus, bulk polymer is well protected but UV would still damage the polymer surface. On the other hand, quenchers stabilizers have a protective effect that is not based on the absorption of damaging UV radiation. In fact, they dissipates the photo-energy absorbed by the polymer chromophores groups inhibiting the successive degradative reactions. The energy is generally dissipated in the form of heat and/or long-wave harmful radiation. In other words, the protective effect of UV quenchers consists in inhibiting the subsequent photochemical reactions of the photo-oxidation and in contrast to the UV absorbers, their efficiency do not significantly depend on polymer product thickness. The most representative quenchers are the the n-butyl-amine even if, for ecological reasons, this product class is being used less and less [227].

4.7 PROMOTION OF BIODEGRADABILITY

Many biopolymers such as PLA, PHAs, PCL, PBS and PBAT can be not easily biodegradable under the common conditions of industrial composter. In addition, the possibility to have articles able to biodegrade also at room temperature condition is nowadays more and more researched since home composting would decrease the amount of the wastes industrially treated. For these reasons, the ways to accelerate or trigger the degradability of environmentally disposable biopolymers after their service are as important as the ways involved for withstand and postpone the degradation. The main ways of promoting the biodegradation of biopolymers are generally two: a) the control of physical features of the biopolymers and b) the use of different biodegradation promoting compounds (Fig.53).
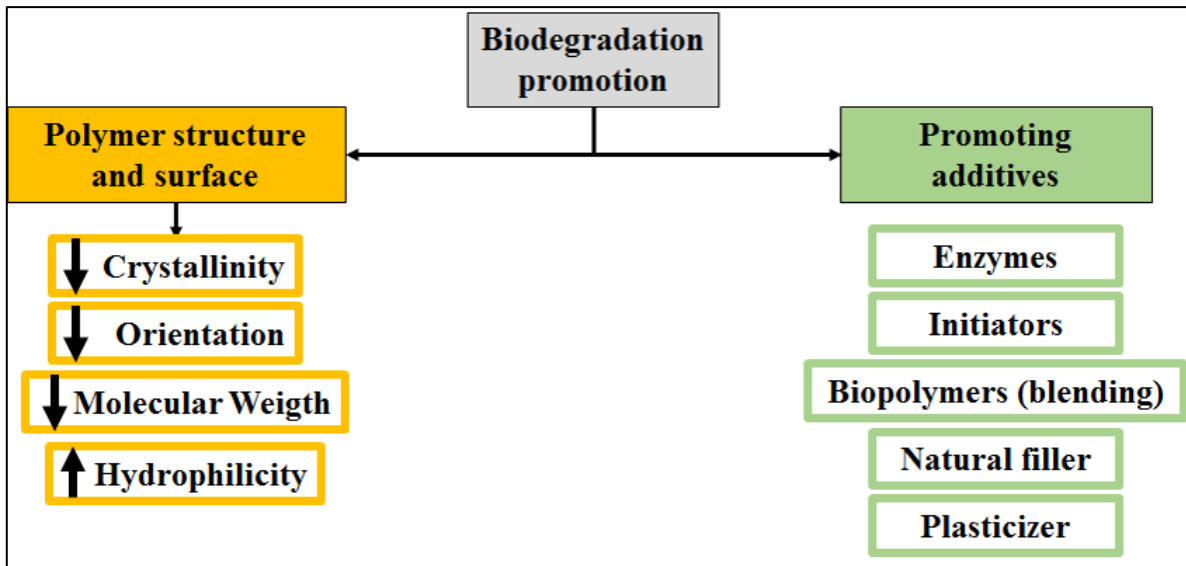
Fig.53 Ways to promote biodegradation.

4.7.1 Control of the physical features of the biopolymer

Physical features of biopolymers have a great influence on the biodegradation rates. These physical features regard the biopolymer molecular weight, morphology and orientation as well as the biopolymer backbone chemical structure and surface. Most of these parameters are governable during the biopolymer synthesis and during the processing steps.

The degradation rate of a biopolymer is generally increased by lowering the molecular weight (M_w) of the polymer. Considering for example the PDLA, it is possible to observe that PDLA with M_w higher than 5000 Da, is typically rigid and hard meanwhile, below that value, PDLA is semisolid and soft, which allows increased water penetration, if compared to high M_w polymers [106, 230]. In addition, low-M_w biopolymers have shorter chain and thus, more acid free ends groups per unit of length that can catalyse the biodegradation are released. Finally, low- M_w biopolymers show enhanced biodegradation rates also because there are more accessible chain groups that can be attacked by microorganisms enzymes [230, 231].

From a morphological point of view, decrease of crystallinity leads to an increase of degradation. In fact, the amorphous phase is more susceptible to degradation than crystalline phase because the molecules are loosely packed and have more "free volume" into which water and/or enzymes can penetrate accelerating significantly the biodegradation [232] . Thus, in the case of the PLA, increasing the ratio of the stereoisomer D-lactide and decreasing the L- form content more degradable polymers are obtainable. Similarly, since PCL degradation time is of nearly 2 years, copolymers of ε-caprolactone with D,L-lactide or with glycolide can be realized to increase the amorphous phase and thus, increase the biodegradation rate [106].

Finally, other factors such as the presence of residual monomer (ca. 2-8% of unreacted cyclic ester) or other impurities, the absence of chain orientation (trough processing) usually shortens the useful life biopolymer.

4.7.2 Biodegradation promoting compounds

From another point of view, biodegradation can be accelerated through the addition of biodegradation promoting compounds. These compounds regard enzymes and microbial nutrients, depolymerisation initiators, plasticizers, other biopolymers with faster biodegradation (blending), capsules and nanoparticles, acidic or basic additives and natural fillers [106]. Generally, through this strategy, the biopolymer biodegradation promotion happens only in processing phase (compounding) and not in the synthesis step. Examples may regard the use of plasticizers such as citrate esters, poly (ethylene glycol) (PEG) and acetyl-tri-n-butyl citrate (ATBC to enhance the PLA biodegradation [233, 234], or blending with low-M_w PCL that can reduce the biodegradation times of PHB [235].

4.7.2.1 Biofiller as biodegradation promoting compounds.

From a large-scale point of view, one of the most interesting strategy regards the use of bio-filler. In fact, as seen in chapter 3, bio-filler would simultaneously enhances also the mechanical properties of the biopolymer in a cost-advantageous way.

There are several works in which different natural fillers have been found able to increase the biodegradation rate of biopolymers [236-239]. Generally, the increased biodegradability of bio-composites can be explained as consequence of three concomitant effects. Firstly, natural fillers increase the biopolymer hydrophilicity [240] and thus, the adsorption and the transport of water within the composite material would be favoured promoting the microbial degradation [241]. Secondly, the not excellent filler-polymer adhesion could create cap-shaped voids between filler and matrix, and this porosity would lead to a preferential channel for the transport of water from the surface to the composite's bulk. In addition, these microstructural defects increase the fragility of composites, favouring their disintegration and resulting in higher contact surfaces suitable by more microorganisms colonies [239]. Finally, many bio-fillers, aggregating in clusters, can decrease the overall crystallinity of the biopolymer facilitating the composite biodegradability since crystalline zones are less accessible for the microorganisms [232, 240].

5. AIM OF THE THESIS

In the introduction, the main drawback of the classical petrochemicals polymers, indeed oil & gas crisis and plastic pollution, have been deeply analyzed, indicating bio-based and/or biodegradable polymers as possible solution of these problems. The synthesis techniques of bio-based polymers have been investigated in chapter 2 where it is has been also pointed out the importance of the raw material substrate. In chapter 3, the main aspects regarding the bio-composites have been discussed, pointing out the potential of this class of material from an environmental, economic and technological point of view. Finally, in chapter 4, degradation and biodegradation have been analyzed showing their importance for the product lifetime and post-life purposes and pointing out how control and manipulate them through (also) natural compounds such as biofiller and natural polyphenols.

Therefore, from an overall point of view, it is possible to notice how natural raw materials could be simultaneously exploited as substrate for polymer synthesis, as polymer reinforcing fillers and as polymer stabilizers or biopolymer biodegradation promotors. Thus, fully natural plastics in which each ingredient such as polymer, antioxidants and reinforcing particles/fibers are derived from renewable agro-wastes are theoretically possible.

In this work, the possibility to exploit the natural by-products exclusively derived from winemaking companies as polymer substrates, stabilizer and reinforcing fillers has been investigated.

Therefore, the aim of the present work is to show the potentiality, the drawbacks, the possible applications and the scaling-up of the main wine wastes within the apparent far plastic worlds in order to extent the empirical and theoretical knowledge of these new bio-plastics elements (Fig.54).
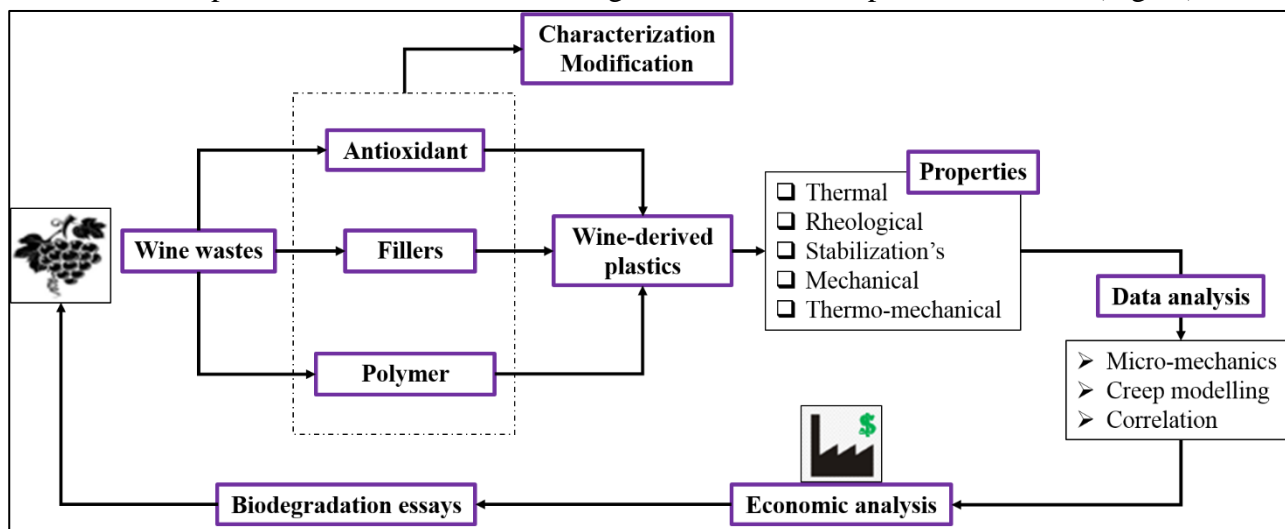
Fig.54 A route to a fully wine-derived plastic.

6. WINE BY-PRODUCTS

6.1 BACKGROUND

Wine is one of the most produced beverage in the world, and it is estimated that in 2018 the worldwide wine production has been of nearly 29 million of tons (Mt). Europe is the producing leader with the 57% of the total production followed by Americas (26%), Asia (7.5%), Oceania (5,4%) and Africa (4.5%) [242] (Fig.55). In terms of country, in 2018, Italy has been the top wine producer with an estimated production of almost 5.4 Mt (18.8% of the total) followed by France and Spain (only these three countries produce almost the 50% of the total worldwide wine). Considering an average wine-grape yield of 0.7 L/kg and an average wine density of 0.99 kg/L, it can be calculated that the processed grapes for winemaking purposes have been nearly of 41 Mton. Considering that total grapes production in 2013 has been of 77 Mt [243] (fourth most produced fruit after water melons, bananas and apples), it can be stated that more than 50% of the world's grapes have been processed into wine and that in the top wine producers country percentages are almost arrived to 100%.
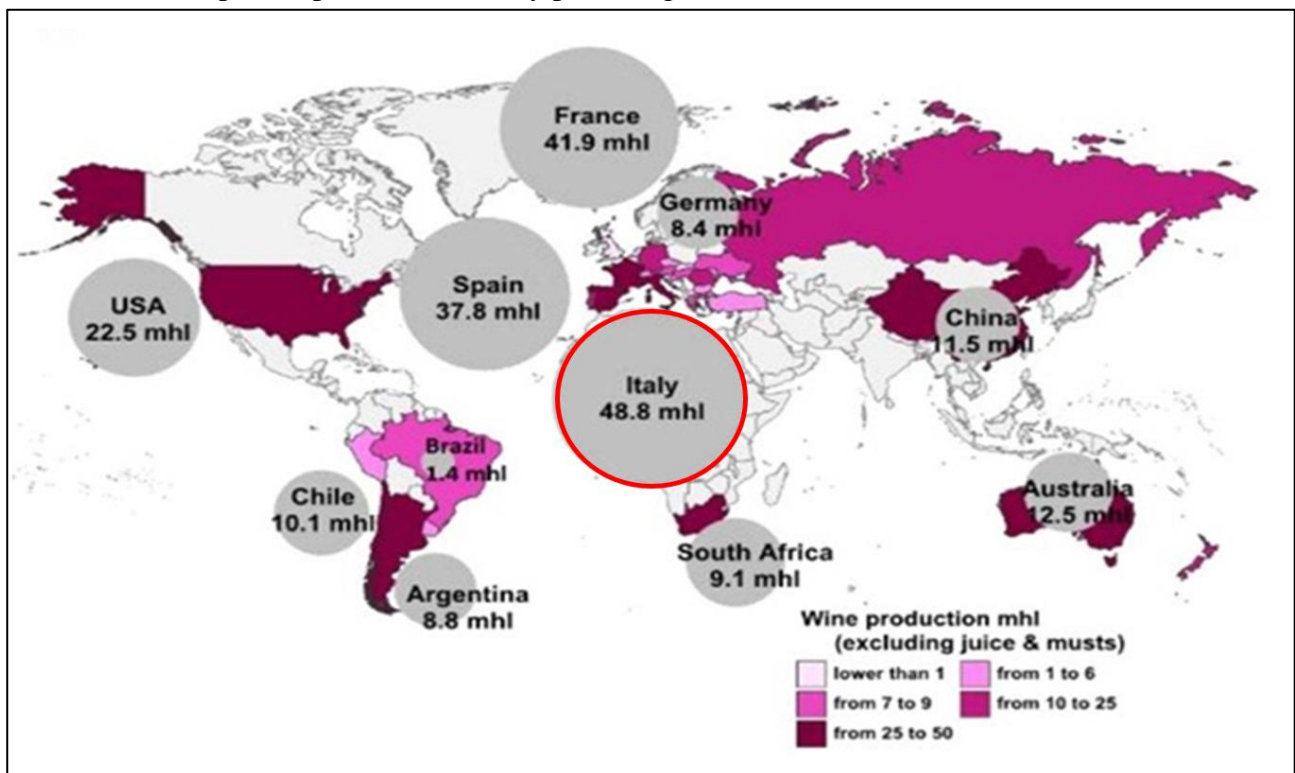
Fig.55 2016 Worldwide wine production. Taken from [244].

Considering the production scheme of red and white wine from the harvest phase to the bottling (Fig.56), it is possible to notice that many wine wastes are produced. At the primary production level, vine shoots (or vine trimming) derive from in-filed intervention in order to preserve the grapevine reproduction. At the processing levels, destemming step is carried out for both red and white wines with the generation of another second residue, the grape stalks (or stems). At this point, grapes are pressed and grape juice is extracted and the solid fractions of this operation, namely grape pomace (or grape marc) is obtained. It is necessary specify that grape pomace is formed by two different solid wastes present in 1:1 (w/w) ratio: the grape seeds and the grape peels (or skins). Grape pomace is immediately discarded in the case of white wines, meanwhile in the case of red wines is left with the

juice (now called must) for a certain fraction of the fermentation period in order to allow the grape constituents extraction. Nevertheless, after this maceration step, grape pomace is removed from the must and pressed, becoming a wine by-product. After completion of alcoholic and/or malolactic fermentations, the last wine waste, namely wine lees, is collected by one or more of the following steps: decanting (or clarification), tartaric stabilization and filtration.
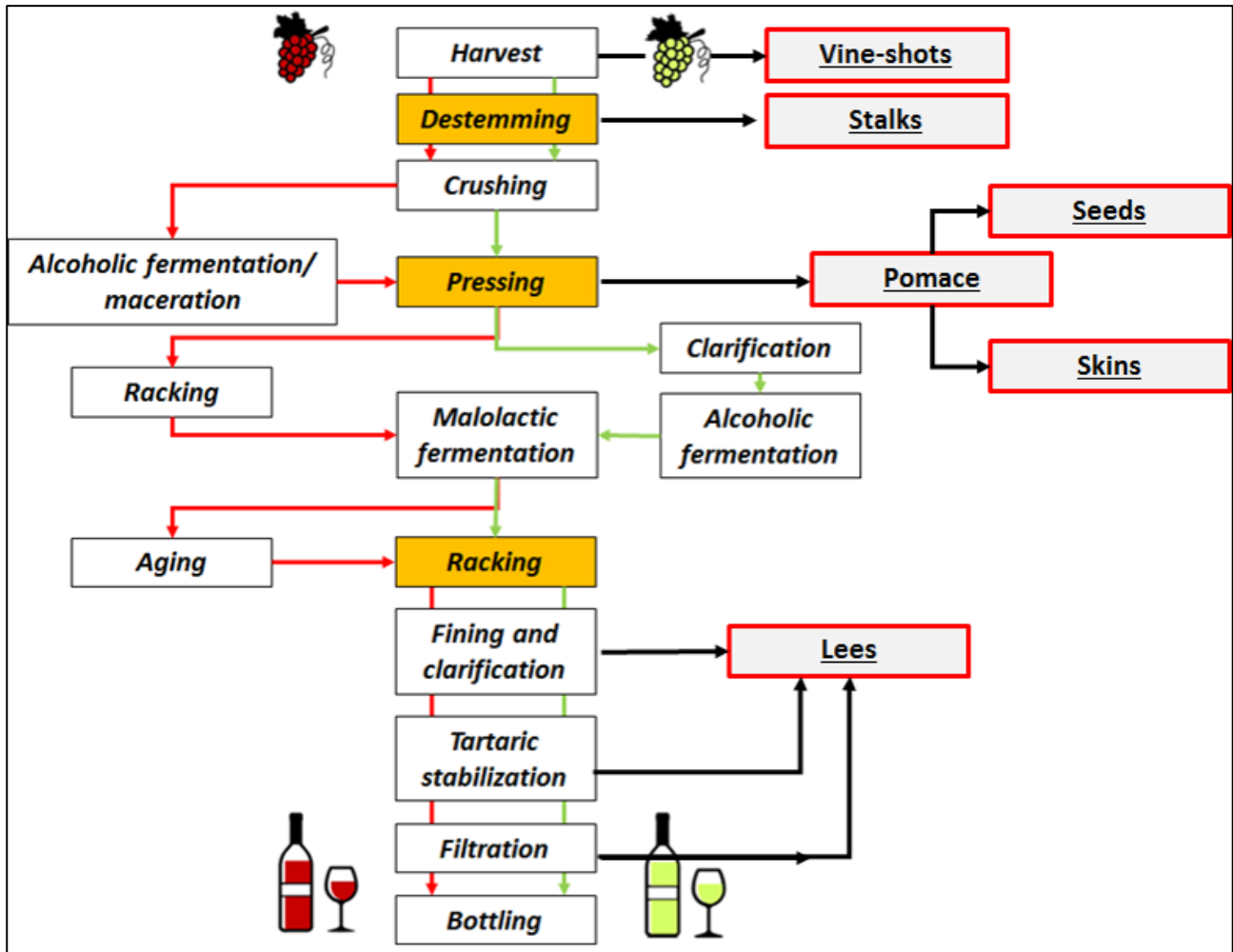
Fig.56 Red and white wine processes and obtainment of the solid wine wastes. Adapted from [244].

Summarizing, the solid by-products obtained during the wine-making processes are: vine shoots, grape stalks, grape pomace (formed by grape peels and grape seeds (1:1 w/w) and wine lees. Considering their generation rate expressed as kg of waste generated for each kg of processed grape it is possible to notice that their production's volumes in 2018 have been very impressive (Table 15), pointing out the possibility to scale up in large scale their use.

Table 15 Grape, wine and wine waste production. Calculation have been made considering [242, 244, 245] data.

	%.wt*	World [10^3ton]	Europe [10^3ton]	Italy [10^3ton]	Emilia-Romagna [10^3ton]
Grape processed	-	41300	26700	7800	1200
Wine	-	28900	18700	5400	800
Vine shoots	1.4-2 t/ha	5500-7800	3560-5050	1030-1460	150-220

Grape stalks	3-5	1240-2070	800-1340	230-390	35-60
Grape seeds	10-12.5	4130-5170	2675-3345	775-970	115-144
Grape peels	10-12.5	4130-5170	2675-3345	775-970	115-144
Wine leeds	2-6	830-2500	530-1600	160-470	20-70

Until recently, these wine wastes have been generally destined to: a) distillation, b) landfilling, c) incineration and d) land-spreading operations. In particular, grape stalks have been mainly destined to land-spreading (76% in Italy, 55% in Spain and 40% in France), disposed in landfill (50% Greece) or destroyed by incineration (36% in France). Grape pomace wastes has been mainly destinted to distillation (100% Italy, 90% France, 30-60% Spain) and land-spreading (50% in Spain) meanwhile in Greece, the 67% has gone to landfill and the 33% has been sold as animal fodder. Finally, wine lees have been generally distilled in all considered country. Nevertheless, these conventional uses of the wine wastes have been severely reconsidered in the past years. As example, because of their low pH, high organic matter and high concentrations of macronutrients wine wastes are not ideal fertilizers without expensive pre-treatments or conditioning steps [246]. Similarly, wine by-products can inhibit or modify the germination properties when used as amendments and landfilling is strongly discouraged since wine wastes affect the soil erosion and decrease the groundwater quality because of the high organic matter losses [247, 248]. As animal feed, grape pomace represents a problem because their high amount of polyphenols that bonding with proteins, lead to compounds not suitable for nutritional goals [249, 250]. In addition, with the 2013, Reg. No 1308/2013 - European Decree in matter of wine wastes disposal rules – distillation of wine by-products has definitely stopped to be a remunerative option for the wine companies [244]. Therefore for these reasons, connected with the necessity to invest in new sustainable and renewable materials, wine wastes have been started to be investigated also within other different sectors.

6.2 COMPOSITION AND NEW USES OF THE WINE WASTES

In this section, the chemical composition and the new applications of the wine wastes will be described. In terms of composition, it can be said that, among all compounds, polyphenols represent one of the most abundant and surely, the most high-valued products findable within the wine wastes. Polyphenols are a natural family of more than 5000 compounds chemically characterized by the presence of several phenol rings and hydroxyl groups. They are originated directly by plants and fruits (2-3 mg/ g of fresh fruit) [251, 252] as secondary metabolites with the aim to defense the plant itself from the UV lights and from the pathogens aggressions [253].

Natural polyphenols are generally classified in: a) Flavonoids, b) non-Flavonoids and c) Phenolic acids (Fig.57). Within wine wastes, most present and abundant polyphenols are flavanols (catechins and gallocatechin), anthocyanidins, stilbenes and hydrobenzoic acids. In addition, it is useful mention that catechins can form oligomeric compounds called condensed tannins (or proanthocyanidinis) with a polymerization degree ranging from 2.4 to 16.7 [254] and similarly, hydrobenzoic acids as gallic and ellagic acid can be assembled in oligomeric polyphenols called hydrolysable tannin. The most important polyphenolic structures have been reported in Fig.58.
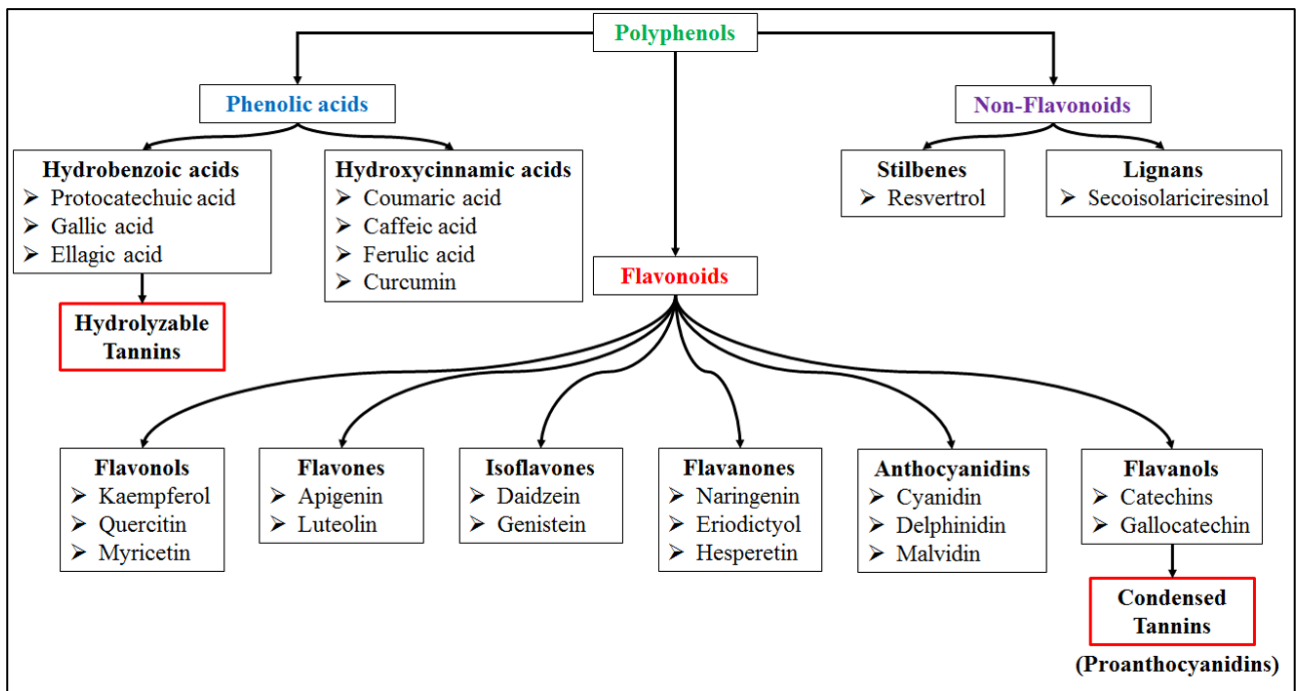
Fig.57 Polyphenols classification.
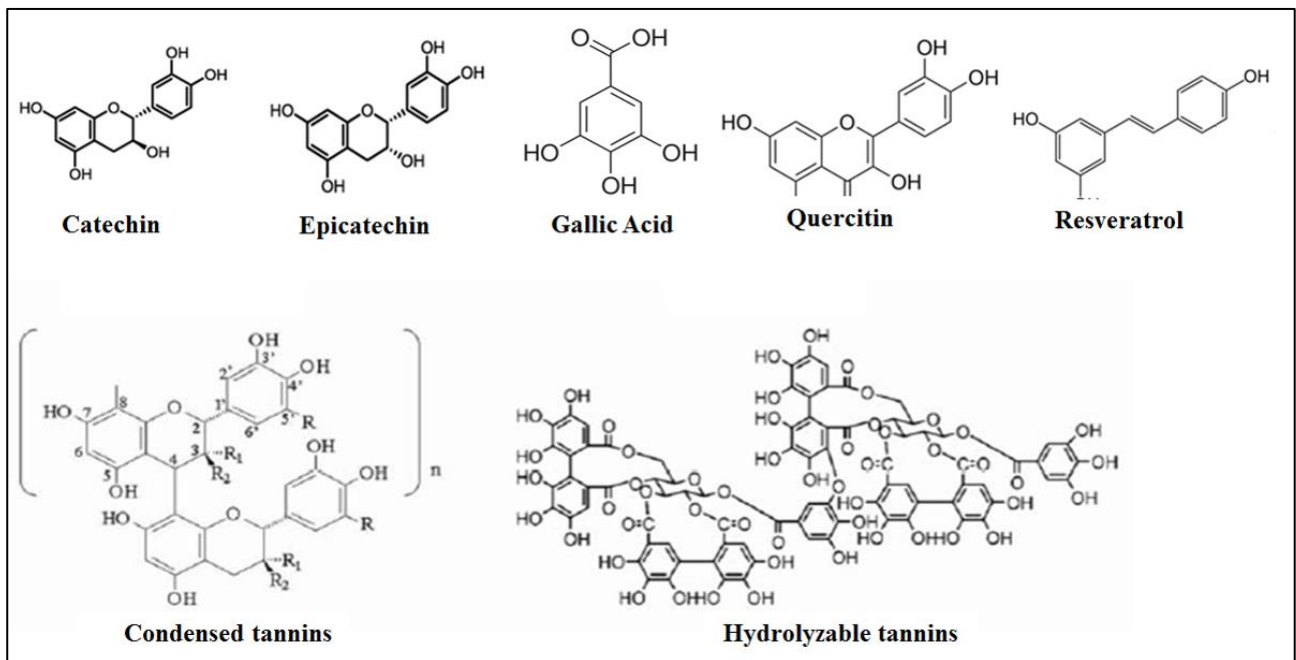
Fig.58 Chemical structure of several polpyhenols.

6.2.1 Vine shoots

Vine shoots are a non-food lignocellulosic agricultural residue with a yield of approximately 1.4-2 ton/ha per year [255] and they represent the major amount of the wastes obtained in viticulture. They are generated during the vine pruning, the necessary process that equilibrates the growth of vegetation and fruit and that influence the grape quality and quantity. The main component of vine shoots are cellulose (34%), hemicellulose (27%) and lignin (19%) [256]. Vine shoots have been commonly destined to the land-spreading or burned in the field. Recently, they have been investigated as source

of antioxidant [257] and bio-stimulating extracts [258], as woody flavorings [259] , as absorber of toxic compounds [260] and as biomass for energy production [261].

6.2.2 Grape stalks

Grape stalks represent about the 14% in weight of the total winemaking solid wastes and 3-5% of the processed grapes [244]. They are lignocellulosic materials with a reported composition of 17%-26% lignin, 20%-30% cellulose, 15%-20% hemicelluloses, 6%-9% ash and with high amounts of tannins (around 16%) [262, 263]. These tannins are structurally associated with lignin and for this reason the extraction of pure cellulose from grape stalks is not easy. Tannins represent the 80% of the stalks' phenolic compounds and their average of polymerization is of nearly 9 [264]. Most present polyphenols in stalks are flavanols (catechin, gallocatechin and condensed tannins) as well as ellagitannins (hydrolysable tannins). The uses of grape stalks have been and are similar to the ones previously described for vine shoots since their similar composition. Until recently, grape stalks were generally land-spread, burned or land-filled meanwhile today, researches are valorising grape stalks as absorbers of toxic compounds [265], as fermentable biomass for bio-ethanol production [266], as substrate for the preparation of activated carbons [267] and as source of high-valued antioxidants [248].

6.2.3 Grape pomace

Grape pomace is the main fraction among the solid wine wastes derived from the winemaking processes steps. It represent up to 60% of the wine solid wastes and 20-25% of the processed grapes. They are formed by a mixture (generally 1:1 in weight) of peels and seeds, and sometimes residual stalks are also findable [244]. When grape pomace is derived from red winemaking processes, it is a fermented waste in which generally less phenolic compounds and sugars are present because of the extraction processes occurred during the fermentation. On the contrary, if obtained from white wines (or grape juices), grape pomace is unfermented and potentially richer in sugars and in polyphenols. Anyway, this material is a complex substrate composed by 30% of neutral polysaccharides, 20% of acid pectic substances, 15% of insoluble proanthocyanidins (condensed tannins), lignin, proteins and other polyphenols. Polyphenols and proteins are often cross-linked to the lignin-carbohydrate fractions [268]. As previously said, grape pomace have been almost exclusively destined to distillation plants (especially in the three top producer countries: Italy, France and Spain). Nowadays, there is a great interest in the recovery of high-valued products such as polyphenols [269], colorant pigments [270] and organic acids as maleic, citric and tartaric [271]. From another hand, because the high quantity of sugars, grape pomace are also investigated as fermentative substrate [272-274] and as substrate for the pullulan polymer production [275].

6.2.4 Grape peels

Grape peels (or skins) represent nearly the 50% in weight of the grape pomace, even if the ratio of peels and seeds can significantly vary depending on the grape variety. Grape skins are formed by interesting contents of proteins (5-12%), ashes (2-8%), soluble sugars (from 1% up to 70%, strongly depending on the applied wine process), and of polyphenols and dietary fibers. The total dietary fiber content is almost the 60% of the dry matter, and nearly the 98.5% are insoluble fibers [276]. Grape peels are also well-known for their important content of polyphenols. These natural compounds are present both within and outside the cell-wall. Cell-wall polyphenols are bound to cellulose and hemi-

cellulose trough hydrophobic interactions and hydrogen bonds and therefore they can be scarcely extracted. On the other hand, non-cell-wall polyphenols (they include also the phenols present in the vacuoles and those associated with the nucleus), being not bounded, are more easily extractable [277]. From a qualitative point of view, the peels polyphenols are characterized by many condensed tannins with high polymerization degrees (average value of 28 and maximum value of 80 [244]) and low amounts of hydrolyzable tannins (nearly 5%). In addition, not negligible amounts of anthocyanins such as delphinidin, cyaniding and malvidin are findable within wine peels [244]. Finally, regarding the new techniques of valorization, it is possible to state that they are the same (or very similar) to the ones previously described for the grape pomace.

6.2.5 Grape seeds

Grape seeds, the other fraction of grape pomace, typically contain high contents of fiber (48%), proteins (11.5%) and lipids (13-15%) [278]. Wine seed oil contain generally high tocols and unsaturated fatty acids such as linoleic and oleic acids [279]. Within wine seeds are also present important quantitatives of polyphenols that are generally formed by the same constitutive units of the peels polyphenols (catechins and gallocatechins) but that have lower polymerization degrees since they tend to be in monomeric form. On the other hand, the content of acid gallic derived polyphenols (hydrolyzable tannins) are more than 30% higher than those findable within the skins and the stalks [277]. From an applicative point of view, wine seeds have been generally exploited for the oil recovery, that is used as food ingredient, and in other cases they have been directly in land burned to avoid expensive transportation costs. Nowadays, research is looking at wine seeds as an interesting source of antioxidants for the food, farmaceutical and cosmetic fields [280-282], as raw material for the fabbrication of green graphene [283] and/or as source of proteins [244].

6.2.6 Wine lees

Wine lees are defined as the residue formed at the bottom of recipients containing wine, after fermentation, during storage or after other allowed treatments as well as the residue obtained by filtration or centrifugation of this product [244, 284] (Council Regulation (EEC) No. 337/79 [285]). They represent the 2-6% of the processed grapes (in some cases also the 7.5% [286]) and, depending on their particle size and on the number of raking processes, wine lees can classified as heavy and light lees. In each case, wine lees are mainly composed by microorganisms (yeast and bacteria), insoluble carbohydrates (from cellulosic and hemi-cellulosic fractions), phenolic compounds, lignin, proteins, organic salts (mainly tartrates) [244]. Because they are also generated during the clarification and filtration treatments, significant inorganic fractions can be findable within wine lees as consequence of the fact that bentonite and kaolin are usually used in those winemaking steps. Wine lees have been (and also today) generally implied as feedstock for alcohol distillation and for tartaric acid recovery [287]. Nevertheless, recent wine lees applications have involved their antioxidant extraction [288], their use in food as ice-cream ingredients [289] and their exploitation as biochar for metals absorption [290].

7. EXPERIMENTAL SECTION

7.1 RESULT'S KEY OF LECTURE

In the present work, each solid wine waste has been investigated following different approaches and using several characterization techniques. As claimed in the Aim chapter (5), it is possible to notice from Fig. 59 that three different valorizing approaches have been adopted. Wine wastes have been investigated as a) polymer antioxidants, b) polymer reinforcing filler and in one case as c) polymer substrate. Each tested wine waste has been also characterized in terms of particle size, density, moisture content, thermal stability, organic and inorganic fractions, sugar content and/or morphologically in order to collect important information on their intrinsic properties. Among all the work reported in Fig.59, only five case-studies have been here reported in order to not overload the work. Therefore, the results and discussions as well as the interpretations of the five selected p have been shown within the sections 7.2-7.6, meanwhile their main features and highlight have been reported in Table 16. Finally, in the Conclusion's chapter (8), the obtained results of each investigated wine waste have been summarized, evidencing their scaling up potentials and their main drawbacks.
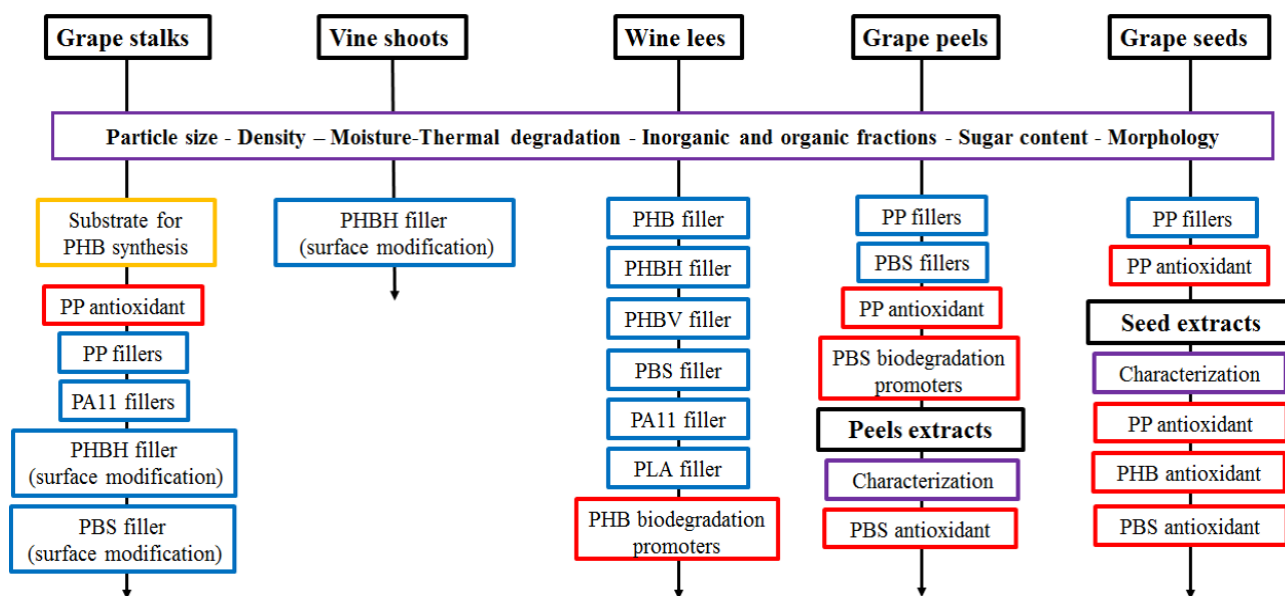
Fig.59 Work scheme: wine wastes as polymer fermentative substrate, antioxidants and reinforcing fillers.

Table 16 Selected works.

1) Title: A comparative study of different winemaking by-products derived additives on oxidation stability, mechanical and thermal proprieties of polypropylene. **Stage**: Published [291] **Wine wastes**: Grape stalks, grape peels, grape seeds and a grape seed tannin extract. **Polymer**: Unstabilized PP **Topics:** Wine wastes characterization – Wine wastes effect on PP thermal and mechanical properties – Wine wastes effect on thermal short-term PP stabilization. **Section**: 7.2
2) **Title**: Thermal and UV aging of polypropylene stabilized by wine seeds wastes and their extracts **Stage**: Published [292] **Wine wastes**: Grape seeds and seed extracts. **Polymer**: Unstabilized PP **Topics:** Seed extracts characterization– Seed extracts and wine seeds effect on thermal and UV long-term PP stabilization – Discussion of the polyphenol structure's role. **Section**: 7.3
3) **Title**: Effect of the wine lees wastes as cost-advantage and natural fillers on the thermal and mechanical properties of poly(3-hydroxybutyrate-*co*-hydroxyhexanoate) (PHBH) and poly(3-hydroxybutyrate-*co*-hydroxyvalerate) (PHBV) **Stage**: Published [177] **Wine wastes**: Wine lees **Polymers**: PHBH and PHBV **Topics:** Wine lees characterization – Wine lees effect on PHBH and PHBV properties – Micro-mechanics – Silane role – Economic essay **Section**: 7.4
4) **Title**: Thermo-mechanical properties and creep modelling of wine lees filled Polyamide 11 (PA11) and Polybutylene succinate (PBS) bio-composites **Stage**: Published [157] **Wine wastes**: wine lees **Polymer**: PA11 and PBS **Topics:** Wine lees characterization – Wine lees effect on PA11 and PBS properties – Creep modelling – Storage modulus prediction formula. **Section**: 7.5
5) **Title**: How modulate thermal stabilization, mechanical reinforcement and biodegradation of Poly(3-hydroxybutyrate) (PHB) using wine derived additives **Stage**: Submitted **Wine wastes**: Seed extracts and wine lees **Polymer**: Unstabilized PHB **Topics:** Wine lees effect on mechanical PHB properties – Seed extracts effect on PHB thermal stability – Wine lees and seed extracts effects on PHB biodegradation. **Section**: 7.6

7.2 WINE WASTES AS POLYPROPYLENE REINFORCING FILLERS AND SHORT-TERM THERMAL STABILIZERS

7.2.1 Materials and methods

Materials

Un-stabilized isotactic PP (MFI 12 g/10 min) has been kindly supplied in the form of a reactor powder by LyondellBasell. White and red grape peels (Pe), white grape stalks (St) and white and red seeds (Se) from wine processing wastes, and the commercial seed tannin extract powder (T) have been obtained from the winery Cevico Group S.R.L, Lugo (RA), Italy during the 2016 harvest and wine-making. Materials have been labelled as follow: PP XY, where X is a number indicating the % in weight of the additive, and Y is the letter(s) indicating the additive typology. "PP powd" and" "PP proc" refer to the virgin PP powder and to the processed PP respectively.

Additive characterization

Solid wine wastes have been hand-washed with distilled water and a cloth in order to remove smug and other impurities. Then they have been oven-dried at 65 °C, monitoring at regular intervals the weight, until it has been constant (48h) and final moisture has been calculated in this phase. Despite the drying treatment can affect the composition and the structure of the wastes it is reasonable to suppose that at 65°C no relevant chemical modification occurs, especially regarding the polyphenol content [293]. Finally, dried wine wastes have been grounded in a batch analytical mill with liquid nitrogen. The different powders have been manually sieved and different granulometry observed.For each powder, solvent extraction has been conducted. The extraction has been carried out for 90 min at 55 °C; the solvent/solid ratio has been of 2 ml g^{-1} and the used solvent has been ethanol. The total polyphenol content of these extracts has been kindly evaluated by Cevico Group S.R.L, Lugo (RA). Extracts have been properly diluted with distilled water and the absorbance has been directly read at 280 nm in a UV/VIS Jasco V-730 spectrophotometer. Total polyphenol content has been expressed as weight percentage referring to the dry matter, and as equivalent tannic acid. For this step, a calibration curve obtained with different concentration tannic acid solution has been used.

Sample preparation

Additives have been mixed at 6% by weight with PP in a Haake Polylab Rheomix internal mixer. Virgin PP powder has been processed in the same conditions to obtain the reference sample for comparisons. Operating conditions have been: 10 minutes of mixing, 180 °C and 32 rpm as rotors speed. The mixed materials have been used for thermal and stability measurements, processed in a hot plate hydraulic press (Carver) to obtain rectangular samples used for the SEM analysis and for DMA tests and processed by injection molding to obtain specimens for mechanical characterization of tensile proprieties.

Experimental techniques

Thermal proprieties

Thermal proprieties have been evaluated by Differential Scanning Calorimetry (DSC). DSC measurements have been performed by a DSC TA 2010, using 8 ± 1 mg of sample. The chamber

has been purged by nitrogen at 50 ml min-1. Each sample have been firstly heated from 25°C to 200 °C at 20 °C min^{-1},to erase the previous thermal history. Therefore, after 2 minutes, samples have been cooled from 200°C to 25°C at 20 °C min^{-1} and then, after 2 minutes, re-heated from 20°C to 200°C at 20°C/min. The crystallization temperature T_c and crystallization enthalpy T_c have been measured in the cooling cycle, while melting temperature T_m and enthalpy of fusion H_m have been obtained in the second heating cycle. The enthalpy values have been calculated considering the weight fraction occupied by additives. Crystallinity percentage has been evaluated considering the value of 208 J g^{-1} (average of [294, 295]) for the 100% crystalline PP melting enthalpy.

Mechanical proprieties

Tensile tests have been performed by means of the INSTRON 5567 dynamometer equipped with a 1 kN load cell and a 25 mm extensimeter. Dumbbell-shaped specimens according to technical standard ISO527 (type 1BA) have been used. Tests have been performed at room temperature with a 10 mm min^{-1} clamp separation rate. The reported data are the average values of at least six determinations. TA DMA Q800 instrument in the single cantilever flexural configuration has been used to evaluate the dynamic mechanical behavior of the different samples. Sizes of the rectangular specimens have been $2 \times 10 \times 17$ mm^3. The tests have been run at a heating rate of 3 °C min^{-1} from -40 °C to 80 °C. Oscillation frequency and strain have been 1 Hz and 0.1%, respectively. Glass transition temperatures (T_g) have been evaluated as the maximum value of the tan d curves. The creep proprieties of the samples have been also measured on the same instrument with same size specimens. The creep tests have been carried out at temperature ranging from 20 °C to 80 °C at 20 °C temperature increments. At each temperature, samples have been firstly loaded for 10 min by 1 MPa stress and then followed by a 20 minutes relaxation. Master curves have been generated from the creep data using the William-Landel-Ferry (WLF) equations at a reference temperature of 20 °C.

Morphological proprieties

Morphology, adhesion, distribution and dispersion of the additives on the samples, have been observed with an environmental Scanning Electron Microscope, SEM (ESEM Quanta FEI 2000). Rectangular specimens, identical to the ones used for the DMA analysis, have been broken in liquid nitrogen. The cross section of the specimen has been covered by a 10 nm thickness gold layer (Gold Sputter Coater – Emitech K550). The obtained surfaces have been observed with the SEM operating in low-vacuum conditions.

Thermal stability behavior

The thermal stability of samples has been investigated by Oxidation Induction Time (OIT) and Oxidation Onset Temperature (OOT) tests performed with the TA DSC 2010 and by thermogravimetric analysis (TGA) performed with the TA TGA Q50. OIT values have been measured in open Al pans, containing 4.8 ± 0.5 mg of sample. The material has been then heated under nitrogen flow (50 ml min^{-1}) with a rate of 15 °C min^{-1}, from room temperature to the set temperature (200 °C or 175 °C), and after 6 min of isothermal the purging gas have been switched to air. The heat flow has been recorded in isothermal conditions as function of the time. The beginning of oxidation has coincided with the sudden increase of the slope of the exothermal heat flow. The time interval elapsed between the gases switch and the exothermic degradative peak has been considered as the OIT, and it has been evaluated by the tangent method according to the ISO 11357-

6. OOT values have been also measured in open Al pans, containing 4.8 ± 0.5 mg of sample. After 5 min of room temperature isothermal under nitrogen flow (50 ml min^{-1}), heating has been started at 20°C min^{-1} and in the same moment, nitrogen has been switched to air. OOT has been evaluated as the temperature at which begin the increase of slope of the exothermal degradative peak. Thermogravimetric analysis (TGA) have been conducted on 15 ± 5 mg of sample using a ramp temperature of 15 °C min^{-1} from 50 °C to 650 °C. Tests have been conducted both in inert atmosphere (nitrogen, 50 ml min^{-1}) and in oxidative atmosphere (oxygen, 50 ml min^{-1}). Temperatures at 5 wt.% loss ($T_{5\%}$) and at 15 wt.% loss ($T_{15\%}$), residues at 650 °C (Res_{650}) and the peak temperatures of the degradation (T_{peak}) have been extrapolated from the graphs for both atmosphere conditions. T_{peak} is the temperature at which the maximum of the derivate of the weight in respect to temperature is observed.

7.2.2 Results and discussion

7.2.2.1 Additives' characterization

Table 17 reports the additives' mean size diameter, the total polyphenol content (TP), the moisture data (% w/w) and the TGA data of temperatures at 15 wt. % loss ($T_{15\%}$) and of percentage residue at 650 °C (Res_{650}) of wine by-products additives under nitrogen and oxygen atmosphere, respectively.

Table 17 Additives' diameter, moisture content (%), total polyphenol content (TP) and TGA data

Material	Diameter [mm]	TP [% wt.]	Moisture (%)	Nitrogen atmosphere		Oxygen atmosphere	
				$T_{15\%}$ [°C]	Res_{650}[%wt]	$T_{15\%}$ [°C]	Res_{650}[%wt]
Se	0.75	0.95	24	267	31.0	261	3.6
Pe	0.35	0.64	47	192	29.2	190	6.0
St	0.20	1.40	22	208	32.0	209	8.3
T	0.15	30.0	-	269	49.8	268	1.1

Additives show no differences regarding the mean size diameter except for the seed (Se) powder that exhibits the highest value, and this can be explained by the important presence of both oleic and linoleic acids [296] in the wine seeds that can aggregate the particles. The total polyphenol content of each wine by-product (Se, St, Pe) is approximately around at 1%wt, while the commercial seed tannin extract (T) has a concentration of polyphenols equal to 30% wt. Despite both extraction conditions and total polyphenol evaluation method can affect the result and be more or less suitable according to the investigated substance characteristics [248, 297], the deep gap evaluated between by-products and commercial powder does not leave room to doubts in this case. Table 18 shows the other constituents typically present in the wine wastes. Despite these data have not been obtained by the wine wastes used in this work, it is reasonable to believe that the eventual differences are not bigger than the ones that exist in the same wastes from one year to another. In Fig.60, TGA curves under nitrogen and oxygen respectively are reported. It is possible to notice that seeds "Se" and tannin extract "T" start their weight loss at about 60-70 °C later than stalks "St" and peels "Pe". $T_{15\%}$ of each additive is the same whatever the purging gas and always higher than the PP melt temperature. For this reason, wine additives are stable to thermal oxidation and are suitable to be mixed with the PP. The wine by-products additives residues at 650 °C under nitrogen are about 30-50 % in weight (Table

17), while residues of 1-8 % wt. are observed under oxygen. This gap is due by the combustion in presence of oxygen of the organic additives that leads to an instantaneous and huge loss of weight (Fig. 60b). Stalks "St" is the additive that suffer earlier this phenomena (at about 250 °C) because of its important composition of cellulose, hemicellulose and lignin [262].

Table 18 Main constituent present in the different solid wine wastes.

Peels [276, 298]		Seeds [298-300]		Stalks [262, 263]	
Constituent	[% w/w]	Constituent	[% w/w]	Constituent	[% w/w]
Ash	2-8	Carbohydrates	11.8	Ash	6-9
Carbohydrates	12.5	Complex Polyphenols	7	Cellulose	20-30
Dietary fiber	60	Dietary fiber	40-50	Hemicellulose	3-20
Lipids	5	Lipids	15	Lignin	17-26
Protein	5-12	Protein	11	Protein	6
Soluble sugars	1-70			Tannin	16
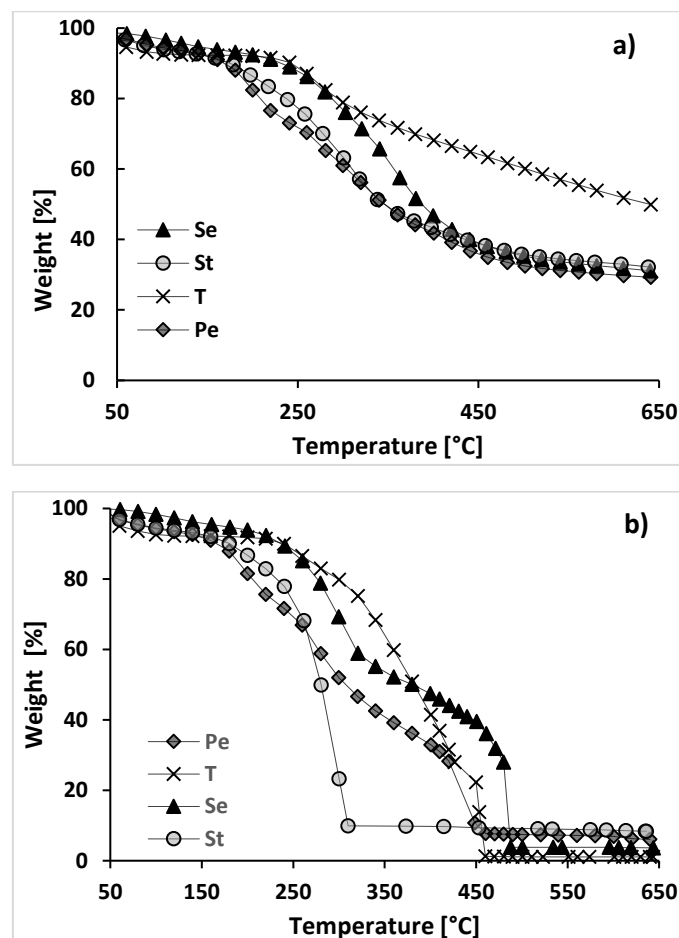
Fig.60 TGA curves of wine wastes derived additives: a) under nitrogen gas flow; b) under oxygen gas flow.

7.2.2.2 Thermal proprieties: DSC

Fig.61 reports the DSC curves of the cooling step after the thermal history reset and the second heating scan of the different compounded materials. Table 19 lists for each material the crystallization temperatures T_c and the melting temperatures T_m and melting enthalpies H_m and crystallization enthalpies H_c. Referring to curves of Fig.61, it is evident that the crystallization and melting phenomena are not significantly influenced by the presence of the additive. Moreover, also the typology of wine waste derived additive does not exhibit any particular behavior. Table 19 shows how the T_cs of compounded materials are lower than PP one, but the maximum deviation ("Se") is limited to 2.1 °C. T_ms are always higher, but also in this case never more than 1.5 °C ("Pe"). These facts demonstrate how characteristics transition temperatures of PP are not affected by the natural additives in accordance to other similar work with PP [301]. Melting enthalpies of compounded materials are lower than the one of neat PP as well as the percentage of crystallinity that results 15% lower than neat PP. The decreasing of the crystallinity is in perfect accord with a similar study on PHB where crystallinity of compounded materials has been observed 10% lower of the neat polymer [302].

Table 19 DSC data comparison between neat PP and compounded PPs.

Material	T_c [°C]	H_c [J g^{-1}]	T_m [°C]	H_m [J g^{-1}]	% Crystallinity
PP powd	115.1	100.6	165.6	145.8	70
PP 6Se	113.0	94.0	166.7	106.4	55
PP 6St	113.4	93.7	167.6	109.4	56
PP 6Pe	113.7	104.3	167.1	115.0	59
PP 6T	114.7	100.7	165.7	112.6	58
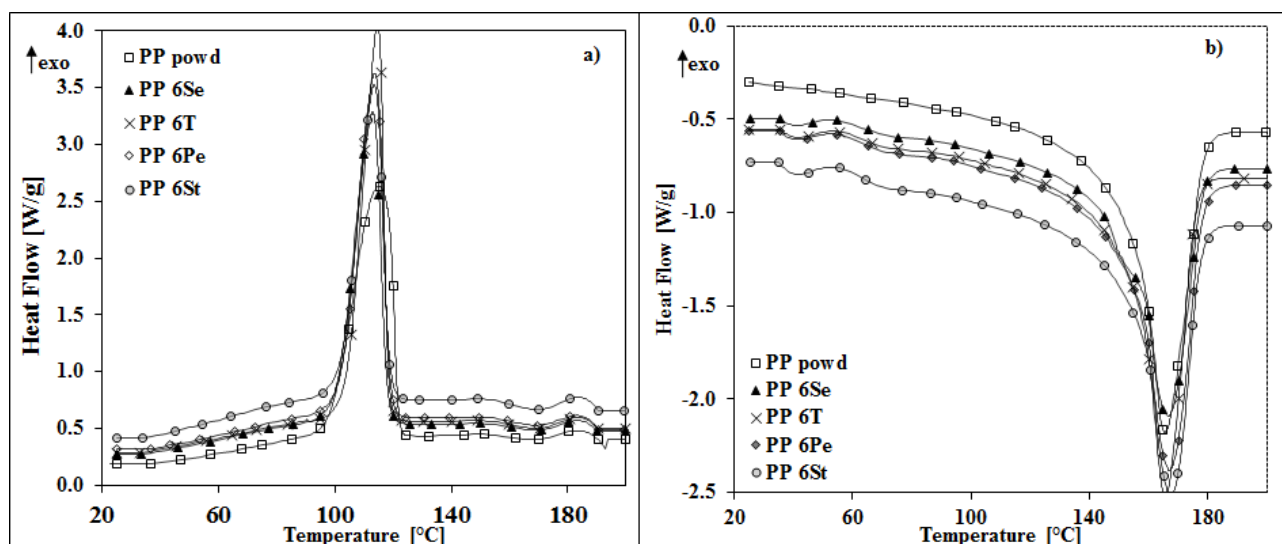
Fig.61 Cooling step (a) and second heating scan (b) of "PP powd" and PP based samples.

7.2.2.3 Mechanical proprieties: DMA, creep tests, tensile tests.

Table 20 Glass transition temperatures (T_g), storage modulus at different temperatures (E'), Young modulus (E), tensile strength at the yield (σ_Y) and yield strain (ε_Y).

Material	T_g	E' Storage Modulus [MPa]			E	σ_Y	ε_Y

	[°C]	-20 °C	0 °C	25 °C	60 °C	[MPa]	[MPa]	[%]
PP proc	7.6	3460	2779	1749	1036	1544±191	31.9±0.9	8.6±0.7
PP 6Se	8.1	4358	3568	2371	1355	1310±320	27.3±0.8	9.0±0.7
PP 6St	12.1	3762	3218	2111	1224	1680±249	30.8±0.5	7.1±0.5
PP 6Pe	8.7	3865	3113	2032	1134	1602±280	28.6±0.7	7.6±0.9
PP 6T	14.8	3290	2899	1925	1201	1460±149	29.7±0.7	7.8±0.3

In Table 20, the glass temperatures (T_g) and the storage modulus (E') at different temperatures (-20, 0, 25, 60 °C) obtained by DMA as well as the Young's Modulus (E), the yield strength (σ_Y) and yield deformation (ε_Y) values obtained by tensile tests are reported. From Table 20 is also possible to assert that additives slightly increase the T_g values leading to a stiffening of the amorphous phase of PP. Among all the additives, tannin extract powder "T" is the additive that more affects the glass transition temperature compared to "PP powd" (+ 7 °C), while seed and peel additives are the less influential. The improved stiffness of the material could be explained by the restriction of the chain mobility of the PP through the formation of hydrogen bonds between additive's hydroxyl and polymer's carbonyl groups formed by oxidation during the internal mixing and the press-molding steps [303, 304]. This fact is also confirmed by the storage modulus E' values that result always higher than the neat PP ones for each different temperature. The additive "Se" shows the highest storage modulus values and this could appear in contrast with data obtained by tensile tests, where additive Se exhibits the lowest yield strength value σ_Y (-14.4%). Nevertheless, the different processes used for the preparation of DMA and tensile test specimens (press molding and injection molding, respectively) do not allow justified comparisons. Concerning yield strength values σ_Y, compounded materials show practically the same values of the neat PP and the slight decrease can be probably explained by the reduced crystallinity of the filled samples. The Young Modulus E and elongation at yield ε_Y values are again not significantly altered and again additive "Se" lead to a slightly more ductile material, while others additives to a slightly stiffer material. Nevertheless, no important differences on mechanical proprieties and among additives are observed. Conversely, creep resistance is noteworthy enhanced by the natural wine derived additives. In Fig.62, the compliance values obtained after 10 minutes ($J_{C, 10\,min}$) creep tests at four different temperatures (20, 40, 60, 80 °C) are shown. As expected, an increase in temperature have been resulted in higher chain mobility and then in high creep deformations for all materials [305], but it is interesting to notice that from 60 °C the difference between neat PP and the others samples starts to increase. If no different behavior is observed at 20 °C and 40 °C, it is clear how wine-additives increase creep resistance of PP at higher temperature. In particular, seed additive "Se" implies the best creep resistance for any temperatures.
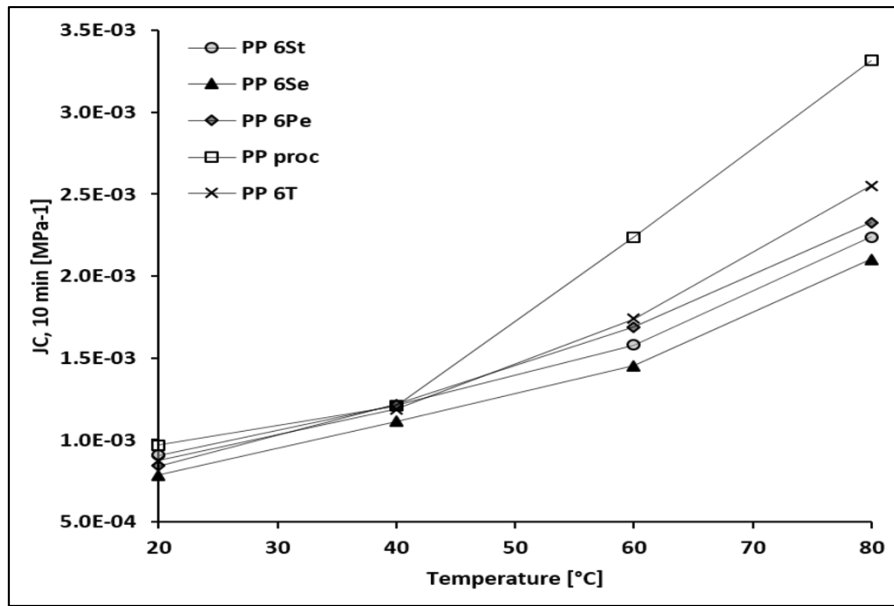
Fig.62. Values of compliance after 10 minutes as function of temperature for unfilled and filled PP samples.

In order to predict compliance behavior as longer times function time-temperature superposition principle has been applied to creep test data. In Fig.63, master curves of PP-based samples at 20 °C are reported. Observing the plot, is possible to notice two different zones: the first one, delimited from 0 to 4 abscissa's range, where PP mix values are slightly higher than compounded materials but the slopes of the lines are practically identical. This is concordant with the data plotted in Fig.62, where not relevant difference material behaviors were observed for short times and low temperatures. In the second zone (4-10 abscissa's range), the slope of the PP mix curve increases considerably and the compliance gap between unfilled PP and wine by-product additive filled PP become higher. As expected, seed additive "Se" is again the best additive that guarantees lowest compliance values. Creep tests show how wine by-products additives improve creep resistance of PP both in time and in temperatures and that the benefit become more and more important increasing temperatures or for longer times.
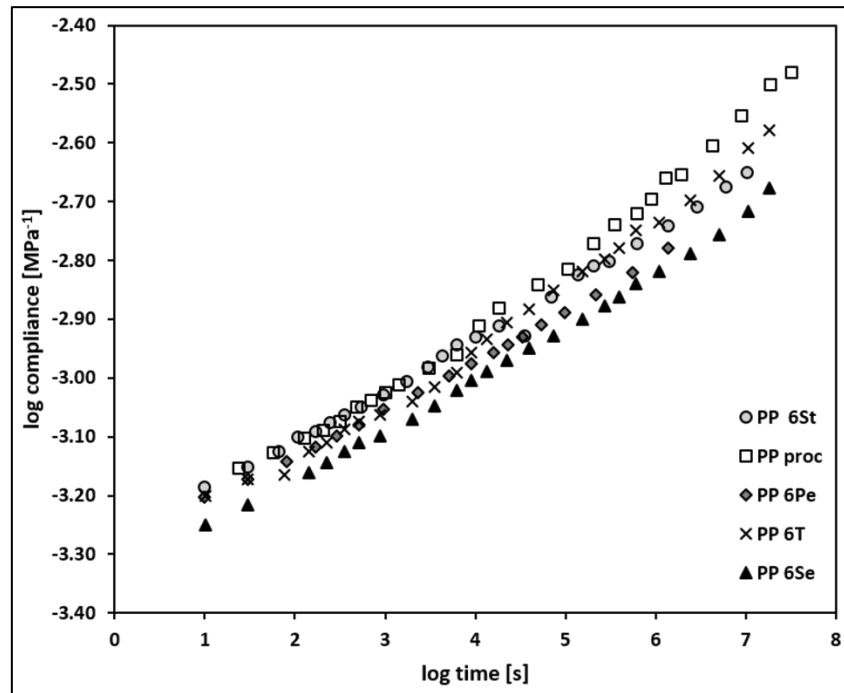
Fig.63 Creep behavior: master curves of filled and unfilled PP through time-temperature superposition principle at 20 °C.

7.2.2.4 Morphology: SEM

In Fig.64, scanning electron micrographs of the morphology of PP mix and PP with wine by-products additives are shown. The micrographs give important information about the distribution and dispersion of the additives and their adhesion to PP matrix. The images captured at lower magnifications (200×, 400×, upper row of Fig.64) show how the additive is dispersed in the PP matrix; they are not easily distinguishable and the morphology of the surface appears not modified and similar to the unfilled PP one. Moreover, they result uniformly distributed and aggregation or preferential additive's zones are not observed. Increasing the magnification (from 800× to 2000×, lower row of Fig.64), is possible to investigate the structure of the additive and the adhesion between the PP and additive surfaces. In each case, the additive is well connected with the PP matrix and no adhesion problems are remarked despite the polarity of the additives surface groups and the non-polarity of the PP chain [306]. Stalks additive "St" (Fig.64 B) and tannin extract additive "T" (Fig.64 D) show the best adhesion with the PP matrix, probably because of their minor particle's sizes. As expected from a natural source, the structures of additives are various and is not possible ascertain any typical shape both among different additives and the same additive typology.
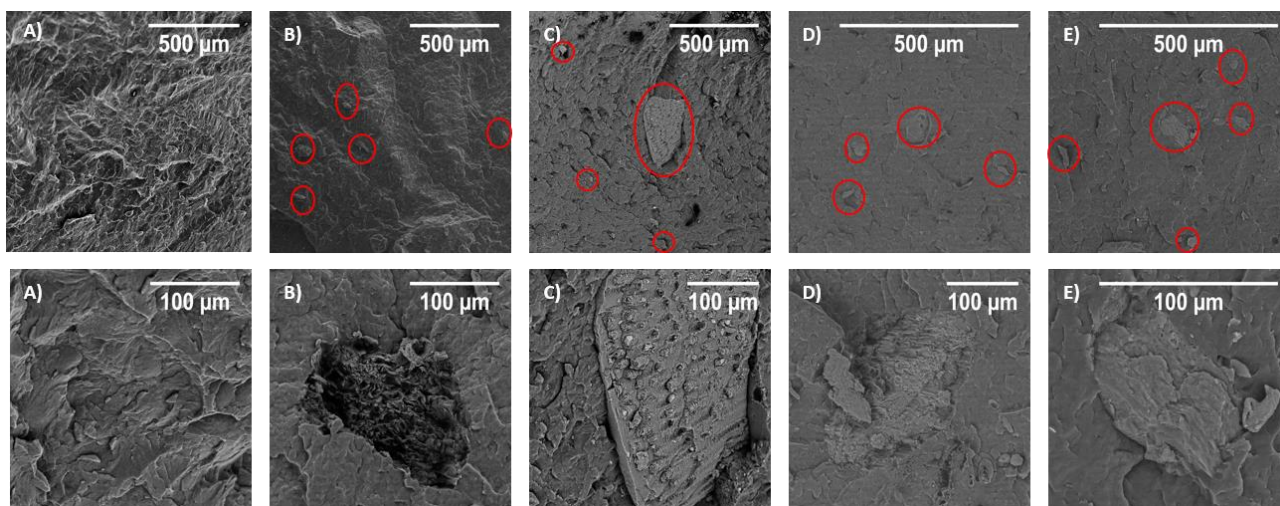
Fig.64 SEM images of: A) PP proc, B) PP 6St, C) PP 6Se, D) PP 6T, E) PP 6Pe. The upper row shows images captured at lower magnifications; the lower row at higher magnifications.

7.2.2.5 Thermal stability: OIT, OOT and TGA

OIT is one of the most reliable and commonly used test for the evaluation of polymer thermal stability, especially for polyolefins [307]. There is a direct correlation between OIT values and stability: higher OIT values involve more stable materials. In this work, OIT have been investigated at 175 °C and 200 °C, two temperatures higher than the PP melting temperature in order to verify the effect of the additives on the thermal stability during typical processing conditions of PP. For this reason, despite the fact that oxidation is a surface phenomenon, the shape of the sample has been not relevant: at the selected temperatures, materials were melt and so, identical surface have been supposed with criteria.
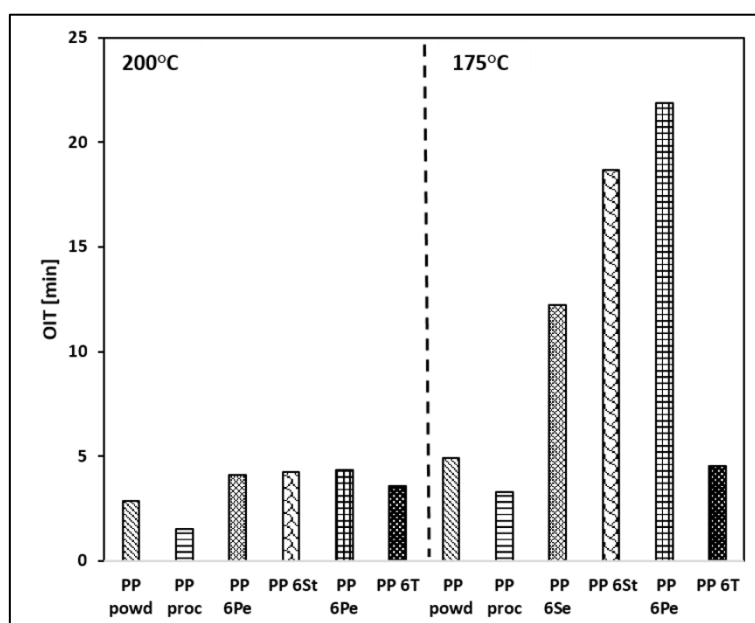
Fig.65 OIT values measured by DSC at 200 °C and 175 °C of PP powd, PP proc and the others PP-based materials under airflow.

Fig. 65 shows the OIT values of the different tested materials for the two temperatures. In this tests two different PP have been used: 'PP neat' intended here as virgin powder and 'PP mix' intended as

PP processed in the same way of the others PP based materials. This distinction allows observing the degradation quota due to the material processing since 'PP mix' values are lower than the 'PP neat' ones, as expected. All the additives lead PP to a higher thermal stability as confirmed by the always higher values at both temperatures. The gap between wine by-products based PP and 'PP mix' OIT values is not exceptional at 200 °C but considerably increases at 175 °C. At higher temperatures, in fact, the major heat generate more and faster free radicals that probably could be not contrasted by wine wastes additives. They are synthetized in nature to withstand with lower temperatures, and some part of the could have been lost due to the high temperatures [308]. Anyway, for the same reasons, is possible to affirm also the contrary which means that at lower temperatures (and at 175 °C is already noteworthy) the OIT values gap should increase as confirmed by other similar works [308]. Among all the additives, peels "Pe" is the best one, but also stalks "St" and seeds "Se" guarantee excellent results. It is interesting notice that seed tannin commercial extract "T" does not significantly improve the PP stability. This fact is unexpected because the great polyphenol concentration of "T" respect to the other additives. Therefore, the obtained results show how the polyphenol quantity does not ensure better results and how polyphenol structure plays a central role for the stability's optimization. Anyway, this result could be of primary interest for industry, since not particular waste treatments or extractions are required to enhance the PP stability. Fig. 66 shows OOT values and again, the effect of additive on thermal stability is confirmed. Onset degradative temperature of "PP powd" is enhanced by 20-25 °C by all wine wastes additives and again is possible to see the effect of the melt processing on the PP stability comparing the "PP powd" OOT value with the "PP proc" one. As opposed to the OIT results, the gap between the efficiency of the additives is limited and "T" exhibits the best performance. Table 21 shows the comparison between the OIT and OOT values.
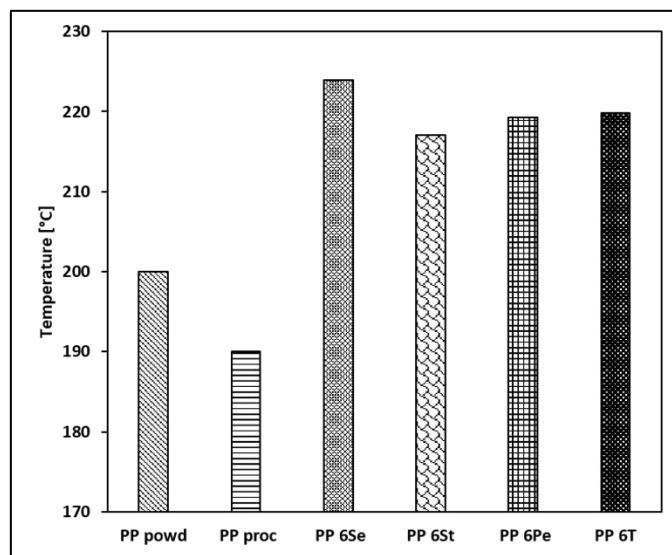
Fig.66 OOT values measured by DSC of PP neat (powder), PP mix (processed) and the others PP based materials under airflow.

Table 21 OIT and OOT data of PP based samples.

Material	OIT [min]		OOT [°C]
	175 °C	200 °C	
PP powd	4.93 ± 0.57	2.88 ± 0.22	200.4 ± 3.6
PP proc	3.29 ± 0.63	1.51 ± 0.16	190.3 ± 5.0

PP 6Se	12.25 ± 1.62	4.08 ± 0.25	223.7 ± 4.5
PP 6St	18.69 ± 1.74	4.24 ± 0.29	217.7 ± 2.1
PP 6Pe	21.91 ± 1.37	4.34 ± 0.47	219.3 ± 5.2
PP 6T	4.53 ± 0.72	3.59 ± 0.1	219.7 ± 3.8

Table 22 shows the temperatures at 5 wt. % loss ($T_{5\%}$) and at 15 wt. % loss ($T_{15\%}$), residue at 650 °C (Res_{650}) and temperature of the degradation peak in the T-dW/DT curves (Tpeak) of wine by-products additives and PP based samples under nitrogen and oxygen atmosphere.

Table 22 Temperatures at 5wt.% ($T_{5\%}$) and at 15wt.% loss ($T_{15\%}$), residue at 650 °C (Res_{650}) and temperature of the degradation peak in the T-dW/DT curves (T_{peak}).

Material	Nitrogen atmosphere				Oxygen atmosphere			
	$T_{5\%}$ [°C]	$T_{15\%}$ [°C]	Res_{650} [%wt]	T_{peak} [°C]	$T_{5\%}$ [°C]	$T_{15\%}$ [°C]	Res_{650} [%wt]	T_{peak} [°C]
PP powd	424	442	1.0	468	240	260	1.0	283
PP proc	401	429	0.3	457	219	236	0.2	276
PP 6Se	405	436	2.4	462	238	255	0.7	290
PP 6St	413	438	2.2	461	237	253	1.2	286
PP 6Pe	399	435	3.5	460	241	257	0.9	301
PP 6T	413	439	3.4	460	240	265	0.8	327
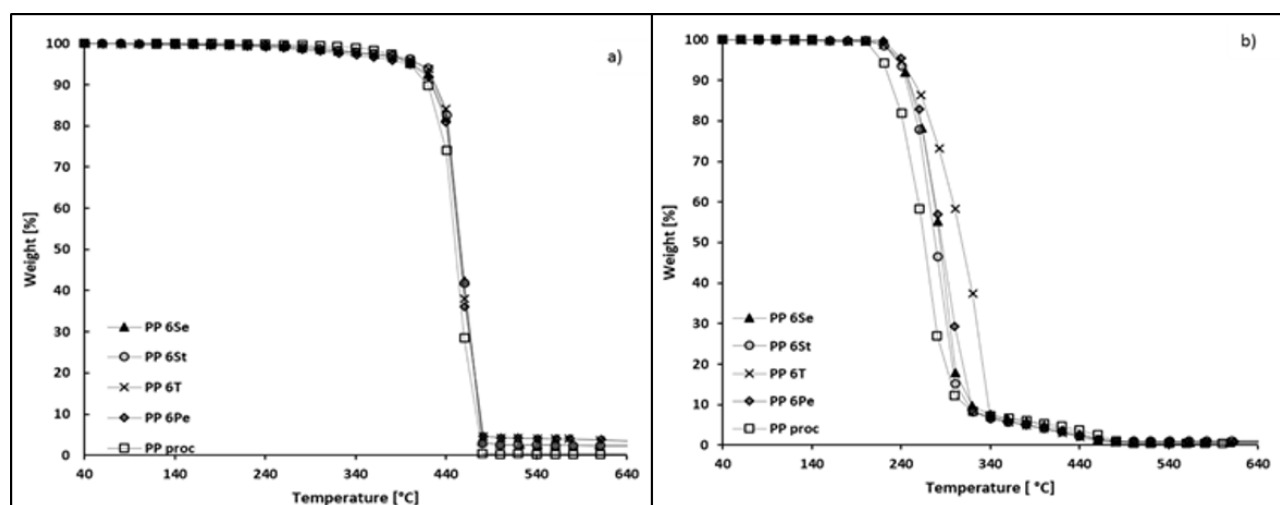
Fig.67 TGA curves of PP based samples: a) under nitrogen gas flow;b) under oxygen gas flow.

In Fig.67 the TGA curves of PP based samples are reported. Both in nitrogen and in oxygen, samples degrade in a single weight loss step close to 460 °C (nitrogen) and 300 °C (oxygen). The thermogravimetric curves of the filled samples have a trend comparable and similar to that of the pure PP but it is noteworthy underline that the curves of PP based samples under oxygen are shifted to the right by about 20-40 °C presumably thanks to the electron donation of the wine by-products additives. In Table 22, it is also possible to observe the difference of values between "PP powd" and "PP proc" that indicates again the degradation process occurred to PP inside the internal mixer. Additives "T" and "Se" are the most efficient stabilizers. Anyway, the observed slight gap between them do not suggest expensive extraction procedures on the seeds. Comparing the OIT and OOT results with the TGA ones emerges a noteworthy consideration. Under the isothermal conditions (OIT tests) peels

101

"Pe" and stalks "St" lead to the best results, while in non-isothermal conditions (OOT and TGA) seeds "Se" and tannin extract "T" result the best choice. It could be supposed that also the conditions of degradation affect the efficiency of these natural antioxidants and data would seem tell that "Pe" and "Re" are more suitable for lower temperatures and longer times, while "T" and "Se" for higher temperatures and shorter time. In conclusion, TGA data confirm that each wine waste derived additive enhances the PP stability against the thermo-oxidative degradation, and that not significant differences are relieved among the different wine additives used in this work.

7.2.3 Conclusions

The use of wine-waste derived additives has been found to be very effective to improve the thermal stability of the PP, increasing its processing window. In fact, wine by-products additives have been able both to increase the OIT and OOT values of PP, typical parameters used for polyolefin stability determination, and to shift the TGA curve to higher temperatures, contrasting the random radical scission degradation behavior of the PP matrix. Among the additives, seed tannin extract "T" has been the less performant in the OIT tests, but the most performant in the TGA and OOT tests opening new interesting questions concerning both the role of natural polyphenol structure in stabilization and the degradative conditions affecting the natural stabilizers. Anyway, what has been gained in OOT and TGA by the use of the extract powder "T" is not enough to justify extraction procedures for large scale operations. No important differences on OIT and TGA values have been t observed among others additives. This fact implies no need of waste separations and makes wine by-products additives low-cost stabilizers suitable for large-scale processes. The images captured by SEM have demonstrated the perfect adhesion and homogenization between additives and PP matrix despite their different polarity. This fact have emerged also in the mechanical proprieties characterization, where no significant differences between unfilled PP and filled PPs have been found. Overall, the reported results demonstrate the possibility to convert an agro-food by-product into a bio-additive able to improve the thermal stability of PP without compromising its mechanical and thermal proprieties, in an environmentally friendly and cost-effective way.

7.3 THERMAL AND UV AGING OF POLYPROPYLENE STABILIZED BY WINE SEEDS AND THEIR EXTRACTS

7.3.1 Material and methods

Materials

Pure isotactic polypropylene (PP) (without any kind of additives and stabilizers and with a MFI 8 g/10 min; 2.16 kg, 235 °C) has been kindly supplied in the form of a reactor powder by LyondellBasell. Wine wastes seeds (Se) have been obtained from the winery Cevico Group C.V.C, Lugo (RA), Italy, during the 2017 harvest and wine-making processes. They have been collected both from white grapes (Mostosa) and red grapes (Sangiovese) in the same weight ratio (1:1). Irganox 1010 (Irg), catechin and gallic acid (HPLC grade) have been supplied by Sigma-Aldrich and the commercial seed tannin extract powder (T) has been supplied by Cevico Group. Materials have been labelled as follow: "PP XY", where X is the number indicating the concentration (%wt) of the additive, and Y is the letter(s) indicating the additive typology. "PP proc" refers to the neat PP after twin-screw extrusion processing step. Table 23 resumes the name, and composition of the investigated materials. It is noteworthy underline that sample PP 01Irg, has been used as testing reference for the sample PP 6Se during the aging tests because of their similar content in effective antioxidant (see further paragraphs), meanwhile sample PP 1Irg, has been compared with PP 6T and PP 2Sext.

Table 23 Code, name and composition of the investigated materials.

Name	Composition
PP Proc	Neat PP processed in the same conditions
PP 01Irg	PP + 0.1 %wt Irganox 1010 (Irg)
PP 6Se	PP + 6 %wt seeds (Se)
PP 6T	PP + 6 %wt commercial tannin extract (T)
PP 2Sext	PP + 2 %wt seed extract (Sext)
PP 1Irg	PP + 1 %wt Irganox 1010 (Irg)

Preparation and characterization of bio-additives

Seed Extraction

The wine wastes seeds have been firstly washed with distilled water and cleaned with a cloth in order to remove smug and other impurities. Then they have been oven-dried at 70 °C overnight and grounded by means a batch analytical mill. In this step, moisture content and mean diameter size have been determined monitoring the weight and sieving manually, respectively. Therefore, a part of grounded seeds has been stored at room temperature and another part has been used for the polyphenol extraction. Extraction has been carried out under magnetic stirring for 120 min at room temperature using a mixture of ethanol-water (7:3 v/v) as solvent (solvent/solid ratio of 5 ml g^{-1}). The solid residue has been separated by filtration under vacuum and the polyphenol fraction has been separated from the solvent by distillation in a rotary evaporator. The yield of collected polyphenol fraction has been 3 %wt with respect to the dried seeds.

Total polyphenol content

The total polyphenol content of seed extracts (Sext), as well as of pristine seeds (Se) and of commercial tannin seed extract powder (T) have been kindly measured by Cevico Group C.V.C., Lugo (RA). Firstly, each sample has been completely (Sext and T) or partially (Se) dissolved in the ethanol-water (7:3 v/v) solvent. Therefore, the solution has been properly diluted with distilled water and the absorbance has been directly read at 280 nm in a UV/VIS Jasco V-730 spectrophotometer. Total polyphenol content has been expressed as weight percentage referring to the dry matter and as equivalent tannic acid. For this step, a calibration curve obtained with different concentration tannic acid solution has been used.

FT-IR and UV/VIS spectra

For each wine-derived additive, FT-IR spectra have been collected using a Perkin-Elmer Spectrum GX Infrared Spectrometer. Spectra have been recorded in ATR mode as an average of 64 scans in the range 4000-400 cm^{-1} and a 4 cm^{-1} resolution. UV/VIS spectra of commercial tannin extract "T" and lab seed extract "Sext" have been collected using a UV/VIS Jasco V-650 Spectrophotometer using absorbance mode at 1nm intervals in 190-490 nm region.

Liquid Chromatography-Mass Spectrometry (LC-MS)

Catechin and gallic acid concentration within the commercial tannin extract "T" and the lab seed extract "Sext" have been carried out by Liquid Chromatography-Mass Spectrometry (LC-MS). LC-MS/MS system has been performed using an Agilent 1200 series HPLC and an Agilent 6410 Triplequdrupole mass spectrometer equipped with an electrospray ionization source (Agilent Technologies, USA). The chromatographic separation has been achieved on a Zorbaz SB-C$_{18}$ (3.5 mm, 2.1 x 30 mm i.d., Agilent). All data have been acquired employing Agilent 6410 Quantitative Analysis version analyst data processing software. The initial mobile phase composition has been a mixture of 0.1% in volume of formic acid in water and acetonitrile (98:2 v/v). After the sample injection (5 mL), the initial mobile phase has been maintained under isocratic conditions for 1 min. A linear gradient has been then programmed to reach a mobile phase composition of 0.1% in volume of formic acid in water and acetonitrile (10:90, v/v) in 12 min, kept constant for further 5 minutes and then switched back to the initial composition in 0.1 min and allowed to re-equilibrate. The flow rate has been fixed at 0.3 mL/min during the whole chromatographic run and the temperature of the analytical column has been of 25° C. Total analysis run time has been of 25 min. "T" and "Sext" have been solubilized in HPLC grade water and injected in 10 ppb concentration. Mass spectrometric detection has been performed on a Series 6410 Triple Quad LC-MS (Agilent Technologies, USA) using multiple reaction monitoring. A turbo electrospray interface in positive ionization has been used.

Preparation of PP-based compounds
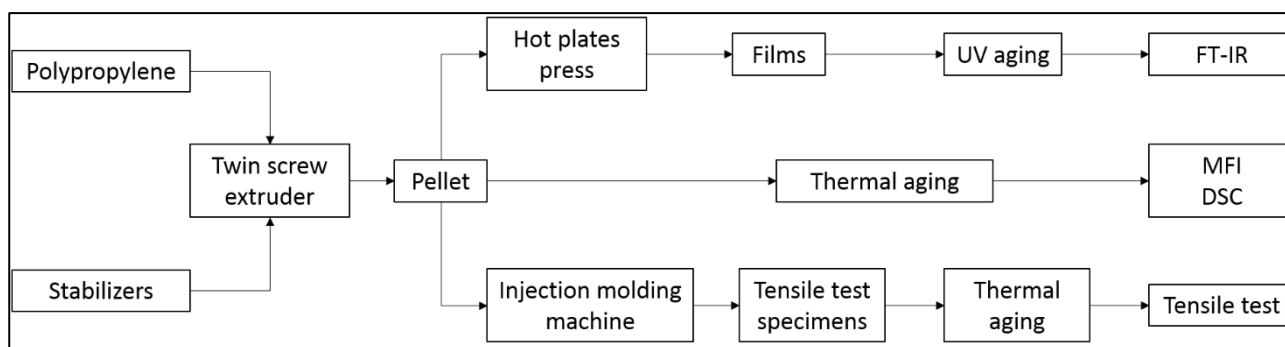
Fig.68 Working scheme.

Following the working scheme (Fig.68), PP has been firstly mixed with the stabilizers and bio-stabilizers through melt-compounding in a laboratory twin-screw extruder Rheomex 557 (Screw length: 300 mm, L/D screw ratio 10).

Table 24 Processing conditions resuming.

Extrusion Conditions		Injection molding conditions		Hot plates press conditions	
Feed zone Temp [°C]	180	Hopper Temp [°C]	185	Plate Temp [°C]	200
Barrel Temp [°C]	200	Screw-barrel Temp [°C]	205	Holding Pressure [MPa]	5
Die Temp [°C]	200	Die Temp [°C]	200	Holding time [min]	3
RPM [min^{-1}]	12±3	Injection Pressure [bar]	100	Cooling time [min]	5
Pressure [bar]	20±5	Holding Pressure [bar]	25		
		Holding time [s]	3		
		Cooling time [s]	4		

The compounded pellets obtained by twin-screw extrusion have been used for the preparation of suitable specimens for tensile test (type 1BA, according to technical standard ISO 527) by using a MegaTech Tecnica DueBi injection molding machine (see processing conditions in Table 24) and for the preparation of suitable films ($20 \times 20 \times 0.5$ mm^3) for photo- and thermal-oxidation by using a Carver hot plate press operating at 200°C for 3 min under a pressure of 5 MPa.

Accelerated aging

UV aging of PP-based films has been carried out by irradiations in air in a SEPAP 12/24 unit (ATLAS) at a wavelength l > 300 nm and 60 °C. The apparatus was equipped with four medium-pressure mercury lamps with borosilicate envelope able to filter wavelengths below 300 nm and it was designed for accelerated artificial UV aging tests, in conditions comparable to natural outdoor weathering. Thermal aging has been carried out in a forced-air oven at 110°C for PP-based pellets and PP-based tensile specimens.

Characterization techniques

Oxidation induction time (OIT) by FT-IR

FTIR spectroscopy has been carried out on films subjected to accelerated aging by means of a Perkin-Elmer Spectrum GX Infrared Spectrometer. Spectra have been recorded in transmission mode as an average of 32 scans in the range 4000-400 cm^{-1} and a 4 cm^{-1} resolution. Both photo-oxidation and thermal-oxidation have been followed by monitoring the intensity of the maximum absorbance in the 1800-1690 cm^{-1} range (C=O vibration stretching band range) as a function of time. In order to avoid

differences due to film thickness absorption, the degradation peak has been normalized to the absorption peak at 2723 cm^{-1} (C-H vibration stretching band of PP). Each film has been analyzed at a fixed time and then returned to the UV apparatus or to the oven to continue the aging treatment. The Oxidation Induction Time (OIT) have been calculated as the time at which the C=O peak start to increase linearly with time and the slope of that line has been indicated as the degradation rate (DR). The reported data are the average values of two determinations.

Tensile test

Tensile tests have been performed by means of the INSTRON 5567 dynamometer equipped with a 1 kN load cell and a 25 mm gauge length extensimeter. Tests have been performed at room temperature with a speed of testing of 10 mm min^{-1} . For each oven aging time, at least six specimens have been tested. Young's modulus (E), tensile strength (σ_M), and tensile strain at break (ε_b) have been measured as function of aging time.

Melt Flow Index

Melt flow index (MFI) of the oven aged PP-based pellets has been monitored according to ISO 1133 at a temperature of 235 °C, and load of 2.16 kg.

Differential Scanning Calorimetry

Thermal properties of oven aged PP based pellets have been evaluated by Differential Scanning Calorimetry (DSC). DSC measurements have been performed by a DSC TA 2010, using 7 ± 1 mg of sample and the chamber has been purged by nitrogen at 50 mL min^{-1}. Each sample has been firstly heated from 20 °C to 220 °C at 15 °C min^{-1} in order to erase the previous thermal history. Therefore, after a 2 min isothermal step at 220 °C, samples have been cooled at 15 °C min^{-1} to 20 °C and finally, re-heated to 220 °C at 15 °C min^{-1}. The crystallization temperature (T_C) has been evaluated as the peak maximum of the heat flow in the cooling cycle. The melting temperature (T_m), as well as the melting enthalpy (H_m) have been obtained from the second heating cycle as the peak maximum and as the integral of the area under the heat flow curve, in the 125 - 200 °C range, respectively. Melting enthalpy has been calculated considering the additives weight fraction. In order to evaluate the crystallinity percentage of the PP-based pellets, the value of 208 J g^{-1} [309] has been considered as reference for the 100% crystalline PP melting enthalpy.

Morphology

Morphology, adhesion, distribution and solution of the additives on the PP matrix have been observed with an Environmental Scanning Electron Microscope, SEM (ESEM Quanta FEI 2000). Tensile specimens have been broken in liquid nitrogen and the cross section has been covered by a 10 nm thickness gold layer (Gold Sputter Coater – Emitech K550). The obtained surfaces have been observed with the SEM, operating in low-vacuum conditions.

7.3.2 Results and discussion

7.3.2.1 Bio-additives characterization

In Table 25, particle size, total polyphenol content, catechin and gallic acid concentrations are reported. It is useful to state that catechin and gallic acid have been chosen as targets among other

many polyphenols because their usually abundancy in grape seeds and because they are the simplest molecules representative the two major polyphenol family, condensed tannins (catechin) and hydolyzable tannins (gallic acid). The reported wine wastes values can be affected by viticultural or environmental factors [310, 311] and by extraction techniques and analysis methods [248], but it is noteworthy to underline that they are still in accord with those carried out by different authors [312-314]. Despite these mentioned affecting factors, comparing "Sext" and "T" additives it can be surely said that "T" contains an higher level of total polyphenols and catechins meanwhile gallic acid seems to be more present in "Sext". This difference in gallic acid concentration could be a key point for the further presented results, suggesting that gallic acid could be better than catechin to withstand the PP degradation. The extreme antioxidant power of gallic acid has been reported numerously. R.Pulido et all. (2000) [315], through the ferric reducing ability of plasma (FRAP assay) have measured the concentration of different dietary antioxidants having a ferric reducing ability equivalent to that of a 1 mmol/L of $FeSO_4,7H_2O$ (CE), finding gallic acid almost two times more active than catechin (CE of gallic acid: 180 mmol/L; CE of catechin: 348 mmol/L). Brand-Williams et al. (1995) [316], using the DPPH radical scavenging method, found that gallic acid was the most effective polyphenol scavenging the DPPH• radical, and similar results have been carried out by other authors [317, 318]. By the way, these results can not state the antioxidant power superiority of gallic acid over catechin in PP stabilization because the antioxidant ability of polyphenols is strictly connected with the systems they are dealing, but nevertheless indicate a clue for the "Sext" additive's antioxidant power explanation. In addition to (+)-catechin and gallic acid, other simple polyphenols typically present in wine seeds extracts are (-)-epicatechin, (-)-epigallocatechin, (-)-epicatechin gallate, (-)-epigallocatechin gallate (ECG), quercetin, resveratrol, ferulic and ellagic acid [319, 320]. Moreover, grape seeds result to be rich in procyanidins, a class of polpyhenols members of the condensed tannins family, which are olygomers formed by catechins and/or epicatechin as building blocks and a degree of polymerization ranging from 2.4 to 16.7 [254]. The chemical structure of the mentioned simple and polymerized polyphenols are reported in Fig.69.

Condensed tannin in branched (a) or linear form (b)
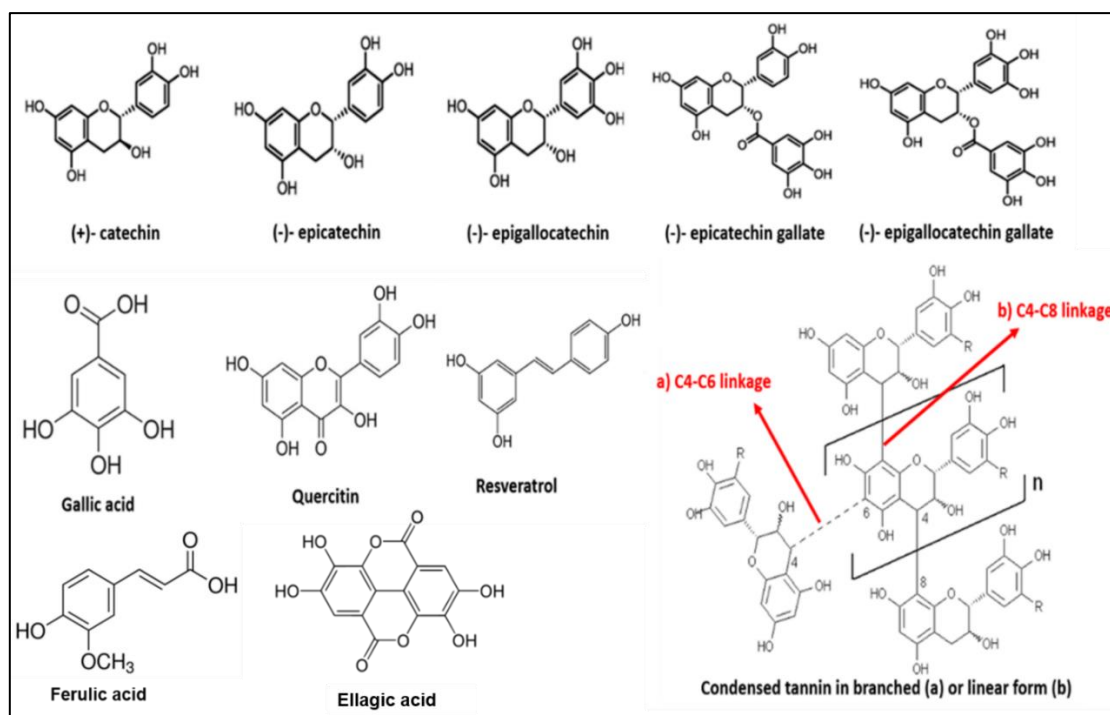
Fig.69 Wine seeds polyphenol extracts: chemical structure of the most important moieties.

FTIR has been used in order to collect and compare information on the chemical structure of the wine wastes seeds (Se), of their extract (Sext) and of the commercial seed tannin extract powder (T). Fig. 70 shows the acquired ATR spectra (normalized with respect to the most intense peak) and Table 26 lists the main bands.

Table 25
Particle size, total polyphenol content [% wt], catechin and gallic acid concentrations of bio-additives.

	Se	Sext	T
Mean particle size [mm]	0.30	0.17	0.17
Total polyphenol content [%wt]	1.4	15.7	38.2
Effective polyphenol content in PP-based sample [%wt]	0.084	0.31	2.29
(+)- Catechin [mg/g ext]		4.61	37.4
Gallic acid [mg/g ext]		3.75	0.67

From a qualitative point of view, it is possible to note that the spectrum of Se presents three sharp and intense peaks (**b**, **c** and **d**) in the 3000-2500 cm^{-1} range related to the stretching of aliphatic CH and CH$_2$ groups that confirm the relevant amount of unsaturated lipids in wine seeds (10-15 %wt) [299, 300]. Moreover, an intense peak at 1745 cm^{-1} (**e**) related to C=O stretching typical of galloylated compounds confirms the typical high content of procyanidins galloylation in grape seeds [254, 321]. Comparing the spectra of Se and T, it is observable how commercial extract T presents a cleaner signal presumably thanks to the industrial extraction method. By the way, the OH stretching band (3700-3000 cm^{-1}) has its maximum peak at the same frequency in both extracts and the breadth of the band results similar. Because the used solvent in the polyphenol and tannins extraction process affects the relative position of the maximum for the OH stretching [322], it is reasonable to believe that Sext and T have been obtained by solvent with similar polarity (maybe pure water has been used for T, being more suitable for large scale extractions). In the 3000-2850 cm^{-1} region, "Sext" spectrum presents two peaks (**c** and **d**) that could be assigned to the asymmetric stretching of aliphatic CH groups [323] or to a residual lipid fraction. The 1800-1680 cm^{-1} region is significant for qualitative analysis because shows a distinctive peak for carbonyl stretching of hydrolysable tannins [324, 325], whereas only a weak signal, if any, appears with condensed compounds [326]. The low intensity of the **e** peak (1740 cm^{-1}) shows the predominance of condensed tannins in both grape seed extracts confirming the grape seed tannin composition [254, 327]. In the 1150-900 cm^{-1} region it is remarkable a sharp peak (**h**) that results more intense in Sext spectra than in T one. This region is characterized by the combination of different substituents in the phenolic rings. The bands appearing in this region are strongly affected by the number and position of substituents and provide a useful indication for the determination of tannin monomeric constituents [328]. Therefore, it is reasonable to conclude that Sext is characterized by tannins with a lower degree of polymerization [326] and many free phenolic hydroxyl groups. Thus, it could be explained the high intensity of **h** peak in Sext spectrum. This aspect is important for two reasons: firstly, the quantification of total polyphenols is highly affected by the extent of polymerization of tannins when using direct reading at 280 nm as reference method [329] and secondly, the free phenolic hydroxyl groups result to be more reactive than long chain tannins [330-332]. Despite the possible underestimation on the Sext polyphenol content, comparing

PP 2Sext and PP 6T it is clear that an important gap concerning the effective polyphenol content within the PP samples still remains, because of the two different antioxidant percentages used (Table 25). In other words, the differences detected and discussed in **h** peak, testimonies again the role and the importance of the polyphenol structure and typology over the polyphenol content.

Table 26 ATR absorption signals and corresponding assignments.

Peak code	Wavenumber [cm^{-1}]	Assignment
a	3290	O-H and N-H stretching vibration of polysaccharides and proteins; O-H of polyphenols
b	3006	=CH stretching vibration of unsaturated lipids
c	2920	CH$_2$ asymmetric stretching vibration of lipids (mainly), proteins, polysaccharides and nucleic acid; CH$_2$ of catechins.
d	2852	CH$_2$ symmetric stretching vibration of lipids (mainly), proteins, polysaccharides and nucleic acids; CH$_2$ of polyphenols
e	1740	C=O stretching vibration of phospholipids and triglycerides; C=O of gallic acid
f	1615	C=O stretching vibration of amide (I) in proteins and nucleic acids; C=O of catechin
g	1458	CH$_2$ bending vibration of lipids and proteins; CH$_2$ of polyphenols
h	1160	C-C, C-O and C-N stretching vibrations
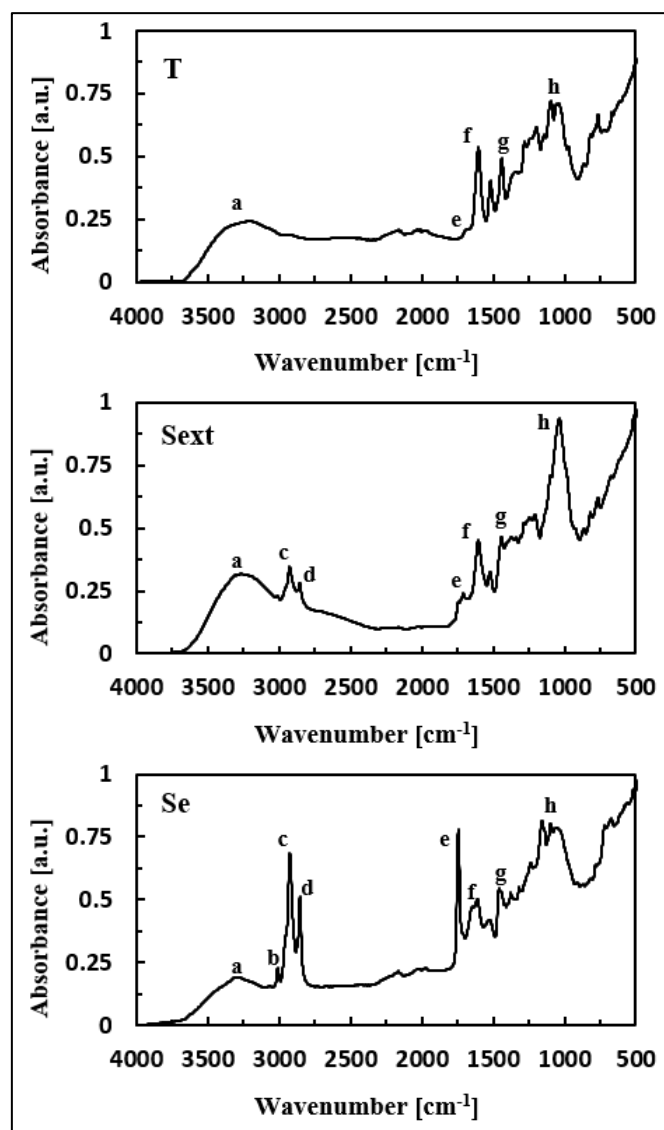
Fig.70 FT-IR ATR spectra of wine seeds (Se), wine seed extracts (Sext) and commercial tannin seed extract (T).

In fig. 71, the UV/VIS spectra of neat powders "T", "Sext", "Se" and Irganox 1010 are shown. As expected, Irganox 1010 exhibits a maximum absorbance peak in the 280 nm region followed by a decreasing absorbance in the UV-A region (315-400 nm) and becoming totally transparent in the visible region (400-700 nm). The different wine seeds derived additives exhibit comparable spectra and, contrary to Irganox 1010, they are able to absorb in the whole UV and visible region. Thus, if mixed in polypropylene, they can act also as UV absorber screening the UV rays and discouraging the UV absorption by the PP chromophores groups. This prevention mechanism reminds both the one played by polyphenolic pigments when a UV barrier screen is needed by the plant or the fruit as sun protection and the effect of some zinc oxide nanoparticles used for UV shielding [333, 334]. By the way, absorbing also in the visible, the use of wine derived additives involve a change of color and opacity in PP matrix as main drawback.
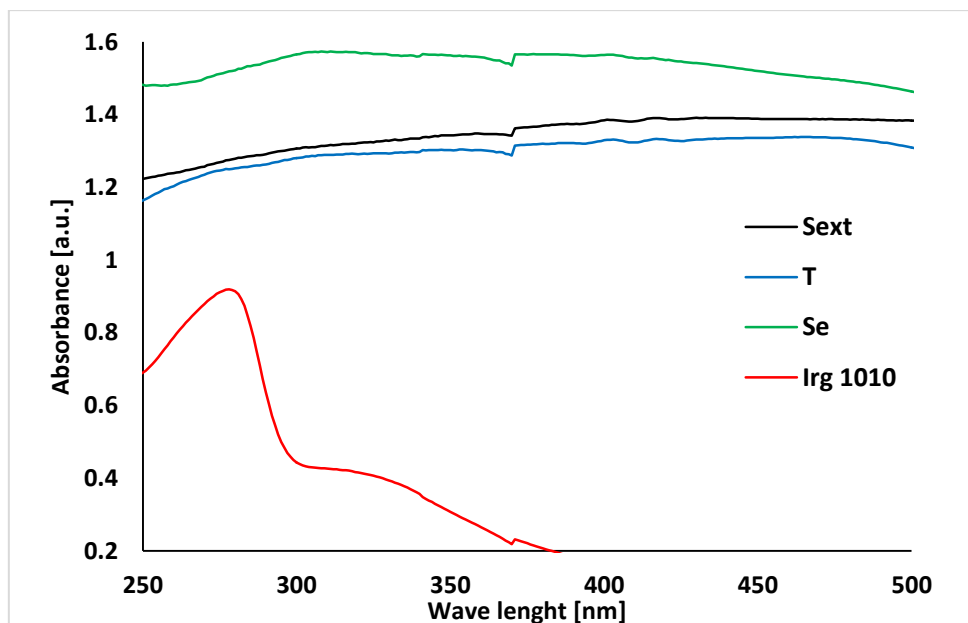
Fig.71 UV/Visible spectra of "Sext", "T", "Se" and Irganox 1010 additives.

7.3.2.2 UV aging of the PP-based films

The photo-oxidation mechanism of isotactic PP has been reported numerous times in literature [335-339]. The main product of the combined action of UV-radiation and oxygen is the formation of the tertiary hydroperoxide. The oxidation continues up to the production of carboxylic acids, esters, peresters, lactones and other oxidized species. Therefore, the analytical detection of oxidation products has been performed by monitoring the intensity of C=O absorption in the 1800-1650 cm^{-1} IR-spectrum range. Fig.72 shows the FTIR absorption spectra, in particularly the carbonyl range, of the PP proc at different UV aging times. It is possible to notice (Fig.72b) that the carbonyl content remains constant up to approximately 10 hours which represents the induction time and then increases at a high rate up to 80 hours. The increasing of absorption intensity over time was caused by the accumulation of carbonyl groups in the polymer. In particular, three different peaks can be distinguished: ketons at 1725 cm $^{-1}$, isolated carboxylic acids at 1755 cm^{-1} and peresters or lactones at 1780 cm^{-1}. This kinetic behavior of the carbonyls reveals the typical outline of photo-oxidation reactions: an induction period followed by an auto-acceleration step. A similar trend of carbonyl evolution has been observed for all PP-based films, pointing out the fact that wine derived additives do not modify the photo-oxidation mechanism.
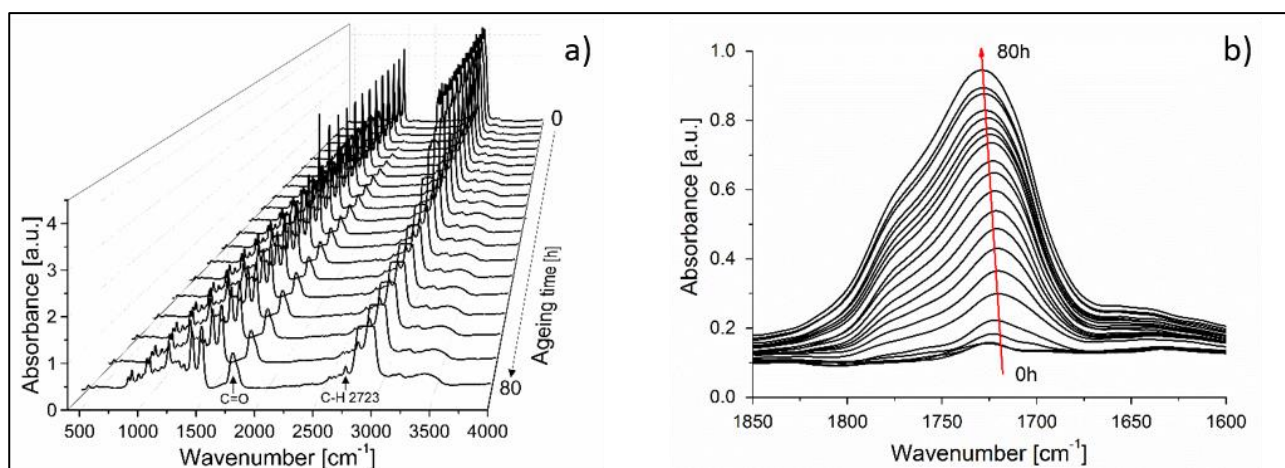
Fig.72 FTIR spectra of photo-oxidized "PP proc" film in 4000-400 cm^{-1} range (a) and in C=O 1850-1600 cm^{-1} zoom (b).

Table 27 UV aged PP-based samples: OIT, slope and R^2 of the experimental data interpolating lines and film breaking time.

PP based sample	OIT [h]	Slope [%]	R^2	Film breaking [h]
PP Proc	10.2 ± 0.4	2.23	0.9979	50 ± 2
PP 01Irg	16.5 ± 0.8	1.60	0.9931	62 ± 2
PP 6Se	14.4 ± 0.6	1.76	0.9950	56 ±8
PP 6T	32.8 ± 1.7	1.30	0.9863	Not occurred
PP 2Sext	43.5 ± 0.6	1.57	0.9971	Not occurred
PP 1Irg	23.2 ± 0.1	1.72	0.9939	60 ± 4

In Fig.73, it is reported the kinetic evolution of the maximum of the carbonyl bands (within the 1800-1650 cm^{-1} range) normalized to the peak at 2723 cm^{-1} (to compensate slight thickness differences) for each PP-based film. Three different behaviors are observable: one without any form of stabilization, the second one with good UV stabilizers and the last one characterized by excellent UV stabilization results. As predictable, unstabilized PP (PP proc) lies on the upper part of the graph: photo-oxidation starts just after 10 h and its rate is the highest among all the samples (Table 27). Subsequently, in the central part of the graph it is possible recognize three similar OIT lines which represent, in decreasing order of UV stabilization efficiency, the PP 1 Irg, PP 01 Irg and PP 6Se degradation responses. These samples are able to protect the PP matrix from 14.4 to 23.2 hours of UV aging (41% and 123% more than unstabilized PP) and the slopes of these lines are comparable and within the range of 1.6-1.76. It is noteworthy underline the fact that PP 6Se and PP 01Irg behaviors are comparable in agreement with their effective antioxidant content (0.084% wt and 0.1% wt, respectively) pointing out the seeds ability to work as long-term stabilizer in a way proportional to their polyphenol content. This aspect indicates that the polyphenols released from the seeds during the extrusion process remain within the PP matrix without be absorbed again by the wine seed surfaces. In fact, fillers, absorbing stabilizers at their surface and therefore reducing their protective effect, may have a negative effect on the long-term properties of plastics [227]. Finally, as expected, PP 1 Irg exhibits the highest OIT value of this group being able to inhibit the photo-oxidation until

23 hours (+7 h than PP 01 Irg and +9 h than PP 6Se). As observable in the bottom right side of Fig.73, polyphenol extracts are the best PP bio-stabilizers against UV aging. This can be explained by the fact that polyphenols can work both as radical scavenger donating hydrogen from their hydroxyl groups (like Irganox 1010) and also as UV absorber as shown in 3.1 paragraph. The OIT values of PP 6T and PP 2Sext are here of around 33 and 44 hours, respectively (41% and 88% more than PP 01 Irg). The PP 6T samples exhibits the lowest interpolating line slope (1.30), and, especially in the beginning of the photo-oxidation, the degradation rate occurs slower than in the PP 2Sext, but then, towards the end, the PP 6T values seem to convert to the PP 2Sext ones. Therefore, it is possible to state that PP 2Sext, despite its lower effective polyphenol content, is able to delay the photo-oxidation of other 11 h, respect to PP 6T. Thus, as explained in the 3.1 paragraph, the polyphenol structure and quality have been proven to be the key role in long-term UV stabilization.
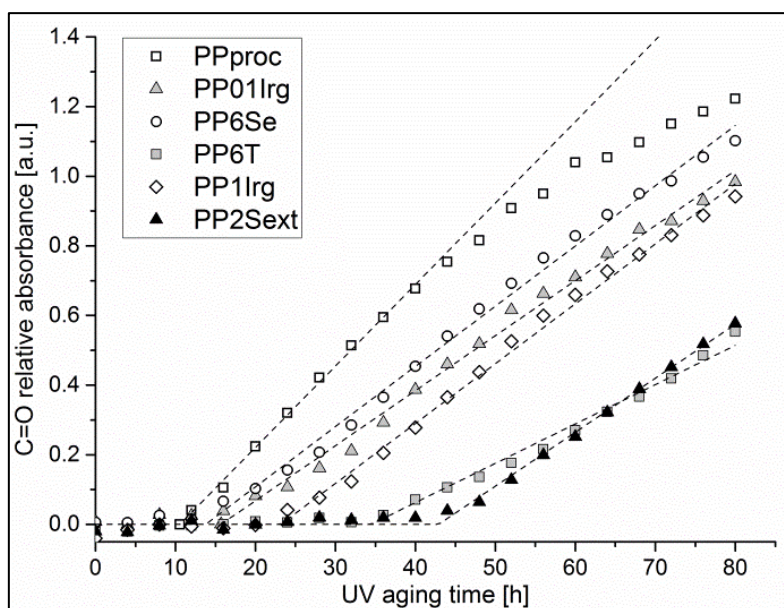
Fig.73 Relative absorbance of carbonyl bands versus UV aging time for PP-based films.

7.3.2.3   Thermal aging of PP-based tensile specimens and pellets.

Young's modulus (E), tensile strength (σ_M) and strain at break (ε_b) at different thermal aging times of each PP-based sample are reported in Table 28. Considering the unaged samples, no significant difference are notable except for PP 6Se and PP 6T samples that present very much lower elongation at break values and a higher elastic modulus (PP 6Se). This could be explained by the presence of micrometric solid inclusions in the polymer matrix, as already seen in a previous work [291], resulting in an embrittlement of the material and in the formation of defects able to accelerate the crack propagation. On the contrary, it is noteworthy underline that, despite the polarity difference between not polar PP and polar wine seeds extracts, PP 2Sext exhibit the same mechanical properties of PP proc (Fig.75). This can be explained because of the complete solubility of the natural additive within the PP matrix that gives to PP 2Sext the same morphology of the processed PP, as confirmed by the captured SEM images (Fig.74).
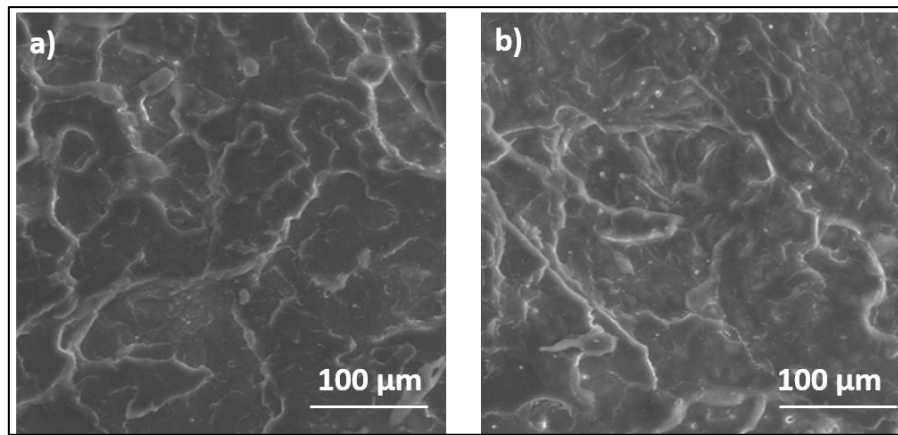
Fig. 74 Captured SEM images at 1000x magnitude of a) PP proc b) PP 2Sext.

Table 28 Young's modulus (E), tensile strength (σ_M) and strain at break (ε_b) of PP-based sample at different aging times.

PP proc			
Aging time [h]	E [MPa]	σ_M [MPa]	ε_b [%]
0	1574±113	28.7±1.6	1146±206
192	1727±130	28.5±0.7	27.8±3.6
271	1901±88	26.7±1.1	14.9±0.6
360	1774±102	27.9±1.4	16.0±1.3
PP 6Se			
Aging time [h]	E [MPa]	σ_M [MPa]	ε_b [%]
0	1938±232	29.2±1.2	12.6±3.5
192	1904±141	24.3±2.5	7.4±2.7
271	1997±58	27.0±2.7	11.1±1.5
360	1757±248	21.5±5.0	8.6±2.0
PP 6T			
Aging time [h]	E [MPa]	σ_M [MPa]	ε_b [%]
0	1656±214	27.3±0.7	44.2±4.2
192	1985±186	25.4±3.2	39.3±4.9
271	1762±178	27.9±0.9	28.9±4.1
360	2033±142	28.6±1.8	32.3±0.3
PP 1Irg			
Aging time [h]	E [MPa]	σ_M [MPa]	ε_b [%]
0	1664±69	28.7±3.0	1060±140
192	1626±108	29.0±1.3	820±104
271	1714±73	26.7±2.2	795±77
360	1893±102	30.1±1.9	18.2±0.8
PP 2Sext			
Aging time [h]	E [MPa]	σ_M [MPa]	ε_b [%]
0	1611±48	27.1±1.0	1138±200
192	1735±98	29.7±1.6	899±170
271	1714±121	28.8±2.6	890±99

360	1969±48	29.5±1.0	760±42
	2103±104	31.6±1.2	19.8±6.2
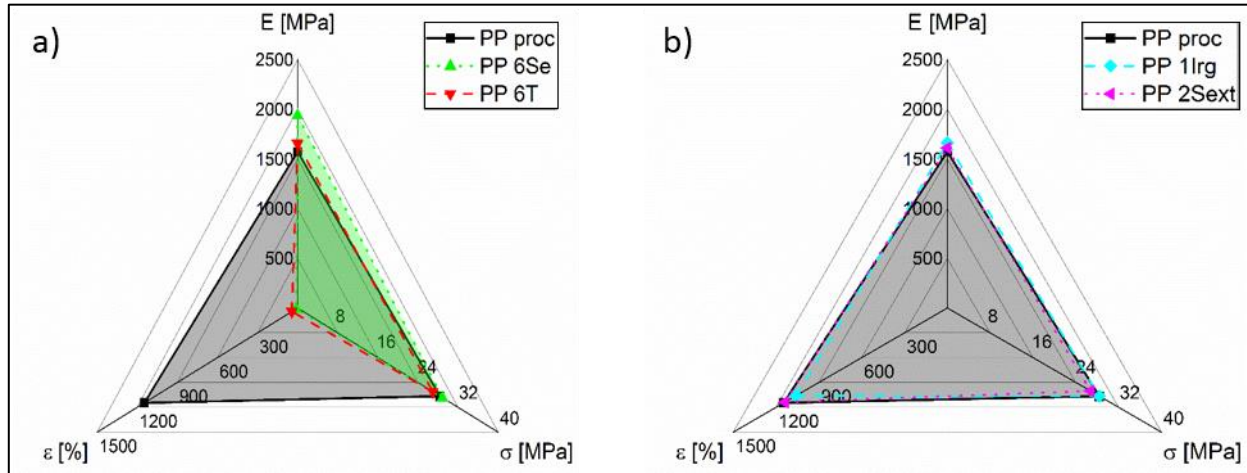
Fig. 75 Comparison of the mechanical properties between a) PP proc, PP 6Se and PP 6T; b) PP proc, PP 1Irg and PP 2Sext.
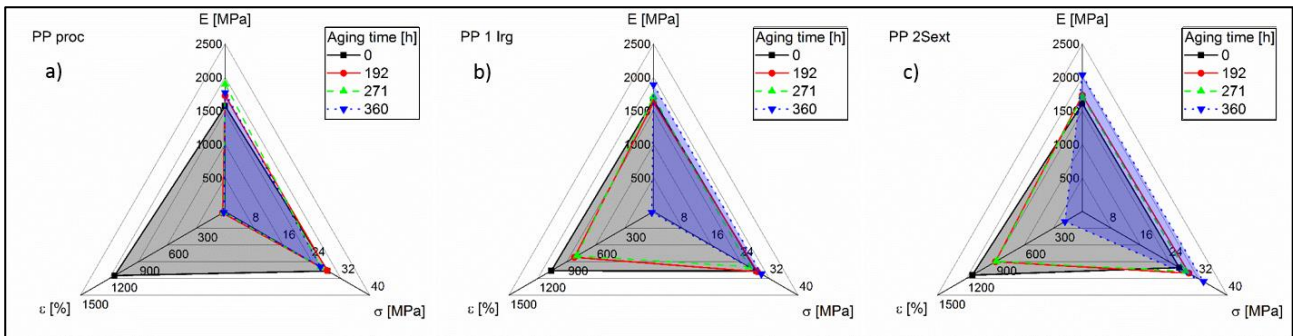
Fig. 76 Comparison of the mechanical properties between a) oven aged PP proc, b) oven aged PP 1 Irg and c) oven aged PP 2Sext.

The relative changes of deformation at break for PP-based specimens as a function of aging time is reported in Fig.77. A significant loss in deformation at break at 360 h and a not relevant difference in behavior between 192 h and 271 h of aging time can be observed for all the samples. From Fig.76, it also emerges the tendency of each sample, as expectable, to increase their Young Modulus and tensile strength during the aging time as embrittlement consequence of the thermal aging. PP proc is not able to withstand the thermal treatment for long time, showing a dramatic loss in the strain at break already at 192 h. The significant loss of mechanical properties in the course of oven aging can be explained by the decrease in the average molecular weight of the polymer due to the degradation phenomena. Therefore, PP 1 Irg and PP 2Sext are the samples that exhibit the best response to the thermal aging. They have an analogous behavior characterized by a slow loss of mechanical properties during the first 271 hours, followed by a fast loss of strain at break during the 271-360 h range. The only difference regard the final value of strain at break: in fact, at 360 h, PP 1 Irg shows a dramatic loss in deformation at break (-98% of its initial value) leaving no doubts on the occurred thermal degradation. Differently, in PP 2Sext it is possible to note two different groups of specimens at 360 h (Table 28):

the 50% of the specimens have shown a total loss of the mechanical properties similarly to PP 1 Irg, meanwhile, the other 50% continue to exhibit significant strain at break values. This aspect could be explained by a not perfect distribution of the polyphenol seed extract within the PP matrix during the compounding processes, leading to specimens with less effective antioxidant content.
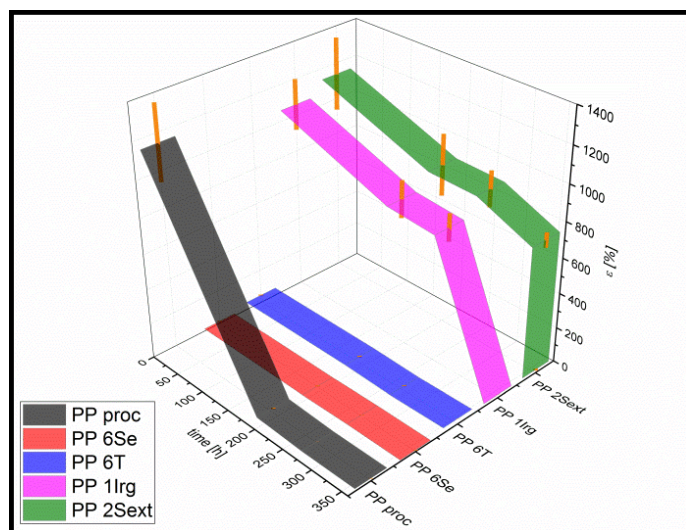
Fig.77 Strain at break as aging time function for PP-based tensile specimens.

The thermal degradation occurred by unzipping mechanism with related loss of molecular weight has been confirmed by the MFI test and by the DSC analysis. Fig.78 shows the MFR values of the oven aged PP-based pellets against the oven aging time. These data are in perfect accord with both the tensile test results and with the UV-aging OIT curves. In fact, is possible to notice how PP proc exhibits a fast and dramatic increasing in MFR values after only 20 h of oven aging and after 50 h, it has been not possible measure the MFR value because of the too high melt fluidity (PP proc has been aged in this case only until 140 h). PP 01 Irg and PP 6Se, as well as for the UV aging, exhibit a comparable behavior being able to maintain their initial MFR value almost until 140-200 h. Despite PP 6Se and PP 6T have not been analyzed in terms of mechanical properties loss due to the thermal aging, because their already low initial elongation at break values, MFR confirms the ability of these bio-additives to work also as long-term thermal stabilizers. Finally, PP 1Irg and PP2Sext withstand the thermal aging for the longest times. In particular, PP 1Irg starts its degradation at around 300 h exhibiting a small increasing MFR value, meanwhile PP 2Sext seems to be undamaged even at 600 h. This last aspect gives rise to the possibility of optimize the polyphenol extract distribution in the compounding step, pointing out that tensile specimens could be able to maintain their properties longer than 360h. Finally, the similar MFR values of the unaged samples indicate that the wine additives do not affect in a significant way the PP rheological properties.
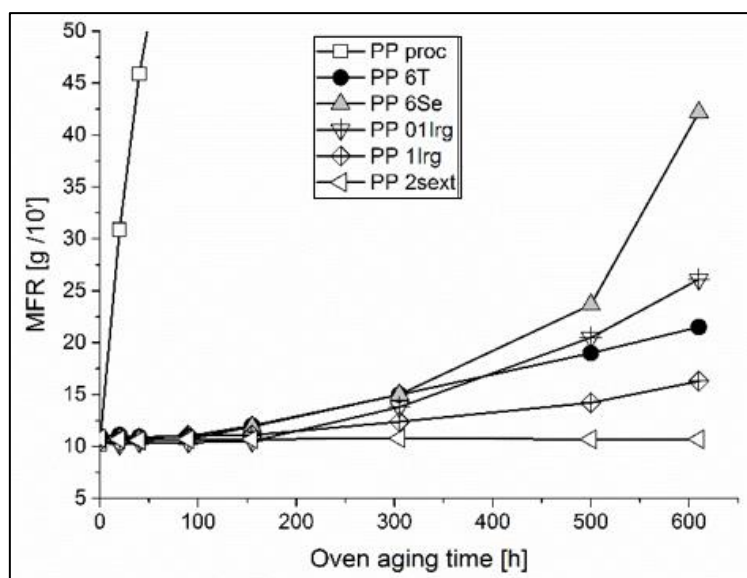
Fig.78 Melt Flow Rate values of PP-based pellets against oven aging time.

The degradative unzipping mechanism is confirmed also by the DSC data (Table 29) that shows the reduced molecular weight of the oven aged PP proc pellets both by the decreasing of the melting temperature (-26 °C) and by the increasing in crystallinity (+24%) testifying an occurred breakage of the PP molecular chains. These thermal properties differences between unaged and oven aged pellets have been not observed for the other PP-based pellets. By the way, referring to the unaged samples, it is noteworthy underline how polyphenol extracts as well as virgin wine seeds do not affect the PP thermal properties.

Table 29 Scanning Calorimetry data of the PP-based pellets.

Material	Oven aging [h]	T_c [°C]	T_m [°C]	H_m [J g^{-1}]	% Crystallinity
PP proc	0	117	167	85	41
	140	105	141	107	51
PP 6Se	0	116	167	79	41
	610	119	166	82	42
PP 1 Irg	0	114	167	88	43
	610	115	165	87	42
PP 6T	0	118	165	79	41
	610	116	166	79	41
PP 01 Irg	0	114	166	86	41
	610	113	164	87	42
PP 2Sext	0	114	167	87	43
	610	112	166	85	42

In conclusion, the thermal aging of tensile specimens has shown the polyphenol extracts (Sext) ability to interrupt the PP thermal radical degradation chain, guarantying remarkable mechanical properties even better than synthetic commercial antioxidant, Irganox 1010. In fact, despite Sext has been mixed with PP in percentages two times higher than Irg 1010 ones, the effective antioxidant content in the PP 2Sext is still less than in PP 1 Irg (0.31% wt against 1.0%wt). Moreover, the results exhibited at

360 h (both from tensile test and MFR) open a further possibility to improve the thermal stability optimizing the polyphenol distribution through extrusion and injection molding processes.

7.3.3 Conclusions

The UV-oxidative stability as well as the thermo-stability of PP containing synthetic or natural antioxidants derived from wine seeds wastes has been studied. Long-term stability has been investigated through UV and thermal aging tests, monitoring the development of degradation products by FT-IR and the loss of mechanical properties. The main results obtained are summarized as follow:

➢ The polyphenol extract (Sext) is able to protect PP against UV aging and the OIT value of the PP 2Sext sample has been the highest among all the investigated samples. This has been due by the ability of Sext of working both as radical scavenging and UV absorber.

➢ The polyphenol extract (Sext) is able to protect PP against thermal aging and the mechanical properties of the PP 2Sext sample have not significantly changed until 360 h of thermal aging. Moreover, a better distribution of the additive within the PP could lead to a degradative resistance even for longer aging time as confirmed by MFR. In addition, despite the difference in polarity between polyphenol extracts and PP, the mechanical properties of the unaged specimens have been similar to the neat PP ones. Finally, also thermal and rheological properties have been not affected by the seed extract.

➢ Wine seeds (Se) are also able to protect PP from long-term UV and thermal aging in a way proportional to their effective antioxidant content as confirmed by the results similar to the PP 01Irg ones. The main drawback regards the necessity to mix high contents of wine seeds(6%wt) with PP to obtain an adequate polyphenol quantity, affecting in a dramatic way the PP mechanical properties (elongation at break values).

➢ The results obtained with Sext, if compared with the commercial tannin seeds extract T, show how the quality of the polyphenol compound plays a key-role in the PP stabilization. It is reasonable to believe that PP 2Sext has worked better than PP 6T, even with a lower content of antioxidants, because of the higher presence of free phenolic hydroxyl groups that result more reactive than long tannin chains. It is also possible to propose the superior antoxidant power of gallic acid (respect to catechin) in PP stabilization comparing the LC-MS data of Sext and T.

➢ The obtained results open new interesting works on the optimization of the PP stabilization using different percentages of the polyphenol extract (Sext) and/or combining their effect with synthetic antioxidants and/or virgin wine seeds.

7.4 WINE LEES AS PHBH AND PHBV NATURAL AND COST-EFFECTIVE REINFORCING FILLERS

7.4.1 Materials and methods

Materials

Poly(3-hydroxybutyrate-*co*-hydroxyhexanoate) (PHBH) − typology "I Am Nature AH131 C1" (melting temperature = 145 °C, density = 1.20 g cm^{-3}) − has been supplied by Gruppo Maip S.R.L. (Turin, Italy). Poly(3-hydroxybutyrate-*co*-hydroxyvalerate) (PHBV) − typology PHI 002 (melting temperature = 175 °C, density = 1.23 g cm^{-3}) has been supplied by NaturePlast (Caen, France). The wine lees (WL) have been obtained from the winery Cevico Group C.V.C (Lugo (RA), Italy) by raking after alcoholic fermentation of red Sangiovese grapes. 3-Methacryloxypropyltrimethoxysilane GENIOSIL® GF31 (sil) (purity > 98%, density = 1.05 g cm^{-3}) has been provided by Wacker Chemie AG (München, Germany). This silane typology has been selected since the high compatibility between the methacrylic organofunctional group and the polyester polymer family as also reported and suggested by the technical datasheet [340, 341]. Finally, the paraffinic oil "Vestan" has been provided by Tizi, S.R.L (Arezzo, Italy). The chemical structure of PHBH, PHBV and sil are shown in Figure 79.
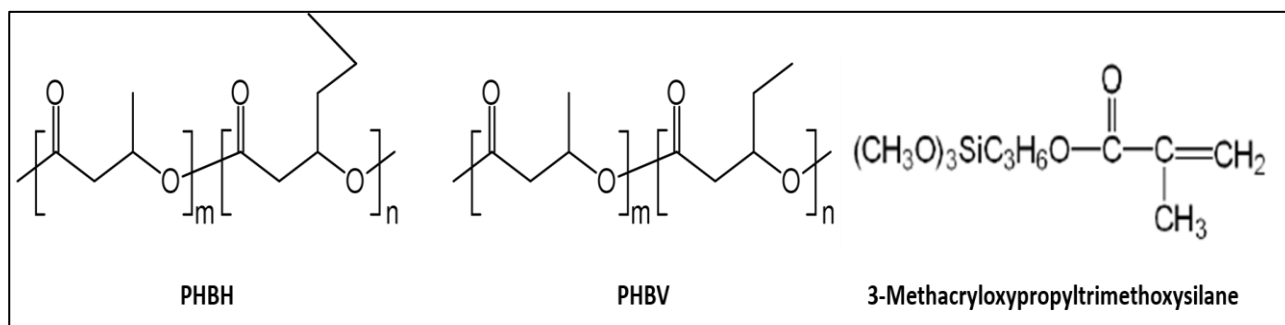
Fig.79 Chemical structure of PHBH, PHBV and sil.

Preparation of the PHBH and PHBV based materials

PHBH and PHBV pellets have been firstly manually mixed with 1 phr (parts for hundred parts of polymer) of Vestan paraffinic oil in order to make the polymer wet and sticky improving the adhesion between the WL and the pellets surfaces and the polymer/filler homogeneity before the extrusion. Therefore, the WL have been mixed in different contents: 10, 20 and 40 phr. Clearly, the paraffinic oil has not been used in the formulations containing silane (inherently sticky) that has been mixed in a content equal to 5 %wt with respect to the WL (or 1 phr of silane referring to the polymer). The compositions of the investigated samples are reported in Table 30.

Table 30 Code and composition of the investigated materials.

PHBH-based samples	Composition	PHBV-based samples
PHBH pellet	Virgin polymer pellet (not processed)	PHBV pellet
PHBH proc	Neat polymer processed in the same conditions	PHBV proc
PHBH 10WL	Polymer + 1 phr Vestan + 10 phr WL	PHBV 10WL

PHBH 20WL	Polymer + 1 phr Vestan + 20 phr WL	PHBV 20WL
PHBH 40WL	Polymer + 1 phr Vestan + 40 phr WL	PHBV 40WL
PHBH 20WL sil	Polymer + 20 phr WL + 1 phr sil	PHBV 20WL sil

Therefore, each formulation has been extruded in a laboratory twin-screw extruder Rheomex 557 (screw length L: 300 mm - L/D screw ratio:10 – Cylindrical Nozzle with L_{Die} of 4 mm and D_{Die} 2 mm) and each extruded wire has been cooled by air, manually spooled and finally grounded. The obtained pellets have been used for the preparation of suitable specimens for tensile test and for the preparation of rectangular specimens for DMA and creep tests by the means of a MegaTech H10/18-1 Tecnica DueBi injection molding machine. The extrusion and injection molding conditions are shown in Table 31. Before of all these mentioned steps, polymer and wine lees have been oven dried at 80°C for 4 hours in order to remove eventual absorbed moisture.

Table 31 Extrusion and injection molding conditions for the PHBH and PHBV-based samples processing.

Extrusion conditions	PHBH	PHBV	Injection molding conditions	PHBH	PHBV
Feed zone Temperature [°C]	145	160	Hopper Temperature [°C]	140	150
Barrel Temperature [°C]	160	170	Screw Temperature [°C]	155	165
Die Temperature [°C]	160	170	Barrel Temperature [°C]	155	155
RPM [min^{-1}]	30	35	Die Temperature [°C]	150	165
Pressure [bar]	15 ± 5	35± 5	Injection Pressure [bar]	120	120
			Holding Pressure [bar]	60	60
			Holding time [s]	3	3
			Cooling time [s]	7.5	7.5

Wine lees characterization

WL have been firstly oven-dried at 70 °C until the monitored weight has resulted to be constant; in this step moisture content has been evaluated. Subsequently, they have been grounded in a batch analytical mill and the particle size distribution has been evaluated as well as the density, by water and air weight measurements exploiting the Archimedes' balance. The volatile (S_v) and not-volatile (S_{nv}) solid fractions have been determined by means of a muffle-furnace operating at 650 °C for 2 hours through the following equations:

$$S_{nv}(\%) = \frac{W_{650}}{W_{80}} * 100 \ (1); \ S_v = \frac{W_{80} - W_{650}}{W_{80}} * 100 \ (2)$$

where W_{650} and W_{80} represent the weight of the residues at 650 and 80 °C, respectively. The grounded and dried WL have been characterized from a morphological point of view using the Scanning Electron Microscopy (SEM) as described in next paragraph (2.4.4.). The elementary composition has been detected by Energy Dispersive Spectroscopy (EDS) using INCA software (ETAS Group, Germany) for the quantification analysis.

Characterization techniques for the PHBH and PHBV-based materials

Differential Scanning Calorimetry (DSC)

Thermal properties of PHBH and PHBV-based materials have been evaluated by Differential Scanning Calorimetry (DSC). DSC measurements have been performed by a DSC TA 2010, using 8 $\pm$ 2 mg of sample and purging the chamber with nitrogen at 50 mL min^{-1}. Each sample has been firstly heated from T_{AMB} to 200 °C at 10 °C min^{-1} in order to erase the previous thermal history. After a 2 min isothermal step at 200 °C, cooling cycle has been conducted at 10 °C min^{-1} to -20 °C and finally, samples have been re-heated to 200 °C at 10 °C min^{-1}. Crystallization temperature (T_C) and crystallization enthalpy (H_C) have been evaluated as the maximum peak and the peak area of the heat flow in the cooling cycle, respectively. The same approach has been used for the melting temperature (T_m), as well as the melting enthalpy (H_m) determinations during both the first and second heating cycle. When present, also post-crystallization temperature (T_{PC}) and enthalpy (H_{PC}) have been evaluated during the heating cycles. The crystallinity has been calculated by the mean of the following formula:

$$\% \, Crystallinity = \left(\frac{H_M - H_{PC}}{H_{ref} * (1 - w_{add})} \right) * 100 \quad (3)$$

where H_{ref} represents the reference melting enthalpy of the polymer 100% crystallinity and w_{add} the weight fraction of the different additives (WL, paraffinic oil, sil). The values of 146 J g^{-1} has been used for PHBH and PHBV as reference melting enthalpy [342].

Tensile test

Tensile tests have been performed by means of the INSTRON 5567 dynamometer equipped with a 1 kN load cell and a 25 mm gauge length extensimeter. The tensile specimens have been of 1BA typology (according to technical standard ISO 527) with the following dimensions: overall length: 75 mm, gauge length: 25 mm, thickness: 2 mm, width of the narrow portion: 5 mm and width at the ends: 10 mm. Tests have been conducted at room temperature with a 10 mm min^{-1} clamp separation speed. Young's modulus (E), tensile strength (σ_M), and tensile strain at break (ε_b) have been measured and the reported data are the average of at least six determinations. WL particles modulus (E_P) has been extrapolated from the micromechanical models for composites modulus (E_C) prediction of Voigt [343] and Halpin-Tsai [344, 345] (Eq. 4 and 5, respectively) considering both PHBH and PHBV data. Analogously, the tensile strength data have been used within Pukanszky's equation [346] (Eq.6) in order to investigate the interfacial adhesion and interaction between the WL particles and the polymer matrices through the extrapolation of the constant B [347, 348]. In fact, B is an empirical constant, which depends on the surface area of particles and on their interfacial bonding energy and for poorly bonded particles, B value tends to zero meanwhile it increases improving the adhesion [349]. The mentioned models are hereafter reported:

$$Voigt: E_C = E_P V_P + E_M (1 - V_P) \quad (4)$$

$$Halpin - Tsai: E_C = E_M \frac{1 + 2\eta V_P}{1 - \eta V_P} \quad (5) \quad \eta = \frac{E_P/E_M - 1}{E_P/E_M + 2}$$

$$Pukanszky: \sigma_C = \sigma_M \frac{1 - V_P}{1 + 2.5 V_P} \exp(B V_P) \quad (6)$$

where E_C is the composite modulus, E_M is the polymer matrix modulus, E_P is the filler particle modulus, V_P is the filler particle volume fraction and B is the Pukanszky's empirical adhesion constant.

Dynamic Mechanical Analysis and creep tests

TA DMA Q800 instrument in the single cantilever flexural configuration has been used to evaluate the dynamic mechanical behavior of the different samples. Size of the used rectangular specimens (l, w, t) has been: $17 \times 5 \times 2$ mm^3. Tests have been conducted with a 3 °C min^{-1} heating rate from -20 °C to 80 °C. The used oscillating frequency has been of 1 Hz meanwhile the strain has been set and maintained equal to 0.1%. Glass transition temperature (T$_g$) has been estimated as the peak maximum of the tanδ curves. The creep properties of the different samples have been measured on the same instrument using the same size specimens. Creep tests have been performed at 20, 40, 60 and 80 °C. At each temperature, samples have been loaded by 1 MPa for a creep time of 10 min followed by a 10 min of relaxation. Creep compliance curves have been obtained for each temperature and subsequently have been used as source for the master curves generation. Master curves have been obtained at the reference temperature of 20 °C using the William-Landel-Ferry (WLF) equation model. Similarly, the Kohlrausch–Williams–Watts (KWW) creep model has been fitted on experimental data in order to extrapolate the 4 KWW theoretical parameters useful for creep behavior description.

Melt Flow Rate (MFR)

Melt mass flow rate (MFR) of the investigated materials has been determined according to ISO 1133 (part II, materials sensitive to moisture) with a load of 2.16 kg at 180 °C.

Scanning Electron Microscope (SEM)

Morphology, adhesion, distribution and dispersion of the WL within the polymer matrix have been observed with an environmental Scanning Electron Microscope, SEM (ESEM Quanta FEI 2000). Rectangular specimens, identical to the ones used for the DMA analysis, have been broken in liquid nitrogen. The cross section of the specimen has been covered by a 10 nm thickness gold layer (Gold Sputter Coater – Emitech K550). The obtained surfaces have been observed with the SEM operating in low-vacuum conditions.

7.4.2 Results and discussion

7.4.2.1 Wine Lees Characterization

The WL have reported an initial moisture value of 16% in weight and a density of 1.36 ± 0.6 g cm^{-3}. In Fig.80, the WL particle size distribution and the cumulative passing curves have been reported. The particle-size distribution curve shows a Gaussian behavior with the mean value (D$_{50}$) placed at around 25 μm meanwhile the 10% of the particles result smaller than 5 μm (D$_{10}$) and the 90% smaller than 63 μm (D$_{90}$). The possibility to obtain relatively tiny particles without many difficulties could encourage further investigations aimed to the obtainment of WL nanoparticles able to improve even more the WL-based composites mechanical properties (as discussed in next paragraph).
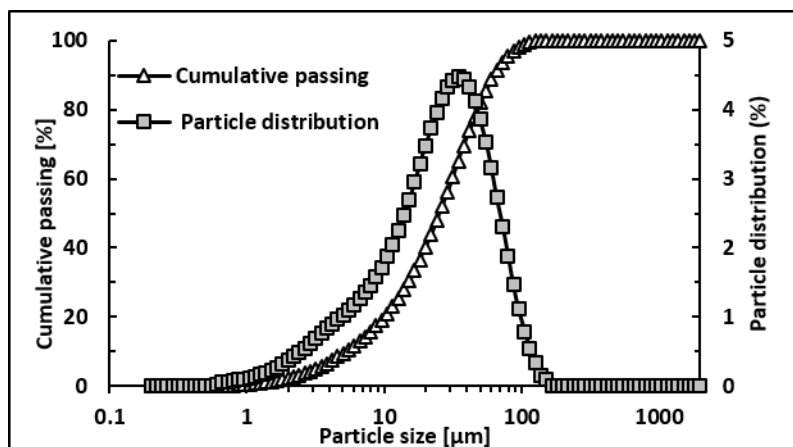
Fig.80 Particle size distribution and cumulative passing curves of the wine lees.

Morphologically, WL particles have been characterized by a spherical-flakes shape as shown in Fig. 81. From a chemical point of view, high inorganic and not volatile fractions have been found out in WL, as demonstrated by the huge muffle-furnace residues ($S_{nv} = 40\%$; $S_v = 60\%$). This high inorganic fraction has been also confirmed by the EDS spectra shown in Fig. 82, where important amounts of Potassium (13.5 ± 0.2 % wt.), Silicon (12.3 ± 0.2 % wt.) and Aluminum (2.6 ± 0.1 % wt.) as well as traces of Calcium, Iron and Cupper have been found out. The Potassium and Calcium presence could be explained by the presence of tartrate salts derived by the significant tartaric acid content often reported in WL [287, 288]. Similarly, the Silicon and Calcium presence could represent the consequence of WL contaminations with materials as bentonite and kaolin, usually used in wine clarification treatments [350].
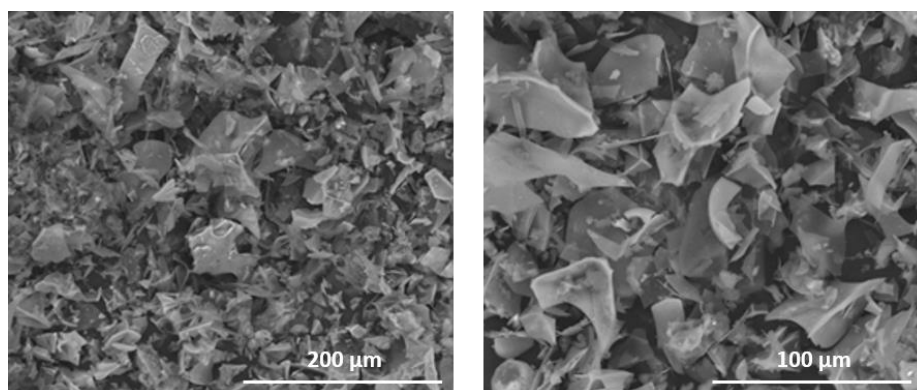
Fig.81 Captured SEM images of the dried and grounded wine lees.
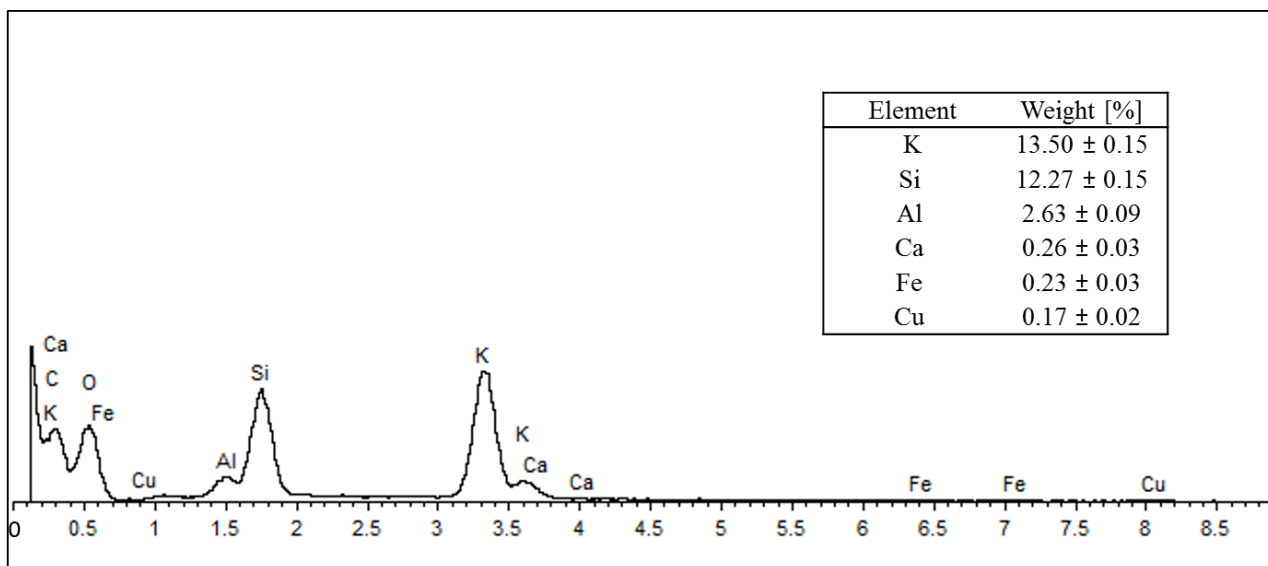
Fig.82 EDS spectra of the wine lees ashes (image created by INCA software, ETAS group (GER)).

Therefore, because of both the elevated inorganic content and the small and homogenous spherical shape, WL seem to promise an excellent filler potential despite being an agro-industrial waste.

7.4.2.2   Thermal properties and Melt Mass Flow Rate

In Figure 83, the crystallinity percentages of PHBH and PHBV-based samples evaluated during the second heating cycle have been reported as WL function. Looking at PHBH data (Fig.5a), it is possible to notice that crystallinity is enhanced using 10-20 phr of WL meanwhile it decreases for 40 phr of WL. This aspect combined with the higher T_C recorded during the cooling step and with the lower T_{PC} recorded during the second heating cycle (Table 32), confirms the possibility of the WL to work, under certain conditions and content range, as heterogonous nucleating agents [351, 352]. By the way, crystallinity percentage can be lowered by high WL loading (e.g. PHBH 40WL) because of possible aggregation phenomena that hinder the crystals formation. In the case of PHBV-based sample (Fig.83b), WL are not able to enhance the crystallinity because the already high crystallinity values of the neat PHBV. Nevertheless, crystallinity decreases again using 40 phr of WL also in this case confirming the aggregation phenomena.
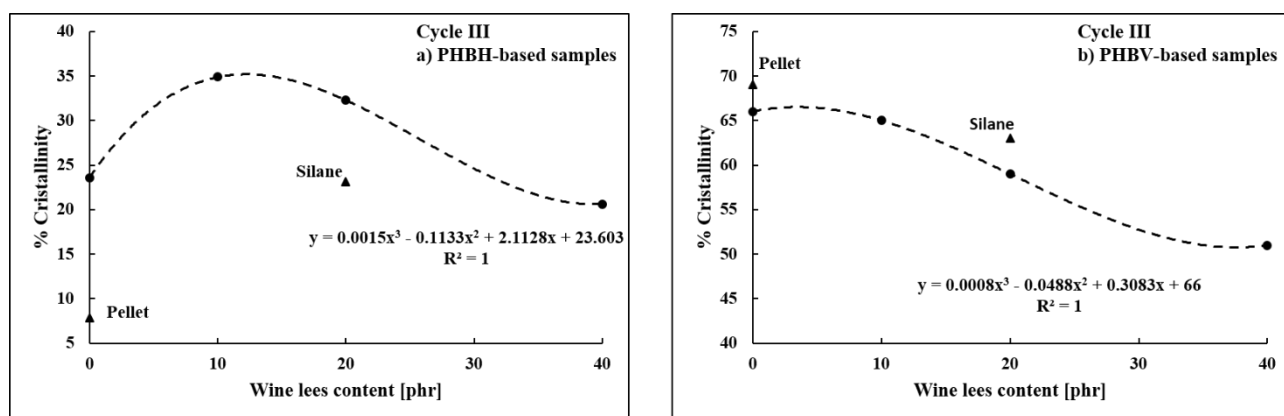
Fig.83 Crystallinity of a) PHBH and b)PHBV-based samples as wine lees content function evaluated during the second heating cycle.

Finally, first and second heating cycle data of PHBH-based samples (Table 32) could seem to be in conflict with one another. From one side, the cooling rate occurred during extrusion (air cooling) seems to have been slower of that set in DSC (10 °C min^{-1}) since post crystallization is present only in the second heating cycle. On the other hand, the overall higher crystallinity evaluated during the second heating cycle suggests the opposite (i.e. cooling rate occurred during extrusion faster than 10 °C min^{-1}). Nevertheless, results are not in contradiction if it is considered that during the first heating cycle (up to 200 °C) degradation may have occurred. In fact, it is often reported in literature that thermal degradation increases the crystallinity percentage (and decrease the melting temperatures) since degraded short-chains can be more easily assembled in ordered domains [195, 292]. For this reason, PHBH crystals domains formed during the third cycle have been more than ones of first cycle despite higher cooling rates [292]. This hypothesis is also supported by the lower melting temperatures recorded during the third cycle and by the significant PHAs susceptibility to the high temperatures [201, 353]. Same reasoning may be applied also considering PHBV data.

Table 32 PHBH and PHBV based samples DSC data.

PHBH based samples											
	T_{PC} [°C]		H_{PC} [J g^{-1}]		T_m [°C]		H_m [J g^{-1}]		% Cristall.		T_C [°C]
Cycle	I	III	I	III	I	III	I	III	I	III	II
Pellet	-	51	-	44.0	149	144	37.1	55.4	25	8	52
Processed	-	38	-	14.3	149	142	32.4	48.8	22	24	48
10 WL	-	35	-	3.6	148	144	33.1	49.4	25	35	65
20 WL	-	35	-	1.5	146	143	31.2	40.5	26	32	64
40 WL	-	37	-	14.9	146	141	26.6	36.3	26	21	51
20WL_sil	-	37	-	21.0	147	143	34.5	49	29	23	53
PHBV based samples											
	T_{PC} [°C]		H_{PC} [J g^{-1}]		T_m [°C]		H_m [J g^{-1}]		% Cristall.		T_C [°C]
Cycle	I	III	I	III	I	III	I	III	I	III	II
Pellet	-	-	-	-	177	168	67.9	100.5	47	69	115
Processed	-	-	-	-	176	166	70.6	97.0	48	66	114
10 WL	-	-	-	-	176	166	69.2	86.5	52	65	110
20 WL	-	-	-	-	175	163	55.0	64.5	45	59	106
40 WL	-	-	-	-	175	163	49.6	53.6	47	51	107
20WL_sil	-	-	-	-	175	165	60.2	77.4	49	63	112

WL have been also able do not modify the melt viscosity as reported in Figure 84. In PHBV based samples, MFI values have ranged between 8 and 10 g/10' for all formulations, perfectly according to the values reported in PHBV technical data sheet (5-10 g/10'). Comparing PHBH processed (12.5 g/10') and PHBH pellet (6.6 g/10') values, a partial degradation seems to be occurred during twin-screw extrusion. In fact, scl-PHAs are particularly susceptible to thermal degradation [201, 353] and the adopted PHBH extrusion temperature (15 °C higher than PHBH melting temperature) could have decreased the molecular weight and thus increased the polymer fluidity. Therefore, looking at PHBH composites data, it could be supposed that WL seems have increased the viscosity of the PHBH based samples balancing the effects due to the degradation.
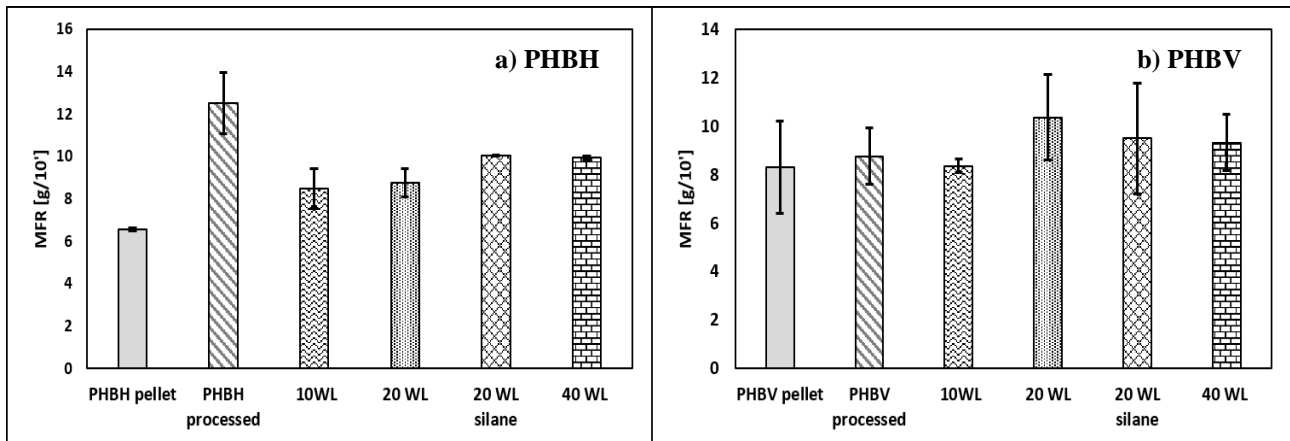
Fig.84 MFR values of PHBH (a) and PHBV (b) based samples.

7.4.2.3 Mechanical properties

Tensile test

PHBH and PHBV tensile test data are reported in Fig. 85 and Table 35. In composites filled with particles the tensile properties (Young's modulus, tensile strength and elongation at break) depend mainly on three factors: particles size, particle-matrix interface adhesion and the particle loading [156]. The Young's modulus increases progressively with the WL content similarly to other works on composites [171-173]. In fact, among the three previous mentioned factors, particle loading is the one more effecting the Young's modulus. Particle size can enhance the modulus only below a critical value (often placed at 30 nm [178-180]), otherwise elastic modulus results to be independent on this factor [156, 354, 355]. The critical particle size cannot be predicted a priori because depending both on particle and matrix typology, but in this case, being the WL mean size of 25 μm, it can be stated to be far away from this criticality. Further WL size optimizations should be conducted only in large-scale approaches evaluating the cost-benefits of the grinding operations. Finally, elastic modulus is also not affected by the particle-matrix adhesion since it is evaluated at relatively low deformations and therefore there is insufficient dilatation to cause interface separation [156]. Thus, it is easy to understand that the adhesion strength does not noticeably affect the elastic modulus as reported in other works [356, 357]. Looking data reported in Fig. 85, Young's modulus is increased especially in PHBH samples with the content of 40 phr of WL where the elastic modulus is enhanced of about the 25% from the initial value (7.3% in the case of PHBV 40WL). The gain in elastic modulus is explained by the fact that WL have higher stiffness than the polymer matrices In PHBV samples, the linearity between the WL content and the Young modulus gain is much less marked. A similar behavior has been found out in other bio-composites works [174-176] where, however, interpretations were rarely or scarcely given. Here, it is proposed that this unconventional mechanical properties trend could be consequence of not optimal processing conditions. As filler content is increased, polymer chains are more and more hindered to orient their selves alongside the axis of the resistant section of the tensile specimen during the injection molding process. Thus, the final stiffness would be balanced by these two opposite effects. Moreover, the stiffening WL contribute (theoretically proportional to the WL content) could have been also balanced by the decreasing crystallinity (inversely related to the WL content as previously reported in DSC data). In any case, further investigation should be carried out to confirm these hypotheses. The WL Young's moduli (E_P)

evaluated by the means of Voigt and Halpin-Tsai models are reported in Table 33. From this table, it is possible to notice that Voigt model matches better the experimental and that the predicted E_P using PHBH data is higher than the one calculated using PHBV data. PHBV data are characterized by much lower standard deviations and the two models predictions are similar. These mentioned differences as well as the high standard deviations may be due to the intrinsic limitations of use of these models as reported in literature [358]. Indeed, these models do not account for the variability in the modulus of the constituents, for the particles break and for the variation of quantity and properties of fillers and matrices through the mixing processes [189]. Moreover, corresponding calculated E_P for the WL are not available in scientific literature and thus, comparisons can not be done. For these reasons, accurate WL elastic modulus values can not be stated in this work. By the way, considering the E_P values of other natural fillers reported in literature (wheat straws 8 GPa [187], hazelnut 5.8 GPa, corn cob 5.0 GPa, wood 4.9 GPa [359] and grape stalks 6.8 GPa [189]) it is possible to notice that the orders of magnitude coincide with WL ones.

Table 33
Wine lees elastic moduli extrapolated through Voigt and Halpin-Tsai models.

	Voigt Model	Halpin-Tsai Model	Average of the two models
	Mean value [MPa]	Mean value [MPa]	[MPa]
Considering PHBH data	4242 ± 839	7318 ± 3274	5780 ± 2757
Considering PHBV data	2505 ± 391	2797 ± 638	2651 ± 514
Considering both	3373 ± 1108	5057 ± 3257	4215 ± 2506
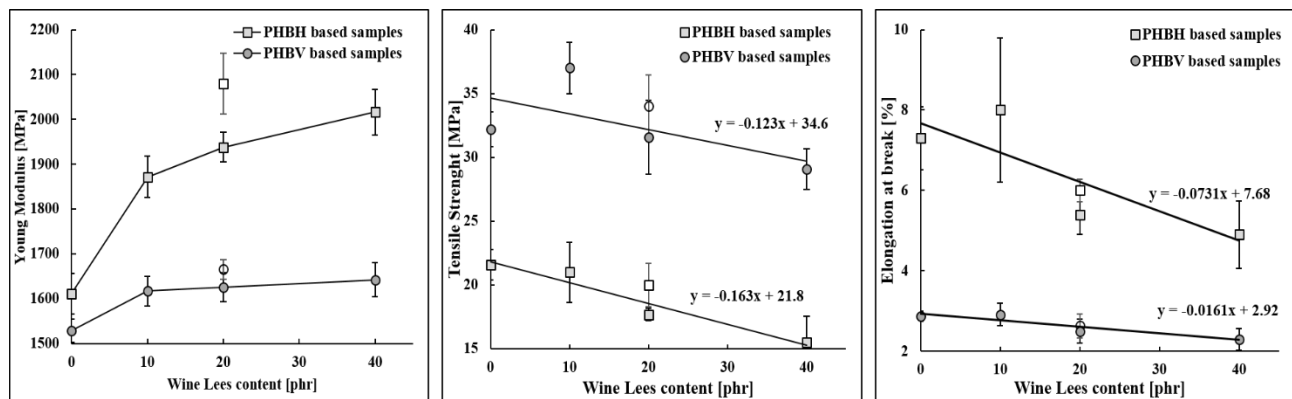
Fig.85 Young Modulus, tensile strength and elongation at break of PHBH and PHBV based samples. Unfilled symbols refer to formulation containing silane.

The maximum tensile strength decreases almost proportionally to the WL content in both PHBH and PHBV-based samples. Summarily, tensile strength loss is "faster" in PHBH where the slope is 1.3 times higher than in PHBV (Fig. 85). This fact could be explained by the fact that PHBH, having one more hydrophobic $-CH_2$ group than PHBV, results in a lower adhesion with the hydrophilic WL than PHBV. This hypothesis is supported by several works in which PHBH water contact angles were reported significantly higher than PHBV ones (approximately 85-105° for PHBH [360, 361] and 70-76 ° for PHBV [362, 363]. In composites, the tensile strength depends mainly on the particle-matrix adhesion but particle size also effect this property. Generally, tensile strength increases with decreasing the particle size because the higher particle specific areas (inversely proportional to the

mean size) guarantee better stress transfers between particle and polymer matrix. Therefore, also well-bonded particles can decrease the tensile strength if not small enough. In literature, this aspect has been reported numerously [355, 364, 365] and in some cases the same particles have both increased and decreased the tensile test depending on their mean size. By the way, the particle-matrix adhesion is the factor more effecting the tensile strength because poorly bonded particles are not able to transfer the stress through the particle-matrix interface. This discontinuity makes the particle unable to sustain any stress load and tensile strength decreases increasing the particle content. Moreover, with poorly bonded particles, craze formation happens earlier than with well-bonded particles because the de-wetting phenomenon connected to the bad adhesion creates cap-shaped cavity already for low applied stresses [156, 357]. For these reasons, considering the PHBH and PHBV-based samples data, is possible to state that the limited tensile strength loss is more connected with the particle size rather than with bad adhesion mechanisms (in which case the observed loss should have been higher [357]). In addition, increasing the particle load can decrease the tensile strength because of aggregation phenomena that deteriorates the stress transfer efficiency [172]. Concluding, is possible to state that WL marginally effect the PHBH and PHBV tensile strengths and even better results could be probably obtained decreasing the particle sizes. The WL-PHAs adhesion seems to be good also without GF31 silane as coupling agent that however is able to work enhancing the particle-matrices interface adhesion. In fact, comparing "PHBH 20WL" with "PHBH 20 WL sil" and "PHBV 20WL" with "PHBV 20 WL sil", a tensile strength increase of 13% in PHBH and of 7.6% in PHBV is noticed when the coupling agent is used. What has been said is confirmed also by the B empirical factors extrapolated by Pukanszky's equation (Table 34). B values are higher in PHBV based samples confirming the best adhesion of WL to PHBV matrix and silane effectiveness is confirmed by higher B values in both polymers. Finally, comparing Table 34 data with other B factors extrapolated in literature for other natural fillers (hemp chips (B=2.10), grape stalks (B=1.69) [189], chemically treated rice husk (B=2.57) [366]), a global and excellent adhesion of the here investigated systems comes out.

Table 34 Empirical B adhesion factor extrapolated from Pukanszky's equation.

	10 WL	20 WL	40 WL	Average	20 WL sil
PHBH based	2.96	1.83	1.77	2.19 ± 0.67	2.68
PHBV based	4.19	3.08	2.69	3.32 ± 0.78	3.58
B factor for PHAs-WL composites: without and with silane				2.76 ± 0.90	3.13 ± 0.64

As expectable, the elongation at break values (Table 35) have been decreased by increasing the particle loading as often reported in literature [156, 367]. In PHBH case, elongation at break increases of nearly 10% in PHBH 10 WL sample confirming the very good particle-matrix adhesion [156, 368] and subsequently decreases at higher WL particles loads, probably because of occurred aggregation phenomena [367, 369]. Nevertheless, from a technological point of view, because of the already low initial elongation at break values of neat PHBH and PHBV (especially), the WL seem do not change the suitable application fields of these biopolymers.

Table 35 PHBH and PHBV tensile test data.

	E [MPa]	ΔE [%]	σ_M [MPa]	$\Delta\sigma_M$ [%]	ε_b [%]	$\Delta\varepsilon_b$ [%]
PHBH proc	1611 ± 46	-	21.6 ± 1.2	-	7.3 ± 0.8	-

10 WL	1872 ± 46	+ 16.2	21.0 ± 2.4	- 2.8	8.0 ± 1.8	+ 9.6
20 WL	1938 ± 33	+ 20.3	17.7 ± 0.5	- 18.1	5.4 ± 0.5	- 26.0
40 WL	2016 ± 51	+ 25.1	15.5 ± 2.0	- 28.2	4.9 ± 0.8	- 32.9
20 WL sil	2080 ± 68	+ 29.1	20.0 ± 1.7	- 7.4	5.4 ± 0.3	- 26.0
PHBV proc	1529 ± 25	-	32.2 ± 1.4	-	2.9 ± 0.1	-
10 WL	1617 ± 33	+ 5.8	37.0 ± 2.0	+ 14.9	2.9 ± 0.3	-
20 WL	1626 ± 32	+ 6.3	31.6 ± 1.9	- 1.9	2.5 ± 0.3	- 13.8
40 WL	1642 ± 38	+ 7.4	29.1 ± 1.6	- 9.6	2.3 ± 0.3	- 20.7
20 WL sil	1666 ± 22	+ 9.0	34.0 ± 1.9	+ 5.6	2.6 ± 0.2	-10.3

Dynamic Mechanical Analysis

The collected DMA data are presented in Table 36, meanwhile Fig.86 shows the storage modulus behavior of PHBH and PHBV-based samples as temperature function.
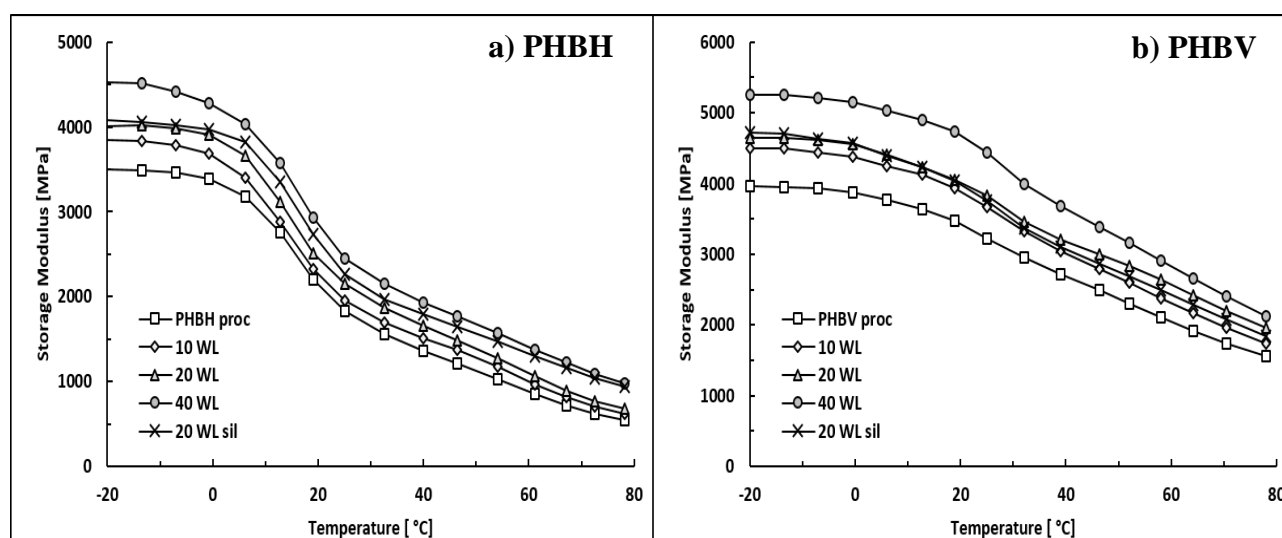
Fig.86 Storage modulus of PHBH (a) and PHBV (b) based sample as temperature function.

Globally, PHBV-based samples have higher storage moduli rather than PHBH-based samples, especially at upper temperatures. In PHBH-based samples, the glass transition region seems to affect more the conservative modulus: E' modulus decreases from 0 °C to 25 °C of almost 46% meanwhile in PHBV based samples this variation is only of 16%. This could be explained by the higher amorphous fraction present in PHBH-based samples as previously reported in DSC data. Considering the WL role, it is possible to confirm the stiffening effect of the WL within both polymer matrices. In fact, an increase in WL content lead to a proportional increase in storage modulus as shown in Fig. 87, and again PHBV-based samples have a slope approximately 1.5 times higher than PHBH one (equations of Table 36). In PHBH-based samples a positive and significant effect of the silane as coupling agent has emerged. In fact, "PHBH 20 WL sil" storage modulus curve is always higher than PHBH 20WL, especially for high temperature (50-75 °C) where their values seem to converge to the PHBH 40WL ones. Conversely, no differences have been detected by the use of silane in PHBV based samples.
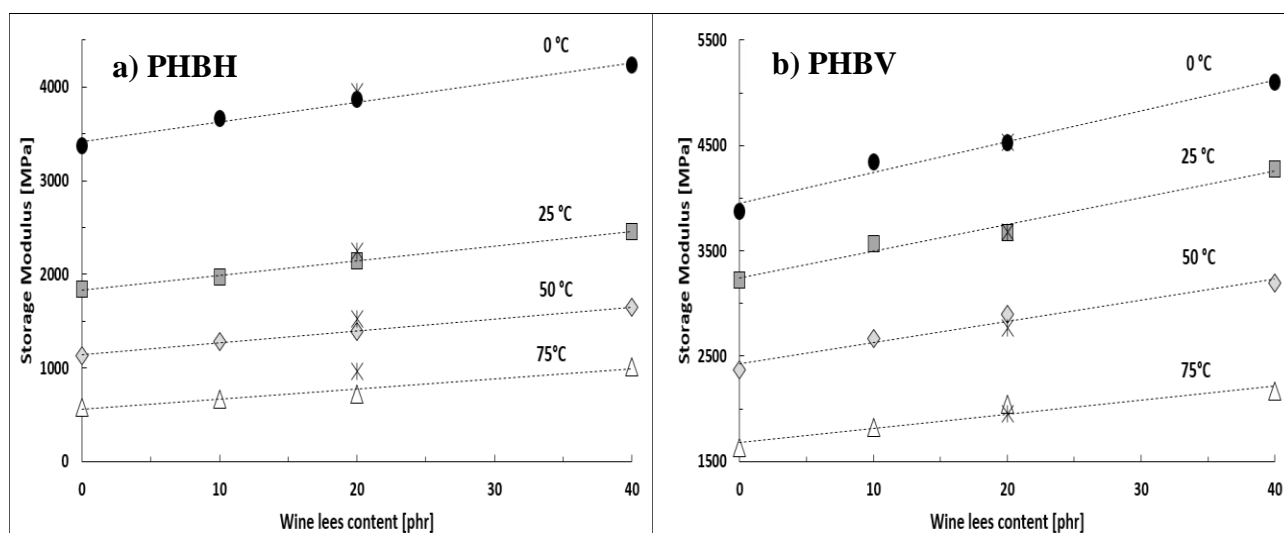
Fig.87 Storage moduli of PHBH (a) and PHBV (b) based sample as wine lees function. Star (✳) symbols refer to samples with silane as coupling agent.

Looking at the glass transition temperatures (T_g), evaluated as the peak maximum of the damping curve and reported in Table 36, is possible to state that WL do not affect significantly this property. Only PHBH 40WL and PHBV 40WL have reported little bit higher T_g temperatures explainable as consequence of the polymer chains immobilization made by the particle along the particle-matrix interface [190-192].

Table 36 Max tan δ values, storage modulus at different temperatures and interpolating equations for PHBH and PHBV-based samples.

	PHBH proc	10 WL	20 WL	40 WL	20 WL sil	Interpolating equation*
E' @0 °C [MPa]	3373	3663	3868	4234	3958	y=21.1x + 3416 R^2=0.998
E' @25 °C [MPa]	1836	1971	2147	2454	2254	y=15.6x + 1829 R^2=0.999
E' @50 °C [MPa]	1131	1285	1384	1643	1533	y=12.6x + 1141 R^2=0.996
E' @75 °C [MPa]	582.9	663.8	723.1	1009	967.4	y=10.7x + 558 R^2=0.966
Max tan δ [°C]	20.2	18.4	19.8	22.0	17.5	
	PHBV proc	10 WL	20 WL	40 WL	20 WL sil	Interpolating equation*
E' @0 °C [MPa]	3873	4345	4522	5097	4532	y=29.3x + 3965 R^2=0.978
E' @25 °C [MPa]	3225	3567	3676	4275	3684	y=25.4x + 3242 R^2=0.981
E' @50 °C [MPa]	2374	2666	2896	3193	2774	y=20.0x + 2431 R^2=0.972

130

E' @75 °C [MPa]	1632	1827	2043	2170	1957	y=13.3x + 1685 R^2=0.920
Max tan δ [°C]	28.7	27.1	27.5	30.5	28.3	

[*] Suitable equations for the prediction of the storage modulus (y) as WL content function (x) at different temperatures for PHBH and PHBV WL composites.

Creep tests

The strain in isothermal creep tests depends on time and on the applied stress and its trend can be usually described as result of three different components [370-372] including a pure elastic component ε_e (σ) (stress-depending, instantaneous and reversible), a viscoelastic component ε_{ve} (t) (time-depending and reversible) and a plastic component ε_p (t, σ) (time and stress depending and irreversible) as reported in Eq.7.

$$\varepsilon(t,\sigma) = \varepsilon_e(\sigma) + \varepsilon_{ve}(t) + \varepsilon_p(t,\sigma) \ (7)$$

In the linear viscoelastic region, the magnitude of these three components is linearly proportional to the magnitude of the applied stress and therefore it is possible to introduce the only time depending creep compliance (J (t) = ε (σ,t)/ σ) and refer to Eq.8.

$$J(t) = J_e + J_{ve}(t) + J_p(t) \ (8)$$

In the present work, no plastic deformation has been produced as testified by the total recovery of the initial length after the unloading and therefore the contribute J_p (t) has not came forward. The creep compliance curves of PHBH and PHBV-based samples carried out at each different testing temperature have been reported in Fig.88, meanwhile the maximum creep compliance values have been reported as temperature function and for different WL contents in Fig. 89. It is evident that WL have been able to markedly reduce the creep compliance and the gap with the not filled polymers has become higher with both increased temperatures and WL contents. Once again, the use of silane have been very efficient as shown by the compliance values of both "PHBH 20WL sil" (always the lowest) and "PHBV 20WL sil" (really close to PHBV 40WL values).
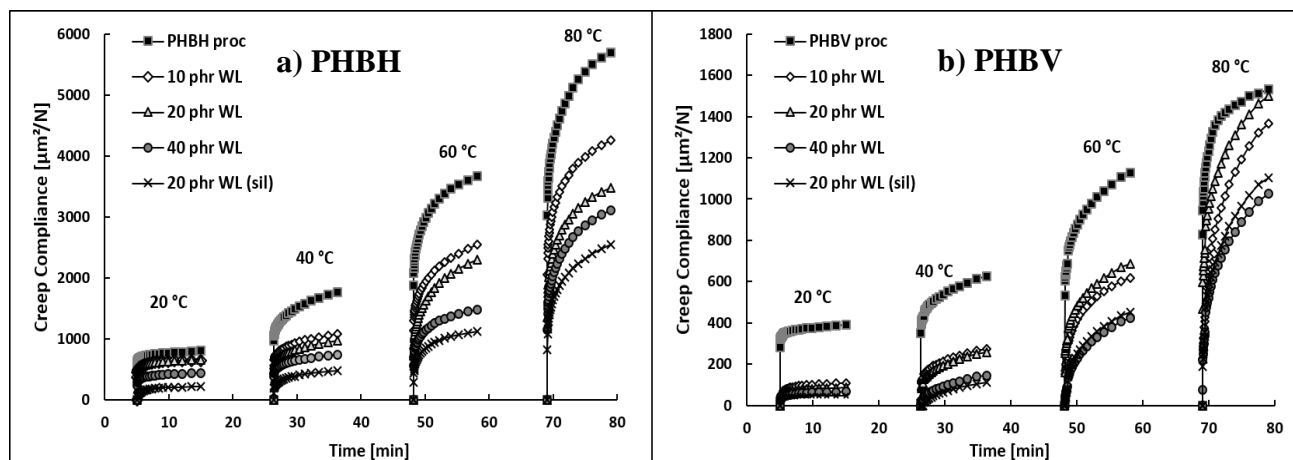
Fig.88 Creep compliance curves of PHBH (a) and PHBV (b) based samples at different temperatures.
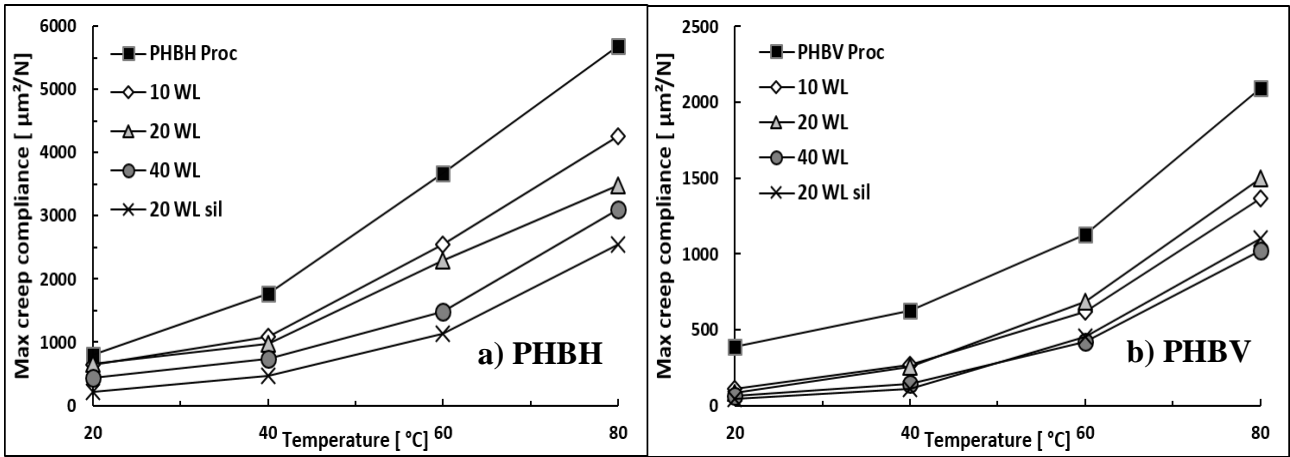
Fig.89 Maximum creep compliance values after 10' of 1 MPa load: PHBH (a) and PHBV (b) based samples curves as temperature and wine lees content.

In order to understand better the viscoelastic mechanisms and responses, a theoretical creep model has been adapted on the obtained creep data to extrapolate useful viscoelastic parameters. In fact, the ability to model the viscoelastic response can provide useful tools to design for long-term load-bearing applications [373]. A mechanical model that has been successfully applied for the analysis of creep data of both glassy solids [374] and semi-crystalline polymers [373, 375] is the Kohlrausch–Williams–Watts (KWW) model. This model arises from the consideration that viscoelastic changes in polymeric matrices occur with incremental jumps due by the fact that, at the molecular level, several segments of macromolecules jumps between different positions of relative stability [376]. According to the KWW model, the time-depending creep compliance is described by a four parameters Weibull-like function [376] and it can be expressed as following (Eq.9):

$$J(t) = J_i + J_c \left\{ 1 - exp\left[-\left(\frac{t}{t_c}\right)^{\beta_c} \right] \right\} \ (9)$$

where J_i is the instantaneous elastic creep compliance component, J_c is the limit creep compliance value reached for time (t) tending to infinite, t_c is the scale characteristic time at which nearly the 63% of the J_c compliance is obtained and β_c represent a shape parameter.

An excellent accordance between experimental and KWW predicted creep compliances data has been found over the entire experimental range ($R^2 \cong 1$) confirming the possibility to use the KWW model as prediction tool for design operation. As example, in Fig. 90 different comparisons between experimental data and the KWW fitting curves at 40 °C have been shown, meanwhile in Table 37, the extrapolated parameters at the temperatures of 40 and 60 °C have been reported for each PHBH and PHBV based samples. Overall, it is possible to notice that the instantaneous elastic component of the creep compliances (J_i) has been reduced by increasing the WL content according perfectly with the changes observed for the tensile elastic modulus. Similarly, a significant reduction of the viscous compliance at very long times (J_c) has been observed in both matrices using WL as fillers. In particular, a reduction of nearly 40% (PHBH) and 30% (PHBV) can be already achieved exploiting only 10 WL phr. Although β_c seems to be only slightly affected by the wine lees presence, the characteristic times (t_c) have been markedly enhanced by the winery by-products. This aspect

132

underlines the fact that wine lees have been able to guarantee both lower strain extents and slower deformation rates.
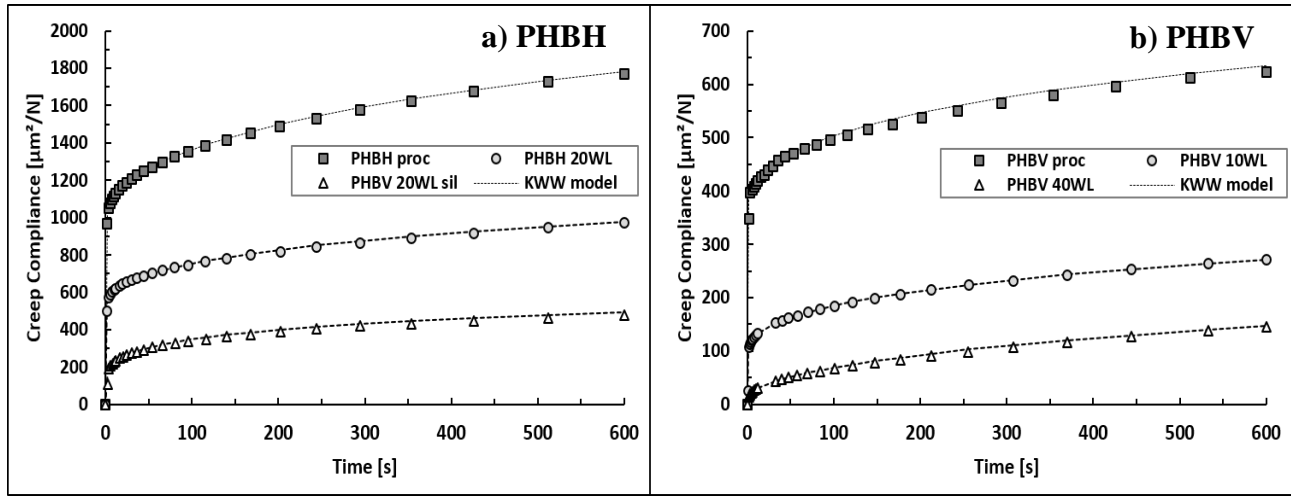
Fig.90 Examples of the KWW model fitting on different PHBH (a) and PHBV (b) based samples creep compliance data at 40 °C.

Table 37 PHBH and PHBV based samples creep compliance: KWW fitting parameters extrapolated at 40 and 60 °C and their R^2 values.

	KWW fitting parameters for creep compliance data at 40 °C									
	PHBH based samples					PHBV based samples				
	J_i	J_c	t_c	β_c	R^2	J_i	J_c	t_c	β_c	R^2
	[μm²/N]	[μm²/N]	[s]	[-]	[-]	[μm²/N]	[μm²/N]	[s]	[-]	[-]
Proc	985.7	1851.5	1891.2	0.5023	1.000	360.4	640.4	2239.6	0.4427	0.998
10 WL	580.6	1108.7	2275.1	0.4090	1.000	93.5	502.5	4041.4	0.4348	1.00
20 WL	512.5	1121.7	2545.2	0.4371	0.999	74.5	566.9	3693.3	0.4701	0.998
40 WL	384.1	873.9	2678.4	0.4008	1.000	11.3	360.0	2294.9	0.5587	1.000
20WL sil	99.9	843.1	2449.0	0.3295	0.998	0.0	196.8	694.7	0.7449	0.999
	KWW fitting parameters for creep compliance data at 60 °C									
	PHBH based samples					PHBV based samples				
	J_i	J_c	t_c	β_c	R^2	J_i	J_c	t_c	β_c	R^2
	[μm²/N]	[μm²/N]	[s]	[-]	[-]	[μm²/N]	[μm²/N]	[s]	[-]	[-]
Proc	1575.5	3652.6	871.7	0.3508	1.000	485.6	1182.1	1056.7	0.4090	0.998
10 WL	1124.6	2661.5	1034.7	0.4470	0.998	77.2	1035.5	1313.2	0.3830	1.000
20 WL	681.5	2971.9	950.6	0.4455	0.999	212.3	935.4	1276.5	0.4552	1.000
40 WL	420.3	1884.3	974.4	0.3312	1.000	13.1	774.0	1053.0	0.5067	1.000
20WL sil	143.2	1664.7	849.8	0.2976	1.000	0.0	716.0	575.8	0.5371	0.999

The enhanced creep resistance mechanism (lower strain and slower deformations) has been also confirmed by the master curves generated at 20 °C using the William-Landel-Ferry (WLF) equations as shown in Fig.91. Through the time-temperature superposition principle, it has been possible to estimate and predict the creep compliance at 20 °C of both PHBH and PHBV based samples until

nearly 60 years. It is possible to notice how final compliance values have been again much lower in filled polymers and perfectly in accord with the J_c values extrapolated by the KWW model.
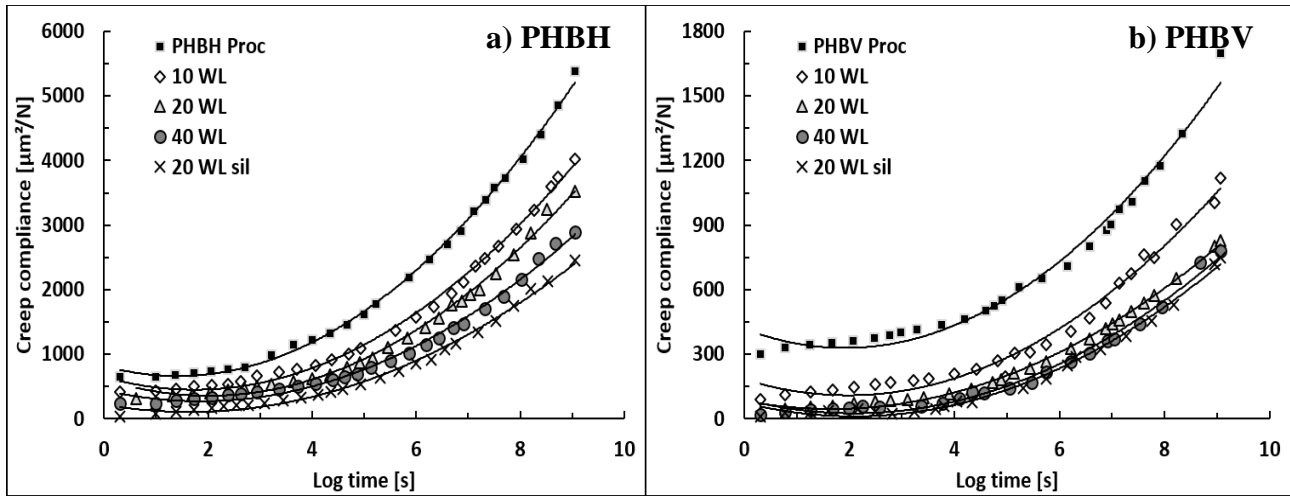
Fig.91 Master curves of PHBH (a) and PHBV (b) generated by time-temperature superposition principle (through WLF equations) at 20 °C.

7.4.2.4 Discussion of the silane role

As previously and often reported in this work, the direct use of silane (5% wt. with respect to the WL content) during the twin-screw extruder processing has led to composites with enhanced mechanical properties. Among them, tensile strength and creep resistance have been the most improved properties because of the improvement of both particle-matrix adhesion and matrix stiffness. If the latter effect could be also viewed as direct consequence of the intrinsic Silicon stiffness (Young's modulus of Silicon particles ranges between 130 and 190 GPa [377, 378]), the enhanced adhesion implies for sure that also chemical/physical interactions between polymer, WL and silane have taken place during the extrusion. Possible reaction schemes between the three compounds have been reported in Fig.92. Briefly, it can be supposed that silanol groups (derived by silane hydrolysis, Fig.92-1) have been able to interact with the OH WL hydroxyl groups to form hydrogen (Fig.92-2a) or covalent (Fig.92-2b) bonding as already reported in other works regarding the use of silane as coupling agent for natural fillers [379, 380]. Concerning the silane-polymer interactions (Fig.92-3), the silane's organo-functional groups could have reacted with the OH terminal group of the used polymers by forming a covalent bond. In fact, the introduction of high energy groups in the interphase area and the relatively low molecular weight of thermoplastics polyesters could have led to significant possibilities for end-group reactions [381, 382].
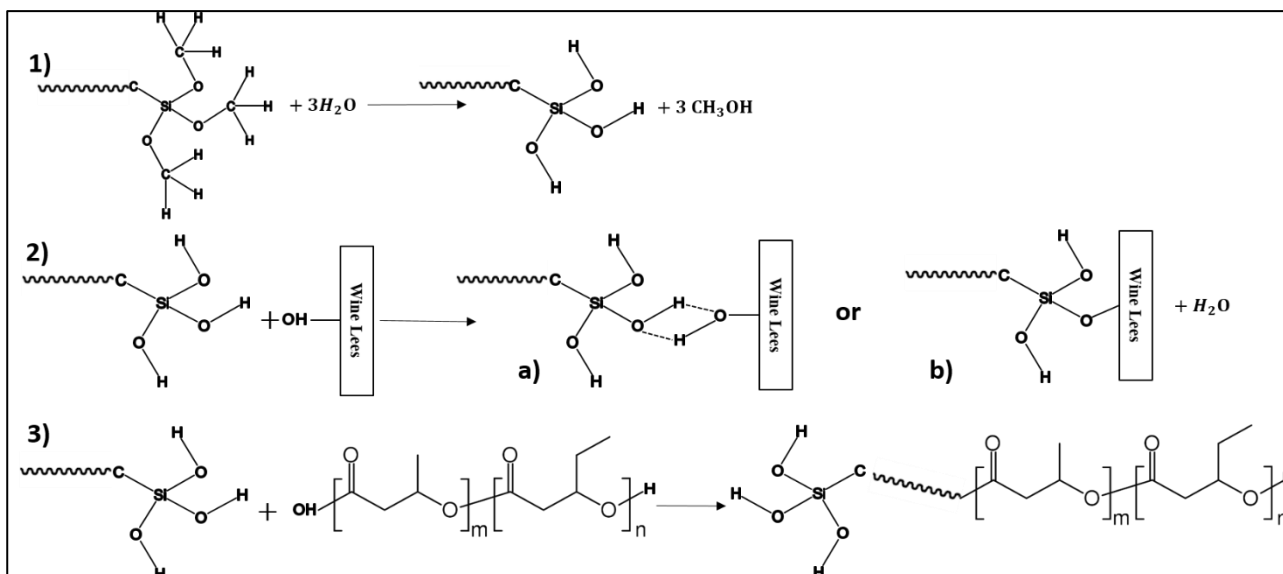
Fig.92 Scheme of possible reactions between silane, wine lees and polymers.

Interactions between particles and matrices have been indirectly confirmed also by the captured SEM images of "PHBH 20WL" and "PHBH 20WL sil" samples (Fig.93). Some of the shortcomings derived by bad particle-matrix adhesions, as cap-shaped cavities and not well-bonded particles, have been noticed within "PHBH 20WL" meanwhile these defects have not been detected (or only marginally) in "PHBH 20WL sil" pointing out the silane efficiency also from a morphological point of view. In the PHBV-based samples, less adhesion problems have been found in both case (with and without silane) because of the higher particle-matrix adhesion (B adhesion factor of 3.32 against the PHBH one of 2.19). Therefore, it is possible to state that also few amounts of sil (1 g each 100 g of polymer) have been able to improve the PHBH and PHBV-WL adhesion without any shortcoming. By the way, because of the already intrinsic good adhesion exhibited between WL and polymers without silane, its use in large scale should be verified only after accurate economic analysis.
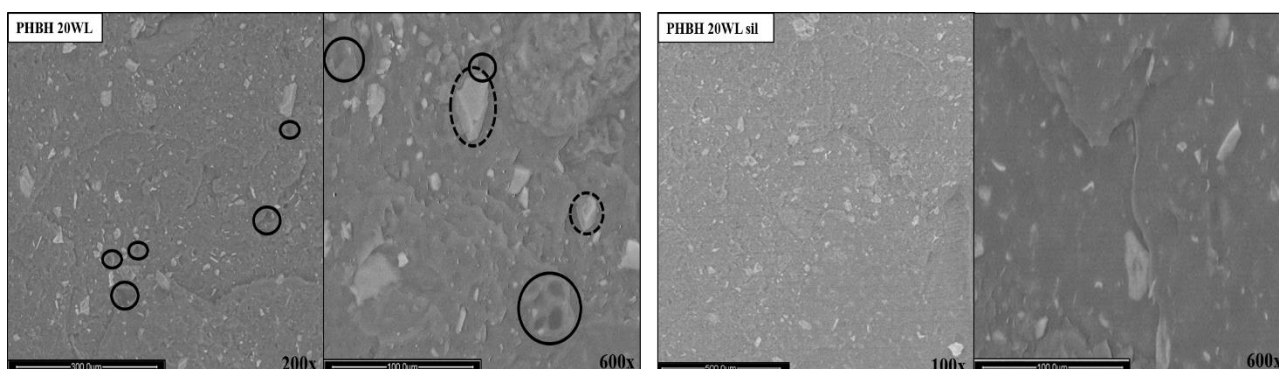
Fig.93 Captured ESEM images of PHBH 20WL and PHBH 20WL sil. The full circles indicate the cap-shaped cavities meanwhile the dotted circles indicate bad-bonded particles.

In conclusion, proposed possible coupling reactions have been supported only by indirect evidences as higher tensile strength and improved morphology meanwhile quantitative proofs of the functionalization have been not reported. This has been due since the difficulty on detecting silicon-bonds differences between samples containing and not containing silane caused by the intrinsic initial

135

presence of the Silicon element within the WL fillers, as previously reported by EDS spectra in Fig.82.

7.4.2.5 Economic analysis

In order to assess the economic feasibility of these investigated bio-composites, an economic analysis has been carried out. It has been supposed that final composite price depends mainly on three economic factors: (i) the polymer price, (ii) the WL prices and (iii) the extrusion cost. In this work, the following costs have been initially adopted: PHBH and PHBV pellets price of 5 €/kg [131, 132], WL price of 0.045 €/kg (iii) [383] and extrusion cost of 0.4 €/kg (estimated cost of commercial extrusion for 10 tons of material [359]). The economic profits have been evaluated comparing the composite final cost with that of pure polymer as well as the Break-Event-Point (BEP) has been estimated as the minimum or maximum value of an economic factor leading, again, to the composite final cost equal to that of pure polymer. As example, examining the formulation with 20 phr of WL, it is possible to state that the polymer price of 2.44 €/kg is the minimum value that balance the composite and pure polymer prices considering fixed to the initial supposed prices the other two economic factors. Indeed, for lower polymer prices no economic profit would be reached. This approach has been followed for each economic factor and formulations and all the estimated profits as well as the economic factors BEP are reported in Table 38. Keeping fixed all three economic factors, the BEP is reached using 8.8 phr of WL anticipating poor economic returns with the 10 phr WL formulation.

Table 38 Economic profits at different WL contents evaluated considering polymer, WL and extrusion costs equal to: 5, 0.045 and 0.4 €/kg respectively. BEP values evaluated keeping fixed two of the previous mentioned costs and varying the other one to reach composite and polymer costs equality.

		BEP economic factor values		
	Economic Profit [€/kg]	Min polymer price [€/kg]	Max WL price [€/kg]	Max Extrusion cost [€/kg]
10 phr WL	0.05	4.44	0.6	0.45
20 phr WL	0.43	2.44	2.60	0.83
40 phr WL	1.02	1.45	3.60	1.42

Nevertheless, the exact initial biopolymer price is difficult to know or suppose a priori since it strongly depends on market requests and trends and on the purchased quantity. Moreover, in this case, being the biopolymers produced by fermentation, other factors as typology, costs and availability of the used fermentable biomasses as well as the polymer purification grade affect significantly the initial price. Similar consideration could also be done referring to the extrusion costs. Therefore, profit surfaces at different WL contents have been generated ranging the initial polymer price from 2.5 to 7.5 €/kg and the extrusion cost from 0.1 to 0.7 €/kg (Fig.16) in order to extent the economic analysis.
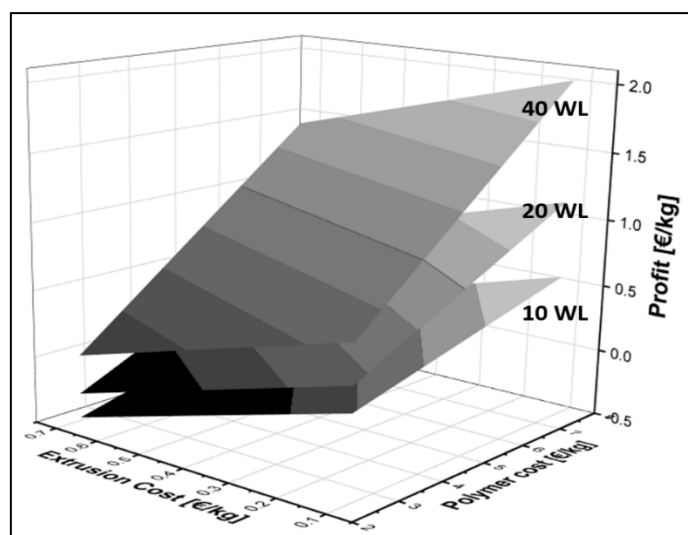
Fig.94 Profit surfaces for different WL contents obtained ranging the extrusion cost from 0.1 to 0.7 €/kg and the polymer cost from 7.5 to 2.5 €/kg and considering the WL cost fixed to 0.045 €/kg.

It is possible to notice that using 40 phr of WL an economic profit is always obtained (no black zones in the surface of Fig.94) and it can reach the maximum value of 2.03 €/kg. Using 20 phr of WL, economic profit is obtained in the 88.1% of the tested combinations and it can reach the maximum value of 1.14 €/kg. As expectable, the 10WL formulation is the less attractive for large-scale operations: no economic returns are observed in the 43% of the cases and the final composite could even cost 0.48 €/kg more than virgin polymer. Finally, considering the 20WL formulation with silane and supposing silane price ranging between 5 and 10 €/kg, the final economic profit (0.38-0.42 €/kg) still remains very similar to the 20WL formulation because of the silane amount littleness.

7.4.3 Conclusions

In the present study, bio-composites consisting of PHBH and PHBV filled with different content (10, 20 and 40 phr) of WL have been prepared by twin-screw extrusion and injections molding. The main thermal and mechanical properties of the obtained samples have been evaluated and compared. Moreover, the use of a 3-methacryloxypropyltrimethoxysilane (Geniosil ® GF31, 1phr) as coupling agent has been investigated comparing samples filled with 20 phr of WL (with and without silane). The main obtained results can be summarized as follow:

➢ Thermal properties as well as MFR values of both PHBH and PHBV based samples have not significantly affected by the WL presence.

➢ The obtained tensile properties have shown how WL are able to increase the Young's modulus without worsen too much the tensile strength. These aspects have been explained by a stiffening effect due to the WL particles and by a good particle-matrix adhesion. In particular, PHBV-based samples have exhibited an excellent adhesion interface as shown by the very high extrapolated Pukanszky empirical B factors.

➢ A stiffening effect has been noticed also considering the creep test results. The creep compliance has been decreased almost proportionally to the WL content in both PHBH and PHBV based samples. The theoretical creep model of Kohlrausch–Williams–Watts (KWW) and the time-temperature superposition equations of William-Landel-Ferry (WLF) have pointed out the ability of WL to decrease at the same time the compliance extent and the compliance velocity.

➤ The coupling agent 3-methacryloxypropyltrimethoxysilane has been found to be very efficient in increasing the adhesion between the tested polymers and the WL. Samples with silane (PHBH 20WL sil and PHBV 20WL sil) have manifested higher creep resistances and tensile strength values than the ones without the coupling agent (PHBH 20WL and PHBH20WL). The mechanical properties of those samples have been even better than the ones filled with 40 phr of WL although the main 40WL composites drawback were avoided. Possible reactions schemes have been proposed and further specific works could validate their existence evidencing and quantifying analytically the functionalization degree.

Finally, the obtained results demonstrate the possibility to replace in the future certain petro-chemicals polymers with these cost-effective bio-composites, solving both the wine-making disposal problem and the necessity to invest in more eco-friendly products. In fact, since the WL abundancy, cost-effectiveness, renewability and excellent workability, these WL-bio-composites could be really attractive for large-scale applications in which biodegradability and certain mechanical properties are simultaneously required, and the reported data could help the selection of the most suitable formulation depending on the economic and technological constrains.

7.5 THERMO-MECHANICAL AND CREEP MODELLING OF PBS AND PA11-WINE LEES FILLED COMPOSITES

7.5.1 Material and methods

Materials

Polyamide 11 (PA11) – typology "Rilsan® BMNO" (melting temperature = 189 °C, density = 1.03 g cm^{-3}, melt mass flow rate (2.16 kg, 235 °C) = 18.5 g/10') – has been supplied by Arkema (Paris, France) meanwhile poly(butylene succinate) (PBS) – typology PBE 003 (melting temperature = 115 °C, density = 1.26 g cm^{-3}, melt mass flow rate (2.16 kg, 190 °C) = 4-6 g/10') - has been supplied by NaturePlast (Caen, France). The wine lees (WL) have been obtained from the winery Cevico Group C.V.C (Lugo (RA), Italy) in 2018 September by raking after alcoholic fermentation of red Sangiovese grapes. 3-Methacryloxypropyltrimethoxysilane GENIOSIL® GF31 (sil) and the paraffinic oil "Vestan" have been provided by Wacker Chemie AG (München, Germany) and Tizi, S.R.L (Arezzo, Italy), respectively.

Preparation of the PA11 and PBS-based materials

PA11 and PBS pellets have been mixed with different contents of WL (10, 20 and 40 phr) by the means of a laboratory twin-screw extruder Haake Rheomex 557. Reactive extrusion has been also tested adding 1 phr of sil to the formulation containing 20 phr of WL. In other cases, 1 phr of sticky Vestan oil has been used to enhance adhesion between WL and pellet surfaces before extrusion. Polymers and WL have been oven-dried at 80 °C for 4 hours to remove eventual absorbed moisture before this step. The extruded filaments have been air-cooled, manually spooled and grounded. The compounded pellets have been fed in a Tecnica DueBi MegaTech H10/18-1 injection-molding machine to obtain tensile test specimens (type 1BA, ISO 527) and rectangular specimens for dynamic-mechanical analysis, creep and heat distorsion temperature tests. The composition of each investigated formulation is reported in Table 39.

Table 39 Codes and compositions of the investigated materials.

PA11-based samples	Composition	PBS-based samples
PA11 proc	Neat polymer processed in the same conditions	PBS proc
PA11 10WL	Polymer + 1 phr Vestan + 10 phr WL	PBS 10WL
PA11 20WL	Polymer + 1 phr Vestan + 20 phr WL	PBS 20WL
PA11 40WL	Polymer + 1 phr Vestan + 40 phr WL	PBS 40WL
PA11 20WL sil	Polymer + 20 phr WL + 1 phr sil	PBS 20WL sil

Wine lees characterization

The WL used in this work have been the same used in a previous work [177], where moisture content, particle size distribution, organic and inorganic fractions (by muffle-furnace), morphology and elementary composition were reported. To extend the WL characterization, thermogravimetric analysis (TGA) and FT-IR spectra have been reported and discussed in the present work. WL powder

FT-IR spectra have been collected using a Perkin-Elmer Spectrum GX Infrared Spectrometer. Spectra have been obtained in ATR mode as an average of 64 scans in the 4000-400 cm^{-1} range with a 4 cm^{-1} resolution. TGA conditions have been the same of the ones reported in paragraph 2.4.3. Finally, the real density of the WL powder has been calculated using the gas pycnometer ACCUPYC 1330.

PA11 and PBS-based materials characterization

Differential Scanning Calorimetry (DSC)

Thermal properties of PA11 and PBS-based samples have been evaluated by Differential Scanning Calorimetry (DSC) (DSC TA 2010), using 7 ± 2 mg of sample and purging the chamber with 50 mL min^{-1} of nitrogen. Each sample has been firstly heated from 25 to 230 °C at 20 °C min^{-1} (PA11-based materials) [from 25 to 180 °C at 15 °C min^{-1} (PBS-based materials)] to erase previous thermal history and subsequently cooled to -30 °C at 15 °C min^{-1} (PA11-based materials) [to -40 °C at 10 °C min^{-1} (PBS-based materials)]. Finally, samples have been heated again to 230 °C at 15 °C min^{-1} (PA11-based materials) [to 180 °C at 10 °C min^{-1} (PBS-based materials)]. Crystallization temperature (T_C) and enthalpy (H_C) have been collected from the cooling cycle, meanwhile melting temperature (T_m) and enthalpy (H_m) and, when detectable, glass transition temperature (T_g) have been carried out from second heating cycle. Melting enthalpies have been calculated considering the additives and fillers weight fractions. Crystallinity percentages (% Cr) have been obtained using the values of 206 J g^{-1} [384] and 110 J g^{-1} [385] as PA11 and PBS reference melting enthalpies values, respectively.

Melt Mass Flow Rate (MFR)

Melt mass flow rate (MFR) has been determined according to ISO 1133 (part II, materials sensitive to moisture) with a load of 2.16 kg and a temperature of 235 °C for PA11-based samples and 190 °C for PBS-based ones.

Thermogravimetric Analysis

TGA has been conducted on 15 ± 5 mg of sample by the means of TG-NETZSCH STA 409 using a ramp temperature of 10 °C min^{-1} from 25 °C to 600 °C and purging the chamber by 50 mL min^{-1} of air. Temperatures at 5%, 10% and 15% weight loss (T_5, T_{10} and T_{15}, respectively) as well as the residue at 600 °C (Res_{600}) have been measured from the thermograms.

Tensile tests

Tensile tests have been performed using the INSTRON 5567 dynamometer equipped with a 1 kN load cell and a 25 mm gauge length extensimeter. Tests have been conducted with a clamp separation speed of 10 mm min^{-1} for the PA11-based samples and of 20 mm min^{-1} for the PBS-based ones. Young's modulus (E), tensile strength (σ_M) and elongation at break (ε_b) have been measured and reported for each formulation as average of at least six determinations. The micro-mechanics models for composites of Voigt [343] and Halpin-Tsai [344] have been exploited to extrapolate the Young's modulus of WL particles (E_P). Similarly, Pukanszky's equation has been used on tensile strength data to extrapolate the empirical adhesion B factor [346]. The mentioned model equations are reported as follow:

$$Voigt: E_C = E_P V_P + E_M (1 - V_P) \ (Eq. 1)$$

$$Halpin - Tsai: E_C = E_M \frac{1 + 2\eta V_P}{1 - \eta V_P} \ (Eq.\,2) \ with \ \eta = \frac{E_P/E_M - 1}{E_P/E_M + 2}$$

$$Pukanszky: \sigma_C = \sigma_M \frac{1 - V_P}{1 + 2.5 V_P} \exp(B V_P) \ (Eq.\,3)$$

where E_C is the composite modulus, E_M is the polymer matrix modulus, E_P is the filler particle modulus, V_P is the filler particle volume fraction, σ_C is the composite tensile strength, σ_M is the polymer matrix tensile strength and B is the Pukanszky's empirical adhesion constant.

Dynamic Mechanical Analysis

TA DMA Q800 instrument has been used in single cantilever configuration to evaluate the dynamic mechanical behavior of PA11 and PBS-based samples. Tests have been run from -40 °C to 80 °C with a heating rate of 3 °C min^{-1}, an oscillating frequency of 1 Hz and an applied strain of 0.1%. Glass transition temperatures (T_g) values have been recorded as the maximum values of the tanδ curves.

Creep tests

Creep properties have been measured at 20, 40, 60 and 80 °C using the TA DMA Q800. Creep compliance has been recorded loading the specimens with a 1 MPa stress for 10 min. The experimental data have been fitted with the micromechanical models of Burger, Kohlrausch–Williams–Watts (KWW) and Findley in order to extrapolate and model useful information on the creep behavior of the tested samples. First attempt values have been assigned to the model's parameters and subsequently they have been optimized minimizing the difference between empirical and theoretical values and imposing the coefficient of determination (R^2) equal to one.

Heat Distortion Temperature

The heat distortion temperature (HDT) of the PA11 and PBS-based samples have been carried out adapting the ASTM International Standard D 648 on the DMA Q800 as here described [386]. Rectangular specimens (5 mm of width and 2 mm of thickness) have been placed on the tree-point bending clamps (50 mm of length) and stress of 0.455 MPa has been applied raising the temperature from 25 °C at 2 °C min^{-1}. HDT has been recorded as the temperature at which the test bar has deflected by 0.25 mm.

Scanning Electron Microscope

Specimens have been broken in liquid nitrogen and cross section covered by a 10 nm thickness gold layer. The treated surface has been observed with an environmental Scanning Electron Microscope ESEM Quanta FEI 2000 operating in low-vacuum conditions and equipped with a microanalysis X-EDS Oxford INCA-350 system.

7.5.2 Results and discussion

7.5.2.1 Wine Lees characterization

As mentioned in paragraph 2.3, WL were characterized also in a previous work [177]. Briefly, WL were found to be spherical-flakes particles with a mean diameter value of around 25 μm and formed

by high inorganic fractions (nearly 40%wt). The inorganic content was evaluated by muffle-furnace tests and was confirmed also by Energy Dispersive Spectroscopy (EDS) spectra that pointed out important amount of Potassium (14%wt.), Silicon (12%wt.) and Aluminum (3%wt.) as well as traces of Calcium, Iron and Cupper. In the present work, the real density of WL particles has been found to be 1.43 ± 0.2 g cm^{-3} and inorganic compounds have been confirmed by thermogravimetric analysis (Fig.95) that has reported a WL Res$_{600}$ value of nearly 40%, in perfect accordance with the previous above mentioned work [177]. The organic fraction has started to thermally degrade in one step at 257 °C (T$_5$) and already at 267 °C (T$_{15}$) the 15% of the mass weight was lost. Despite this very fast weight loss, is appreciable that WL degradation has begun at temperatures higher than PBS and PA11 processing ones.
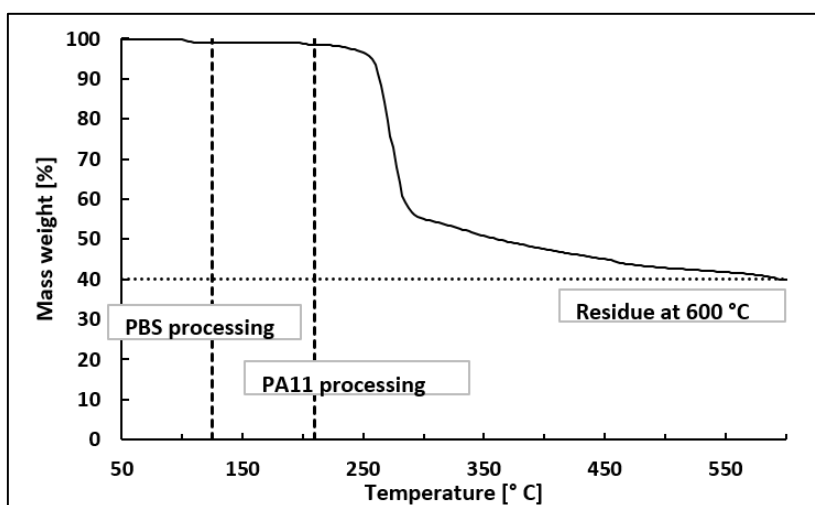
Fig.95 TGA curve of WL under air gas flow.

The organic fraction of WL has been confirmed to be composed mainly by yeast (peaks b, e, f, g, h and i), tartaric acid and their derivate (peaks a, d and i), carbohydrates (peaks h and i) and traces of lipids derived by the grape seeds (peaks c and d), as shown by FT-ATR analysis (Fig.96 and Table 40).
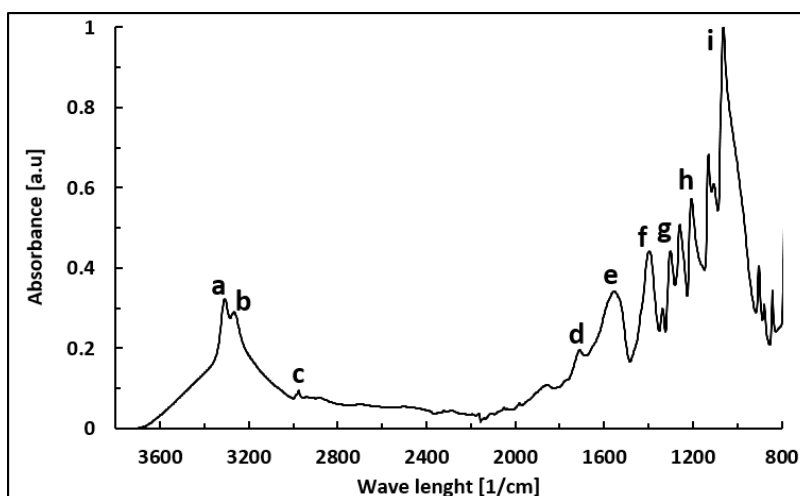
Fig.96 FT-IR ATR spectrum of the WL.

Table 40 WL FT-IR ATR spectrum: absorption peaks and corresponding assignments.

142

Peak code	Wave number [cm^{-1}]	Assignment
a	~ 3400	O-H and N-H stretching vibration of polysaccharides and tartaric acid
b	~ 3300	N-H stretching of proteins and peptides
c	~ 2920	Asymmetric stretching vibration of CH2 lipids (Hydrocarbon tails)
d	~ 1740	C=O stretching in lipid esters and in tartaric acid
e	~ 1550	Amide II: N–H and C–N vibrations of the peptide bond in different protein conformations
f	~ 1390	CO of COO− symmetric stretching in proteins
g	~ 1300	Amide III: C–N and C–O stretching, N–H and OC–N bending
h	~ 1210	C–O stretching free nucleotides/ C–O–C carbohydrates
i	~ 1160	C-C, C-O and C-N stretching vibrations

7.5.2.2 Thermal properties and Melt Mass Flow Rate

The main thermal properties and the MFR values of the investigated composites have been reported in Table 41. No significant differences in thermal behavior of both PA11 and PBS-based samples have been found by adding WL as filler. Crystallinity has been improved using 20 phr of WL (+10.9% in PA11 20WL and +17.7% in PBS 20WL) pointing out the WL possibility to partially work as nucleating agent [352]. This property has disappeared using 40 phr of WL because of probable agglomeration phenomena of WL particles.

Table 41 PA11 and PBS-based samples thermal properties.

Sample code	MFR [g/10']	T_C [° C]	H_C [J g^{-1}]	T_g [° C]	T_m [° C]	H_m [J g^{-1}]	% Cr
PA11 Proc	19.0 ± 1.1	159.0	43.3	51.3	189.3	49.1	23.8
PA11 10 WL	15.1 ± 0.2	161.3	40.1	49.2	189.1	46.0	24.8
PA11 20 WL	12.3 ± 0.3	161.0	41.8	49.9	189.3	44.9	26.4
PA11 40 WL	10.6 ± 0.4	160.4	29.2	48.0	190.1	32.1	21.9
PA11 20 WL sil	8.2 ± 0.4	161.2	37.3	48.4	189.0	40.3	23.7
PBS Proc	7.6 ± 0.2	89.0	71.0	-	114.7	68.7	62.1
PBS 10 WL	7.9 ± 0.3	86.5	65.1	-	114.6	65.2	65.4
PBS 20 WL	10.5 ± 0.7	85.7	69.3	-	114.9	66.8	73.1
PBS 40 WL	8.6 ± 0.8	82.9	53.4	-	115.0	55.1	70.2
PBS 20 WL sil	7.4 ± 0.4	84.7	57.1	-	116.1	59.3	64.9

Finally, WL have slightly increased the viscosity of PA11-based samples as shown by MFR values, similarly to other works on composites. Nevertheless, the increased viscosity has not been enough to affect the injection molding processability. On the other hand, PBS-based samples MFR values have not been significantly modified by the WL particles remaining close to the PBS proc ones.

7.5.2.3 Mechanical and thermo-mechanical properties

Tensile test

143

Table 42 PA11 and PBS-based samples tensile properties.

Sample code	V_P [-]	E [MPa]	ΔE [%]	σ_M [MPa]	$\Delta\sigma_M$ [%]	ε_b [%]	$\Delta\varepsilon_b$ [%]
PA11 proc	-	1113 ± 57	-	33.8 ± 2.6	-	305 ± 26	-
PA11 10 WL	0.067	1200 ± 42	+ 7.9	28.3 ± 2.2	- 16.2	227 ± 36	- 25.6
PA11 20 WL	0.126	1318 ± 78	+ 18.5	26.1 ± 3.8	- 22.8	167 ± 30	- 45.2
PA11 40 WL	0.224	1494 ± 65	+ 34.3	24.7 ± 1.0	- 26.9	48 ± 5	- 84.7
PA11 20 WL sil	0.126	1260 ± 51	+ 13.2	26.5 ± 0.6	- 21.6	177 ± 16	- 42.1
PBS proc	-	683 ± 28	-	32.7 ± 2.1	-	394 ± 24	-
PBS 10 WL	0.081	775 ± 12	+ 13.5	28.9 ± 1.1	- 11.6	286 ± 41	-27.4
PBS 20 WL	0.150	865 ± 26	+ 26.6	23.6 ± 0.7	- 27.8	188 ± 43	- 52.3
PBS 40 WL	0.261	946 ± 30	+ 38.5	21.3 ± 1.8	- 34.9	50 ± 13	- 87.2
PBS 20 WL sil	0.150	834 ± 23	+ 22.2	24.8 ± 0.6	- 24.1	151 ± 54	- 61.7

The tensile properties of PA11 and PBS-based samples are reported in Table 42. It is possible to notice a WL stiffening effect on both polymeric matrices. Young modulus (E) has been linearly increased with the WL content and this fact has denoted a good dispersion of the particles inside the matrix as also confirmed by SEM image of Fig.99a. In particular, PA11 40WL and PBS 40WL samples have respectively shown enhanced elastic moduli of nearly + 34% and + 39% if compared to neat polymers. The gain in Young modulus has been explained by the higher intrinsic stiffness of WL particles rather than polymer matrices due to their high inorganic fractions. As example, Aluminum silicates and Potassium tartrates found out within PBS 20WL sample have been reported in Fig.97. The WL elastic modulus (E_P), quantified fitting Voigt and Halpin-Tsai models on experimental data has been calculated to lie between 1.8 and 3.4 GPa (Table 43). In this work, WL elastic modulus seems inferior to the one extrapolated previously [177], but in this case E_P values are more convergent (especially considering Halpin-Tsai model).
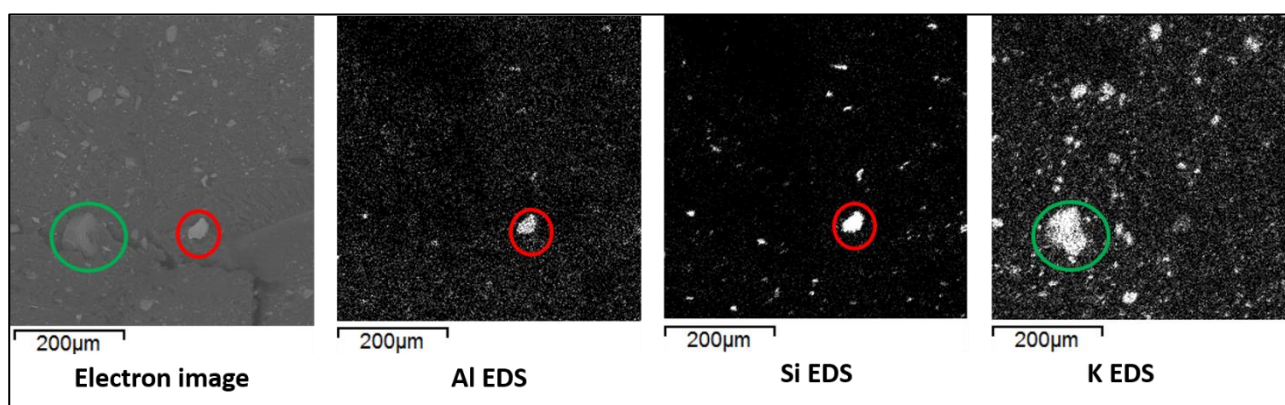
Fig.97 SEM image of PBS 20WL and overlap of Al, Si and K EDS revelations. Green circle refers to Potassium tartrates meanwhile red circle to Alumina silicates.

The tensile strength has been decreased increasing the WL content in both PA11 and PBS-based samples. In composites, this mechanical property is strongly affected by the particle-matrix adhesion. Poorly bonded particles are not able to transfer the stress through the interface; thus discontinuities and de-wetting phenomena are generated and crazes formation happens earlier and for low applied stresses than with well-bonded particles [156, 357]. The Pukanzsky's B adhesions factors is an

empirical constant able to quantify the particles-matrix adhesion. It tends to zero for poorly bonded particle meanwhile raises up progressively with the increasing of the particle-matrix interactions. In this case, because of polymers hydrophobicity and WL hydrophilicity, B factors have not been too great if compared to other works [177, 366, 387], but neither too bad, being higher than zero (Table 43).

Table 43 Micro-mechanics: WL elastic moduli (E_P) evaluated through both Voigt and Halpin-Tsai models and empirical B adhesion factor from Pukanszky's equation. Micromechanical values have been obtained using the volume particle fractions reported in Table 42.

	10 WL	20 WL	40 WL	20 WL sil	Average
E_P [MPa] using Voigt Model					
PA11-based	2416	2744	2817	2283	2565 ± 222
PBS-based	1874	1948	1730	1735	1822 ± 93
E_P [MPa] using Halpin-Tsai Model					
	10 WL	20 WL	40 WL	20 WL sil	Average
PA11-based	3162	3960	3936	2801	3465 ± 500
PBS-based	3252	3371	2379	2562	2891 ± 428
Pukanszky's B adhesion factor					
	10 WL	20 WL	40 WL	Average	20 WL sil
PA11-based	0.71	1.18	1.72	1.20 ± 0.41	1.31
PBS-based	1.73	0.95	1.39	1.35 ± 0.39	1.29

Tensile strength has been drastically reduced using 10 WL phr, and subsequently, with 20 and 40 WL phr, a smaller reduction tending to an asymptote has been observed, especially for PA11-based samples (Fig.98). This mechanical behavior in which tensile strength is related to filler content by a power law is described theoretically by several authors [388, 389] and observed experimentally also in other composites-related works [184, 390]. By the way, other authors believe that tensile strength in particle composites decreases only when the filler content exceed a critic volume fraction V_{pc} and the strength loss is proportional to the square of the filler volume fraction and no asymptotic trends are predicted [391, 392]. In each case, the explanation of this mechanical loss is attributed to the particles tendency to aggregate their selves after a certain filler content in clusters and in high-stress concentrated spots that affect and worse the stress transfer of the composite. From another point of view, also particle size affects the tensile strength that decreases for higher mean particle diameters following a power law [392, 393]. Therefore, it is here suggested that the observed asymptotic tensile strength trend could have been due by the fact that tiny particles have formed aggregated clusters able to act as larger particles. It would be like that if fillers aggregate weakly, tensile strength would collapse abruptly increasing the filler content, meanwhile when clusters aggregate are strong, tensile strength loss would be smoother as in the case of larger particles. An example of aggregated particles within PA11 40WL is shown in Fig.99b. Finally, the not significant enhancement of the tensile strength values of samples containing silane has pointed out the inefficiency of the reactive extrusion for these bio-composites. Possible reactions have been anyway investigated analytically comparing samples with and without silane trough ATR-IR spectra, EDS maps, water contact angles and surface morphology (by SEM) but no differences have been detected similarly to what happened in another work where, however, tensile strength was enhanced. Thus, in this case, because both indirect and

direct evidences of silane have been absent, it is reasonable to believe that no coupling reactions have taken place.
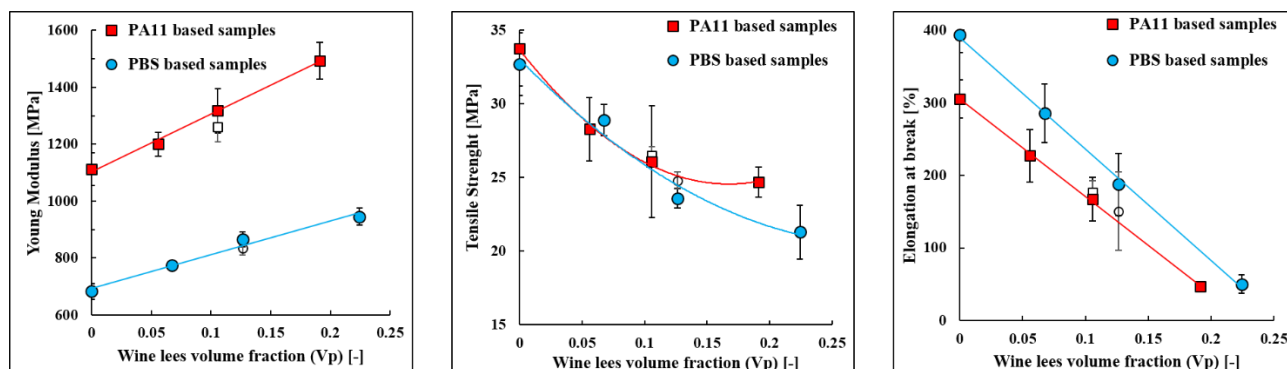
Fig.98 Young modulus, tensile strength and elongation at break as WL content function for PA11 and PBS-based samples. Unfilled symbols refer to containing silane formulations.
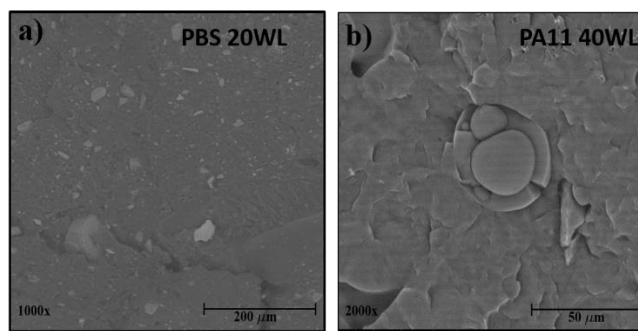
Fig.99 SEM images of a) well distributed particles within PBS 20WL and b) aggregated particles within PA11 40WL.

As expectable, the elongation at break (ε_b) of neat polymers have been decreased by WL concentration as often reported [156, 367]. Nevertheless, it is noteworthy underline that also with high particles loadings significant elongation at break values have been maintained (167% in PA11 20WL and 188% in PBS 20WL) if compared with other PA11 and PBS-based composites (Table 44). Small decreases in ductility can be due to both partial plasticization effects and good miscibility between WL and polymers that not completely decrease the chain mobility [181, 394]. The possibility of a partial plasticization induced by WL on matrices is also supported by the lower T_g values carried out in filled polymers (Tables 41 and 45). Concluding, WL have been able to guarantee mechanical properties comparable to the ones obtained using other different bio-fillers (Table 44), with the advantage to preserve significant elongation at break values even for high loading.

Table 44 Tensile properties and HDT values of different PA11 and PBS bio-composites reported in literature.

PA11-based	E [MPa]	ΔE [%]	σ_M [MPa]	$\Delta\sigma_M$ [%]	ε_b [%]	$\Delta\varepsilon_b$ [%]	ΔHDT [°C]	Ref
20%wt. stone ground fibers	-	-	45.0 ± 0.8	+17	10	-	-	[395]
15%vol PHB whisker	1270 ± 40	+118	25.0 ± 3.8	-41	8±3	-97	-	[396]

25%wt. lignin	1663±90	+67	39 ± 1	+5	9±2	-95	-	[181]
20% wood fiber	1610±100	+54	40.0 ± 1.2	+13	-	-	+0-2	[193]
PA10.10-based								
20%wt. rice husk ash	2090±100	+44	36.4±0.4	-22	18±4	-95	+1	[182]
PA6.10-based								
10%wt. rice husk ash	2000±60	+15	45.6±0.4	-14	44±3	-86	+4	[182]
PBS-based								
30%wt.lignin	1100 ±300	+80	26 ± 2	-26	4.6±0.3	-96	+5	[183]
20%wt. jute fibers	-	-	-	-	3 ± 2	-95	-	[176]
10% wt. oil palm fibers	300 ± 6	+20	25.5 ± 1.6	-31	20 ± 3	-96	-	[184]

Dynamic Mechanical Analysis

Table 45 Storage moduli E' at different temperatures (0, 25, 50 and 75 °C), T_g (max tanδ) and interpolating equation of PA11 and PBS-based samples.

E'(T) [MPa]	PA11 proc	10 WL	20 WL	40 WL	20 WL sil
E'(0)	1178	1354	1412	1602	1448
E'(25)	1111	1255	1301	1489	1335
E'(50)	842	849	892	1079	928
E'(75)	342	333	364	459	353
T_g [°C]	66.2	64.2	62.6	63.9	63.7
E'(T) [MPa]	PBS proc	10 WL	20 WL	40 WL	20 WL sil
E'(0)	888	1026	1178	1293	1131
E'(25)	629	719	831	920	798
E'(50)	474	553	635	700	613
E'(75)	318	385	442	482	421
T_g [°C]	-20.2	-19.3	-19.3	-20.0	-19.6

The storage moduli (E') of PA11 and PBS-based samples have been reported as temperature's function in Fig.100 as well as in Table 45. The WL stiffening effect has been confirmed within the whole range of tested temperatures appearing more markedly below T_g, but still appreciable at 75 °C where the use of 40 phr of WL has guaranteed E' values 1.3 and 1.5 higher than PA11 proc and PBS proc, respectively. T_g has been confirmed to be lowered by WL fillers in both PA11 and PBS-based samples, similarly to what noticed in DSC measurements (only for PA11). As previously mentioned discussing the elongation at break values, WL have been able to induce a certain plasticization on the polymer matrix. This aspect could be explained by the fact that WL contain not negligible amounts

(1.67%wt. [397]) of lipids as linoleic and oleic acid [397, 398] that can work as polymer plasticizers as reported in other papers [399, 400]. In addition, the presence of a single T_g (one $\tan\delta$ peak) confirms also the existence of a single phase system with good miscibility [181, 401].
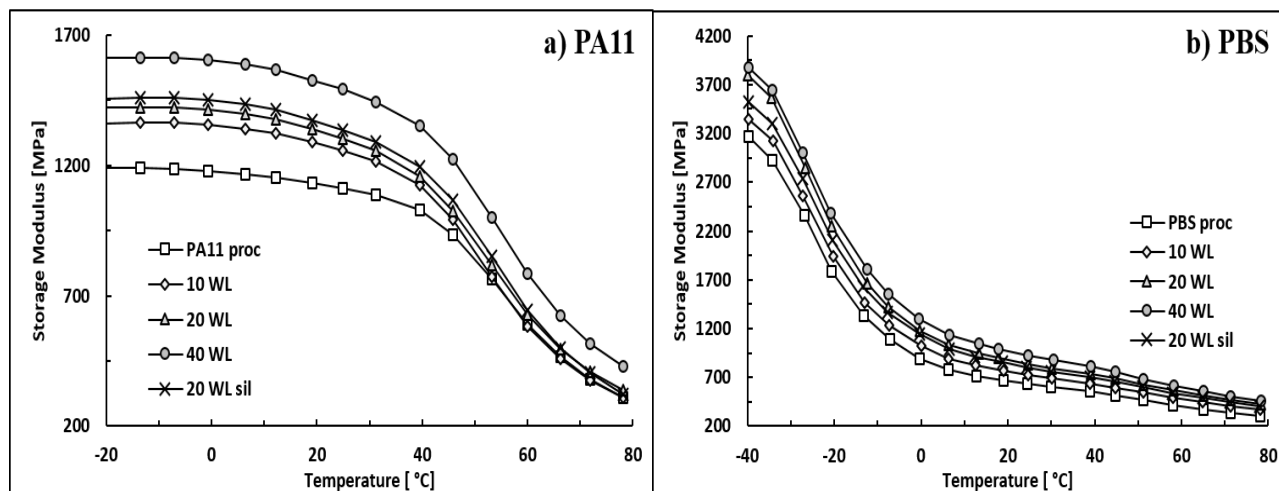
Fig.100 Storage modulus of (a) PA11and (b) PBS-based samples as a function of temperature.

From Table 45, it is observable that storage modulus has increased almost linearly with the WL content similarly to what observed in other works regarding WL-filled composites. Plotting all these collected storage modulus data (Fig.101a), it has been possible carry out a correlation formula suitable for the prediction of the storage modulus of a WL-filled composite at a certain temperature. In particular, WL have been used as filler within poly(3-hydroxybutyrate-*co*-hydroxyvalerate) (PHBV) and poly(3-hydroxybutyrate-*co*-hydroxyvalerate) (PHBH) [177], poly(3-hydroxybutyrate) (PHB) [402] and poly(lactic acid) [no published data, available upon request]. The mentioned equation has the following form:

$$\frac{E_C'(T)}{E_M'(T)}(V_{WL}) = e^{1.24 V_{WL}} \ (Eq.\,4)$$

where $E_M'(T)$ is the storage modulus of the neat polymer at temperature T, $E_C'(T)$ is the storage modulus of the WL filled composite at temperature T, and V_{WL} is the wine lees volume fraction.

Despite the equation simplicity, the coefficient of determination R^2 has been reasonably high (0.831) as well as standard deviation has been limited in terms of extension (7.5%) and well distributed, as evidenced by Fig.101b in which predicted values have been not systematically higher or lower than experimental ones. Thus, from an engineering perspective, the proposed formula could represent a useful tool in a preliminary engineering design phase to estimate the stiffness gain induced by the WL content.
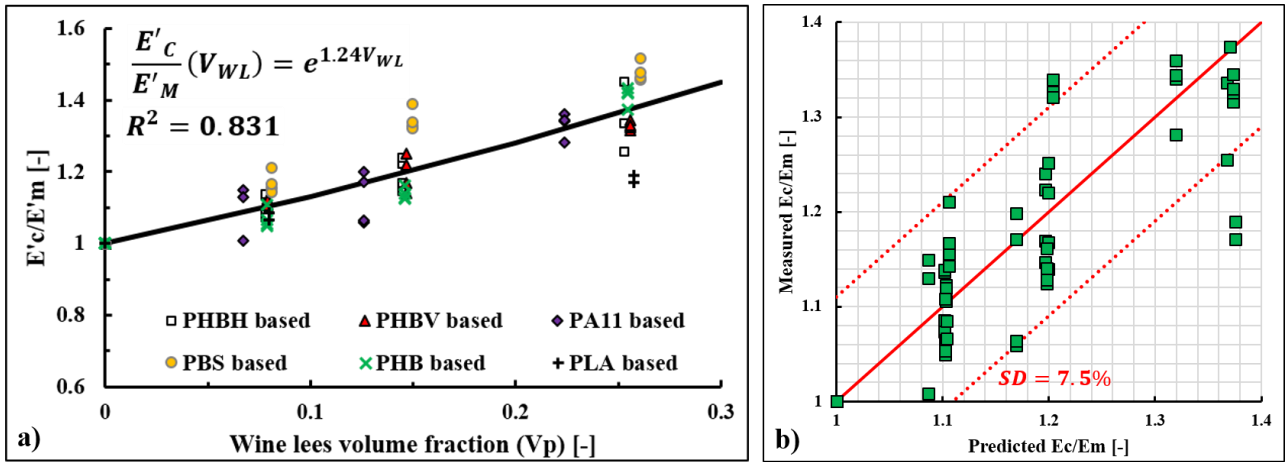
Fig.101 Storage moduli of several WL filled bio-composites: a) proposed predictive curve and b) its standard deviation.

7.5.2.4 Modelling of the creep behavior

The creep compliance curves at different temperatures of PA11 and PBS-based samples have been reported in Fig.102, where is possible to notice how WL have been able to significantly increase the creep resistance. The creep resistance gap between neat polymers and composites has become greater especially for high particles loadings (40WL phr) and for high temperatures (60 and 80 °C). From an applicative point of view, this mechanical enhancement is particularly useful for PA11-based composites that are often applied for long-life applications [403] since their not biodegradability.
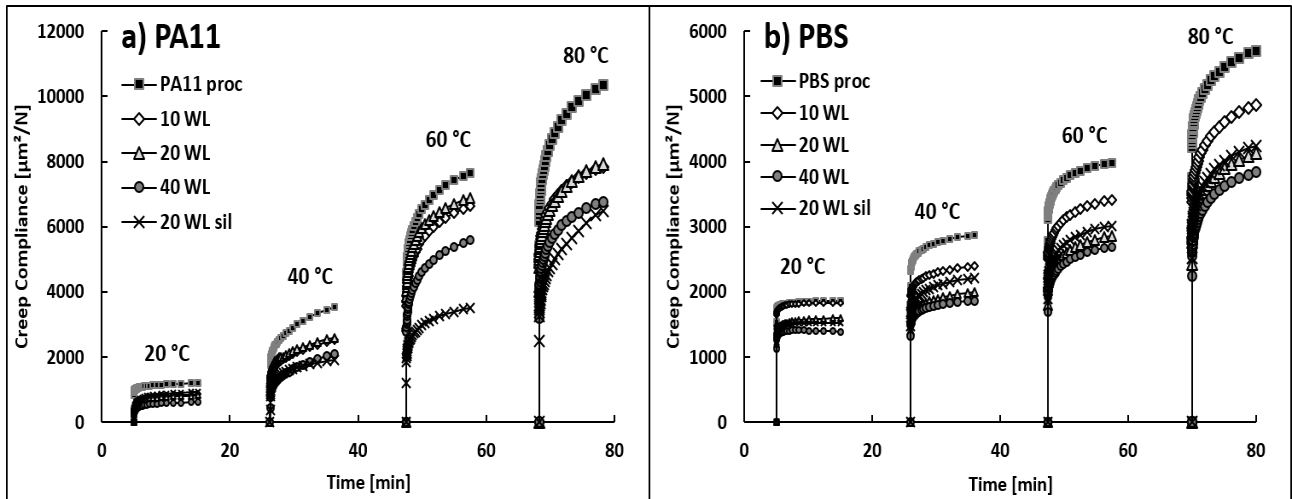
Fig.102 Creep compliance curves for PA11 and PBS-based samples at 20, 40, 60 and 80 °C.

Generally, the trend of the isothermal creep compliance can be described by three different components: a pure elastic component, a viscoelastic component and a plastic irreversible component [372]. In this work, no plastic deformations have been produced since total recovery of the initial length has been observed after unloading. Therefore, to evaluate the effects of WL on the elastic and viscoelastic components of the creep response three different micro-mechanics theoretical creep models have been fitted on experimental data. Burgers model [404] is based on a four-element mechanical system composed by the combination of Maxwell series and Kelvin elements and it has

been successfully applied for creep data analysis of various semi-crystalline polymers [405]. The creep compliance formula of this model is given by:

$$J(t) = \frac{1}{E_M} + \frac{1}{\eta_M} + \frac{1}{\eta_K}\left[1 - exp\left(-\frac{E_K}{\eta_K}t\right)\right] \quad (Eq.5)$$

where E_M and η_M are the elastic and viscous parameters of the Maxwell series elements, meanwhile E_K and η_K are the elastic and viscous parameters of the Kelvin parallel elements. Another successful model applied to creep data of glassy solids [374] and semi-crystalline polymers [373] is the Kohlrausch-Williams-Watts (KWW) model. KWW model derives from the consideration that viscoelastic changes in polymeric matrices occur because of molecular incremental jumps due to several segments chains jumps between different positions of relative stability [376]. The KWW model describes the creep compliance through a four parameters Weibull-like function and its formula is given by:

$$J(t) = J_i + J_c\left\{1 - exp\left[-\left(\frac{t}{t_c}\right)^{\beta_c}\right]\right\} \quad (Eq.6)$$

where J_i is the instantaneous elastic creep compliance component, J_c is the limit viscous creep compliance value and t_c and β_c are the scale (characteristic time) and shape parameters, respectively. Expanding the KWW function as a series and ignoring all terms except the first one is possible to obtain a power law consistent with Findley's equation [406], here reported:

$$J(t) = J_i + kt^n \quad (Eq.7)$$

where J_i is again the elastic instantaneous creep compliance contribute, k is a coefficient related to the underlying retardation process and n is an exponent taking into account the time dependence of creep response. As an example, in Fig.103 creep data of PA11 proc, PA11 10WL and PA11 40WL at 40 °C as well as PBS proc, PBS 10WL and PBS 40WL at 60°C have been fitted by Burgers and KWW equations, meanwhile all extrapolated parameters are available in Supplementary data.
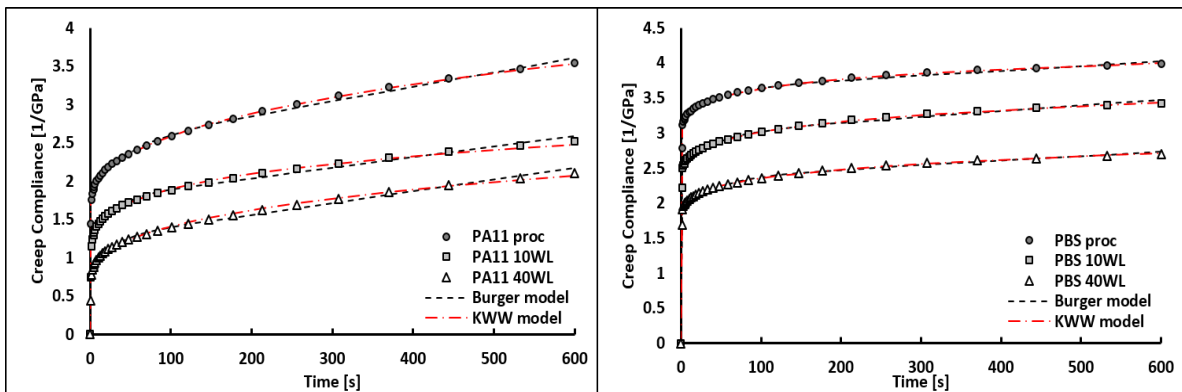
Fig.103 Creep compliance data of some PA11-based samples at 40 °C and some PBS-based samples at 60° C and fitting Burger and KWW models curves.

In Fig.103, it is possible to observe that for PA11-based samples Burger model is only partially able to fit the experimental curve because at longer times a linear increase in creep compliance caused by the Maxwell dashpot element (η_M) contribution is observable. Physically, the creep deformation

150

associated with this element is irreversible after unloading and this fact is in contrast with this experiment as before mentioned. Further, according to Burger model, the creep compliance reduction should have been reflected by an increasing of both elastic (E_M, η_M) and viscous parameters (E_K, η_K) and this has occurred in most of both PA11 and PBS-based samples cases. Considering KWW parameters, it is possible to state that elastic creep contribute (J_i) have been decreased by the WL particles in both PA11 and PBS-based samples and for each temperature, in perfect agreement with the WL stiffening effect revealed by tensile test and DMA. Similarly, the viscous creep compliance with time tending to infinite ($J_i + J_c$) has been found to be reduced in almost each tested sample and temperature (-27% in PA11-based samples and -14% in PBS-based samples, on average) confirming the WL ability to decrease the creep extent as carried out in previous work [177]. Nevertheless, contrarily to PHBH and PHBV-WL based samples [177], t_c has been reduced by the WL adding in both polymer matrices. This means that bio-composites deform more rapidly than neat polymers but to a lower extent. Finally, it is noteworthy underline that a certain aggregation degree within PA11-based samples has been denoted also by creep tests. In fact, it has been shown that particle aggregations affect and degrade the composite creep resistance, and that their contribute should be taken into account by the predictive creep model [407]. Possible aggregation phenomena could be testified experimentally by Fig.102 in which PA11 40WL creep resistance is lower than PA11 20WL for certain temperatures. Nevertheless, it seems that these aggregates have still an interphase region in which interaction between polymer matrix and particle still take place because the creep response is however positive. Concluding, each investigated model has led to the same physical creep behavior interpretation. KWW and Findley's models have been able to excellently fit both PA11 and PBS-based samples experimental data meanwhile Burger's model should not be used to describe PA11-based samples compliances data. For PA11 composite, better fitting could be reached using predictive models able to take in account the viscoelastic response of the aggregation interphase.

Heat Distortion Temperature (HDT) and Thermogravimetric Analysis (TGA*)*

Heat Distortion Temperature (HDT) is a key parameter for the identification of the maximum service temperature for a plastic product. HDT values of PA11 and PBS-based samples have been reported in Table 46. It is possible to notice that WL have enhanced this property of nearly +6 °C and +12 °C, if compared with neat PA11 and PBS, respectively. This improvement is a consequence of the WL stiffening effect caused by the hindering of segmental polymer chains that makes materials more resistant to deflection [408, 409]. As observable from Table 44, the HDT increments (ΔHDT) induced by WL have been slightly higher than the ones reported in literature in which other bio-filler were tested within PBS or PA11. As example, PA11 filled with 20%wt. of wood fiber reported the ΔHDT of ≃ +0-2 °C [193], meanwhile PBS filled with 30%wt. of lignin reported the ΔHDT of +5 °C [183]. Thus, it is reasonable to state that if not dramatic HDT increases are required, WL could represent an optimal solution among bio-fillers. To enhance more the HDT, other fillers typology should be chosen, as basalt fibers (ΔHDT ≃ + 20 °C within PBS) [410] or carbon fibers (ΔHDT ≃ + 60 °C within PA11) [193] but with the inconvenience of increasing the composite costs. Despite the ΔHDT enhancement, it is noteworthy underline that TGA curves (Fig.104) have been significantly shifted to lower temperatures by WL. The thermal degradation behavior has been the same for all samples as confirmed by the identical TGA curves shape, but WL filled samples have started to lose weight much earlier (T_{10} reduction of nearly -80 °C and -35 °C comparing respectively PA11 and PBS-filled

samples with neat polymers). This has been due by the intrinsic lower thermal stability of WL fillers respect to the neat polymers. In fact, WL start their degradation at 257 °C meanwhile PA11 at 392 °C and PBS at 306 °C, as reported in Table 46. Therefore, it is reasonable to believe that in PBS-based samples also biodegradation should be favorited by using WL as filler even if degradative agents are different. This consideration is supported by other works regarding biodegradation of composites [236]. Thus, PBS-based samples with improved HDT and encouraged biodegradation could represent particularly useful materials for applications in which heat resistance and composability are simultaneously needed.
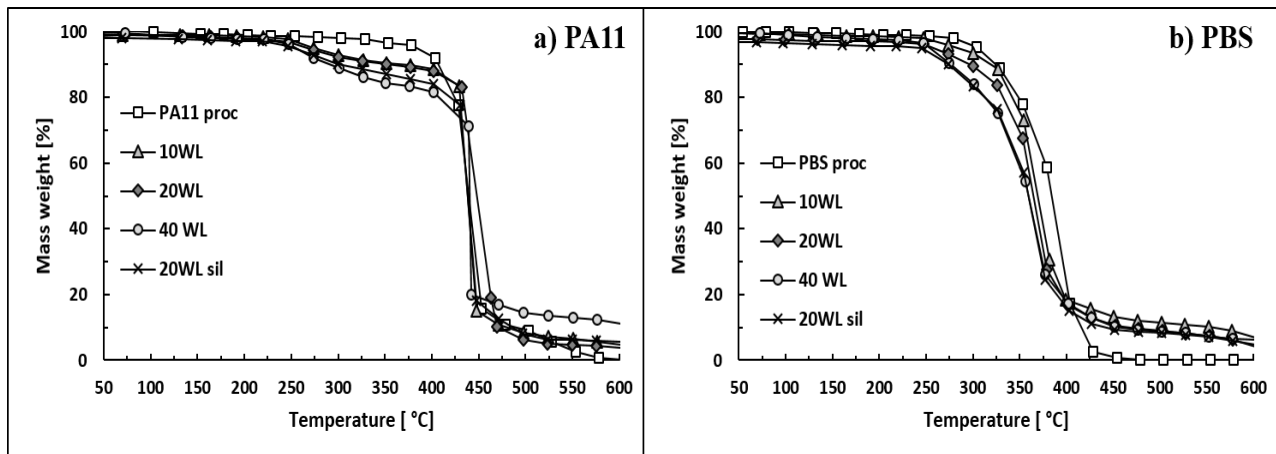
Fig.104 TGA curves of (a) PA11 and (b) PBS-based samples under air flow.

Table 46 Temperatures at 5, 10 and 15 % mass loss and residues at 600 °C for WL, PA11 and PBS-based samples.

Sample code	HDT [°C]	T_5 [°C]	T_{10} [°C]	T_{15} [°C]	Res_{600} [%]
PA11 proc	55.3	392	408	418	0.0
PA11 10 WL	61.1	284	369	425	3.9
PA11 20 WL	60.0	262	351	427	4.6
PA11 40 WL	61.6	253	289	336	11.2
PA11 20 WL sil	59.8	251	303	387	5.5
PBS proc	67.5	306	325	339	0.0
PBS 10 WL	79.5	284	321	336	4.4
PBS 20 WL	79.5	261	298	322	6.2
PBS 40 WL	78.6	257	276	297	7.1
PBS 20 WL sil	79.1	248	274	293	5.0
WL	-	257	264	267	40.0

7.5.3 Conclusions

New bio-composites formed by PA11 or PBS and WL in different contents have been processed by twin-screw extruder and injection molding machine and deeply characterized. Thermal properties have been not significantly altered by WL: only T_g values have been slightly decreased by WL particles suggesting a plasticization effect of the filler on the matrix. This aspect has been reflected in elongation at break values that have been maintained particularly high despite the significant WL loading. Tensile test has also pointed out a good WL stiffening effect (Young modulus of WL of

around 2-3 GPa) and a good polymers-WL adhesion (Pukanszky's B adhesion factor of around 1.3). The WL stiffening effect have been reflected also on higher storage modulus (E') within a broad temperature range. Moreover, a correlative prediction formula for WL filled bio-composites storage modulus has been proposed. Three different micro-mechanical models have been fitted on experimental creep test data to extent and predict the viscoelastic behavior of investigated composites. Each model has pointed out the WL ability to improve both the instantaneous elastic and the final viscous creep resistance. By the way, using WL the time needed to reach the maximum asymptotic creep compliances has been reduced if compared with neat polymers. Thermal and heat resistance of bio-composites has been smartly modified by WL. In fact, HDT has been enhanced meanwhile TGA curves have been significantly shifted to lower temperatures. Finally, reactive extrusion with silane seems to have not given special benefits to composites and alternative coupling strategies should be investigated in order to further improve their mechanical properties.

7.6 HOW MODULATE PHB THERMAL STABILIZATION, REINFORCEMENT AND BIODEGRADATION USING WINE DERIVED ADDITIVES

7.6.1 Material and methods

Materials

Unstabilized Poly(3-hdroxybutyrate) (PHB), in form of powder, has been kindly supplied by Bio-On s.p.a. (Bologna, Italy), meanwhile wine lees (WL) and grape seeds (Se), have been collected and provided by CEVICO C.V.C (Lugo (RA), Italy) during the winemaking 2018 season, and Irganox 1010 (Irg1010) has been purchased by Sigma Aldrich. Preparation methods of WL powder as well extraction conditions for the wine seed polyphenolic extract (Sext) are reported in [177] and [292], respectively.

Processing

PHB and wine derived additives have been melt mixed by the means of a twin-screw extruder Haake Rheomex 557. Extrusion has been carried using a feed-zone temperature of 160 °C, barrel and die temperatures of 170 °C, screw velocity of 30 rpm and pressure die of 35 ± 5 bar. Each extruded wire has been air cooled, manually spooled and grounded in new-compounded pellets that have been used as feed for a MegaTech Tecnica DueBi injection-molding machine to obtain tensile specimens (type 1BA, according to technical standard ISO 527). The investigated formulation have been reported in Table 47, where is useful to notice that asterisk (*) distinguishes between neat PHB processed with or without stabilizers. Before each process, each material has been oven dried for 4-6 hours at 80 °C.

Table 47 Name and composition of the investigated samples.

Stabilization essay	
PHB neat	Neat PHB powder not processed
PHB proc	PHB processed without any stabilizers
PHB 0.6Irg	PHB + 0.6 phr Irg1010
PHB 03Irg_03Sext	PHB + 0.3 phr Irg 1010 + 0.3 phr Sext
PHB 0.6Sext	PHB + 0.6 Sext
PHB 1.2Sext	PHB + 1.2 Sext
Reinforcing essay	
PHB proc*	PHB + 0.6 phr Irg1010
PHB 10WL	PHB + 0.6 phr Irg1010 +10 phr WL
PHB 20WL	PHB + 0.6 phr Irg1010 +20 phr WL
PHB 40WL	PHB + 0.6 phr Irg1010 + 0.3 phr Irg1076 +20 phr WL

Wine derived additives characterization

The WL and Sext used in this work have been the same used within other works. In particular, WL characterization can be found in [177, 411], meanwhile Sext characterization can be found in [292]. However, for a better readability, the main properties of these wine derived additives have been summarized in paragraph 3.1.

Characterization techniques
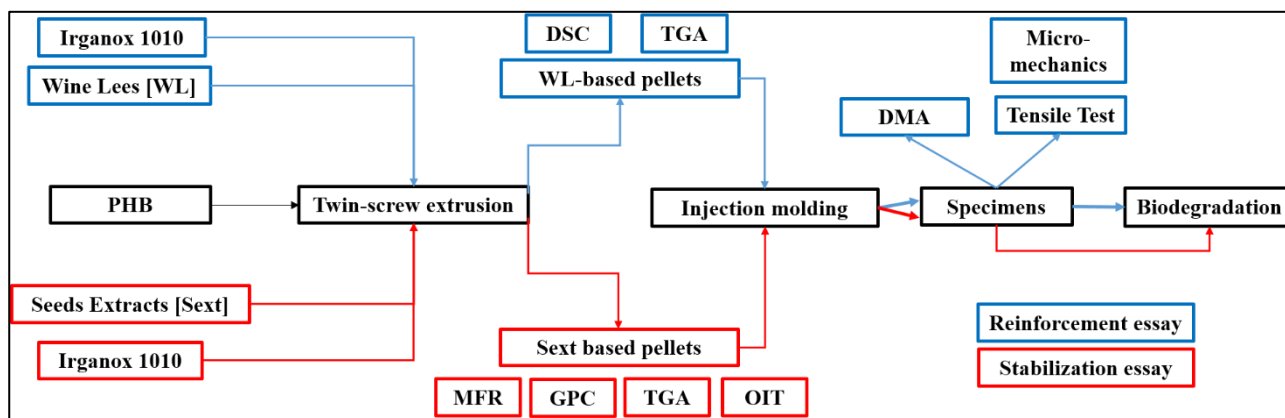
Fig.105 Scheme of work.

Since Sext and WL have been tested for different goals (PHB stabilization and PHB reinforcement, respectively) and both Sext and WL based samples have been biodegraded (Fig.105), material and methods, as well as results and discussion have been split in three different essays for a better readability.

Stabilization Essay

Gel Permeation Chromatography (GPC)

Molecular weight of stabilized PHB samples has been evaluated trough Gel Permeation Chromatography (GPC). Firstly, processed samples have been solubilized in chloroform (1g/L), filtered by celite powder, precipitated in cold methanol, and again filtered by a paper filter 1300/80. This operation has been conducted to remove low molecular weight products (such as antioxidants and other) from extruded pellet in order to not affect GPC measurements. Therefore, purified PHB has been again solubilized in chloroform (1g/L) and injected in the chromatographic system Agilent 1260 Infinity System equipped with a Reflective Index Detector. The separation system has been formed by the PLgel MiniMIX-A column (20 μm particle size, 4.6 x 250 mm) suitable for the separation of molecules with molecular weight up to $40x10^6$ g/mol, followed by the TOSOH TSKhel SuperMultipore HZ-M (4 μm particle size, 4.6 x 150 mm) column for the separation of small molecules with molecular weight ranging between 10^2-$2x10^6$ g/mol. Columns have worked at 35 °C during the analysis and the injection volume has been of 20 μL of which 2-2.5 μL has been toluene, used as flow marker. Calibration curve has been made using standard polystyrene samples at different molecular weights.

Thermogravimetric Analysis (TGA)

TGA has been conducted on 15 ± 5 mg of sample by the means of TG-NETZSCH STA 409 using a ramp temperature of 10 °C min^{-1} from 25 °C to 600 °C and purging the chamber by 50 mL min^{-1} of air. Temperatures at 10% weight loss ($T_{10\%}$) as well as the residue at 600 °C (R_{600}) have been measured from the thermograms. Same conditions have been adopted also for PHB-WL composites.

Melt Mass Flow Rate (MFR)

Melt mass flow rate (MFR) has been determined according to ISO 1133 (part II, materials sensitive to moisture) with a load of 2.16 kg and a temperature of 190 °C.

Oxidation Induction Time (OIT)

Oxidation Induction Time (OIT) tests have been performed with the TA DSC 2010 using 5 ± 0.5 mg of sample. The material has been heated under nitrogen flow (50 ml min^{-1}) with a rate of 15 °C min^{-1}, from room temperature to the set OIT temperature (250 °C), and after 1 min of isothermal, the purging gas have been switched to air. The heat flow has been recorded in isothermal conditions as function of the time. The beginning of oxidation has coincided with the sudden increase of the slope of the exothermal heat flow. The time interval elapsed between the gases switch and the exothermic degradative peak has been considered as the OIT, and it has been evaluated by the tangent method according to the ISO 11357-6.

Reinforcement Essay

Differential Scanning Calorimetry (DSC)

Thermal properties of PHB-based samples have been evaluated by Differential Scanning Calorimetry (DSC) (DSC TA 2010), using 10 ± 1 mg of sample and purging the chamber with 50 mL min^{-1} of nitrogen. Each sample has been firstly heated from 25 to 200 °C at 10 °C min^{-1} to erase previous thermal history and subsequently cooled to -30 °C at 10 °C min^{-1}. Finally, samples have been heated again to 200 °C at 10 °C min^{-1}. Crystallization temperature (T_C) and enthalpy (H_C) have been collected from the cooling cycle, meanwhile melting temperature (T_m) and enthalpy (H_m) as well as glass transition temperature (T_g) have been measured from second heating cycle. Melting enthalpies have been corrected considering the fillers weight fractions. Crystallinity percentages (%Cr) have been obtained using the values of 146 J g^{-1} as PHB reference melting enthalpy [342].

Tensile tests

Tensile tests have been performed using the INSTRON 5567 dynamometer equipped with a 1 kN load cell and a 25 mm gauge length extensimeter. Tests have been conducted with a clamp separation speed of 10 mm min^{-1} and Young's modulus (E), tensile strength (σ_M) and elongation at break (ε_b) have been measured and reported for each formulation as average of at least five determinations. Finally, the micro-mechanical models for composites modulus prediction of Voigt [343] and Halpin-Tsai [344] have been exploited to evaluate the WL particle modulus, meanwhile Pukanszky's equation [346] has been adopted to extrapolate the empirical B adhesion factor. Mentioned models present the following forms:

$$Voigt: E_C = E_P V_P + E_M(1 - V_P)$$

$$Halpin - Tsai: E_C = E_M \frac{1 + 2\eta V_P}{1 - \eta V_P} \; with \; \eta = \frac{E_P/E_M - 1}{E_P/E_M + 2}$$

$$Pukanszky: \sigma_C = \sigma_M \frac{1 - V_P}{1 + 2.5 V_P} \exp(B V_P)$$

where E_C and E_M are the composite and polymer matrix Young's moduli, respectively, E_P is the filler particle modulus, V_P is the filler particle volume fraction, σ_C and σ_M are the composite and polymer tensile strength, respectively, and B is the Pukanszky's empirical adhesion constant.

Dynamic Mechanical Analysis

TA DMA Q800 instrument has been used in single cantilever configuration to evaluate the visco-elastic behavior of the PHB-based samples. Tests have been run from -20 °C to 80 °C with a heating rate of 3 °C min^{-1}, an oscillating frequency of 1 Hz and an applied strain of 0.1%. Glass transition temperatures (T_g) values have been recorded as the maximum values of the tanδ curves.

Biodegradation Essay

Two injected moulded specimens (thickness of 2 mm) for each PHB formulation (of both stabilization and reinforcement essays) have been buried in separated plastic jars containing nearly 100 g of the same soil. The soil, generally used as cultivation substrate for different garden purposes, has been purchased by Valcofert s.r.l. (Florence, Italy). Each jar has been watered constantly in order to maintain humid the soil. Biodegradation has been evaluated monitoring the weight loss over time. Samples have been unearthed over time, carefully cleaned, oven-dried 24 hours under vacuum and then weighted. Marine water biodegradation has been done placing PHB samples on the bottom of an aquarium in which fresh marine water has been regularly filled to keep constant the level. Biodegradation extent has been evaluated analogously to as it has described for biodegradation in soil.

7.6.2 Results and discussion

Wine derived additives characterization

The same here-used WL and Sext wine derived additives were used also within other works ([177, 411] and [291, 292], respectively) and Table 48 lists their main properties. Briefly, WL fillers are spherical-flakes particles with a mean diameter of 25 μm and a real density of 1.43 g cm^3, characterized by high inorganic fractions, carbohydrates and dead yeasts, significant amounts of organic acids (mainly tartaric), lipids and phenols. Sext is a crystalline powder formed by particles with a mean diameter of nearly 170 μm, characterized by a significant high total polyphenol content (nearly 16%). It is also useful to remind that within Sext high-amounts of small simple polyphenolic molecules, as Gallic acid and Catechins were detected meanwhile long-chains polyphenolic oligomers were absent or negligible (Fig.106).

Table 48 Main WL and Sext properties.

WL properties [177, 398, 411-413]				Sext properties [292]	
Moisture content [%]	16	Degradation temp. [°C]	267	Mean particle size [μm]*	170
Real density [g/cm^3]*	1.43	Mean particle size [μm]*	25	Polyphenol content [%]*	16
Inorganic fraction [%]*	30-40	Organic fraction [%]	60-70	(+)- Catechin [mg/g]*	4.6
Potassium content [%]*	14	Tartaric acid [g/kg]	20-30	Gallic acid [mg/g]*	3.75
Silicon content [%]*	12	Other organic acids [g/kg]	5-15		
Aluminum content [%]*	3	Phenolic compounds [g/kg]	1-2		
Calcium, Iron, Cupper*	traces	Lipids [g/kg]	1-2		

*Properties determined by the same authors of the present work from the same WL and Sext. Others are from literature.
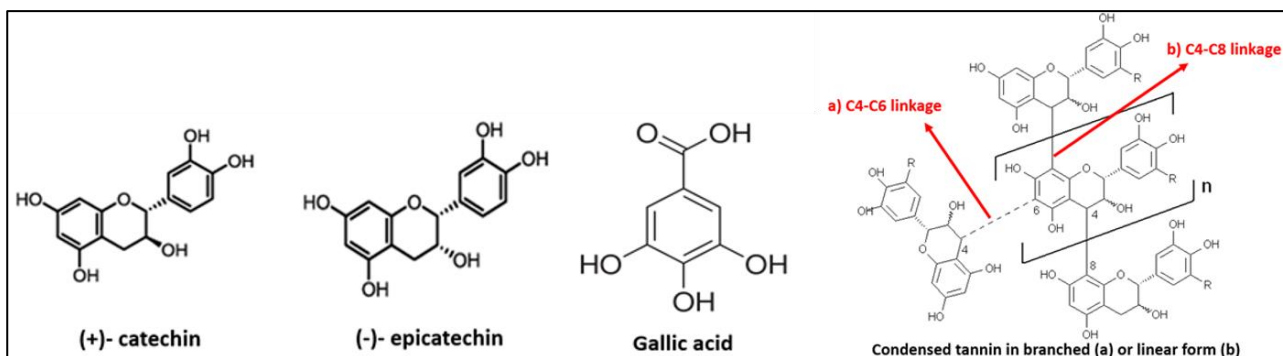
Fig.106 Example of polyphenol structures usually present in wine wastes: simple molecules and oligomeric procyanidins,

7.6.2.1 Stabilization essay

Thermal degradation of PHB has been deeply investigated and described in literature [197-202]. Briefly, PHB becomes thermally unstable even before of its melting temperature, in the 160-200 °C range. In this phase, the main degradative pathway is represented by random chain scission (cis-elimination) that lead to low molecular weight PHB oligomers with a carboxylic acid and an unsutarated propenyl as ends groups. It is very widely accepted that chain scission usually occurs by ester decomposition mechanism involving a six-membered ring transition state. Before the M_W reduction, it is believed that esterification reactions between hydroxyl and acid groups originally present as the end group of the PHB polymer could take place leading to M_W increases, and that M_W starts to decline only when hydroxyl groups are consumed. Random chain scission reactions will continue untill formed oligomers will be volatile enough to leave the matrix. Crotonic acids and their dimers and trimers represent the first and most formed volatile compounds [203, 204] that at high temperatures (ca. 500 °C) can be further degraded by decarboxylation reactions leading to carbon dioxide and propene (especially) as well as to ketene and acetaldhyde. The PHB degradation pathway is schematized in Fig.107, meanwhile the above mentioned reactions are reported in Fig.110b. At PHB processing temperatures (170-190 °C), volatile products are pratically never produced since they are mostly genereted at 200-300 °C or, at lower temperaturers, for degradation times significantly higher than processing residence times. This is explained by the fact that since thermal degradation occurs almost exclusively via random chain scission reactions, the probability of volatile species are lower than chain scission probabilities [205], and even at 220 °C, mass losses could be scarcely detactable [205]. By the way, processed PHB exhibits significantly decreased M_W and important oligomeric fractions as random chain scission consequence [206].
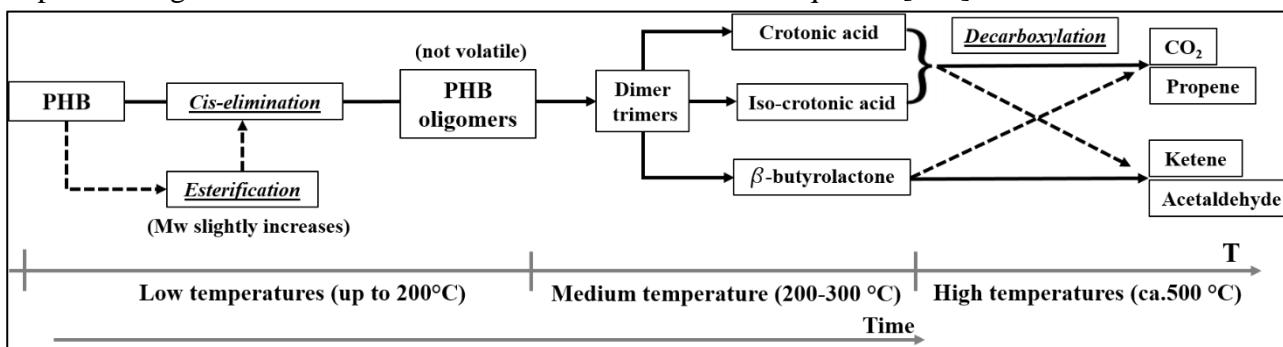
Fig. 107 PHB thermal degradation pathway

Looking at the elution curves reported in Fig.108a, it is possible to notice that these mentioned aspects have been occurred also in the here investigated PHB samples. Processed PHB samples have shown elution curves shifted of nearly 2 min if compared with unprocessed PHB, testifying a significant M_W reduction. In fact, as reported in Table 49, M_W has decreased more than two times, passing approximately from 700'000 g/mol to 350'000 g/mol. This huge loss has been similarly reported in another work concerning stabilized PHB [414], where M_W was abruptly reduced of 50% already after short processing times. From a quantitative point of view, looking at data reported in Table 49, it seems that Sext has been able to protect the PHB matrix slightly better than the other tested stabilizers (PHB 0.6 and 1.2 Sext ≃ 346'000 g/mol, PHB processed ≃ 328'000 g/mol). By the way, these limited differences could be also a consequence of the intrinsic GPC measurement errors and thus, stabilization effect can be only suggested by this singular evidence and not stated. In Fig.108b, the elution curves of the formed PHB oligomers detected with the second column (optimized for low-molecular weight compounds) have been shown. Even if molecular weights have been practically the same in terms of values (800-1000 g/mol), the signal intensity has significantly changed. PHB powd has exhibited the lower signal, meanwhile PHB proc the maximum one. The fact that small oligomeric fractions have been detected also within unprocessed PHB could be explained as consequence of some extraction or purification treatments that, during the PHB downstream processes, have partially damaged the M_W (e.g extraction with hydrogen peroxide [415]). Comparing the signal intensities is possible to notice a certain hierarchy that seems to correspond to what previously observed. In fact, PHB 0.6 Sext has exhibited the lower signal followed by PHB 1.2 Sext, PHB 0.3Sext 0.3Irg and PHB 0.6Irg. Since signals intensities are connected with the PHB oligomers amounts, it is reasonable to believe that Sext has been able to work as thermal stabilizer reducing the oligomer formations.
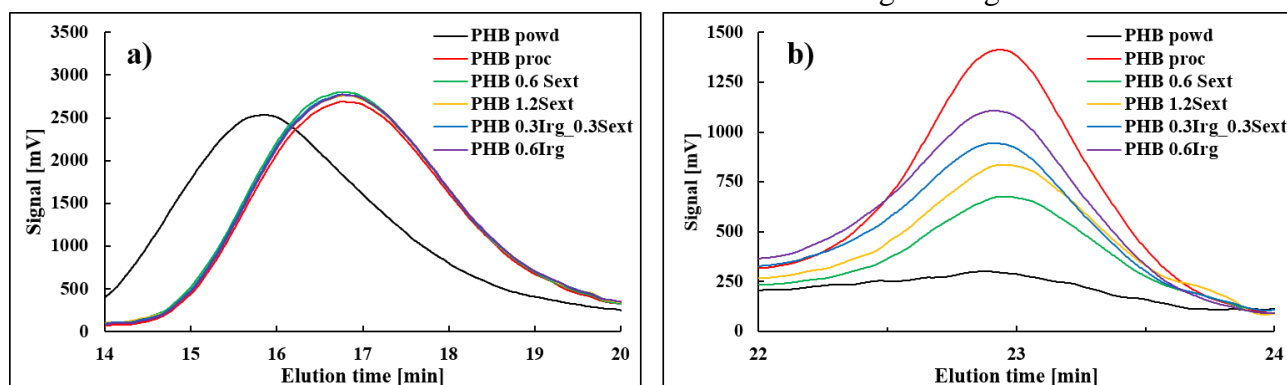
Fig.108 GPC elution curve of high molecular weight (a) and oligomeric (b) fractions

This hypothesis has been also supported by MFR data, that are connected with the viscosity of the material and thus indirectly with the molecular weight. The effect of the extrusion on the flow properties has been evident since MFR has increased by an order of magnitude, passing from 1.6 g/10' (PHB powd) to 11-14 g/10'. As expectable, PHB proc has exhibited the highest MFR value even if stabilized PHB values have been not too lower (Table 49). The ability of the tested antioxidants to slightly postpone the degradation has been further confirmed by TGA analysis and OIT tests. TGA curves, reported in Fig.109, show that each sample has been degraded at nearly 280 °C through a unique and fast mass loss step. If compared with unstabilized PHB, TGA curves of stabilized PHB samples have been found to be approximately 5-6 °C shifted to the right, confirming a certain stabilization effect. Similar moderate improvements have been found out also by the OIT test conducted at 250 °C (Table 49). Comparing the antioxidant efficiency within these two tests, it

is possible to note that PHB 0.6 Sext has exhibited the best TGA response meanwhile PHB 0.6Irg has guaranteed the higher OIT times. This discrepancy could be explained by the different conditions involved in the two tests (isothermal for OIT and dynamic for the TGA) that may affect differently the stabilizer efficiency as also reported in a previous work [177].
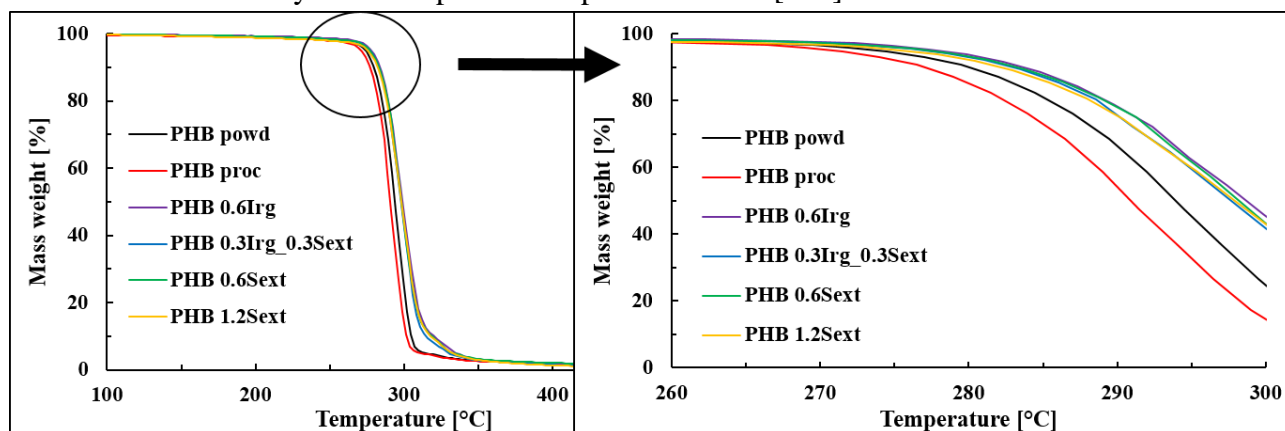
Fig.109 TGA curves and their zoom of stabilized PHB samples.

Table 49 Molecular weights, TGA, OIT and MFR data of stabilized PHB samples.

| Sample | GPC analysis | | | $T_{10\%}$ | R_{600} | OIT | MFR |
| | M_n | M_w | PD | | | | |
	[g/mol]	[g/mol]	[-]	[° C]	[%]	[min]	[g/10']
Unprocessed PHB	206'000	710'000	3.45	279.9	0.1	3.4	1.6 ± 0.3
Processed PHB	120'900	327'600	2.71	276.9	0.1	2.4	14.2 ± 0.6
0.6 Irg	128'700	328'200	2.55	283.6	0.4	5.6	11.6 ± 0.4
0.3 Irg_0.3Sext	110'000	338'500	3.08	282.9	0.3	5.5	11.7 ± 0.2
0.6 Sext	135'100	345'700	2.56	283.2	-	4.8	12.1 ± 0.3
1.2 Sext	131'200	347'100	2.65	282.1	-	5.1	11.4 ± 0.4

Summarizing the results, it is possible to state that Sext and Irganox 1010, independently by their amount or combination, have been able to stabilize the PHB matrix only moderately. A certain stabilization effect has been evidenced but, globally, it has been less marked than one observed using the same polyphenols extracts within polypropylene [292]. This can be explained considering that natural antioxidants are mainly able to work as thermal stabilizers trough electron donation and ring resonance stabilization during radical degradation. As previously mentioned, the degradation mechanism of PHB, and in general of aliphatic polyester, is almost exclusively governed by non-radical random chain scissions reactions, even if, in presence of oxygen, minor thermo-oxidative reactions can also take place. Possible thermo-oxidative reactions, supported by other works on PHB [213-215] and on poly(lactic acid) (PLA) [416], have been reported in Fig.110a.

Therefore, it is reasonable to believe that Sext has been able to slow down the degradation, stabilizing the secondary radical degradation contributes (P•), (POO•) and (PO•) formed by thermo-oxidation (Fig. 110a), and thus, the moderate stabilization effect would be explained.
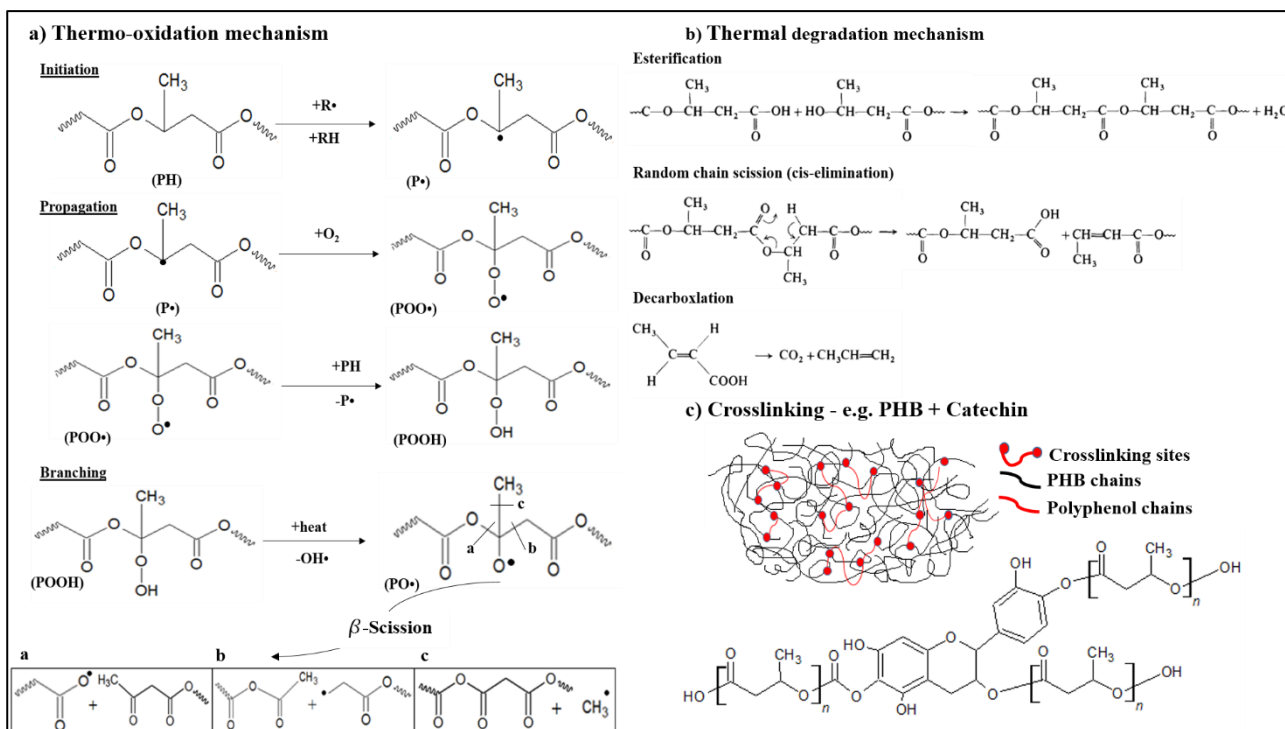
Fig. 110 a) Possible radical reactions during thermo-oxidation, b) thermal degradation trough not radical random chain scission (widely accepted mechanism) and c) polyphenols as cross-linking agents within PHB.

From another point of view, obtained results (no evident differences between formulations with 0.6 and 1.2 phr of Sext) have suggested that polyphenol typology, rather than polyphenol quantity, could represent a key role to further improve the PHB stabilization. In fact, as depicted in Fig. 110c, polyphenols would be theoretically able to act as cross-linker between the PHB chains. Several studies have demonstrated the PHB chemical bonding affinity, and reactions with chain extender or other highly functionalized additives have been exploited to improve the PHB thermal stability [417, 418]. Nevertheless, to achieve this goal, Sext should have had enough long polyphenolic chains to enhance the linking probability [414], instead of be formed by simple reactive molecules and low polymerization degree. In fact, the absence of any cross-linking reactions has been evidenced by the complete solubility of processed PHB samples in chloroform. This thesis is also supported by Nisshin Spinning Co., Ltd., that patented [A] (EP1354917 A1) a hindered phenol with a M_W higher than 400 g/mol as stabilizer for aliphatic polyesters (including PHB) and by [414], in which tannic acid (a long-chains polyphenol) was used to stabilize PHB making it at the same time partially insoluble in chloroform, and thus cross-linked. Concluding, it seems that PHB polyphenolic hierarchy is opposed to the one noticed for polypropylene [292], in which long-chains polyphenols were less efficient than small polyphenolic molecules because their steric hindrance reduced the number of effective collisions between hydroxyl groups and PP macro-radicals. By the way, it is useful to remind that crosslinking reactions, even if able to withstand the molecular weight loss, could be undesired for certain purposes since resulting PHB will be no more or much less biodegradable [232].

7.6.2.2 Reinforcement essay

Thermal properties

Thermal properties of filled PHB samples, evaluated through DSC and TGA, have been reported in Table 50. From DSC data, it is possible to notice that WL fillers have not significantly affected the

PHB thermal behavior. Unique divergences regard the crystallization temperatures (T_C) of filled samples that have been nearly 15 °C higher than PHB proc* one, pointing out a faster crystallization and a possible nucleating effect of the WL [351, 352] explainable by its small mean size diameter (25 μm). By the way, no significant differences have been noticed in terms of crystallinity extent (%Cr) as reported by the data collected during the second heating cycle (Table 50) and this fact, as it will be shown in 3.3, represents surely a positive thing for biodegradation purposes since microorganisms mainly attack amorphous domains where chains are loosely packed [232].

Table 50 Thermal properties of the PHB-WL biocomposites

	DSC data						TGA data	
	T_g [°C]	T_C [°C]	H_C [J g^{-1}]	T_m [°C]	H_m [J g^{-1}]	%Cr	$T_{10\%}$ [°C]	R_{600} [%]
PHB proc*	3.1	67	51	168	78	53	283.4	0.3
PHB 10WL	3.5	81	55	170	70	53	261.1	3.0
PHB 20WL	3.4	80	51	166	62	51	259.8	3.8
PHB40WL	4.1	83	46	166	55	53	257.5	5.9

Finally, thermal degradation behavior has been again the same for each filled and unfilled samples, as confirmed by the identical TGA curves shape reported in Fig.111. Nevertheless, in this case, WL filled samples have started their degradation much earlier as testified by the temperatures at 10%wt. loss ($T_{10\%}$) which have resulted approximately 20-25 °C lower (Table 50) than the one of PHB proc*. This has been due by the intrinsic lower thermal stability of the WL filler that starts its degradation at nearly 257 °C. Finally, the high amount of residues at 600 °C (R_{600}) has confirmed the high inorganic fraction intrinsically present within WL.
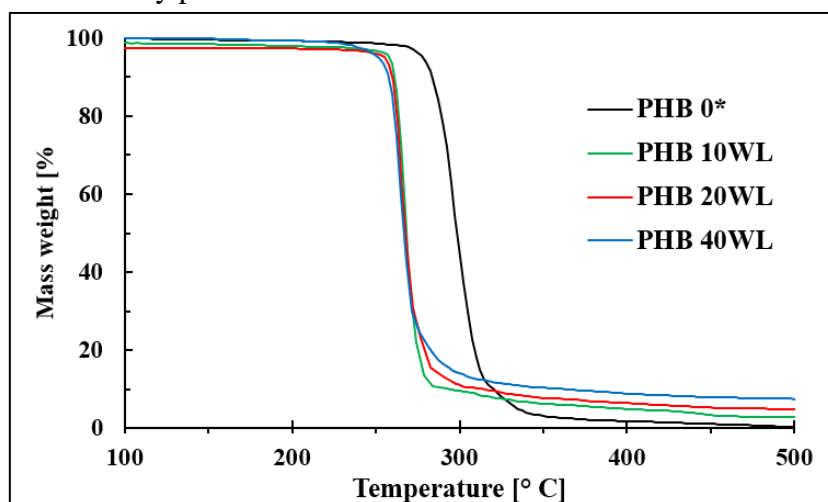
Fig.111 TGA curves of WL-filled PHB samples.

Mechanical Properties

Filled PHB tensile properties have been reported in Fig.112 and in Table 51. Tensile properties of polymer composites filled with spherical particles essentially depend on particle size, particle-matrix interface adhesion and particle loading [156]. Young's modulus of tested samples has increased progressively with the WL content, and the PHB 40WL sample has shown the maximum increment (almost +40%), if compared with unfilled PHB. This fact confirms that particle loading is the parameter that more affect this mechanical property. In fact, tensile modulus is usually independent from particle size, other than it is smaller than a critical value, often placed at nanometer scale [156,

162

179], and similarly, it is not affected by the particle-matrix adhesion since it is evaluated at low deformation for which interface separation are not allowed. The other parameter that plays a key role for the enhancement of the Young's modulus of composites is the intrinsic stiffness of the used filler (E_P). To evaluate this property, two micro-mechanical models have been exploited and the extrapolated values have been reported in Table 51. Some discrepancies are notable comparing the results obtained using Voigt and Halpin-Tsai models. Halpin-Tsai model gives higher particle modulus values and higher error, meanwhile Voigt model exhibits lower but more uniform E_P values. These mentioned differences may be due to intrinsic limitations of use of these models, as also reported in literature [177, 358, 387], but it is still notable that WL stiffness values (3-5 GPa, approximately) have been in accordance with the magnitude order of other tested natural fillers [187, 387] and with the same WL values evaluated within other polymer matrices [177, 411]. Thus, the gain in elastic modulus is explainable by the fact that WL filler as a higher stiffness than neat PHB.
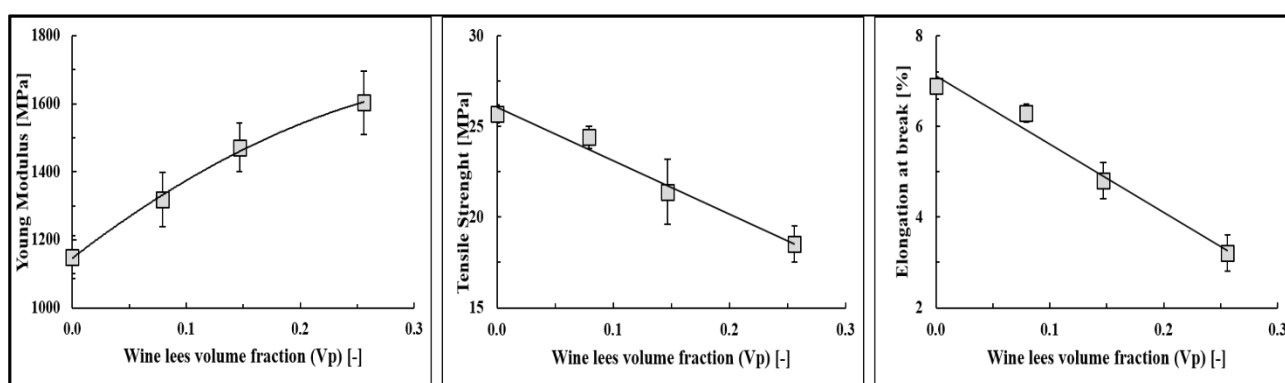
Fig.112 Tensile properties of the WL-filled PHB based samples as WL volume fraction's function.

On the other hand, tensile strength (σ_M) has decreased linearly with the WL content. Particle-matrix adhesion is the parameter that more effect this mechanical property. In fact, poorly bonded particles are not able to transfer the stress load trough the particle-matrix interface and these local discontinuities make global tensile strength decreased [156]. Nevertheless, only PHB 40WL has exhibited an important σ_M loss, maybe because of aggregation phenomena that have worsen the stress transfer, meanwhile PHB 10WL and PHB 20WL losses have been not so dramatic (5% and 16%, respectively). This aspect has been confirmed also by Pukanzky's B adhesion factor. This micro-mechanical parameter is an empirical constant able to quantify the polymer-filler adhesion. It raises up with the increasing of the particle-matrix interactions and tends to zero whit not well-bonded particles. Thus, the reported B mean value of 2.2 has confirmed a global intrinsic good adhesion between WL and PHB. As example, the B values of polyamide 11 (PA11) and poly(butylene succinate) (PBS) filled with WL (1.20 and 1.35, respectively) [411], or of poly(lactic acid) filled with grape stalks (1.69) [387] have been definitely lower. The intrinsic good adhesion between WL and PHB could be explained by the fact that PHB, among polymeric materials, is rather hydrophilic as demonstrated by its water contact angle value (70-76 °) [362, 363]. Concerning the elongation at break (ε_b), it is possible to notice that it has decreased linearly with WL loading, as expectable and as often reported in literature [156, 367]. By the way, from a technological point of view, this loss seems to do not change the suitable application fields of these bio-composites because of the already high fragility of neat PHB.

Table 51 Tensile properties and extrapolated micro-mechanicals values.

Tensile properties							
Sample code	V_p [-]	E [MPa]	ΔE [%]	σ_M [MPa]	$\Delta\sigma_M$ [%]	ε_b [%]	$\Delta\varepsilon_b$ [%]
PHB proc*	0	1150 ± 63	-	25.7 ± 0.5	-	6.9 ± 0.3	-
PHB 10 WL	0.079	1318 ± 80	+ 14.6	24.4 ± 0.6	- 5.1	6.3 ± 0.2	- 8.7
PHB 20 WL	0.147	1472 ± 71	+ 28.0	21.4 ± 1.8	- 16.7	4.8 ± 0.4	- 30.4
PHB 40 WL	0.256	1603 ± 94	+ 39.4	18.5 ± 1.0	- 28.0	3.2 ± 0.4	- 53.6
Micro-mechanicals values			
Sample code	E_P [MPa] (Voigt)	E_P [MPa] (Halpin-Tsai)	B factor [-] (Pukanszky)
PHB 10 WL	3271	6039	2.7
PHB 20 WL	3344	5946	2.0
PHB 40 WL	2920	4012	1.8
Average	3178 ± 227	5332 ± 1144	2.2 ± 0.5

Finally, it is noteworthy underline that the WL mechanical reinforcing effect has been observed also within a wide range of temperatures as evidenced by the DMA data reported in Fig. 113 and in Table 6. Storage modulus has increased proportionally to the WL content (Fig.113b) and filled PHB have been stiffer than PHB proc* for the whole temperatures' range (Fig.113a). In particular, the maximum stiffening effect has been observed at 75-80 °C, at which PHB 40WL has exhibited an E' value enhanced of 43%, if compared with unfilled PHB. This aspect is particularly important because denotes the WL ability to improve the thermal resistance of filled PHB samples although the decreased thermal stability, as previously shown by TGA curves. Finally, looking at the glass transition temperatures (T_g), evaluated as the peak maximum of the damping curve and reported in Table 52, it is possible to notice that WL have increased these values as also observed, even if less markedly, by DSC. It is reasonable to suppose that these increments have been consequence of the polymer chains immobilization made by the WL particles along the particle-matrix interface zone [190, 192].
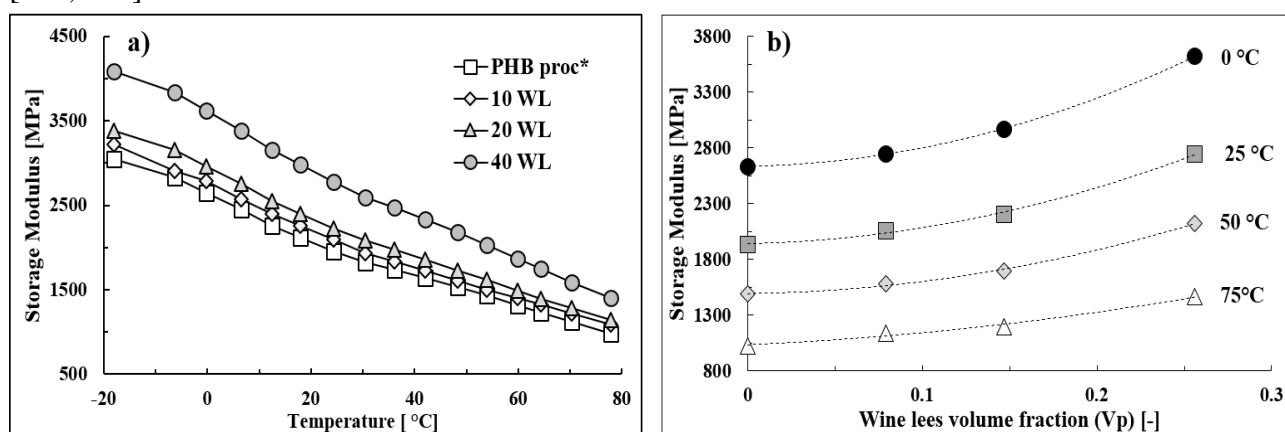

Fig. 113 Storage modulus as a) temperature and b) WL content function.

Table 52 DMA data:Storage modulus values at different temperatures (E' (T)) and glass transition temperatures (T_g).

	Max tan δ	E'(T) [MPa]			
Sample	T_g [°C]	E'(0 °C)	E'(25 °C)	E'(50 °C)	E'(75 °C)
PHB proc*	14.3	2635	1935	1490	1028

PHB 10 WL	18.5	2750	2060	1581	1139
PHB 20 WL	17.0	2971	2207	1700	1199
PHB 40 WL	19.7	3622	2744	2124	1468

7.6.2.3 Biodegradation essay

In addition to the thermal and thermo-oxidation, PHB can be degraded also by microorganisms. During biodegradation, PHB molecular structure is broken down through enzymes secreted by naturally occurring microorganism such as bacteria, fungi or actinomycetes. The process involves metabolic or enzymatic reactions inversely similar to the ones used by the same microorganisms to synthesis the polymer. Biodegradation can occur in aerobic or anaerobic conditions giving biomass (humus and compost) and carbon dioxide (aerobically) or biomass and methane (anaerobically) as main biodegradation's products. In this work, biodegradation tests (in soil and in marine water) have been conducted for each PHB formulation, comparing the PHB proc response with the one of stabilized and WL-filled PHB samples in terms of mass loss. In Fig. 114, the mass loss curves have been reported for both bio-degradative environments as time function. Globally, it is possible to notice that biodegradation has been more significant in soil rather than in marine water and that WL filled samples have exhibited the highest mass losses in both environment. Biodegradation seems to increase proportionally to the WL content (especially in soil), and PHB 40WL has been able to biodegrade almost two times faster than PHB proc both in soil and in marine water. There are several works in which different natural fillers have been found able to increase the biodegradation rate of biopolymers [236-239]. Generally, the increased biodegradability of bio-composites can be explained as consequence of three concomitant effects. Firstly, natural fillers increase the biopolymer hydrophilicity [240] and thus, the adsorption and the transport of water within the composite material would be favoured promoting the microbial degradation [241]. Secondly, the not excellent filler-polymer adhesion could create cap-shaped voids between filler and matrix, and this porosity would lead to a preferential channel for the transport of water from the surface to the composite's bulk. In addition, these microstructural defects increase the fragility of composites, favouring their disintegration and resulting in higher contact surfaces suitable by more microorganisms colonies [239]. Finally, many bio-fillers, aggregating in clusters, can decrease the overall crystallinity of the biopolymer facilitating the composite biodegradability since crystalline zones are less accessible for the microorganisms [232, 240]. It is reasonable to believe that increased hydrophilicity and greater porosity have facilitated the biodegradation also in this work (Fig. 115); meanwhile morphological effects should have been of little importance since the similar crystallinity observed between neat and filled PHB samples. Nevertheless, WL fillers could have accelerated biodegradation also thanks to their high content of organic acids. In fact, organic acids have been found able to improve the neat biopolymers biodegradation [106],[B] and WL, as mentioned in 3.1, are very rich in tartaric acid (20-30 g/kg) and in other organic acids (5-15 g/kg) such as lactic, succinic, acetic and maleic. Actually, the acid organics presence could represent one of the main reasons of the impressive weight losses exhibited in this work, despite the unfavourable conditions. In fact, it is useful remind that biodegradation tests have been conducted using relative thick samples (2 mm) in a generic and not optimized soil, at room temperature and in oxygen absence, and for only 100 days. As comparative example, in [419], the biodegradation in soil of a PHBV-wood specimen (1.6 mm of thickness,

50%wt. of wood flour) has been investigated under similar environmental condition and the weight loss after one year was of just 12%.
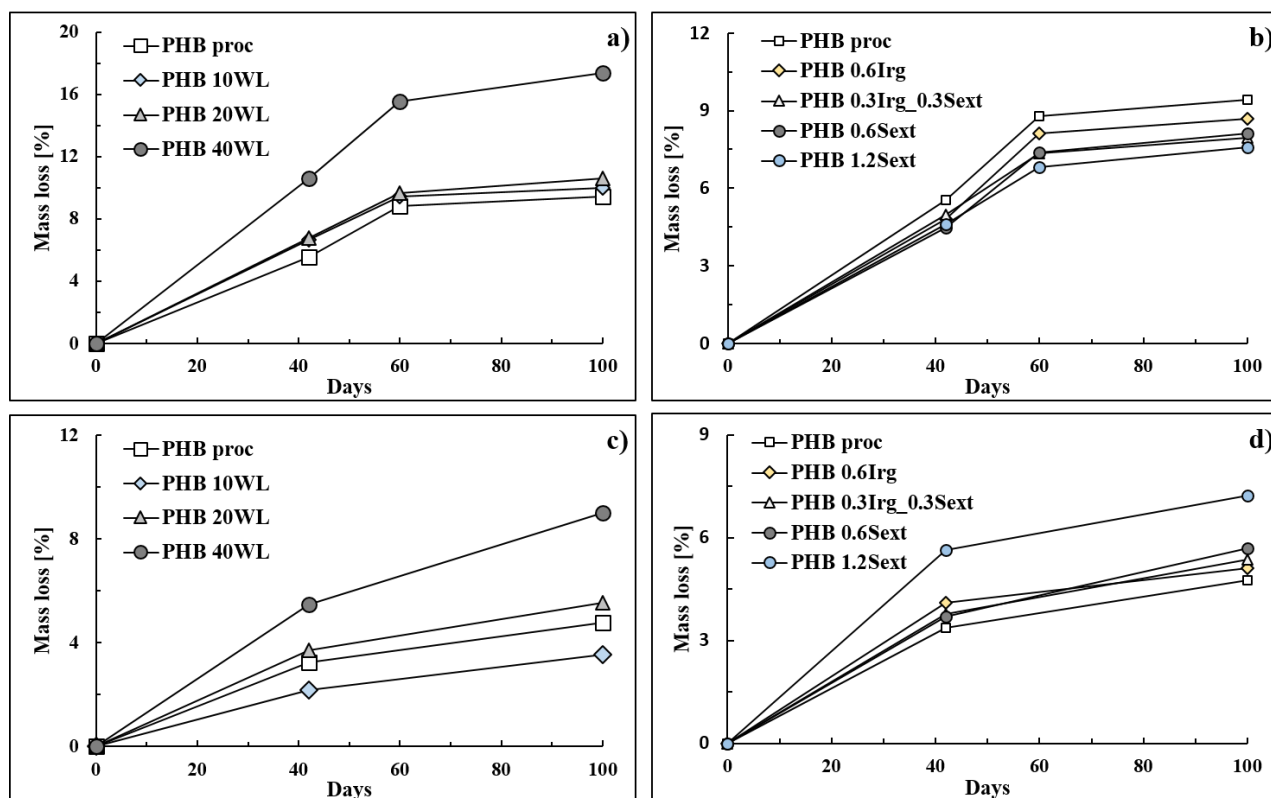
Fig. 114 Biodegradation curves for: a) PHB-filled composites in soil, b) PHB-stabilized samples in soil, c) PHB-filled composites in marine water and d) PHB-stabilized samples in marine water.

Considering the stabilized PHB samples (Fig.114 b-d), it is observable that antioxidants have moderately postponed the biodegradation in soil. From a qualitative point of view, comparing thermal stabilization and biodegradation results, it seems that stabilizers have worked similarly under both degradative conditions and as they slightly resisted to thermal degradation, they slightly have resisted to microorganism. From an applicative point of view, this aspect could be exploited when both certain stabilizations and biodegradation rates are simultaneously needed. Among the tested samples, PHB 1.2 Sext has been the more resistant one, degraded approximately 20% less than PHB proc. This aspect is explainable by the well-known anti-microbial activity of natural polyphenols that could have discouraged microorganisms in attacking the polymer chains [420]. On the contrary, because of the high solubility of polyphenols in water, PHB 1.2 Sext sample has exhibited the highest mass loss (+50% respect to PHB proc) during the biodegradation in marine water.
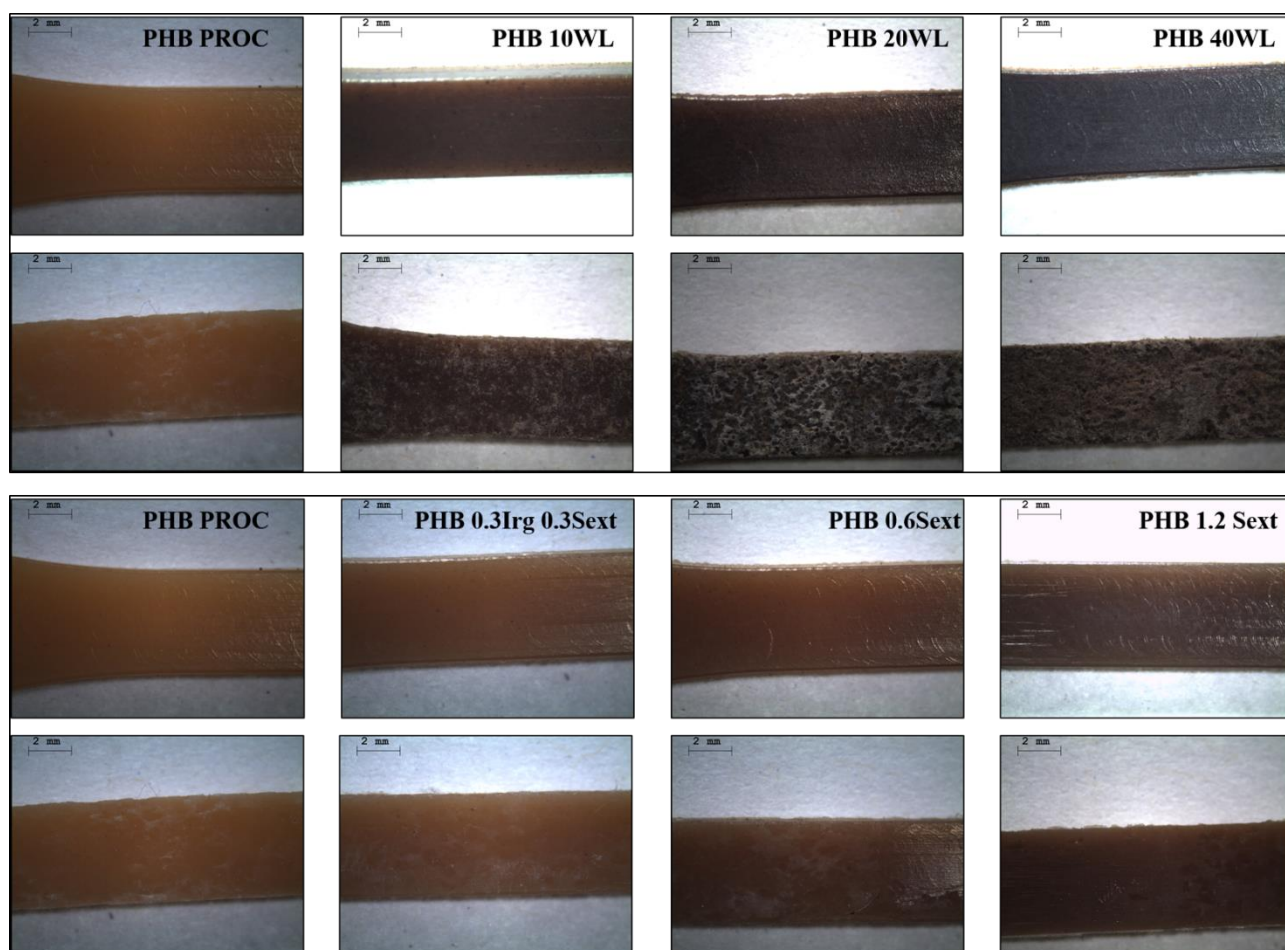
Fig. 115 Pictures of WL filled and stabilized PHB samples before biodegradation (titled figures) and after 40 days in soil (respectively below).

7.6.3 Conclusions

Concerning thermal stabilization, wine seed extracts (Sext) have been able to withstand the PHB thermal degradation only in part. This has been explained by the fact that, Sext, being rich in simple polyphenols, has mainly worked as hydrogen donator, contrasting the formed PHB macro-radicals that, however, in PHB and, generally, in aliphatic polyesters, represent fewer degradation products. Similarly, biodegradation has been slighlty reduced but not totally inhibited, pointing out the possible Sext use within applications in which certain grade of stabilizations and biodegradation are simultaneously needed. To achieve better stabilization results with natural additives, long-chain polyphenols should be used with the inconvenience of inhibit or slow-down the biodegradation because of cross-linking reactions. From another hand, wine lees (WL) fillers have significantly reinforced the PHB matrix without affecting its mechanical and thermal properties as shown by tensile and DSC data. In addition, the WL stiffening effect has worked also at higher temperatures despite the decreased degradation temperatures. Finally, because of their high organic fractions, WL have been able to significantly promote the PHB biodegradation, overcoming the Irganox presence, and candidating their potential for large-scale disposable applications.

8. CONCLUSIONS

In this section, the main engineering aspects emerged by the cased studies presented in 7.2-7.6 and by the other works conducted on the wine wastes (Fig. 59) have been summarized. In particular, the potentials and the drawbacks of each wine wastes have been highlighted and the large-scaling feasibility has been commented. Finally, further related works have been proposed in section 8.2.

8.1 SUMMARY OF RESULTS

8.1.1 Grape stalks

Grape stalks have been tested as natural fillers within polypropylene (PP), polyamide 11 (PA11) and poly(3-hydroxybutyrate-*co*-exanoate) (PHBH). In general, these wastes have been found able to reinforce the polymer matrices and t enhance the polymer Young Moduli thanks to their significant cellulosic (30%) and hemi-cellulosic fractions (20%). In addition, through the modification of the grape stalks surface (e.g. silanization and acetylation), better tensile strength values of PHBH and PBS-based composites can be obtained. Nevertheless, from an industrial point of view, these treatments should be discussed also in economic terms for assess the scaling-up feasibility. Concerning the grape stalks processability, it is possible to say that their inherent thermal stability (209 °C, evaluated by TGA) has been suitable for the melt compounding with PHBH, PBS and PP but not sufficiently high for PA11 matrix (T_m=190 °C). Within PP, wine stalks have been able to improve the short-term stabilization even without expensive antioxidant extractions procedures because of their important polyphenolic content.

From another hand, grape stalks have been selected as the most promising substrate for the PHB biosynthesis. In fact, among all the tested wine wastes, wine stalks have released the highest amounts of glucose and, at the same time, important amounts of C5-sugars. This aspect has been explained by the lignocellulosic composition of the grape stalks (20-30% cellulose and 15-20% hemicellulose). Similarly, the other lignocellulosic wine wastes, namely vine shoots, have also generated significant amounts of sugars. By the way, grape stalks have especially released xylose and other pentose sugars and only little amounts of glucose, if compared with the grape stalks. Thus, vine shoots have been not selected as first option because microorganism's growth is more efficient when C6-sugars are used. The grape stalks hydrolysis has been optimized as well as the detoxifying treatments and bio-fermentation reactors have been build up in order to investigate the ability of *Burkholderia sacchari IPT 101* to produce PHB using wine stalks hydrolysate as substrate. Unfortunately, the final amounts of PHB and the PHB yields have been not excellent. This has been explained by the fact that PHB accumulation's phase has started later than expected (nearly to the bioreactor shutdown) as consequence of the microorganism's difficulty to adapt and grow within the unconventional grape stalk hydrolysate. By the way, it is reasonable to believe that introducing a pre-inoculation phase, microorganisms could be able to synthetize more PHB within the usual bioreactor time (72 hours). In addition, other fermentative strategies as fed-batch reactors or continues reactors could improve the PHB final yield as described in 2.3.5. These hypotheses seems to be confirmed by the results obtained from recent new tests in which a pre-inoculum reactor has been involved and no lag-phases have been not observed. Thus, grape stalks could represent a new ecological and cost-effective raw material suitable for the PHAs production, and/or for other building blocks based on sugar

fermentation. In addition, further works could investigate the possibility to use both grape stalks and vine shoots as lignocellulosic raw materials for the obtainment of a suitable hydrolysate.

Anyway, the main drawbacks of grape stalks for large-scale purposes are represented by their pre-treatments and logistic operations. In fact, when collected, grape stalks present very low densities values (100-300 kg m^{-3}) and not negligible water content (20-25%) that could significantly affect the transport costs. In addition, because of their fibrous nature and intrinsic hardness, the grinding operation needed for the obtainment of a grape stalks powder (especially for the use of grape stalks as natural filler) could be difficult or not cost-advantageous.

8.1.2 Wine peels

Selected work: 7.2

Wine peels have been tested within PP investigating simultaneously their effect on PP thermal and mechanical properties and on PP short-term stabilization. Despite results have been generally positive, wine peels are not recommended as industrial natural fillers because of their intrinsic low thermal stability (190 °C by TGA) that do not allow compounding processes with many polymers and because their high moisture contents (47%) that would involve expensive drying pre-treatments. Nevertheless, grape peels could be used within biopolymers characterized by low processing temperatures (e.g. PBS and PBAT) with the aim of increase their biodegradation rates. As example, it is noteworthy mention that the use of 30%wt. of grape peels has been able to enhance the PBS biodegradation rate of around 15-20 times and thus, wine peels fillers could be exploited as biodegradation promoting agents, especially within high crystalline polymer as PBS. On the other hand, polyphenolic grape peels extracts have been found to be less efficient than the ones obtained by the wine seeds. They have been tested as PBS thermal stabilizers, and it has been noticed that long-chain polyphenols extracted from wine seeds were far more efficient to postpone the PBS molecular weight loss. New studies should verify the possibility to obtain suitable polyphenol extracts using the grape pomace (peels and seeds) as initial raw material in order to improve the antioxidant activity of the extract and to eliminate the sorting step between peels and seeds.

8.1.3 Wine seeds

Selected work: 7.2 and 7.3

As the wine peels, wine seeds have been tested within PP investigating simultaneously their effect on its thermal and mechanical properties. As reinforcing fillers (6%wt.), they have guaranteed the best creep resistance among the all tested wine wastes, meanwhile as short-term stabilizers they have exhibited very good responses. In addition, wine seeds thermal stability (268 °C) has been found to be acceptable for almost each common polymer. For these encouraging characteristics, wine seeds have been tested also as long-terms stabilizers within PP. From that work (7.3), it has been pointed out the wine seeds ability to withstand the PP aging in a way proportional to their polyphenol content. Nevertheless, since their low neat polyphenol amount, high wine seed contents should be added within PP matrix to reach significant stabilization responses with the inconvenience to decrease the tensile strength and the elongation at break values. Therefore, it could be stated that wine seeds could be used simultaneously as reinforcing fillers and antioxidants within applications that do not require ductile properties and that are not particularly stressed by degradative agents as heat or UV.

8.1.4 Wine seeds extracts

Selected work: 7.3 and 7.6

Two different wine seeds extracts have been tested and analysed: a commercial tannin seed extract (T) characterized by long-chain polyphenols and Sext, a lab-made wine seed extract characterized by simple low polyphenolic molecules. T has been tested within PBS, Sext within PHB and both extracts have been used as stabilizers within PP. The obtained results have evidenced important differences in terms of stabilization mechanisms and response between the two extracts. It could be stated that within polymers that degrade radically (as PP), simple polyphenols as Sext are more preferable since they can work better as radical scavengers. In fact, simple polyphenols are more reactive than long-chain polyphenols and being not sterically hindered, they guarantee more numbers of efficient collisions between phenolic hydroxyl groups and the polymer chains. It is noteworthy underline that the Sext antioxidant power has been even higher of the one of Irganox 1010, the most common used PP stabilizer.

On the other hand, when dealing with polyesters (not radical degradation pathway), long-chain polyphenols as T are preferred because they could mitigate the molecular weight loss due by degradation acting as chain extenders. Nevertheless, in biodegradable polyesters such as PHB and PBS, this strategy should lead also to unwanted cross-linking reactions that could inhibit or reduce the biodegradation's rates.

Finally, as previously mentioned, it could be useful to test polyphenol extracts obtained directly by the grape pomace (peels and seeds) in order to avoid the sorting step that could increase the final costs in large-scale operations.

8.1.5 Wine lees

Selected work: 7.4, 7.5 and 7.6

From a technological and industrial point of view, wine lees have been surely the most promising bio-filler. Wine lees are cheap natural wastes (0.05-0.1 €/kg) characterized by an excellent intrinsic thermal stability (268 °C by TGA) that could be exploited within many different biopolymers. They can be easily grounded in a fine powder (25μm) and their density and water contents values not involve expensive large-scale pre-treatments. Wine lees have been able to significantly reinforce many biopolymers such as PA11, PBS, PHB, PHBH and PHBV, improving their Young's moduli and creep resistances without drastically affect their thermal or rheological properties. In addition, wine lees have been simultaneously able to enhance the biopolymers high-temperatures resistance and to act as biodegradation promoters agents pointing out their potential for disposable applications in which both heat resistance and biodegradability are requested. WL-filled biocomposites have exhibited good tensile strength values even without the use of coupling agents and without filler's surface modifications. In conclusion, wine lees have many skills for their transfer in large-scale operation and for this reason, predictive correlation formula, economic analysis and micro-mechanics models have been often used to extent their knowledge and to promote their industrial use.

8.2 FURTHER WORKS

Wine lees and wine seed extracts are potentially scalable in large scale because of their excellent exhibited results. Further improvements could regard the polyphenol extraction phase in which more green extractive systems such as supercritical fluid extraction should be adopted, especially for large-scale purposes. In addition, the extraction's parameters should be optimized in order to selectively extract suitable polyphenols in accordance with the polymer degradative mechanism. Thus, short or long-chain polyphenol's varieties would be extracted depending on the polymer that want to be stabilized (e.g. simple polyphenols for polyolefin and long-chains polyphenols for polyesters).

On the other hand, operations such as drying and grinding should be tested using large-scale apparatuses in order to evaluate the feasibility and the costs to obtain wine lees fillers "ready to use". In addition, wine lees should be compounded within several biopolymers using pilot or industrial processing apparatuses (e.g. extruders and injection molding machines) in order to evaluate the properties of these industrially obtained bio-composites. If large-scale results would be similar to the ones obtained at lab scales, wine lees fillers could concretely become commercially available.

From a scientific and applicative point of view, it would be interesting investigate the simultaneous effect of wine lees and seed extracts on the biodegradation's rate of commercial available biopolymers such as PBS, PBAT, PHB, PCL and PLA. In fact, wine lees have been found able to act as biodegradation's promoters meanwhile polyphenol extracts have been found able to partially inhibit or postpone the biodegradation's rate and therefore, their opposite effect could be controlled to manipulate the product lifetime in accordance with their applicative purposes. Even if biodegradable polymers are more and more required for disposable applications, the composting companies are still having troubles to guarantee the complete biodegradation of these bioplastic wastes that thus, despite their purposes, are dumped in landfills. On the other hand, stabilized bioplastics could be exploited within new different applications where particular durability is required. Therefore, the control of the biodegradation seems to be one of the most important parameter of upcoming years and the possibility to modulate the product lifetime playing with natural derived additives could represent an economically and environmentally advantageous key point.

Considering the production of bio-based polymers, it is possible to say that grape stalks and vine shoots could be exploited as low-cost, natural fermentative raw materials. They can release important sugars content, they are abundant (especially in Italy and in Europe) to be exploited in large-scale and they are not food-competitive. The grape stalks hydrolysate has been tested as PHB substrate within this work, but from an overall point of view, the same hydrolysate could be used also for the production of polymer precursors such as lactic acid and succinic acid.

In conclusion, this work has shown only few of the several interesting possibilities in which wine wastes could be valorized within the plastic world. Results have been generally optimistic, and further researches as well as pilot-plants test should be carried out in order to further promote the use of these wastes as plastic constituents.

The idea of a "wine-plastic platform" able to produce polymers, additives and other chemicals represents an attractive solution able to mitigate the environmental problems of our days. Especially within European countries, where wine is a leader sector and a cultural symbol, the idea of a "wine-refinery" could be realized concretely.

could be realized. In fact, joining together all the results, interpretations and approaches covered by this work, it is possible to state a fully wine-derived plastic could be theoretically feasible (Fig.116).
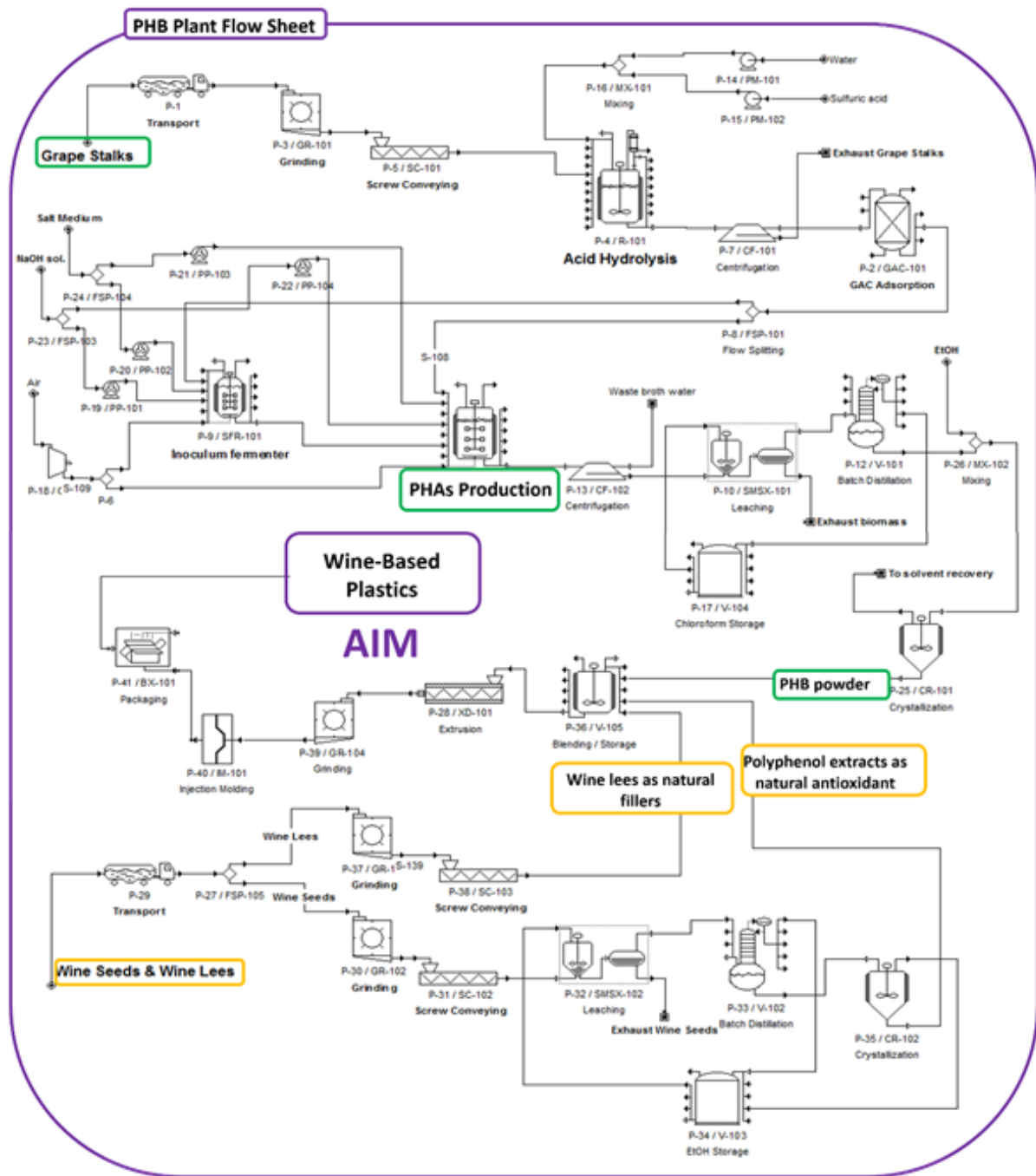

Fig.116 A route to a fully wine-based plastic scheme. Example of a PHB plant flow sheet.

9. REFERENCES

1. Plastics-Europe, *Plastics the fact: an analysis of European plastics production, demand and waste data*. 2018.
2. Osswald, T.A. and G. Menges, *Materials science of polymers for engineers*. 2012: Carl Hanser Verlag GmbH Co KG.
3. Dudley, B., *BP statistical review of world energy, 68th edition*. 2019.
4. Li, M., *World energy 2017-2050: Annual report.* Department of Economics, University of Utah, 2017.
5. Lal, R., *Soil carbon sequestration impacts on global climate change and food security.* science, 2004. **304**(5677): p. 1623-1627.
6. Boden, T.A., G. Marland, and R.J. Andres, *Global, regional, and national fossil-fuel CO2 emissions.* Carbon Dioxide Information Analysis Center, Oak Ridge National Laboratory, US Department of Energy, Oak Ridge, Tenn., USA doi, 2009. **10**.
7. Wuebbles, D.J. and A.K. Jain, *Concerns about climate change and the role of fossil fuel use.* Fuel Processing Technology, 2001. **71**(1-3): p. 99-119.
8. Lund, H., *Renewable energy strategies for sustainable development.* Energy, 2007. **32**(6): p. 912-919.
9. Kazerooni, A., et al. *Dynamic thermal rating application to facilitate wind energy integration*. in *2011 IEEE Trondheim PowerTech*. 2011. IEEE.
10. Olah, G.A., *Beyond oil and gas: the methanol economy.* Angewandte Chemie International Edition, 2005. **44**(18): p. 2636-2639.
11. Raudaskoski, R., et al., *Catalytic activation of CO2: Use of secondary CO2 for the production of synthesis gas and for methanol synthesis over copper-based zirconia-containing catalysts.* Catalysis Today, 2009. **144**(3-4): p. 318-323.
12. Viebahn, P., V. Daniel, and H. Samuel, *Integrated assessment of carbon capture and storage (CCS) in the German power sector and comparison with the deployment of renewable energies.* Applied Energy, 2012. **97**: p. 238-248.
13. Lake, L.W., *Enhanced oil recovery.* 1989.
14. R.Debarre, T.F., B. Lajoie, *Energt Perspectives - Consequences of COP21 for the Oil and Gas Industry: GHG targets and possible outcomes*, AccentureStrategy, Editor. 2016.
15. EIA, U., *Annual energy outlook 2019 with projections to 2050.* 2019.
16. Ediger, V.Ş., *An integrated review and analysis of multi-energy transition from fossil fuels to renewables.* Energy Procedia, 2019. **156**: p. 2-6.
17. Awaja, F. and D. Pavel, *Recycling of PET.* European Polymer Journal, 2005. **41**(7): p. 1453-1477.
18. Ruj, B., et al., *Sorting of plastic waste for effective recycling.* International Journal of Applied Science and Engineering Research, 2015. **4**(4): p. 564-571.
19. Ahmad, S., *A new technology for automatic identification and sorting of plastics for recycling.* Environmental technology, 2004. **25**(10): p. 1143-1149.
20. Plastics-Europe, *Plastics the fact: an analysis of European plastics production, demand and waste data*. 2017.
21. Geyer, R., J.R. Jambeck, and K.L. Law, *Production, use, and fate of all plastics ever made.* Science advances, 2017. **3**(7): p. e1700782.
22. Ritchie, H. and M. Roser, *Plastic Pollution.* Our World in Data, 2018.
23. Lebreton, L.C., et al., *River plastic emissions to the world's oceans.* Nature communications, 2017. **8**: p. 15611.
24. Jambeck, J.R., et al., *Plastic waste inputs from land into the ocean.* Science, 2015. **347**(6223): p. 768-771.
25. Eriksen, M., et al., *Plastic pollution in the world's oceans: more than 5 trillion plastic pieces weighing over 250,000 tons afloat at sea.* PloS one, 2014. **9**(12): p. e111913.
26. Boerger, C.M., et al., *Plastic ingestion by planktivorous fishes in the North Pacific Central Gyre.* Marine pollution bulletin, 2010. **60**(12): p. 2275-2278.

27.   Woodall, L.C., et al., *The deep sea is a major sink for microplastic debris.* Royal Society open science, 2014. **1**(4): p. 140317.

28.   Lebreton, L., M. Egger, and B. Slat, *A global mass budget for positively buoyant macroplastic debris in the ocean.* Scientific reports, 2019. **9**(1): p. 1-10.

29.   Rochman, C.M., et al., *The ecological impacts of marine debris: unraveling the demonstrated evidence from what is perceived.* Ecology, 2016. **97**(2): p. 302-312.

30.   Law, K.L., *Plastics in the marine environment.* Annual review of marine science, 2017. **9**: p. 205-229.

31.   Galloway, T.S., *Micro-and nano-plastics and human health*, in *Marine anthropogenic litter*. 2015, Springer, Cham. p. 343-366.

32.   Revel, M., A. Châtel, and C. Mouneyrac, *Micro (nano) plastics: A threat to human health?* Current Opinion in Environmental Science & Health, 2018. **1**: p. 17-23.

33.   Jabeen, K., et al., *Microplastics and mesoplastics in fish from coastal and fresh waters of China.* Environmental Pollution, 2017. **221**: p. 141-149.

34.   Güven, O., et al., *Microplastic litter composition of the Turkish territorial waters of the Mediterranean Sea, and its occurrence in the gastrointestinal tract of fish.* Environmental Pollution, 2017. **223**: p. 286-294.

35.   Siddique, R., J. Khatib, and I. Kaur, *Use of recycled plastic in concrete: A review.* Waste management, 2008. **28**(10): p. 1835-1852.

36.   Ignatyev, I.A., W. Thielemans, and B. Vander Beke, *Recycling of polymers: a review.* ChemSusChem, 2014. **7**(6): p. 1579-1593.

37.   Al-Salem, S., P. Lettieri, and J. Baeyens, *Recycling and recovery routes of plastic solid waste (PSW): A review.* Waste management, 2009. **29**(10): p. 2625-2643.

38.   Sinha, V., M.R. Patel, and J.V. Patel, *PET waste management by chemical recycling: a review.* Journal of Polymers and the Environment, 2010. **18**(1): p. 8-25.

39.   Paszun, D. and T. Spychaj, *Chemical recycling of poly (ethylene terephthalate).* Industrial & engineering chemistry research, 1997. **36**(4): p. 1373-1383.

40.   Behrendt, G. and B.W. Naber, *The chemical recycling of polyurethanes.* J. Univ. Chem. Technol. Metall, 2009. **44**(1): p. 3-23.

41.   Sharuddin, S.D.A., et al., *A review on pyrolysis of plastic wastes.* Energy conversion and management, 2016. **115**: p. 308-326.

42.   Yamamoto, T., et al., *Bisphenol A in hazardous waste landfill leachates.* Chemosphere, 2001. **42**(4): p. 415-418.

43.   Verma, R., et al., *Toxic pollutants from plastic waste-a review.* Procedia Environmental Sciences, 2016. **35**: p. 701-708.

44.   Themelis, N.J. and P.A. Ulloa, *Methane generation in landfills.* Renewable Energy, 2007. **32**(7): p. 1243-1257.

45.   European-Bioplastics, *Bioplastics market data 2018 - Global production of bioplastics 2018-2023*. 2018.

46.   Van den Oever, M., et al., *Bio-based and biodegradable plastics: facts and figures: focus on food packaging in the Netherlands*. 2017: Wageningen Food & Biobased Research.

47.   European-Bioplastics, *Biobased plastics – fostering a resource efficient circular economy*. 2016.

48.   Wyman, C.E., *Ethanol production from lignocellulosic biomass: overview*, in *Handbook on Bioethanol*. 2018, Routledge. p. 1-18.

49.   Ruiz, D., et al., *LCA of a multifunctional bioenergy chain based on pellet production.* Fuel, 2018. **215**: p. 601-611.

50.   Cherubini, F., *The biorefinery concept: using biomass instead of oil for producing energy and chemicals.* Energy conversion and management, 2010. **51**(7): p. 1412-1421.

51.   Carus, M. and L. Dammer, *Food or non-food: Which agricultural feedstocks are best for industrial uses?* Industrial Biotechnology, 2013. **9**(4): p. 171-176.

52.   Schut, J.H., *Pioneering Sustainability: Biopolymer applications are expanding, in fits and starts.* Plastics Engineering, 2016. **72**(3): p. 6-13.

53.   Emilia, U.R., *Rivelazioni dei prezzi all'ingrosso sulla piazza di Milano 2018*. 2018.

54. Emilia, U.R., *Rivelazioni dei prezzi all'ingrosso sulla piazza di Milano 2019*. 2019.

55. Rajagopal, R., *Sustainable value creation in the fine and speciality chemicals industry*. 2014: Wiley Online Library.

56. Open-Bio, *Validated standard for decentralized composting*. 2016.

57. Reddy, G., et al., *Amylolytic bacterial lactic acid fermentation—a review.* Biotechnology advances, 2008. **26**(1): p. 22-34.

58. Taherzadeh, M.J. and K. Karimi, *Acid-based hydrolysis processes for ethanol from lignocellulosic materials: A review.* BioResources, 2007. **2**(3): p. 472-499.

59. Modenbach, A.A. and S.E. Nokes, *Enzymatic hydrolysis of biomass at high-solids loadings–a review.* Biomass and Bioenergy, 2013. **56**: p. 526-544.

60. Palmqvist, E. and B. Hahn-Hägerdal, *Fermentation of lignocellulosic hydrolysates. I: inhibition and detoxification.* Bioresource technology, 2000. **74**(1): p. 17-24.

61. Moreno, A.D., et al., *A review of biological delignification and detoxification methods for lignocellulosic bioethanol production.* Critical reviews in biotechnology, 2015. **35**(3): p. 342-354.

62. Mussatto, S.I. and I.C. Roberto, *Alternatives for detoxification of diluted-acid lignocellulosic hydrolyzates for use in fermentative processes: a review.* Bioresource technology, 2004. **93**(1): p. 1-10.

63. Chang, C., M. Xiaojian, and C. Peilin, *Kinetics of levulinic acid formation from glucose decomposition at high temperature.* Chinese Journal of Chemical Engineering, 2006. **14**(5): p. 708-712.

64. Podolean, I., et al., *Ru-based magnetic nanoparticles (MNP) for succinic acid synthesis from levulinic acid.* Green Chemistry, 2013. **15**(11): p. 3077-3082.

65. Kiff, B.W. and D.J. Schreck, *Production of ethanol from acetic acid*. 1983, Google Patents.

66. Green Polyethylene, B., *Refer to http://www. braskem. com. br/site. aspx/green-products-USA*. 2013, Accessed 21/11/13.

67. Harmsen, P.F., M.M. Hackmann, and H.L. Bos, *Green building blocks for bio-based plastics.* Biofuels, Bioproducts and Biorefining, 2014. **8**(3): p. 306-324.

68. Rodriguez, B.A., et al., *The production of propionic acid, propanol and propylene via sugar fermentation: an industrial perspective on the progress, technical challenges and future outlook.* Green Chemistry, 2014. **16**(3): p. 1066-1076.

69. Yu, L., et al., *Propylene from renewable resources: Catalytic conversion of glycerol into propylene.* ChemSusChem, 2014. **7**(3): p. 743-747.

70. Kaplan, D.L., *Introduction to biopolymers from renewable resources*, in *Biopolymers from renewable resources*. 1998, Springer. p. 1-29.

71. Zhou, S., et al., *Fermentation of 12%(w/v) glucose to 1.2 M lactate by Escherichia coli strain SZ194 using mineral salts medium.* Biotechnology letters, 2006. **28**(9): p. 663-670.

72. Hartmann, M., *High molecular weight polylactic acid polymers*, in *Biopolymers from renewable resources*. 1998, Springer. p. 367-411.

73. Reeve, M.S., et al., *Polylactide stereochemistry: effect on enzymic degradability.* Macromolecules, 1994. **27**(3): p. 825-831.

74. Averous, L., *Synthesis, properties, environmental and biomedical applications of polylactic acid.* Handbook of Biopolymers and Biodegradable Plastics: Properties, Processing and Applications, 2012: p. 171-188.

75. Wee, Y.-J. and H.-W. Ryu, *Lactic acid production by Lactobacillus sp. RKY2 in a cell-recycle continuous fermentation using lignocellulosic hydrolyzates as inexpensive raw materials.* Bioresource technology, 2009. **100**(18): p. 4262-4270.

76. Bustos, G., et al., *Revalorization of hemicellulosic trimming vine shoots hydrolyzates trough continuous production of lactic acid and biosurfactants by L. pentosus.* Journal of food engineering, 2007. **78**(2): p. 405-412.

77. Melzoch, K., et al., *Lactic acid production in a cell retention continuous culture using lignocellulosic hydrolysate as a substrate.* Journal of biotechnology, 1997. **56**(1): p. 25-31.

78. Mussatto, S.I., et al., *Effects of medium supplementation and pH control on lactic acid production from brewer's spent grain.* Biochemical Engineering Journal, 2008. **40**(3): p. 437-444.

79.   Marques, S., et al., *Lactic acid production from recycled paper sludge by simultaneous saccharification and fermentation.* Biochemical engineering journal, 2008. **41**(3): p. 210-216.
80.   Gullon, B., et al., *L-Lactic acid production from apple pomace by sequential hydrolysis and fermentation.* Bioresource technology, 2008. **99**(2): p. 308-319.
81.   Yun, J.-S., et al., *Fermentative production of dl-lactic acid from amylase-treated rice and wheat brans hydrolyzate by a novel lactic acid bacterium, Lactobacillus sp.* Biotechnology letters, 2004. **26**(20): p. 1613-1616.
82.   John, R.P., K.M. Nampoothiri, and A. Pandey, *Simultaneous saccharification and fermentation of cassava bagasse for L-(+)-lactic acid production using Lactobacilli.* Applied biochemistry and biotechnology, 2006. **134**(3): p. 263-272.
83.   Timbuntam, W., K. Sriroth, and Y. Tokiwa, *Lactic acid production from sugar-cane juice by a newly isolated Lactobacillus sp.* Biotechnology letters, 2006. **28**(11): p. 811-814.
84.   Dumbrepatil, A., et al., *Utilization of molasses sugar for lactic acid production by Lactobacillus delbrueckii subsp. delbrueckii mutant Uc-3 in batch fermentation.* Appl. Environ. Microbiol., 2008. **74**(1): p. 333-335.
85.   Aeschelmann, F. and M. Carus, *Bio-based building blocks and polymers in the world.* Capacities, production and applications: Status quo and trends towards, 2015. **2020**: p. 1-23.
86.   Pinazo, J.M., et al., *Sustainability metrics for succinic acid production: a comparison between biomass-based and petrochemical routes.* Catalysis Today, 2015. **239**: p. 17-24.
87.   Pellis, A., et al., *Renewable building blocks for sustainable polyesters: new biotechnological routes for greener plastics.* Polymer International, 2016. **65**(8): p. 861-871.
88.   Becker, J., et al., *Top value platform chemicals: bio-based production of organic acids.* Current opinion in biotechnology, 2015. **36**: p. 168-175.
89.   Lee, J.W., et al., *Microbial production of building block chemicals and polymers.* Current opinion in biotechnology, 2011. **22**(6): p. 758-767.
90.   Carole, T.M., J. Pellegrino, and M.D. Paster. *Opportunities in the industrial biobased products industry.* in *Proceedings of the Twenty-Fifth Symposium on Biotechnology for Fuels and Chemicals Held May 4–7, 2003, in Breckenridge, CO.* 2004. Springer.
91.   Yim, H., et al., *Metabolic engineering of Escherichia coli for direct production of 1, 4-butanediol.* Nature chemical biology, 2011. **7**(7): p. 445.
92.   Cheng, K.-K., et al., *Improved succinate production by metabolic engineering.* BioMed research international, 2013. **2013**.
93.   Scholten, E. and D. Dägele, *Succinic acid production by a newly isolated bacterium.* Biotechnology letters, 2008. **30**(12): p. 2143-2146.
94.   Becker, J. and C. Wittmann, *Advanced biotechnology: Metabolically engineered cells for the bio-based production of chemicals and fuels, materials, and health-care products.* Angewandte Chemie International Edition, 2015. **54**(11): p. 3328-3350.
95.   Chen, C., et al., *Simultaneous saccharification and fermentation of cassava to succinic acid by Escherichia coli NZN111.* Bioresource technology, 2014. **163**: p. 100-105.
96.   Lee, P., et al., *Batch and continuous cultures of Mannheimia succiniciproducens MBEL55E for the production of succinic acid from whey and corn steep liquor.* Bioprocess and biosystems engineering, 2003. **26**(1): p. 63-67.
97.   Leung, C.C.J., et al., *Utilisation of waste bread for fermentative succinic acid production.* Biochemical Engineering Journal, 2012. **65**: p. 10-15.
98.   Zhang, A.Y.-z., et al., *Valorisation of bakery waste for succinic acid production.* Green chemistry, 2013. **15**(3): p. 690-695.
99.   Dessie, W., et al., *Bio-succinic acid production from coffee husk treated with thermochemical and fungal hydrolysis.* Bioprocess and biosystems engineering, 2018. **41**(10): p. 1461-1470.
100.   Lo, E., et al., *Biochemical conversion of sweet sorghum bagasse to succinic acid.* Journal of bioscience and bioengineering, 2019.

101. Huang, M., et al., *Efficient production of succinic acid in engineered Escherichia coli strains controlled by anaerobically-induced nirB promoter using sweet potato waste hydrolysate.* Journal of environmental management, 2019. **237**: p. 147-154.

102. Salvachúa, D., et al., *Succinic acid production from lignocellulosic hydrolysate by Basfia succiniciproducens.* Bioresource technology, 2016. **214**: p. 558-566.

103. Someya, Y., Y. Sugahara, and M. Shibata, *Nanocomposites based on poly (butylene adipate-co-terephthalate) and montmorillonite.* Journal of applied polymer science, 2005. **95**(2): p. 386-392.

104. Ren, J., et al., *Preparation, characterization and properties of binary and ternary blends with thermoplastic starch, poly (lactic acid) and poly (butylene adipate-co-terephthalate).* Carbohydrate polymers, 2009. **77**(3): p. 576-582.

105. Niaounakis, M., *Definitions and Assessment of (Bio) degradation.* Biopolym. Reuse, Recycl. Dispos, 2013: p. 77-94.

106. Niaounakis, M., *Biopolymers: reuse, recycling, and disposal*. 2013: William Andrew.

107. Haveren, J.v., E.L. Scott, and J. Sanders, *Bulk chemicals from biomass.* Biofuels, Bioproducts and Biorefining: Innovation for a sustainable economy, 2008. **2**(1): p. 41-57.

108. Sun, J. and H. Liu, *Selective hydrogenolysis of biomass-derived xylitol to ethylene glycol and propylene glycol on supported Ru catalysts.* Green Chemistry, 2011. **13**(1): p. 135-142.

109. Huang, Z., et al., *Selective hydrogenolysis of xylitol to ethylene glycol and propylene glycol over copper catalysts.* Applied Catalysis B: Environmental, 2014. **147**: p. 377-386.

110. Zhao, L., et al., *Hydrogenolysis of sorbitol to glycols over carbon nanofiber supported ruthenium catalyst.* Chemical Engineering Science, 2010. **65**(1): p. 30-35.

111. Collias, D.I., et al., *Biobased terephthalic acid technologies: a literature review.* Industrial Biotechnology, 2014. **10**(2): p. 91-105.

112. Tachibana, Y., S. Kimura, and K.-i. Kasuya, *Synthesis and verification of biobased terephthalic acid from furfural.* Scientific reports, 2015. **5**: p. 8249.

113. Anderson, A.J. and E.A. Dawes, *Occurrence, metabolism, metabolic role, and industrial uses of bacterial polyhydroxyalkanoates.* Microbiological reviews, 1990. **54**(4): p. 450-472.

114. Steinbüchel, A., H.E. Valentin, and A. Schönebaum, *Application of recombinant gene technology for production of polyhydroxyalkanoic acids: biosynthesis of poly (4-hydroxybutyric acid) homopolyester.* Journal of environmental polymer degradation, 1994. **2**(2): p. 67-74.

115. Poirier, Y., et al., *Synthesis of high-molecular-weight poly ([R]-(-)-3-hydroxybutyrate) in transgenic Arabidopsis thaliana plant cells.* International journal of biological macromolecules, 1995. **17**(1): p. 7-12.

116. Steinbüchel, A. and H.E. Valentin, *Diversity of bacterial polyhydroxyalkanoic acids.* FEMS Microbiology letters, 1995. **128**(3): p. 219-228.

117. Solaiman, D.K., et al., *Conversion of agricultural feedstock and coproducts into poly (hydroxyalkanoates).* Applied microbiology and biotechnology, 2006. **71**(6): p. 783-789.

118. Castilho, L.R., D.A. Mitchell, and D.M. Freire, *Production of polyhydroxyalkanoates (PHAs) from waste materials and by-products by submerged and solid-state fermentation.* Bioresource technology, 2009. **100**(23): p. 5996-6009.

119. Dietrich, K., et al., *Producing PHAs in the bioeconomy—Towards a sustainable bioplastic.* Sustainable Production and Consumption, 2017. **9**: p. 58-70.

120. Lemoigne, M., *Products of dehydration and of polymerization of β-hydroxybutyric acid.* Bull Soc Chem Biol, 1926. **8**: p. 770-782.

121. DiGregorio, B.E., *Biobased performance bioplastic: Mirel.* Chemistry & Biology, 2009. **16**(1): p. 1-2.

122. Jung, I.L., et al., *Spontaneous liberation of intracellular polyhydroxybutyrate granules in Escherichia coli.* Research in microbiology, 2005. **156**(8): p. 865-873.

123. Koller, M., et al., *Microbial PHA production from waste raw materials*, in *Plastics from bacteria*. 2010, Springer. p. 85-119.

124. Kunasundari, B. and K. Sudesh, *Isolation and recovery of microbial polyhydroxyalkanoates.* Express Polymer Letters, 2011. **5**(7).

125. Koller, M., H. Niebelschütz, and G. Braunegg, *Strategies for recovery and purification of poly [(R)-3-hydroxyalkanoates](PHA) biopolyesters from surrounding biomass.* Engineering in Life Sciences, 2013. **13**(6): p. 549-562.
126. Eyerer, P., M. Weller, and C. Hübner, *Polymers-Opportunities and Risks II: sustainability, product design and processing.* Vol. 12. 2010: Springer.
127. Koller, M. and A. Muhr, *Continuous production mode as a viable process-engineering tool for efficient poly (hydroxyalkanoate)(PHA) bio-production.* Chemical and biochemical engineering quarterly, 2014. **28**(1): p. 65-77.
128. Atlić, A., et al., *Continuous production of poly ([R]-3-hydroxybutyrate) by Cupriavidus necator in a multistage bioreactor cascade.* Applied microbiology and biotechnology, 2011. **91**(2): p. 295-304.
129. Lemos, P.C., L.S. Serafim, and M.A. Reis, *Synthesis of polyhydroxyalkanoates from different short-chain fatty acids by mixed cultures submitted to aerobic dynamic feeding.* Journal of Biotechnology, 2006. **122**(2): p. 226-238.
130. Braunegg, G., R. Bona, and M. Koller, *Sustainable polymer production.* Polymer-plastics technology and engineering, 2004. **43**(6): p. 1779-1793.
131. Choi, J. and S.Y. Lee, *Factors affecting the economics of polyhydroxyalkanoate production by bacterial fermentation.* Applied Microbiology and Biotechnology, 1999. **51**(1): p. 13-21.
132. Choi, J.-i. and S.Y. Lee, *Process analysis and economic evaluation for poly (3-hydroxybutyrate) production by fermentation.* Bioprocess Engineering, 1997. **17**(6): p. 335-342.
133. Obruca, S., et al., *Use of lignocellulosic materials for PHA production.* Chemical and biochemical engineering quarterly, 2015. **29**(2): p. 135-144.
134. Nonato, R., P. Mantelatto, and C. Rossell, *Integrated production of biodegradable plastic, sugar and ethanol.* Applied Microbiology and Biotechnology, 2001. **57**(1-2): p. 1-5.
135. Du, G., et al., *Continuous production of poly-3-hydroxybutyrate by Ralstonia eutropha in a two-stage culture system.* Journal of biotechnology, 2001. **88**(1): p. 59-65.
136. Cesário, M.T., et al., *Enhanced bioproduction of poly-3-hydroxybutyrate from wheat straw lignocellulosic hydrolysates.* New biotechnology, 2014. **31**(1): p. 104-113.
137. Silva, L., et al., *Poly-3-hydroxybutyrate (P3HB) production by bacteria from xylose, glucose and sugarcane bagasse hydrolysate.* Journal of industrial microbiology and biotechnology, 2004. **31**(6): p. 245-254.
138. Obruca, S., et al., *Production of polyhydroxyalkanoates using hydrolysate of spent coffee grounds.* Process biochemistry, 2014. **49**(9): p. 1409-1414.
139. Van-Thuoc, D., et al., *Utilization of agricultural residues for poly (3-hydroxybutyrate) production by Halomonas boliviensis LC1.* Journal of applied microbiology, 2008. **104**(2): p. 420-428.
140. Shen, L., J. Haufe, and M.K. Patel, *Product overview and market projection of emerging bio-based plastics PRO-BIP 2009.* Report for European polysaccharide network of excellence (EPNOE) and European bioplastics, 2009. **243**.
141. Martino, L., et al., *Bio-based polyamide 11: Synthesis, rheology and solid-state properties of star structures.* European Polymer Journal, 2014. **59**: p. 69-77.
142. Devaux, J.-F., G. Lê, and B. Pees, *Application of Eco-Profile Methodology To Polyamide 11.* Arkema, unpublished (www. arkema. com/pdf/EN/products/technical_polymers/rilsan/rilsan_website_2011/rilsan_ecoprofile_article. pdf), 2013.
143. Pilla, S., *Engineering applications of bioplastics and biocomposites-An overview.* Handbook of bioplastics and biocomposites engineering applications, 2011: p. 1-15.
144. Hinrichsen, G., et al., *Natural Fibers, Biopolymers, and Biocomposites: An Introduction*, in *Natural Fibers, Biopolymers, and Biocomposites.* 2005, CRC Press. p. 17-51.
145. Bashir, A.S. and Y. Manusamy, *Recent developments in biocomposites reinforced with natural biofillers from food waste.* Polymer-Plastics Technology and Engineering, 2015. **54**(1): p. 87-99.
146. Bijwe, J., C. Logani, and U. Tewari, *Influence of fillers and fibre reinforcement on abrasive wear resistance of some polymeric composites.* Wear, 1990. **138**(1-2): p. 77-92.

147. Faruk, O., et al., *Biocomposites reinforced with natural fibers: 2000–2010.* Progress in polymer science, 2012. **37**(11): p. 1552-1596.

148. Ismail, H., M. Edyham, and B. Wirjosentono, *Bamboo fibre filled natural rubber composites: the effects of filler loading and bonding agent.* Polymer testing, 2002. **21**(2): p. 139-144.

149. Shalwan, A. and B. Yousif, *In state of art: mechanical and tribological behaviour of polymeric composites based on natural fibres.* Materials & Design, 2013. **48**: p. 14-24.

150. Daniel, I.M., et al., *Engineering mechanics of composite materials*. Vol. 3. 1994: Oxford university press New York.

151. Akpan, E., et al., *Design and Synthesis of Polymer Nanocomposites*, in *Polymer Composites with Functionalized Nanoparticles*. 2019, Elsevier. p. 47-83.

152. Gurunathan, T., S. Mohanty, and S.K. Nayak, *A review of the recent developments in biocomposites based on natural fibres and their application perspectives.* Composites Part A: Applied Science and Manufacturing, 2015. **77**: p. 1-25.

153. Bledzki, A. and J. Gassan, *Composites reinforced with cellulose based fibres.* Progress in polymer science, 1999. **24**(2): p. 221-274.

154. Cousins, W., *Young's modulus of hemicellulose as related to moisture content.* Wood science and technology, 1978. **12**(3): p. 161-167.

155. Satyanarayana, K.G., G.G. Arizaga, and F. Wypych, *Biodegradable composites based on lignocellulosic fibers—An overview.* Progress in polymer science, 2009. **34**(9): p. 982-1021.

156. Fu, S.-Y., et al., *Effects of particle size, particle/matrix interface adhesion and particle loading on mechanical properties of particulate–polymer composites.* Composites Part B: Engineering, 2008. **39**(6): p. 933-961.

157. Nanni, A. and M. Messori, *Thermo-mechanical properties and creep modelling of wine lees filled Polyamide 11 (PA11) and Polybutylene succinate (PBS) bio-composites.* Composites Science and Technology, 2020. **188**: p. 107974.

158. Lee, S.G., et al. *Characterization of surface modified flax fibers and their biocomposites with PHB*. in *Macromolecular symposia*. 2003. Wiley Online Library.

159. Dufresne, A., D. Dupeyre, and M. Paillet, *Lignocellulosic flour-reinforced poly (hydroxybutyrate-co-valerate) composites.* Journal of Applied Polymer Science, 2003. **87**(8): p. 1302-1315.

160. Gibeop, N., et al., *Effect of plasma treatment on mechanical properties of jute fiber/poly (lactic acid) biodegradable composites.* Advanced Composite Materials, 2013. **22**(6): p. 389-399.

161. Chu, B.Y., et al., *Interfacial adhesion of silk/PLA biocomposites by plasma surface treatment.* Adhesion and Interface, 2004. **5**(4): p. 9-16.

162. Gassan, J. and V.S. Gutowski, *Effects of corona discharge and UV treatment on the properties of jute-fibre epoxy composites.* Composites Science and Technology, 2000. **60**(15): p. 2857-2863.

163. Ragoubi, M., et al., *Impact of corona treated hemp fibres onto mechanical properties of polypropylene composites made thereof.* Industrial Crops and Products, 2010. **31**(2): p. 344-349.

164. Pizzi, A., et al., *High resin content natural matrix–natural fibre biocomposites.* Industrial Crops and Products, 2009. **30**(2): p. 235-240.

165. Focher, B., et al., *Steam exploded biomass for the preparation of conventional and advanced biopolymer-based materials.* Biomass and Bioenergy, 1998. **14**(3): p. 187-194.

166. Albano, C., et al., *Analysis of the mechanical, thermal and morphological behaviour of polypropylene compounds with sisal fibre and wood flour, irradiated with gamma rays.* Polymer Degradation and Stability, 2002. **76**(2): p. 191-203.

167. Stamboulis, A., C. Baillie, and T. Peijs, *Effects of environmental conditions on mechanical and physical properties of flax fibers.* Composites Part A: Applied Science and Manufacturing, 2001. **32**(8): p. 1105-1115.

168. Kabir, M., et al., *Chemical treatments on plant-based natural fibre reinforced polymer composites: An overview.* Composites Part B: Engineering, 2012. **43**(7): p. 2883-2892.

169. Kalia, S., B. Kaith, and I. Kaur, *Pretreatments of natural fibers and their application as reinforcing material in polymer composites—A review.* Polymer Engineering & Science, 2009. **49**(7): p. 1253-1272.

170. Rana, A., et al., *Studies of acetylation of jute using simplified procedure and its characterization.* Journal of Applied Polymer Science, 1997. **64**(8): p. 1517-1523.

171. Wang, M., et al., *Young's and shear moduli of ceramic particle filled polyethylene.* Journal of Materials Science: Materials in Medicine, 1998. **9**(11): p. 621-624.

172. Ou, Y., F. Yang, and Z.Z. Yu, *A new conception on the toughness of nylon 6/silica nanocomposite prepared via in situ polymerization.* Journal of Polymer Science Part B: Polymer Physics, 1998. **36**(5): p. 789-795.

173. Zhu, Z.K., et al., *Preparation and properties of organosoluble polyimide/silica hybrid materials by sol–gel process.* Journal of Applied Polymer Science, 1999. **73**(14): p. 2977-2984.

174. Oksman, K., M. Skrifvars, and J.-F. Selin, *Natural fibres as reinforcement in polylactic acid (PLA) composites.* Composites science and technology, 2003. **63**(9): p. 1317-1324.

175. Zainuddin, S.Y.Z., et al., *Potential of using multiscale kenaf fibers as reinforcing filler in cassava starch-kenaf biocomposites.* Carbohydrate polymers, 2013. **92**(2): p. 2299-2305.

176. Liu, L., et al., *Mechanical properties of poly (butylene succinate)(PBS) biocomposites reinforced with surface modified jute fibre.* Composites Part A: Applied Science and Manufacturing, 2009. **40**(5): p. 669-674.

177. Nanni, A. and M. Messori, *Effect of the wine lees wastes as cost-advantage and natural fillers on the thermal and mechanical properties of poly(3-hydroxybutyrate-co-hydroxyhexanoate) (PHBH) and poly(3-hydroxybutyrate-co-hydroxyvalerate) (PHBV).* Journal of Applied Polymer Science 2019.

178. Douce, J., et al., *Effect of filler size and surface condition of nano-sized silica particles in polysiloxane coatings.* Thin Solid Films, 2004. **466**(1-2): p. 114-122.

179. Mishra, S., S. Sonawane, and R. Singh, *Studies on characterization of nano CaCO3 prepared by the in situ deposition technique and its application in PP-nano CaCO3 composites.* Journal of Polymer Science Part B: Polymer Physics, 2005. **43**(1): p. 107-113.

180. Ji, X.L., et al., *Tensile modulus of polymer nanocomposites.* Polymer Engineering & Science, 2002. **42**(5): p. 983-993.

181. Sallem-Idrissi, N., P. Van Velthem, and M. Sclavons, *Fully bio-sourced Nylon 11/raw lignin composites: thermal and mechanical performances.* Journal of Polymers and the Environment, 2018. **26**(12): p. 4405-4414.

182. Battegazzore, D., et al., *Thermo-mechanical properties enhancement of bio-polyamides (PA10. 10 and PA6. 10) by using rice husk ash and nanoclay.* Composites Part A: Applied Science and Manufacturing, 2016. **81**: p. 193-201.

183. Sahoo, S., M. Misra, and A.K. Mohanty, *Enhanced properties of lignin-based biodegradable polymer composites using injection moulding process.* Composites Part A: Applied Science and Manufacturing, 2011. **42**(11): p. 1710-1718.

184. Then, Y.Y., et al., *Oil palm mesocarp fiber as new lignocellulosic material for fabrication of polymer/fiber biocomposites.* International Journal of Polymer Science, 2013. **2013**.

185. Shih, Y.-F. and C.-C. Huang, *Polylactic acid (PLA)/banana fiber (BF) biodegradable green composites.* Journal of Polymer Research, 2011. **18**(6): p. 2335-2340.

186. Cheng, S., et al., *Mechanical and thermal properties of chicken feather fiber/PLA green composites.* Composites Part B: Engineering, 2009. **40**(7): p. 650-654.

187. Ahankari, S.S., A.K. Mohanty, and M. Misra, *Mechanical behaviour of agro-residue reinforced poly (3-hydroxybutyrate-co-3-hydroxyvalerate),(PHBV) green composites: A comparison with traditional polypropylene composites.* Composites Science and Technology, 2011. **71**(5): p. 653-657.

188. Moustafa, H., C. Guizani, and A. Dufresne, *Sustainable biodegradable coffee grounds filler and its effect on the hydrophobicity, mechanical and thermal properties of biodegradable PBAT composites.* Journal of Applied Polymer Science, 2017. **134**(8).

189. Battegazzore, D., A. Noori, and A. Frache, *Natural wastes as particle filler for poly (lactic acid)-based composites.* Journal of Composite Materials, 2019. **53**(6): p. 783-797.

190. Boluk, M. and H. Schreiber, *Interfacial interactions and the properties of filled polymers: I. Dynamic-mechanical responses.* Polymer composites, 1986. **7**(5): p. 295-301.

191. Akay, M., *Aspects of dynamic mechanical analysis in polymeric composites.* Composites science and technology, 1993. **47**(4): p. 419-423.

192. Landel, R.F. and L.E. Nielsen, *Mechanical properties of polymers and composites*. 1993: CRC press.

193. Armioun, S., et al., *Biopolyamide hybrid composites for high performance applications.* Journal of Applied Polymer Science, 2016. **133**(27).

194. Kim, K.-W., et al., *Thermal and mechanical properties of cassava and pineapple flours-filled PLA bio-composites.* Journal of thermal analysis and calorimetry, 2011. **108**(3): p. 1131-1139.

195. Zweifel, H., *Stabilization of polymeric materials*. 2012, Berling (DE): Springer Science & Business Media.

196. Frache, A. and G. Camino, *Degradazione, stabilizzazione e ritardo alla fiamma di polimeri*. Vol. 8. 2012: Edizioni Nuova Cultura.

197. Kunioka, M. and Y. Doi, *Thermal degradation of microbial copolyesters: poly (3-hydroxybutyrate-co-3-hydroxyvalerate) and poly (3-hydroxybutyrate-co-4-hydroxybutyrate).* Macromolecules, 1990. **23**(7): p. 1933-1936.

198. Mitomo, H. and E. Ota, *Thermal decomposition of poly (β-hydroxybutyrate) and its copolymer.* Sen'i Gakkaishi, 1991. **47**(2): p. 89-94.

199. Lehrle, R.S. and R.J. Williams, *Thermal degradation of bacterial poly (hydroxybutyric acid): mechanisms from the dependence of pyrolysis yields on sample thickness.* Macromolecules, 1994. **27**(14): p. 3782-3789.

200. Grassie, N., E. Murray, and P. Holmes, *The thermal degradation of poly (-(D)-β-hydroxybutyric acid): Part 3—The reaction mechanism.* Polymer degradation and stability, 1984. **6**(3): p. 127-134.

201. Grassie, N., E. Murray, and P. Holmes, *The thermal degradation of poly (-(D)-β-hydroxybutyric acid): part 2—changes in molecular weight.* Polymer Degradation and Stability, 1984. **6**(2): p. 95-103.

202. Grassie, N., E. Murray, and P. Holmes, *The thermal degradation of poly (-(d)-β-hydroxybutyric acid): Part 1—Identification and quantitative analysis of products.* Polymer degradation and stability, 1984. **6**(1): p. 47-61.

203. Kopinke, F.-D. and K. Mackenzie, *Mechanistic aspects of the thermal degradation of poly (lactic acid) and poly (β-hydroxybutyric acid).* Journal of Analytical and Applied Pyrolysis, 1997. **40**: p. 43-53.

204. Kopinke, F.-D., M. Remmler, and K. Mackenzie, *Thermal decomposition of biodegradable polyesters—I: Poly (β-hydroxybutyric acid).* Polymer Degradation and stability, 1996. **52**(1): p. 25-38.

205. Aoyagi, Y., K. Yamashita, and Y. Doi, *Thermal degradation of poly [(R)-3-hydroxybutyrate], poly [ε-caprolactone], and poly [(S)-lactide].* Polymer Degradation and Stability, 2002. **76**(1): p. 53-59.

206. Nguyen, S., G.-e. Yu, and R. Marchessault, *Thermal degradation of poly (3-hydroxyalkanoates): preparation of well-defined oligomers.* Biomacromolecules, 2002. **3**(1): p. 219-224.

207. Södergård, A. and M. Stolt, *Properties of lactic acid based polymers and their correlation with composition.* Progress in polymer science, 2002. **27**(6): p. 1123-1163.

208. McNeill, I. and H. Leiper, *Degradation studies of some polyesters and polycarbonates—1. Polylactide: General features of the degradation under programmed heating conditions.* Polymer Degradation and Stability, 1985. **11**(3): p. 267-285.

209. McNeill, I. and H. Leiper, *Degradation studies of some polyesters and polycarbonates—2. Polylactide: degradation under isothermal conditions, thermal degradation mechanism and photolysis of the polymer.* Polymer degradation and stability, 1985. **11**(4): p. 309-326.

210. Kopinke, F.-D., et al., *Thermal decomposition of biodegradable polyesters—II. Poly (lactic acid).* polymer Degradation and Stability, 1996. **53**(3): p. 329-342.

211. Rizzarelli, P. and S. Carroccio, *Thermo-oxidative processes in biodegradable poly (butylene succinate).* Polymer Degradation and Stability, 2009. **94**(10): p. 1825-1838.

212. Bikiaris, D., et al., *Investigation of thermal degradation mechanism of an aliphatic polyester using pyrolysis–gas chromatography–mass spectrometry and a kinetic study of the effect of the amount of polymerisation catalyst.* Polymer Degradation and Stability, 2007. **92**(4): p. 525-536.

213.   Denisov, E.T. and I.B. Afanas' ev, *Oxidation and antioxidants in organic chemistry and biology*. 2005: CRC press.

214.   Denisov, E.T. and E. Denisov, *Handbook of antioxidants*. 1995: CRC press Boca Raton, FL.

215.   Michalak, M., et al., *Oxidative degradation of poly (3-hydroxybutyrate). A new method of synthesis for the malic acid copolymers.* RSC Advances, 2016. **6**(16): p. 12809-12818.

216.   Lucas, N., et al., *Polymer biodegradation: Mechanisms and estimation techniques–A review.* Chemosphere, 2008. **73**(4): p. 429-442.

217.   Hueck, H. *The biodeterioration of materials-an appraisal*. in *Biodeterioration of materials. Microbiological and allied aspects. Proceedings of the 1st international symposium. Southampton, 9th-14th September, 1968*. 1968.

218.   Gu, J.-D., *Microbiological deterioration and degradation of synthetic polymeric materials: recent research advances.* International biodeterioration & biodegradation, 2003. **52**(2): p. 69-91.

219.   Cappitelli, F., P. Principi, and C. Sorlini, *Biodeterioration of modern materials in contemporary collections: can biotechnology help?* Trends in biotechnology, 2006. **24**(8): p. 350-354.

220.   Bonhomme, S., et al., *Environmental biodegradation of polyethylene.* Polymer Degradation and Stability, 2003. **81**(3): p. 441-452.

221.   Warscheid, T. and J. Braams, *Biodeterioration of stone: a review.* International Biodeterioration & Biodegradation, 2000. **46**(4): p. 343-368.

222.   Jennings, D.H. and G. Lysek, *Fungal biology: understanding the fungal lifestyle*. 1996: Bios Scientific Publishers Ltd.

223.   Göpferich, A., *Mechanisms of polymer degradation and erosion.* Biomaterials, 1996. **17**(2): p. 103-114.

224.   Hakkarainen, M., S. Karlsson, and A.-C. Albertsson, *Rapid (bio) degradation of polylactide by mixed culture of compost microorganisms—low molecular weight products and matrix changes.* Polymer, 2000. **41**(7): p. 2331-2338.

225.   Flemming, H.-C., *Relevance of biofilms for the biodeterioration of surfaces of polymeric materials.* Polymer Degradation and Stability, 1998. **59**(1-3): p. 309-315.

226.   Pospíšil, J., *Mechanistic action of phenolic antioxidants in polymers—A review.* Polymer degradation and stability, 1988. **20**(3-4): p. 181-202.

227.   Ehrenstein, G.W. and S. Pongratz, *Resistance and stability of polymers*. 2013: Carl Hanser Verlag GmbH Co KG.

228.   THOMAS, R., *UV-Stabilisierung von elastomeren Werkstoffen.* Gummi, Fasern, Kunststoffe, 1995. **48**(12): p. 864-872.

229.   Kramer, E., *Lichtschutzmittel.* Kunststoffe, 1996. **86**(7): p. 948-953.

230.   Sinha Ray, S., et al., *New polylactide/layered silicate nanocomposites. 3. High-performance biodegradable materials.* Chemistry of Materials, 2003. **15**(7): p. 1456-1465.

231.   Kawai, F. and B. Schink, *The biochemistry of degradation of polyethers.* Critical reviews in biotechnology, 1987. **6**(3): p. 273-307.

232.   El-Hadi, A., et al., *Correlation between degree of crystallinity, morphology, glass temperature, mechanical properties and biodegradation of poly (3-hydroxyalkanoate) PHAs and their blends.* Polymer testing, 2002. **21**(6): p. 665-674.

233.   Labrecque, L., et al., *Citrate esters as plasticizers for poly (lactic acid).* Journal of Applied Polymer Science, 1997. **66**(8): p. 1507-1513.

234.   Arrieta, M.P., et al., *Disintegrability under composting conditions of plasticized PLA–PHB blends.* polymer degradation and stability, 2014. **108**: p. 307-318.

235.   Lovera, D., et al., *Crystallization, morphology, and enzymatic degradation of polyhydroxybutyrate/polycaprolactone (PHB/PCL) blends.* Macromolecular Chemistry and Physics, 2007. **208**(9): p. 924-937.

236.   Teramoto, N., et al., *Biodegradation of aliphatic polyester composites reinforced by abaca fiber.* Polymer Degradation and Stability, 2004. **86**(3): p. 401-409.

237. Mohanty, A., M.A. Khan, and G. Hinrichsen, *Surface modification of jute and its influence on performance of biodegradable jute-fabric/Biopol composites.* Composites Science and Technology, 2000. **60**(7): p. 1115-1124.

238. Mohanty, A., M. Khan, and G. Hinrichsen, *Influence of chemical surface modification on the properties of biodegradable jute fabrics—polyester amide composites.* Composites Part A: Applied Science and Manufacturing, 2000. **31**(2): p. 143-150.

239. Lammi, S., et al., *How olive pomace can be valorized as fillers to tune the biodegradation of PHBV based composites.* Polymer Degradation and Stability, 2019.

240. Wei, L., S. Liang, and A.G. McDonald, *Thermophysical properties and biodegradation behavior of green composites made from polyhydroxybutyrate and potato peel waste fermentation residue.* Industrial Crops and Products, 2015. **69**: p. 91-103.

241. Chevillard, A., et al., *Investigating the biodegradation pattern of an ecofriendly pesticide delivery system based on wheat gluten and organically modified montmorillonites.* Polymer degradation and stability, 2012. **97**(10): p. 2060-2068.

242. OIV, *The International Organisation of Vine and Wine. Available from: http://www.oiv.int/public/medias/6371/oiv-statistical-report-on-world-vitiviniculture-2018.pdf.* 2018.

243. FAOSTAT, *Food and Agriculture Organization of the United Nations—Statistics Division, 2013. Available from: http://faostat3.fao.org/home/E.* 2013.

244. Galanakis, C.M., *Handbook of Grape Processing by-Products: Sustainable Solutions.* 2017, San Diego (US): Academic Press.

245. ANPA, I., *rifiuti del comparto agro–alimentare.* Studio di settore, Rapporti, 2001. **11**: p. 2001.

246. Bustamante, M., et al., *Agrochemical characterisation of the solid by-products and residues from the winery and distillery industry.* Waste Management, 2008. **28**(2): p. 372-380.

247. das Comunidades Europeias, C.-C., *Para um setor vitivinícola sustentável.* Comunicação da Comissão ao Conselho e ao Parlamento Europeu (PT), 2006: p. 319.

248. Spigno, G. and D.M. De Faveri, *Antioxidants from grape stalks and marc: Influence of extraction procedure on yield, purity and antioxidant power of the extracts.* Journal of Food Engineering, 2007. **78**(3): p. 793-801.

249. Devesa-Rey, R., et al., *Valorization of winery waste vs. the costs of not recycling.* Waste management, 2011. **31**(11): p. 2327-2335.

250. Maugenet, J., *Evaluation of the by-products of wine distilleries. II.* Possibility of recovery of proteins in the vinasse of wine distilleries. CR Seances Acad Agric Fr, 1973. **59**: p. 481-7.

251. Pandey, K.B. and S.I. Rizvi, *Plant polyphenols as dietary antioxidants in human health and disease.* Oxidative medicine and cellular longevity, 2009. **2**(5): p. 270-278.

252. Scalbert, A., et al., *Dietary polyphenols and the prevention of diseases.* Critical reviews in food science and nutrition, 2005. **45**(4): p. 287-306.

253. Beckman, C.H., *Phenolic-storing cells: keys to programmed cell death and periderm formation in wilt disease resistance and in general defence responses in plants?* Physiological and Molecular Plant Pathology, 2000. **57**(3): p. 101-110.

254. Prieur, C., et al., *Oligomeric and polymeric procyanidins from grape seeds.* Phytochemistry, 1994. **36**(3): p. 781-784.

255. Jiménez, L., et al., *Comparison of various pulping processes for producing pulp from vine shoots.* Industrial crops and products, 2006. **23**(2): p. 122-130.

256. Max, B., et al., *Extraction of phenolic acids by alkaline hydrolysis from the solid residue obtained after prehydrolysis of trimming vine shoots.* Journal of agricultural and food chemistry, 2009. **58**(3): p. 1909-1917.

257. Rajha, H.N., et al., *Electrical, mechanical, and chemical effects of high-voltage electrical discharges on the polyphenol extraction from vine shoots.* Innovative food science & emerging technologies, 2015. **31**: p. 60-66.

258. Harris-Valle, C., et al., *Polar vineyard pruning extracts increase the activity of the main ligninolytic enzymes in Lentinula edodes cultures.* Canadian journal of microbiology, 2007. **53**(10): p. 1150-1157.
259. Delgado de la Torre, M.P., F. Priego-Capote, and M.D. Luque de Castro, *Comparative profiling analysis of woody flavouring from vine-shoots and oak chips.* Journal of the Science of Food and Agriculture, 2014. **94**(3): p. 504-514.
260. Karaoğlu, M.H., Ş. Zor, and M. Uğurlu, *Biosorption of Cr (III) from solutions using vineyard pruning waste.* Chemical Engineering Journal, 2010. **159**(1-3): p. 98-106.
261. Buratti, C., M. Barbanera, and E. Lascaro, *Ethanol production from vineyard pruning residues with steam explosion pretreatment.* Environmental Progress & Sustainable Energy, 2015. **34**(3): p. 802-809.
262. Prozil, S.O., D.V. Evtuguin, and L.P.C. Lopes, *Chemical composition of grape stalks of Vitis vinifera L. from red grape pomaces.* Industrial Crops and Products, 2012. **35**(1): p. 178-184.
263. Spigno, G., et al., *Influence of cultivar on the lignocellulosic fractionation of grape stalks.* Industrial crops and products, 2013. **46**: p. 283-289.
264. Souquet, J.-M., et al., *Phenolic composition of grape stems.* Journal of Agricultural and Food Chemistry, 2000. **48**(4): p. 1076-1080.
265. Zouboulis, A.I., N.K. Lazaridis, and K.A. Matis, *Removal of toxic metal ions from aqueous systems by biosorptive flotation.* Journal of Chemical Technology & Biotechnology: International Research in Process, Environmental & Clean Technology, 2002. **77**(8): p. 958-964.
266. Egüés, I., et al., *Fermentable sugars recovery from grape stalks for bioethanol production.* Renewable energy, 2013. **60**: p. 553-558.
267. Ozdemir, I., et al., *Preparation and characterization of activated carbon from grape stalk by zinc chloride activation.* Fuel processing technology, 2014. **125**: p. 200-206.
268. Amendola, D., et al., *Autohydrolysis and organosolv process for recovery of hemicelluloses, phenolic compounds and lignin from grape stalks.* Bioresource Technology, 2012. **107**: p. 267-274.
269. Amendola, D., D.M. De Faveri, and G. Spigno, *Grape marc phenolics: Extraction kinetics, quality and stability of extracts.* Journal of Food Engineering, 2010. **97**(3): p. 384-392.
270. Langston, M.S., *Anthocyanin colorant from grape pomace*. 1985, Google Patents.
271. Schieber, A., F.C. Stintzing, and R. Carle, *By-products of plant food processing as a source of functional compounds—recent developments.* Trends in Food Science & Technology, 2001. **12**(11): p. 401-413.
272. Mateo, J.J. and S. Maicas, *Valorization of winery and oil mill wastes by microbial technologies.* Food Research International, 2015. **73**: p. 13-25.
273. Mokochinski, J.B., et al., *Biomass and Sterol Production from Vegetal Substrate Fermentation Using A garicus brasiliensis.* Journal of Food Quality, 2015. **38**(3): p. 221-229.
274. Botella, C., et al., *Xylanase and pectinase production by Aspergillus awamori on grape pomace in solid state fermentation.* Process Biochemistry, 2007. **42**(1): p. 98-101.
275. Israilides, C., et al., *Pullulan content of the ethanol precipitate from fermented agro-industrial wastes.* Applied Microbiology and Biotechnology, 1998. **49**(5): p. 613-617.
276. Deng, Q., M.H. Penner, and Y. Zhao, *Chemical composition of dietary fiber and polyphenols of five different varieties of wine grape pomace skins.* Food Research International, 2011. **44**(9): p. 2712-2720.
277. Pinelo, M., A. Arnous, and A.S. Meyer, *Upgrading of grape skins: Significance of plant cell-wall structural components and extraction techniques for phenol release.* Trends in Food Science & Technology, 2006. **17**(11): p. 579-590.
278. Özvural, E.B. and H. Vural, *Which is the best grape seed additive for frankfurters: extract, oil or flour?* Journal of the Science of Food and Agriculture, 2014. **94**(4): p. 792-797.
279. Fiori, L., et al., *Supercritical CO2 extraction of oil from seeds of six grape cultivars: Modeling of mass transfer kinetics and evaluation of lipid profiles and tocol contents.* The Journal of Supercritical Fluids, 2014. **94**: p. 71-80.

280. Aghamirzaei, M., et al., *Effects of grape seed powder as a functional ingredient on flour physicochemical characteristics and dough rheological properties.* Journal of Agricultural Science and Technology, 2015. **17**(2): p. 365-373.

281. Glampedaki, P. and V. Dutschk, *Stability studies of cosmetic emulsions prepared from natural products such as wine, grape seed oil and mastic resin.* Colloids and surfaces A: Physicochemical and engineering aspects, 2014. **460**: p. 306-311.

282. Shi, J., et al., *Polyphenolics in grape seeds—biochemistry and functionality.* Journal of medicinal food, 2003. **6**(4): p. 291-299.

283. Yaragalla, S., et al., *Preparation and characterization of green graphene using grape seed extract for bioapplications.* Materials Science and Engineering: C, 2016. **65**: p. 345-353.

284. Pérez-Serradilla, J. and M.L. De Castro, *Microwave-assisted extraction of phenolic compounds from wine lees and spray-drying of the extract.* Food Chemistry, 2011. **124**(4): p. 1652-1659.

285. Regulation, C., *No 1208/84 of 27 April 1984 amending Regulation (EEC) No 337/79 on the common organization of the market in wine.* Official Journal of the European Communities.

286. Nerantzis, E.T. and P. Tataridis, *Integrated enology-utilization of winery by-products into high added value products.* J. Sci. Tech, 2006. **1**: p. 79-89.

287. Yalcin, D., et al., *Characterization and recovery of tartaric acid from wastes of wine and grape juice industries.* Journal of Thermal Analysis and Calorimetry, 2008. **94**(3): p. 767-771.

288. Delgado de la Torre, M., F. Priego-Capote, and M. Luque de Castro, *Characterization and comparison of wine lees by liquid chromatography–mass spectrometry in high-resolution mode.* Journal of agricultural and food chemistry, 2015. **63**(4): p. 1116-1125.

289. Sharma, A.K., et al., *Use of fine wine lees for value addition in ice cream.* Journal of Food Science and Technology, 2015. **52**(1): p. 592-596.

290. Zhu, Q., et al., *Adsorption Characteristics of Pb2+ onto Wine Lees-Derived Biochar.* Bulletin of Environmental Contamination and Toxicology, 2016. **97**(2): p. 294-299.

291. Nanni, A. and M. Messori, *A comparative study of different winemaking by-products derived additives on oxidation stability, mechanical and thermal proprieties of polypropylene.* Polymer Degradation and Stability, 2018. **149**: p. 9-18.

292. Nanni, A., et al., *Thermal and UV aging of polypropylene stabilized by wine seeds wastes and their extracts.* Polymer Degradation and Stability, 2019. **165**: p. 49-59.

293. Larrauri, J.A., P. Rupérez, and F. Saura-Calixto, *Effect of drying temperature on the stability of polyphenols and antioxidant activity of red grape pomace peels.* Journal of agricultural and food chemistry, 1997. **45**(4): p. 1390-1393.

294. Hikosaka, M. and T. Seto, *The order of the molecular chains in isotactic polypropylene crystals.* Polymer Journal, 1973. **5**(2): p. 111-127.

295. Keith, H., et al., *Evidence for a second crystal form of polypropylene.* Journal of Applied Physics, 1959. **30**(10): p. 1485-1488.

296. BAYDAR, N.G. and M. Akkurt, *Oil content and oil quality properties of some grape seeds.* Turkish Journal of Agriculture and Forestry, 2001. **25**(3): p. 163-168.

297. Ignat, I., I. Volf, and V.I. Popa, *A critical review of methods for characterisation of polyphenolic compounds in fruits and vegetables.* Food chemistry, 2011. **126**(4): p. 1821-1835.

298. Bates, R. and F. Regulski, *Composition and utilisation of Florida grape pomace.* Proc. Fla. Stale Horl. Soc, 1982. **95**: p. 107-109.

299. Teixeira, A., et al., *Natural bioactive compounds from winery by-products as health promoters: a review.* International journal of molecular sciences, 2014. **15**(9): p. 15638-15678.

300. Özvural, E.B. and H. Vural, *Grape seed flour is a viable ingredient to improve the nutritional profile and reduce lipid oxidation of frankfurters.* Meat science, 2011. **88**(1): p. 179-183.

301. Olejar, K.J., S. Ray, and P.A. Kilmartin, *Enhanced antioxidant activity of polyolefin films integrated with grape tannins.* Journal of the Science of Food and Agriculture, 2015.

302. Persico, P., et al., *Enhancement of poly (3-hydroxybutyrate) thermal and processing stability using a bio-waste derived additive.* International journal of biological macromolecules, 2012. **51**(5): p. 1151-1158.

303. Kwei, T., *The effect of hydrogen bonding on the glass transition temperatures of polymer mixtures.* Journal of Polymer Science Part C: Polymer Letters, 1984. **22**(6): p. 307-313.

304. Ambrogi, V., et al., *Natural antioxidants for polypropylene stabilization.* Polymer degradation and stability, 2011. **96**(12): p. 2152-2158.

305. Houshyar, S., R. Shanks, and A. Hodzic, *Tensile creep behaviour of polypropylene fibre reinforced polypropylene composites.* Polymer Testing, 2005. **24**(2): p. 257-264.

306. Navas, C.S., M.M. Reboredo, and D.L. Granados, *Comparative study of agroindustrial wastes for their use in polymer matrix composites.* Procedia Materials Science, 2015. **8**: p. 778-785.

307. Bigger, S. and O. Delatycki, *New approach to the measurement of polymer photooxidation.* Journal of Polymer Science Part A: Polymer Chemistry, 1987. **25**(12): p. 3311-3323.

308. Cerruti, P., et al., *Effect of natural antioxidants on the stability of polypropylene films.* Polymer Degradation and Stability, 2009. **94**(11): p. 2095-2100.

309. Van Krevelen, D.W. and P. Hoftyzer, *Properties of polymers: their estimation and correlation with chemical structure/by DW van Krevelen; with the collaboration of PJ Hoftyzer.*

310. Ojeda, H., et al., *Influence of pre-and postveraison water deficit on synthesis and concentration of skin phenolic compounds during berry growth of Vitis vinifera cv. Shiraz.* American Journal of Enology and Viticulture, 2002. **53**(4): p. 261-267.

311. Brossaud, F., et al., *Flavonoid compositional differences of grapes among site test plantings of Cabernet franc.* American journal of enology and viticulture, 1999. **50**(3): p. 277-284.

312. Jayaprakasha, G., R. Singh, and K. Sakariah, *Antioxidant activity of grape seed (Vitis vinifera) extracts on peroxidation models in vitro.* Food chemistry, 2001. **73**(3): p. 285-290.

313. Jaitz, L., et al., *LC–MS/MS analysis of phenols for classification of red wine according to geographic origin, grape variety and vintage.* Food chemistry, 2010. **122**(1): p. 366-372.

314. Pascual, O., et al., *Oxygen consumption rates by different oenological tannins in a model wine solution.* Food chemistry, 2017. **234**: p. 26-32.

315. Pulido, R., L. Bravo, and F. Saura-Calixto, *Antioxidant activity of dietary polyphenols as determined by a modified ferric reducing/antioxidant power assay.* Journal of agricultural and food chemistry, 2000. **48**(8): p. 3396-3402.

316. Brand-Williams, W., M.-E. Cuvelier, and C. Berset, *Use of a free radical method to evaluate antioxidant activity.* LWT-Food science and Technology, 1995. **28**(1): p. 25-30.

317. Cuvelier, M., C. Berset, and H. Richard, *Use of a new test for determining comparative antioxidative activity of butylated hydroxyanisole, butylated hydroxytoluene, alpha and gamma-tocopherols and extracts from rosemary and sage.* Sciences des Aliments (France), 1990.

318. Sánchez-Moreno, C., J.A. Larrauri, and F. Saura-Calixto, *A procedure to measure the antiradical efficiency of polyphenols.* Journal of the Science of Food and Agriculture, 1998. **76**(2): p. 270-276.

319. Cotea, V.V., et al., *EVALUATION OF PHENOLIC COMPOUNDS CONTENT IN GRAPE SEEDS.* Environmental Engineering & Management Journal (EEMJ), 2018. **17**(4).

320. Cheng, V.J., et al., *Effect of extraction solvent, waste fraction and grape variety on the antimicrobial and antioxidant activities of extracts from wine residue from cool climate.* Food Chemistry, 2012. **134**(1): p. 474-482.

321. Ma, W., et al. *Isolation of condensed tannins in individual size from grape seeds and their impact on astringency perception*. in *BIO Web of Conferences*. 2016. EDP Sciences.

322. Ajuong, E.-M. and M.C. Breese, *Fourier transform infrared characterization of Pai wood (Afzelia africana Smith) extractives.* Holz als Roh-und Werkstoff, 1998. **56**(2): p. 139.

323. Senvaitiene, J., A. Beganskiene, and A. Kareiva, *Spectroscopic evaluation and characterization of different historical writing inks.* Vibrational Spectroscopy, 2005. **37**(1): p. 61-67.

324. Ragupathi Raja Kannan, R., R. Arumugam, and P. Anantharaman, *Fourier transform infrared spectroscopy analysis of seagrass polyphenols.* Current Bioactive Compounds, 2011. **7**(2): p. 118-125.

325. Jensen, J.S., M. Egebo, and A.S. Meyer, *Identification of spectral regions for the quantification of red wine tannins with Fourier transform mid-infrared spectroscopy.* Journal of agricultural and food chemistry, 2008. **56**(10): p. 3493-3499.

326. Ricci, A., et al., *Application of Fourier transform infrared (FTIR) spectroscopy in the characterization of tannins.* Applied Spectroscopy Reviews, 2015. **50**(5): p. 407-442.

327. Ricci, A., et al., *Analytical profiling of food-grade extracts from grape (Vitis vinifera sp.) seeds and skins, green tea (Camellia sinensis) leaves and Limousin oak (Quercus robur) heartwood using MALDI-TOF-MS, ICP-MS and spectrophotometric methods.* Journal of Food Composition and Analysis, 2017. **59**: p. 95-104.

328. Robb, C.S., et al., *Analysis of green tea constituents by HPLC-FTIR.* 2002.

329. Antoine, M.L., C. Simon, and A. Pizzi, *UV spectrophotometric method for polyphenolic tannin analysis.* Journal of applied polymer science, 2004. **91**(4): p. 2729-2732.

330. Schofield, P., D. Mbugua, and A. Pell, *Analysis of condensed tannins: a review.* Animal feed science and technology, 2001. **91**(1-2): p. 21-40.

331. Vidal, S., et al., *Changes in proanthocyanidin chain length in winelike model solutions.* Journal of Agricultural and Food Chemistry, 2002. **50**(8): p. 2261-2266.

332. Rigo, A., et al., *Contribution of proanthocyanidins to the peroxy radical scavenging capacity of some Italian red wines.* Journal of agricultural and food chemistry, 2000. **48**(6): p. 1996-2002.

333. Becheri, A., et al., *Synthesis and characterization of zinc oxide nanoparticles: application to textiles as UV-absorbers.* Journal of Nanoparticle Research, 2008. **10**(4): p. 679-689.

334. Li, Y.-Q., S.-Y. Fu, and Y.-W. Mai, *Preparation and characterization of transparent ZnO/epoxy nanocomposites with high-UV shielding efficiency.* Polymer, 2006. **47**(6): p. 2127-2132.

335. Battegazzore, D., et al., *Plasticizers, antioxidants and reinforcement fillers from hazelnut skin and cocoa by-products: Extraction and use in PLA and PP.* Polymer Degradation and Stability, 2014. **108**: p. 297-306.

336. Bocchini, S., A. Di Blasio, and A. Frache. *Influence of MWNT on polypropylene and polyethylene photooxidation*. in *Macromolecular Symposia*. 2011. Wiley Online Library.

337. Alongi, J., et al., *Role of β-cyclodextrin nanosponges in polypropylene photooxidation.* Carbohydrate Polymers, 2011. **86**(1): p. 127-135.

338. Bocchini, S., et al., *Influence of nanodispersed hydrotalcite on polypropylene photooxidation.* European Polymer Journal, 2008. **44**(11): p. 3473-3481.

339. Bocchini, S., et al., *Influence of nanodispersed boehmite on polypropylene photooxidation.* Polymer Degradation and stability, 2007. **92**(10): p. 1847-1856.

340. AG, W.C., *GENIOSIL GF31 - Organofunctional Silanes - https://www.wacker.com/h/en-us/medias/GENIOSIL-GF-31-en-2019.11.05.pdf*. 2019.

341. AG, W.C., *For powerful connections - Silanes I organofunctional - https://www.yumpu.com/en/document/view/16039476/for-powerful-connections-wacker-chemie*. 2018.

342. Barham, P., et al., *Crystallization and morphology of a bacterial thermoplastic: poly-3-hydroxybutyrate.* Journal of Materials Science, 1984. **19**(9): p. 2781-2794.

343. Voigt, W., *Ueber die Beziehung zwischen den beiden Elasticitätsconstanten isotroper Körper.* Annalen der Physik, 1889. **274**(12): p. 573-587.

344. Halpin, J., *Stiffness and expansion estimates for oriented short fiber composites.* Journal of Composite Materials, 1969. **3**(4): p. 732-734.

345. Halpin, J.C., *Effects of environmental factors on composite materials*. 1969, Air Force Materials Lab Wright-Patterson AFB OH.

346. Pukanszky, B., *Influence of interface interaction on the ultimate tensile properties of polymer composites.* Composites, 1990. **21**(3): p. 255-262.

347. Móczó, J. and B. Pukánszky, *Polymer micro and nanocomposites: structure, interactions, properties.* Journal of Industrial and Engineering Chemistry, 2008. **14**(5): p. 535-563.

348. Turcsanyi, B., B. Pukanszky, and F. Tüdõs, *Composition dependence of tensile yield stress in filled polymers.* Journal of Materials Science Letters, 1988. **7**(2): p. 160-162.

349. Liang, J. and R. Li, *Prediction of tensile yield strength of rigid inorganic particulate filled thermoplastic composites.* Journal of Materials Processing Technology, 1998. **83**(1-3): p. 127-130.

350. Saywell, L., *Clarification of wine.* Industrial & Engineering Chemistry, 1934. **26**(9): p. 981-982.

351. Barham, P., *Nucleation behaviour of poly-3-hydroxy-butyrate.* Journal of materials science, 1984. **19**(12): p. 3826-3834.

352. Kai, W., Y. He, and Y. Inoue, *Fast crystallization of poly (3-hydroxybutyrate) and poly (3-hydroxybutyrate-co-3-hydroxyvalerate) with talc and boron nitride as nucleating agents.* Polymer international, 2005. **54**(5): p. 780-789.

353. Hablot, E., et al., *Thermal and thermo-mechanical degradation of poly (3-hydroxybutyrate)-based multiphase systems.* Polymer Degradation and Stability, 2008. **93**(2): p. 413-421.

354. Spanoudakis, J. and R. Young, *Crack propagation in a glass particle-filled epoxy resin.* Journal of Materials Science, 1984. **19**(2): p. 473-486.

355. Radford, K., *The mechanical properties of an epoxy resin with a second phase dispersion.* Journal of Materials Science, 1971. **6**(10): p. 1286-1291.

356. Levita, G., A. Marchetti, and A. Lazzeri, *Fracture of ultrafine calcium carbonate/polypropylene composites.* Polymer composites, 1989. **10**(1): p. 39-43.

357. Dekkers, M. and D. Heikens, *The effect of interfacial adhesion on the tensile behavior of polystyrene–glass-bead composites.* Journal of Applied Polymer Science, 1983. **28**(12): p. 3809-3815.

358. Pilla, S., et al., *Polylactide-pine wood flour composites.* Polymer Engineering & Science, 2008. **48**(3): p. 578-587.

359. Battegazzore, D., J. Alongi, and A. Frache, *Poly (lactic acid)-based composites containing natural fillers: thermal, mechanical and barrier properties.* Journal of Polymers and the Environment, 2014. **22**(1): p. 88-98.

360. Rebia, R.A., et al., *Biodegradable PHBH/PVA blend nanofibers: Fabrication, characterization, in vitro degradation, and in vitro biocompatibility.* Polymer degradation and stability, 2018. **154**: p. 124-136.

361. Xu, P., et al., *Effects of modified nanocrystalline cellulose on the hydrophilicity, crystallization and mechanical behaviors of poly (3-hydroxybutyrate-co-3-hydroxyhexanoate).* New Journal of Chemistry, 2018. **42**(14): p. 11972-11978.

362. Hassaini, L., et al., *The effects of PHBV-g-MA compatibilizer on morphology and properties of poly (3-hydroxybutyrate-Co-3-hydroxyvalerate)/olive husk flour composites.* Journal of adhesion science and Technology, 2016. **30**(19): p. 2061-2080.

363. Wang, Y., et al., *Improvement in hydrophilicity of PHBV films by plasma treatment.* Journal of Biomedical Materials Research Part A: An Official Journal of The Society for Biomaterials, The Japanese Society for Biomaterials, and The Australian Society for Biomaterials and the Korean Society for Biomaterials, 2006. **76**(3): p. 589-595.

364. Pukanszky, B. and G. VÖRÖS, *Mechanism of interfacial interactions in particulate filled composites.* Composite Interfaces, 1993. **1**(5): p. 411-427.

365. Reynaud, E., et al., *Nanofillers in polymeric matrix: a study on silica reinforced PA6.* Polymer, 2001. **42**(21): p. 8759-8768.

366. Battegazzore, D., et al., *Rice husk as bio-source of silica: preparation and characterization of PLA–silica bio-composites.* RSC Advances, 2014. **4**(97): p. 54703-54712.

367. Jancar, J. and A. Dibenedetto, *Failure Mechanics in Ternary Composites of Polypropylene with Inorganic Fillers and Elastomer Inclusions. 2. Fracture-Toughness.* Journal of materials science, 1995. **30**(9): p. 2438-2445.

368. Guo, T., et al., *Effects of nano calcium carbonate modified by a lanthanum compound on the properties of polypropylene.* Journal of applied polymer science, 2005. **97**(3): p. 1154-1160.

369. Liu, Z., et al., *Effects of coupling agent and morphology on the impact strength of high density polyethylene/CaCO3 composites.* Polymer, 2002. **43**(8): p. 2501-2506.

370. Ward, I.M. and D.W. Hadley, *An introduction to the mechanical properties of solid polymers*. 1993.

371. Crawford, R.J., *Plastics engineering*. 1998: Elsevier.

372. Lakes, R.S., *Viscoelastic solids*. Vol. 9. 1998: CRC press.

373. Bondioli, F., et al., *Improving the creep stability of high-density polyethylene with acicular titania nanoparticles.* Journal of applied polymer science, 2009. **112**(2): p. 1045-1055.

374. Palmer, R.G., et al., *Models of hierarchically constrained dynamics for glassy relaxation.* Physical Review Letters, 1984. **53**(10): p. 958.

375. Fancey, K.S., *A latch-based weibull model for polymerie creep and recovery.* Journal of polymer engineering, 2001. **21**(6): p. 489-510.

376. Fancey, K.S., *A mechanical model for creep, recovery and stress relaxation in polymeric materials.* Journal of materials science, 2005. **40**(18): p. 4827-4831.

377. Wortman, J. and R. Evans, *Young's modulus, shear modulus, and Poisson's ratio in silicon and germanium.* Journal of applied physics, 1965. **36**(1): p. 153-156.

378. Hopcroft, M.A., W.D. Nix, and T.W. Kenny, *What is the Young's Modulus of Silicon?* Journal of microelectromechanical systems, 2010. **19**(2): p. 229-238.

379. Zhao, Y., et al., *The interfacial modification of rice straw fiber reinforced poly (butylene succinate) composites: Effect of aminosilane with different alkoxy groups.* Journal of Applied Polymer Science, 2012. **125**(4): p. 3211-3220.

380. Then, Y.Y., et al., *Effect of 3-Aminopropyltrimethoxysilane on chemically modified oil palm Mesocarp fiber/poly (butylene succinate) Biocomposite.* BioResources, 2015. **10**(2): p. 3577-3601.

381. Abay, A.K., et al., *Preparation and characterization of poly (lactic acid)/recycled polypropylene blends with and without the coupling agent, n-(6-aminohexyl) aminomethyltriethoxysilane.* Journal of Polymer Research, 2016. **23**(9): p. 198.

382. Arkles, B., *Silane coupling agents: connecting across boundaries.* Morrisville: Gelest, 2003. **2003**: p. 9-12.

383. Novello, V., *Filiera vitivinicola: Valorizzare residui e sottoprodotti.* Informatore Agrario, 2015. **33**: p. 61-63.

384. Mago, G., D.M. Kalyon, and F.T. Fisher, *Nanocomposites of polyamide-11 and carbon nanostructures: Development of microstructure and ultimate properties following solution processing.* Journal of Polymer Science Part B: Polymer Physics, 2011. **49**(18): p. 1311-1321.

385. Xu, J. and B.H. Guo, *Poly (butylene succinate) and its copolymers: research, development and industrialization.* Biotechnology journal, 2010. **5**(11): p. 1149-1163.

386. Sujan EBW, R.R., *Using the DMA Q800 for ASTM International D 648 Deflection Temperature Under Load* TA Instruments, 109 Lukens Drive, New Castle DE 19720, USA

387. Battegazzore, D., A. Noori, and A. Frache, *Natural wastes as particle filler for poly (lactic acid)-based composites.* Journal of Composite Materials, 2018: p. 0021998318791316.

388. Nielsen, L.E., *Simple theory of stress-strain properties of filled polymers.* Journal of Applied Polymer Science, 1966. **10**(1): p. 97-103.

389. Jancar, J., A. Dianselmo, and A. Dibenedetto, *The yield strength of particulate reinforced thermoplastic composites.* Polymer Engineering & Science, 1992. **32**(18): p. 1394-1399.

390. Wang, K., et al., *Mechanical properties and toughening mechanisms of polypropylene/barium sulfate composites.* Composites Part A: Applied Science and Manufacturing, 2003. **34**(12): p. 1199-1205.

391. Dai, H.L., C. Mei, and Y.N. Rao, *A novel method for prediction of tensile strength of spherical particle-filled polymer composites with strong adhesion.* Polymer Engineering & Science, 2017. **57**(2): p. 137-143.

392. Dai, H.-L., et al., *Prediction of the tensile strength of hybrid polymer composites filled with spherical particles and short fibers.* Composite Structures, 2018. **187**: p. 509-517.

393. Hojo, H., et al., *Short-and long-term strength characteristics of particulate-filled cast epoxy resin.* Polymer Engineering & Science, 1974. **14**(9): p. 604-609.

394. Sailaja, R. and M. Deepthi, *Mechanical and thermal properties of compatibilized composites of polyethylene and esterified lignin.* Materials & Design, 2010. **31**(9): p. 4369-4379.

395. Oliver-Ortega, H., et al., *Tensile properties and micromechanical analysis of stone groundwood from softwood reinforced bio-based polyamide11 composites.* Composites Science and Technology, 2016. **132**: p. 123-130.

396. Taesler, C., et al., *Polymer whiskers of poly (4-hydroxybenzoate): Reinforcement efficiency in composites with polyamides.* Journal of applied polymer science, 1996. **61**(5): p. 783-792.

397. Hua, L., *Analysis on amino acid composition and lipid of yellow wine lees [J].* Journal of Anhui Agricultural Sciences, 2009. **34**: p. 153.

398. Gómez, M.E., et al., *Lipid composition of lees from Sherry wine.* Journal of agricultural and food chemistry, 2004. **52**(15): p. 4791-4794.

399. Vieira, M.G.A., et al., *Natural-based plasticizers and biopolymer films: A review.* European Polymer Journal, 2011. **47**(3): p. 254-263.

400. Budi Santosa, F. and G.W. Padua, *Tensile properties and water absorption of zein sheets plasticized with oleic and linoleic acids.* Journal of agricultural and food chemistry, 1999. **47**(5): p. 2070-2074.

401. Mishra, S.B., et al., *Study of performance properties of lignin-based polyblends with polyvinyl chloride.* Journal of Materials Processing Technology, 2007. **183**(2-3): p. 273-276.

402. A.Nanni, M.M., *Thermal Stabilization and mechanical reinforcement of Polyhydroxybutyrate (PHB) using wine derived additives.* Under Submission, 2019.

403. Zierdt, P., et al., *Sustainable wood-plastic composites from bio-based polyamide 11 and chemically modified beech fibers.* Sustainable Materials and Technologies, 2015. **6**: p. 6-14.

404. Burgers, J., *First report on viscosity and plasticity.* Nordemann Pub., New York, 1935.

405. Holmes, D., J. Loughran, and H. Suehrcke, *Constitutive model for large strain deformation of semicrystalline polymers.* Mechanics of Time-Dependent Materials, 2006. **10**(4): p. 281-313.

406. Findley, W.N., *26-Year creep and recovery of poly (vinyl chloride) and polyethylene.* Polymer Engineering & Science, 1987. **27**(8): p. 582-585.

407. Hassanzadeh-Aghdam, M., et al., *Effect of nanoparticle aggregation on the creep behavior of polymer nanocomposites.* Composites Science and Technology, 2018. **162**: p. 93-100.

408. Huda, M.S., et al., *Effect of fiber surface-treatments on the properties of laminated biocomposites from poly (lactic acid)(PLA) and kenaf fibers.* Composites science and technology, 2008. **68**(2): p. 424-432.

409. Lee, J., et al., *Mechanical, thermal and water absorption properties of kenaf-fiber-based polypropylene and poly (butylene succinate) composites.* Journal of Polymers and the Environment, 2013. **21**(1): p. 293-302.

410. Zhang, Y., et al., *Mechanical and thermal properties of basalt fiber reinforced poly (butylene succinate) composites.* Materials Chemistry and Physics, 2012. **133**(2-3): p. 845-849.

411. Nanni, A. and M. Messori, *Thermo-mechanical properties and creep modelling of Wine Lees filled Polyamide 11 (PA11) and Polybutylene succinate (PBS) bio-composites.* Composites Science and Technology 2019. **Accepted paper,**.

412. Versari, A., et al., *Recovery of tartaric acid from industrial enological wastes.* Journal of Chemical Technology & Biotechnology: International Research in Process, Environmental & Clean Technology, 2001. **76**(5): p. 485-488.

413. Jara-Palacios, M.J., *Wine Lees as a Source of Antioxidant Compounds.* Antioxidants, 2019. **8**(2): p. 45.

414. Auriemma, M., et al., *Blending poly (3-hydroxybutyrate) with tannic acid: influence of a polyphenolic natural additive on the rheological and thermal behavior.* European Polymer Journal, 2015. **63**: p. 123-131.

415. De Rooy, S.L., et al., *Purification and characterization of poly-hydroxybutyrate (PHB) in Cupriavidus necator.* Indonesian Journal of Chemistry, 2007. **7**(3): p. 243-248.

416. Bocchini, S., et al., *Polylactic acid and polylactic acid-based nanocomposite photooxidation.* Biomacromolecules, 2010. **11**(11): p. 2919-2926.

417. Duangphet, S., et al., *The effect of chain extender on poly (3-hydroxybutyrate-co-3-hydroxyvalerate): Thermal degradation, crystallization, and rheological behaviours.* Journal of Polymers and the Environment, 2014. **22**(1): p. 1-8.

418. Kolahchi, A.R. and M. Kontopoulou, *Chain extended poly (3-hydroxybutyrate) with improved rheological properties and thermal stability, through reactive modification in the melt state.* Polymer degradation and stability, 2015. **121**: p. 222-229.

419. Chan, C.M., et al., *Insights into the biodegradation of PHA/wood composites: Micro-and macroscopic changes.* Sustainable Materials and Technologies, 2019. **21**: p. e00099.

420.   Daglia, M., *Polyphenols as antimicrobial agents.* Current opinion in biotechnology, 2012. **23**(2): p. 174-181.